ISSN 1732-9353
eISSN 2543-7496

Scientific Review

Engineering and Environmental Sciences

Przegląd Naukowy

Inżynieria i Kształtowanie Środowiska

Vol. 29 (2) 2020 Nr 88

Quarterly – Kwartalnik

SCIENTIFIC REVIEW
ENGINEERING AND ENVIRONMENTAL SCIENCES
Kwartalnik / Quarterly

Lista recenzentów jest publikowana w ostatnim numerze danego rocznika i na stronie http://iks_pn.sggw.pl
The list of reviewers is published in the last issue of the volume and on the http://iks_pn.sggw.pl

ADRES REDAKCJI / EDITORIAL OFFICE ADDRESS
Wydział Budownictwa i Inżynierii Środowiska SGGW
ul. Nowoursynowska 159, 02-776 Warszawa
tel. (22) 59 35 248, 59 35 240
e-mail: iks_pn@sggw.pl
http://iks_pn.sggw.pl

ISSN 1732-9353
e-ISSN 2543-7496

Wydawnictwo drukowane jest pierwotną wersją Przeglądu Naukowego Inżynieria i Kształtowanie Środowiska

„Przegląd Naukowy Inżynieria i Kształtowanie Środowiska" jest indeksowane w bazach: AGRO(Poznań), BazTech, Biblioteka Nauki, CrossRef, DOAJ, E-publikacje Nauki Polskiej, Google Scholar, Index Copernicus, INFONA, POL-Index, SCOPUS, SIGŻ(CBR).

Scientific Review

Engineering and Environmental Sciences

Przegląd Naukowy

Inżynieria i Kształtowanie Środowiska

Vol. 29 (2) **2020** **Nr 88**

Spis treści
Contents

PRACE ORYGINALNE
Original papers

Opracowanie redakcyjne – Anna Dołomisiewicz, Krystyna Piotrowska

ISSN 1732-9353   eISSN 2543-7496

Druk: ZAPOL sp.j., al. Piastów 42, 71-062 Szczecin

PRACE ORYGINALNE
ORIGINAL PAPERS

Scientific Review – Engineering and Environmental Sciences (2020), 29 (2), 123–135
Sci. Rev. Eng. Env. Sci. (2020), 29 (2)
Przegląd Naukowy – Inżynieria i Kształtowanie Środowiska (2020), 29 (2), 123–135
Prz. Nauk. Inż. Kszt. Środ. (2020), 29 (2)
http://iks.pn.sggw.pl
DOI 10.22630/PNIKS.2020.29.2.11

Libor ANSORGE, Lada STEJSKALOVÁ, Jiří DLABAL, Elżbieta ČEJKA

Výzkumný ústav vodohospodářský T. G. Masaryka, v. v. i.
T. G. Masaryk Water Research Institute, p. r. i.

Wpływ oczyszczalni ścieków na redukcję zanieczyszczeń odprowadzanych w czeskiej części dorzecza Odry
Effect of wastewater treatment plants to the reduction of pollution discharged in the Czech part of the Odra river basin

Słowa kluczowe: ocena śladu wodnego, szary ślad wodny, oczyszczalnie ścieków, zanieczyszczenie, obszar dorzecza
Key words: water footprint assessment, grey water footprint, wastewater treatment plants, pollution, river basin district

Wprowadzenie

Wzrost liczby ludności, urbanizacja i uprzemysłowienie to jedne z wiodących problemów współczesnego świata. W związku z tym pojawiają się pytania, jak zapewnić wystarczającą ilość jedzenia, energii i wody. Szacuje się, że znaczna część świata już jest narażona na tzw. stres wodny, to jest niedobór wody, a sytuacja w przyszłości jeszcze się pogorszy (Alcamo, Flörke i Märker, 2007; Mekonnen i Hoekstra, 2016; Wada i in., 2016). Wraz ze wzrostem liczby ludności, rozrastającymi się aglomeracjami i rozwojem przemysłowym rośnie także ilość substancji odpadowych emitowanych do wód. Często wody te są nieodpowiednio oczyszczane, co powoduje problemy z ich dalszym wykorzystaniem poniżej zrzutu do odbiornika do poboru wody dla potrzeb gospodarczych i bytowych, do celów przemysłowych lub w rolnictwie, ale także w celu zapewnienia zaopatrujących ekosystemowych usług wodnych (Keeler i in., 2012). Problemy te będą nasilać się wraz ze zmianami klimatu i z rozwojem społeczno-gospodarczym (Li i in., 2017) i będą miały wpływ na gospodarkę oraz inne dziedziny życia (Hertel i Liu, 2016). Z tych właśnie powodów ONZ zdefiniowała jako jeden z 17 celów zrównoważonego rozwoju cel 6: Zapewnić wszystkim ludziom dostęp do wody i warunków sanitarnych poprzez zrównoważoną gospodarkę zasobami wodnymi (UN, 2015). Aby to osiągnąć, określono konkretne zadania. Zadanie 6.3 ma na celu poprawienie jakości wód poprzez zmniejszenie odprowadzanych do nich zanieczyszczeń. Głównymi źródłami zanieczyszczeń dostających się do wody jest rolnictwo, przemysł i źródła komunalne. Zanieczyszczenia pochodzące z rolnictwa mają charakter zanieczyszczenia obszarowego wynikającego ze stosowania na gruntach rolnych nawozów, pestycydów i innych substancji. Zanieczyszczenia przemysłowe to zazwyczaj zanieczyszczenia punktowe z przedsiębiorstw i zakładów przemysłowych. Skład zanieczyszczeń z jednostek osadniczych zależy od typu zabudowy. W przypadku luźnej zabudowy zanieczyszczenie może być rozproszone. W Europie Środkowej jest jednak bardziej rozpowszechniony układ urbanistyczny w postaci aglomeracji miejskich i stref podmiejskich o dużej koncentracji ludności i powiązanych usługach skupionych na niewielkim obszarze. Ścieki i wody deszczowe z tak zabudowanych obszarów są odprowadzane przez systemy kanalizacyjne, a ich zrzuty do odbiornika są punktowe. W celu zmniejszenia zanieczyszczenia komunalnego generowanego na obszarach zurbanizowanych oraz zanieczyszczeń przemysłowych poszczególne systemy kanalizacyjne są zakończone, zgodnie z prawodawstwem europejskim, oczyszczalniami ścieków.

Przedstawione badania dotyczą oceny wpływu oczyszczalni ścieków na redukcję zanieczyszczeń odprowadzanych do wód z punktowych źródeł zanieczyszczeń. Do oceny wpływu zrzutów zanieczyszczeń na odbiornik stosuje się, w zależności od celu oceny, różne metody. W tym wypadku wybrano metodę analizy śladu wodnego. Ślad wodny to narzędzie, które pozwala wyrazić ilość wody zużytej zarówno bezpośrednio, jak i pośrednio w całym cyklu produkcyjnym (np. wyrobów, firmy lub usługi) w celu rozcieńczenia zanieczyszczenia związanego z tym procesem. Koncepcja śladu wodnego została wprowadzona w 2002 roku (Hoekstra, 2003). Od momentu wprowadzenia wskaźnika ślad wodny, ze względu na jego prostotę i użyteczność w praktyce, zyskał dużą popularność wśród naukowców, organów decyzyjnych i użytkowników. W literaturze można znaleźć coraz więcej badań z wykorzystaniem śladu wodnego (Mubako, 2018; Ansorge, Stejskalová i Vološinová, 2019; Zhu i in., 2019). Szczegółowy opis metodologii określania śladu wodnego jest dostępny w wielu językach, w tym również w języku polskim (Fiałkiewicz, Burszta-Adamiak, Malinowski i Kolonko, 2013; Bergier i in., 2019).

Do oceny zanieczyszczenia wód służy tzw. szary ślad wodny. Określa on objętość wody wymaganą do rozcieńczenia ładunku odprowadzanych zanieczyszczeń do takiego stopnia, żeby jakość uzyskanej wody nie przekraczała obowiązujących standardów (Hoekstra, Chapagain, Aldaya i Mekonnen, 2011). Do wyliczenia śladu wodnego oprócz sposobu opartego na klasyfikacji zrzutów zanieczyszczeń (szary ślad wodny) stosuje się też metodę oceny cyklu życia (ang. *life cycle assessment* – LCA), która jest również określana jako ślad wodny (Bergier i in., 2019). Obliczanie śladu wodnego na podstawie wskaźnika LCA zostało zdefiniowane w międzynarodowej normie ISO 14046:2014.

Oceną prawidłowego funkcjonowania oczyszczalni ścieków za pomocą śladu wodnego zajmowało się w przeszłości wielu autorów i na ten temat zostały opublikowane liczne badania. Shao i Chen (2013) w badaniu śladu wodnego oczyszczalni ścieków zajmowali się bezpośrednimi i pośrednimi kosztami oczyszczania ścieków z użyciem tzw. podejścia hybrydowego i analizy przepływów międzygałęziowych (ang. *input–output*). Analizę przepływów międzygałęziowych wykorzystano również do oszacowania udziału poszczególnych sektorów z obszarów zurbanizowanych (Li, Liu, Yang i Hao, 2016). Gu i inni (2016) zaproponowali, aby zastosować tzw. wskaźnik redukcji śladu wodnego przy określaniu roli oczyszczalni ścieków w zmniejszaniu wpływu człowieka na zasoby wodne. Z kolei Gómez-Llanos, Durán-Barroso i Matías (2018) do oceny poprawy jakości ścieków w procesie oczyszczania wprowadzili nowy wskaźnik – tzw. operatywny szary ślad wodny, tj. różnicę między szarym śladem wodnym bez oczyszczalni i z oczyszczalnią ścieków. Opublikowanych zostało także kilka analiz dotyczących szarego śladu wodnego w wybranych oczyszczalniach ścieków lub na wybranych terytoriach. Fiałkiewicz i inni (2013) zajęli się równowagą hydrologiczną miasta i ustalili ślad wodny Wrocławia. Teodosiu, Barjoveanu, Sluser, Popa i Trofin (2016) porównali metodologię oceny śladu wodnego (ang. *water footprint assessment*) zgodnie z zasadami LCA z metodologią według kwantyfikacji oddziaływania na środowisko (ang. *environmental impact quantification*) na komunalnej oczyszczalni ścieków w Iasi, w Rumunii (Barjoveanu, Cojocariu, Robu i Teodosiu, 2010). Morera, Corominas, Poch, Aldaya i Comas (2016) przetestowali metodologię śladu wodnego w oczyszczalni ścieków o wydajności 4000 m^3 na dobę w miejscowości La Garriga, w Hiszpanii. Martínez-Alcalá, Pellicer-Martínez i Fernández-López (2018) zbadali wpływ 12 komunalnych oczyszczalni ścieków w regionie Murcia (Hiszpania) na zmniejszenie szarego śladu wodnego nie tylko w przypadku powszechnie spotykanych wskaźników zanieczyszczeń, ale także farmaceutyków. Ansorge i inni (2019) wykorzystując szary ślad wodny, dokonali oceny zrzutów ścieków z 14 komunalnych oczyszczalni ścieków w północno-zachodnich Czechach z punktu widzenia kryteriów zrównoważonego rozwoju. Johnson i Mehrvar (2019) opublikowali badanie wykorzystujące ślad wodny do oceny ścieków z przemysłu winiarskiego oczyszczanych w oczyszczalni ścieków komunalnych w rejonie Niagara, w Ontario (Kanada). Stejskalová, Ansorge, Kučera i Vološinová (2019) dokonali oceny zrównoważonego zrzutu ścieków z komunalnych oczyszczalni ścieków w małej zlewni łącznie z obliczeniem śladu wodnego przed modernizacją i po modernizacji tego obiektu. Qin, Sun, Han i Zou (2019) obliczyli szary ślad wodny dla przemysłu, rolnictwa i gospodarstw domowych w 31 prowincjach w Chinach w latach 1998–2012.

W niniejszym badaniu szary ślad wodny jest wykorzystywany do wyrażenia wpływu przemysłowych i komunalnych oczyszczalni ścieków na redukcję odprowadzanych zanieczyszczeń w czeskiej części międzynarodowego dorzecza Odry. Znaczne zanieczyszczenie wód powierzchniowych w dorzeczu Odry jest postrzegane jako istotny problem o znaczeniu ponadregionalnym, którego rozwiązanie wymaga wymiany informacji i uzgodnienia na poziomie międzynarodowym. Oprócz problemów ponadregionalnych w dorzeczu Odry występują także problemy gospodarki wodnej o charakterze regionalnym, a jednym z nich jest niedostateczny w stosunku do obecnego stanu wiedzy i techniki oraz ustalonych celów środowiskowych dla wód powierzchniowych stopień oczyszczania odprowadzanych ścieków w regionalnych zlewniach cząstkowych.

Metodologia badań

Powierzchnia dorzecza Odry w Republice Czeskiej wynosi 7240 km^2, co stanowi zaledwie 6% całego dorzecza (MKOO, 2015). W celu realizacji dyrektywy 2000/60/WE ustanawiającej ramy wspólnotowego działania w dziedzinie polityki wodnej międzynarodowy obszar dorzecza Odry (MODO) podzielono na siedem jednostek, z których część obszarów opracowania górnej Odry i Nysy Łużyckiej znajduje się w Republice Czeskiej.

Dane dotyczące ścieków odprowadzanych do wód w ilościach przekraczających 500 m^3 miesięcznie lub 6000 m^3 rocznie są w Republice Czeskiej ewidencjonowane przez Státní Podniky Povodí (zarządy dorzecza) oraz zapisywane w rejestrze poborów wody i zrzutów ścieków do odbiornika, łącznie z wybranymi danymi dotyczącymi ilości i jakości ścieków surowych na dopływie do oczyszczalni i oczyszczonych odprowadzanych do odbiorników wodnych. Informacje o zanieczyszczeniach na dopływie do oczyszczalni oraz zrzutach ścieków oczyszczonych do odbiornika uwzględniają siedem wybranych wskaźników zanieczyszczenia, którymi są: biochemiczne zapotrzebowanie tlenu (BZT_5), chemiczne zapotrzebowanie tlenu ($ChZT_{Cr}$), zawiesiny ogólne, rozpuszczone związki mineralne, azot amonowy ($N\text{-}NH_4^+$), azot nieorganiczny (N_{norg}) i fosfor ogólny (P_{og}).

Do badania śladu wodnego i analizy redukcji zanieczyszczeń wykorzystano dane charakteryzujące 391 oczyszczalni ścieków i miejsc zrzutu ścieków oczyszczonych do odbiorników wodnych w czeskiej części dorzecza Odry, które zebrano w latach 2004–2018 (tab. 1). Komunalne i przemysłowe oczyszczalnie ścieków identyfikowano na podstawie klasyfikacji działalności gospodarczych w Unii Europejskiej, tj. kodów NACE (Nomenclature statistique des activités économiques dans la Communauté européenne).

Kalkulacja zmniejszenia szarego śladu wodnego w dorzeczu odbywa się w czterech krokach. Zgodnie z równaniem (1) obliczano szary ślad wodny zarówno generowanych (na dopływie do oczyszczalni), jak i odprowadzanych zanieczyszczeń (na odpływie z oczyszczalni) dla każdego wskaźnika zanieczyszczenia *i* oraz punktu zrzutu *j*. Następnie na podstawie wzoru (2) obliczono ślad wodny ścieków surowych doprowadzonych do oczyszczalni i odprowadzanego ładunku zanieczyszczeń dla każdego punktu zrzutu *j*. W trzecim kroku, zgodnie z równaniem (3), określono szary ślad wodny dorzecza jako sumę śladów wodnych wszystkich miejsc zrzutu. Wreszcie redukcję zanieczyszczeń

TABELA 1. Liczba punktów zrzutów ścieków w czeskiej części dorzecza Odry (badania własne)
TABLE 1. Number of wastewater discharges in the Czech part of Odra river basin (own studies)

Wyszczególnienie Specification	Górna Odra Upper Odra	Nysa Łużycka Lusatian Neisse	Razem Sum
Liczba punktów zrzutów ścieków z redukcją odprowadzanych zanieczyszczeń Number of places of wastewater discharges with pollution reduction	329	62	391
Liczba zapisów zrzutów ścieków w rejestrze z redukcją odprowadzanych zanieczyszczeń Number of records concerning discharges with pollution reduction	2607	446	3053

(sprawność oczyszczania ścieków) określono na podstawie wzoru (4) jako stosunek różnicy szarego śladu wodnego na dopływie i odpływie (w miejscu zrzutu do odbiornika) do szarego śladu wodnego na dopływie.

$$SW_{\text{szary},j,i,k} = \frac{L_{j,i,k}}{c_{\max,j,i} - c_{\text{nat},j,i}} \tag{1}$$

$$SW_{\text{szary},j,k} = \max\left\{SW_{\text{szary},j,1,k}, SW_{\text{szary},j,2,k}, \ldots, SW_{\text{szary},j,i,k}\right\} \tag{2}$$

$$SW_{\text{szary},k} \sum\nolimits_{j=1}^{n} SW_{\text{szary},j,k} \tag{3}$$

$$redukcja = \frac{SW_{\text{szary,effluent}} - SW_{\text{szary,influent}}}{SW_{\text{szary,influent}}} \tag{4}$$

gdzie:
k – identyfikator (*influent* – dopływ do oczyszczalni, *effluent* – odpływ z oczyszczalni),
$SW_{\text{szary},j,i,k}$ – szary ślad wodny zanieczyszczenia i w miejscu zrzutu j [objętość / czas],
$SW_{\text{szary},j,k}$ – szary ślad wodny oczyszczalni w miejscu zrzutu j [objętość / czas],
$SW_{\text{szary},k}$ – szary ślad wodny analizowanego systemu [objętość / czas],
$L_{j,i,k}$ – ładunek zanieczyszczenia i na dopływie do oczyszczalni albo ładunek zanieczyszczenia i na odpływie z oczyszczalni w miejscu j [masa / czas],
$c_{\max,j,i}$ – dopuszczalne stężenie zanieczyszczeń i w odbiorniku w miejscu j [masa / objętość],
$c_{\text{nat},j,i}$ – naturalne stężenie zanieczyszczeń i w odbiorniku j [masa / objętość],
n – liczba punktów zrzutów.

Poziomy granicznych zawartości monitorowanych zanieczyszczeń podaje czeska norma techniczna wydana w 2017 roku – ČSN 75 7221. Zgodnie z nią maksymalne stężenia zanieczyszczeń w odbiorniku ($c_{\max}$) zostały ustalone na podstawie poziomów dla wód II klasy, a poziom naturalnego stężenia (c_{nat}) określono zgodnie z wartościami dla wód I klasy (tab. 2).

TABELA 2. Maksymalne i naturalne poziomy monitorowanych wskaźników
TABLE 2. Monitored parameters with their natural and maximum concentration values

Wskaźnik Parameter	c_{nat} [mg·l^{-1}]	c_{max} [mg·l^{-1}]
Biochemiczne zapotrzebowanie tlenu Biochemical oxygen demand	2	4
Chemiczne zapotrzebowanie tlenu Chemical oxygen demand	15	25
Zawiesiny ogólne General suspensions	15	25
Rozpuszczone związki mineralne* Dissolved minerals	300	450
Azot nieorganiczny Inorganic nitrogen	2,75	5,55
Fosfor ogólny General phosphorus	0,05	0,15
Azot amonowy Ammonium nitrogen	0,2	0,4

*Wartość zdolności asymilacyjnej (c_{max}–c_{nat}) rozpuszczonych związków mineralnych wyprowadzono na podstawie założenia, że rozpuszczone związki mineralne są podzbiorem całkowitej ilości rozpuszczonych substancji stałych. Wartość zdolności asymilacyjnej dla rozpuszczonych związków mineralnych określono na poziomie 3/4 zdolności asymilacyjnej całkowitej ilości rozpuszczonych substancji stałych zgodnie z normą ČSN 75 7221 (Ansorge, Stejskalová, Dlabal i Kučera, 2019).

Wyniki oraz ich dyskusja

Szary ślad wodny zanieczyszczeń odprowadzanych z oczyszczalni ścieków waha się w czeskiej części dorzecza Odry od 1,87 do 4,00·10^9 m^3 rocznie (rys.). Zlewnia cząstkowa górnej Odry ma w nim udział na poziomie 71–92%, a zlewnia Nysy Łużyckiej zaledwie 8–29%. Szary ślad wodny zanieczyszczeń na dopływie do oczyszczalni ścieków wynosi od 21,66 do 30,14·10^9 m^3 rocznie. Skuteczność usuwania zanieczyszczeń w oczyszczalniach ścieków w czeskiej części dorzecza Odry wynosi 85–95% i podobne wyniki osiąga się również w cząstkowej zlewni górnej Odry, gdzie wielkość redukcji badanych wskaźników osiąga od 86 do 95%. W czeskiej części zlewni Nysy Łużyckiej redukcja zanieczyszczeń kształtuje się w granicach od 58 do 92%. Szczegóły podano w tabeli 3.

Odpływy z oczyszczalni komunalnych (tab. 4) stanowią od 68 do 90% szarego śladu wodnego zrzucanych zanieczyszczeń. W zlewni Nysy Łużyckiej zrzuty z miejskich oczyszczalni ścieków stanowią od 88 do 99% całkowitego szarego śladu wodnego. Podobnie jest z zanieczyszczeniami w ściekach surowych na dopływie do oczyszczalni. Zanieczyszczenia dopływające do miejskich oczyszczalni ścieków stanowią od 68 do 93% szarego śladu wodnego zanieczyszczeń wytwarzanych w całym do-

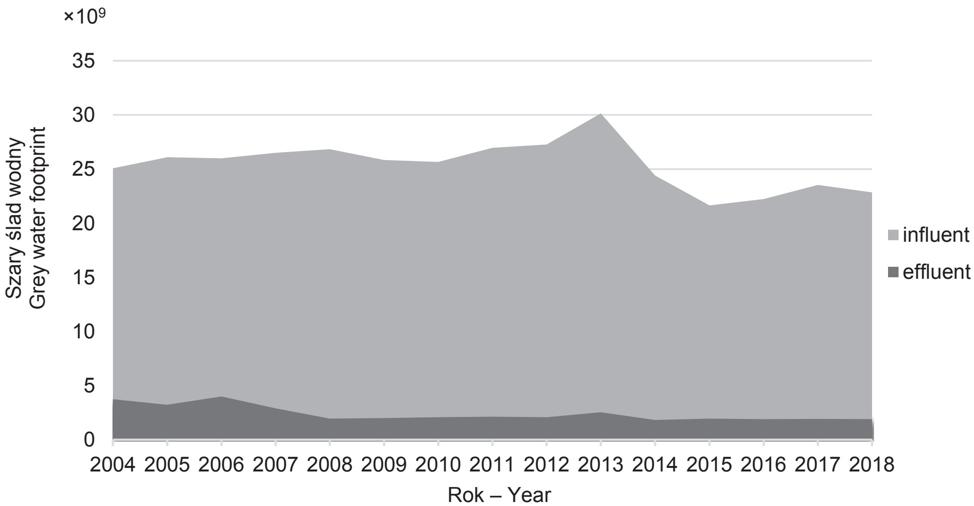

RYSUNEK. Szary ślad wodny odpływu z oczyszczalni ścieków (ang. *effluent*) i dopływu do oczyszczalni (ang. *influent*) w czeskiej części dorzecza Odry (badania własne)
FIGURE. Grey water footprint of pollution discharged from WWTPs (effluent) and pollution entering the WWTPs (influent) in the Czech part of Odra river basin (own studies)

rzeczu Odry – od 65 do 93% w dorzeczu górnej Odry, a od 92 do 99% w zlewni Nysy Łużyckiej. Ścieki odprowadzane z przemysłowych oczyszczalni ścieków (tab. 5) stanowią zatem jedynie niewielką część szarego śladu wodnego.

Przeprowadzone badania mają kilka ograniczeń:

1. W przypadku 168 zapisów dotyczących zrzutów zanieczyszczeń do odbiornika (co stanowi 5,5%) w rejestrze jest brak niektórych danych odnośnie wskaźnika zanieczyszczenia na dopływie do oczyszczalni ścieków, determinującego wartość śladu wodnego w odpływie z oczyszczalni. Zatem obliczenie stopnia zmniejszenia zanieczyszczenia w powyższych przypadkach może nie być całkowicie dokładne.
2. W trakcie badań dysponowano danymi o siedmiu podstawowych wskaźnikach zanieczyszczenia ujętych w centralnym rejestrze, ale, jak pokazują badania zagraniczne (Martínez-Alcalá i in., 2018), na szary ślad wodny mogą mieć wpływ również substancje inne niż standardowo monitorowane w oczyszczalniach ścieków czy raportowane do rejestrów centralnych. W przypadku 1837 ewidencjonowanych pomiarów jakości ścieków surowych i oczyszczonych (tj. 60,2%) ze względu na niejednakową skuteczność usuwania poszczególnych zanieczyszczeń doszło do zamiany wskaźnika zanieczyszczenia determinującego ślad wodny na dopływie ścieków do oczyszczalni na wskaźnik dominujący na odpływie z oczyszczalni.
3. W 21 przypadkach (0,7%) na oczyszczalni ścieków nastąpił wzrost szarego śladu wodnego (poza przypadkami, o których mowa w pkt 1). Przyczyną mogły być błędy w centralnej bazie danych albo optymalizacja procesu

TABELA 3. Szary ślad wodny zanieczyszczenia na dopływie do oczyszczalni i na odpływie z oczyszczalni w czeskiej części dorzecza Odry (badania własne)

TABLE 3. Grey water footprint of pollution entering the WWTPs (influent) and pollution discharged from WWTPs (effluent) in the Czech part of Odra river basin (own studies)

Rok Year	Jednostka Unit	Szary ślad wodny na dopływie do oczyszczalni Grey water footprint – influent			Szary ślad wodny na odpływie z oczyszczalni Grey water footprint – effluent		
		dorzecze Odry Odra river basin	górna Odra upper Odra	Nysa Łużycka Lusatian Neisse	dorzecze Odry Odra river basin	górna Odra upper Odra	Nysa Łużycka Lusatian Neisse
2004	$10^9 m^3$	25,07	22,60	2,46	3,75	3,25	0,50
2005	$10^9 m^3$	26,10	23,51	2,59	3,24	2,43	0,81
2006	$10^9 m^3$	25,99	23,61	2,38	4,00	3,00	1,00
2007	$10^9 m^3$	26,51	24,40	2,11	2,91	2,07	0,84
2008	$10^9 m^3$	26,85	24,40	2,44	1,97	1,78	0,18
2009	$10^9 m^3$	25,85	23,27	2,58	2,00	1,76	0,24
2010	$10^9 m^3$	25,65	23,79	1,86	2,09	1,91	0,18
2011	$10^9 m^3$	26,95	24,73	2,22	2,12	1,72	0,40
2012	$10^9 m^3$	27,26	24,67	2,59	2,08	1,71	0,36
2013	$10^9 m^3$	30,14	27,71	2,43	2,55	2,08	0,46
2014	$10^9 m^3$	24,41	21,66	2,75	1,82	1,61	0,22
2015	$10^9 m^3$	21,66	19,00	2,65	1,95	1,52	0,43
2016	$10^9 m^3$	22,23	19,59	2,64	1,90	1,45	0,45
2017	$10^9 m^3$	23,53	20,69	2,84	1,93	1,54	0,39
2018	$10^9 m^3$	22,85	19,74	3,11	1,90	1,47	0,44

TABELA 4. Szary ślad wodny zanieczyszczenia na dopływie do komunalnej oczyszczalni ścieków i na odpływie z oczyszczalni w czeskiej części dorzecza Odry (badania własne)

TABLE 4. Grey water footprint of pollution entering the municipal WWTPs (influent) and pollution discharded from municipal WWTPs (effluent) in the Czech part of Odra river basin (own studies)

Rok Year	Jednostka Unit	Szary ślad wodny na dopływiedo oczyszczalni Grey water footprint – influent			Szary ślad wodny na odpływie z oczyszczalni Grey water footprint – effluent		
		dorzecze Odry Odra river basin	górna Odra Upper Odra	Nysa Łużycka Lusatian Neisse	dorzecze Odry Odra river basin	górna Odra Upper Odra	Nysa Łużycka Lusatian Neisse
2004	10^9 m^3	17,73	15,32	2,41	2,57	2,09	0,48
2005	10^9 m^3	19,23	16,69	2,54	2,45	1,67	0,79
2006	10^9 m^3	18,54	16,21	2,33	2,91	1,92	0,98
2007	10^9 m^3	19,32	17,25	2,08	2,23	1,40	0,82
2008	10^9 m^3	19,81	17,40	2,42	1,34	1,17	0,17
2009	10^9 m^3	18,65	16,13	2,52	1,43	1,20	0,23
2010	10^9 m^3	17,95	16,16	1,79	1,55	1,39	0,16
2011	10^9 m^3	18,79	16,77	2,03	1,60	1,25	0,36
2012	10^9 m^3	19,46	16,94	2,52	1,57	1,22	0,35
2013	10^9 m^3	20,41	18,05	2,36	1,89	1,44	0,45
2014	10^9 m^3	19,96	17,27	2,69	1,45	1,25	0,20
2015	10^9 m^3	20,23	17,64	2,60	1,68	1,26	0,42
2016	10^9 m^3	20,39	17,79	2,59	1,66	1,21	0,45
2017	10^9 m^3	21,13	18,31	2,82	1,74	1,35	0,39
2018	10^9 m^3	21,23	18,16	3,08	1,71	1,28	0,43

TABELA 5. Szary ślad wodny zanieczyszczenia na dopływie do przemysłowej oczyszczalni ścieków i na odpływie z oczyszczalni w czeskiej części dorzecza Odry (badania własne)
TABLE 5. Grey water footprint of pollution entering the industrial WWTPs (influent) and pollution discharged from industrial WWTPs (effluent) in the Czech part of Odra river basin (own studies)

Rok Year	Jednostka Unit	Szary ślad wodny na dopływie do oczyszczalni Grey water footprint – influent			Szary ślad wodny na odpływie z oczyszczalni Grey water footprint – effluent		
		dorzecze Odry Odra river basin	górna Odra upper Odra	Nysa Łużycka Lusatian Neisse	dorzecze Odry Odra river basin	górna Odra upper Odra	Nysa Łużycka Lusatian Neisse
2004	10^9 m^3	7,34	7,29	0,05	1,18	1,16	0,02
2005	10^9 m^3	6,86	6,81	0,05	0,79	0,76	0,03
2006	10^9 m^3	7,45	7,41	0,05	1,09	1,08	0,02
2007	10^9 m^3	7,19	7,15	0,04	0,69	0,67	0,02
2008	10^9 m^3	7,03	7,01	0,02	0,63	0,62	0,01
2009	10^9 m^3	7,20	7,14	0,06	0,57	0,56	0,01
2010	10^9 m^3	7,70	7,64	0,07	0,54	0,52	0,01
2011	10^9 m^3	8,16	7,97	0,19	0,52	0,47	0,05
2012	10^9 m^3	7,80	7,73	0,07	0,51	0,50	0,01
2013	10^9 m^3	9,73	9,66	0,07	0,66	0,64	0,01
2014	10^9 m^3	4,45	4,39	0,06	0,38	0,36	0,01
2015	10^9 m^3	1,42	1,37	0,06	0,27	0,26	0,01
2016	10^9 m^3	1,84	1,79	0,05	0,25	0,24	0,01
2017	10^9 m^3	2,40	2,37	0,03	0,19	0,19	0,00
2018	10^9 m^3	1,61	1,58	0,03	0,19	0,19	0,01

oczyszczania zamierzona z pewnych względów na inny wskaźnik zanieczyszczenia niż te, na podstawie których określano szary ślad wodny.

Wnioski

Jedną z głównych zalet szarego śladu wodnego jest to, że transfiguruje każdy rodzaj zanieczyszczenia wypuszczanego do odbiornika w ilość wody niezbędną do rozcieńczenia wprowadzonego do wody ładunku zanieczyszczenia do takiego stopnia, aby jakość wody nie przekraczała ustalonych standardów. W ten sposób można porównywać ze sobą różne wskaźniki zanieczyszczenia. Jego wadą jest to, że odnosi się wyłącznie do chemizmu wody a nie uwzględnia wpływu odprowadzanych ścieków na stan ekologiczny.

Oczyszczalnie ścieków w znacznym stopniu redukują zanieczyszczenie odprowadzane do odbiornika, a tym samym minimalizują potrzebę rozcieńczania zrzutu ścieków do bezpiecznego stężenia. W czeskiej części dorzecza Odry oczyszczalnie ścieków zmniejszają nawet o 92% ilość wody potrzebnej do rozcieńczenia odprowadzanych zanieczyszczeń, tj. szary ślad wodny. Czeska część dorzecza Odry jest podzielona na dwa obszary opracowania: około 90% szarego śladu wodnego dotyczy dorzecza górnej Odry, a 10% zlewni Nysy Łużyckiej. Na początku monitorowanego okresu 2004–2018 oczyszczalnie komunalne i przemysłowe przyczyniły się do wielkości szarego śladu wodnego w dorzeczu górnej Odry w 65 : 35. Pod koniec tego okresu stosunek ten wynosił 85 : 15. W zlewni Nysy Łużyckiej również wzrósł odsetek komunalnych oczyszczalni ścieków względem oczyszczalni przemysłowych z około 96 : 4 do 98 : 2. Ze względu na niejednakowy stopień redukcji poszczególnych wskaźników zanieczyszczenia w oczyszczalniach ścieków w 60% oczyszczalni wielkość szarego śladu wodnego na wlocie do oczyszczalni była uwarunkowana innym wskaźnikiem niż na wylocie z oczyszczalni.

Literatura

Alcamo, J., Flörke, M. i Märker, M. (2007). Future long-term changes in global water resources driven by socio-economic and climatic changes. *Hydrological Sciences Journal*, *52*(2), 247--275. https://doi.org/10.1623/hysj.52.2.247

Ansorge, L., Stejskalová, L. i Vološinová, D. (2019). Srovnání výzkumu vodní stopy v ČR a ve světě – bibliometrická analýza. *Vodohospodářské technicko-ekonomické informace*, *61*(6), 60-62. Pobrano z: https://www.vtei.cz/2019/12/srovnani-vyzkumu-vodni-stopy-v-cr-a-ve-svete-bibliometricka-analyza [dostęp 19.12.2019].

Ansorge, L., Stejskalová, L., Dlabal, J. i Kučera, J. (2019). Šedá vodní stopa jako ukazatel udržitelného vypouštění odpadních vod – případová studie *Povodí Ohře*. *Entecho*, *2*(2), 12-18. https://doi.org/10.35933/ENTECHO.2019.12.001

Barjoveanu, G., Cojocariu, C., Robu, B. i Teodosiu, C. (2010). Integrated assessment of wastewater treatment plants for sustainable river basin management. *Environmental Engineering and Management Journal*, *9*(9), 1251-1258. Pobrano z: http://eemj.eu/index.php/EEMJ/article/view/634 [dostęp 20.03.2020].

Bergier, T., Burszta-Adamiak, E., Fiałkiewicz, W., Małeck, P., Owsiany, M., Rosiek, K., Rybicki, S.M. i Wojciechowska, E. (2019). *Racjonalizacja wykorzystania zasobów wodnych na terenach zurbanizowanych*. Stowarzyszenie Gmin Polska Sieć „Energie Cités". Pobrano z: http://www.sladwodnymiast.pl/images/2019/20191108/Racjonaliacja_wykorzystania_zasob%C3%B3w_wodnych_na_terenach_zurbanizowanych.pdf [dostęp 27.02.2020].

ČSN 75 7221. Kvalita vod. Klasifikace kvality povrchových vod.

Dyrektywa 2000/60/WE Parlamentu Europejskiego i Rady z dnia 23 października 2000 r. ustanawiająca ramy wspólnotowego działania w dziedzinie polityki wodnej. OJ L 327 z 22.12.2000.

Fiałkiewicz, W., Burszta-Adamiak, E., Malinowski, P. i Kolonko, A. (2013). Urban water Footprint – System monitorowania i oceny gospodarowania wodą w miastach. *Ochrona Środowiska*, *35*(3), 9-12.

Gómez-Llanos, E., Durán-Barroso, P. i Matías-Sánchez, A. (2018). Management effectiveness assessment in wastewater treatment plants through a new water footprint indicator. *Journal of Cleaner Production*, *198*, 463-471. https://doi.org/10.1016/j.jclepro.2018.07.062

Gu, Y., Dong, Y., Wang, H., Keller, A., Xu, J., Chiramba, T. i Li, F. (2016). Quantification of the water, energy and carbon footprints of wastewater treatment plants in China considering a water–energy nexus perspective. *Ecological Indicators*, *60*, 402-409. https://doi.org/10.1016/j.ecolind.2015.07.012

Hertel, T.W. i Liu, J. (2019). Implications of water scarcity for economic growth. W *Economy-Wide Modeling of Water at Regional and Global Scales* (strony 11-35). Singapore: Springer.

Hoekstra, A.Y. (2003). Virtual Water Trade. Proceedings of the international expert meeting on Virtual Water Trade (Value of Water Research Report Series No 12). IHE. Pobrano z: http://waterfootprint.org/media/downloads/Report12.pdf [dostęp 05.05.2015].

Hoekstra, A.Y., Chapagain, A.K., Aldaya, M.M. i Mekonnen, M.M. (2011). The water footprint assessment manual: Setting the global standard. Abingdon, UK: Routledge.

ISO 14046:2014. Environmental management. Water footprint. Principles, requirements and guidelines.

Johnson, M.B. i Mehrvar, M. (2019). An assessment of the grey water footprint of winery wastewater in the Niagara Region of Ontario, Canada. *Journal of Cleaner Production*, *214*, 623-632. https://doi.org/10.1016/j.jclepro.2018.12.311

Keeler, B.L., Polasky, S., Brauman, K.A., Johnson, K.A., Finlay, J.C., O'Neill, A., Kovacs, K. i Dalzell, B. (2012). Linking water quality and well-being for improved assessment and valuation of ecosystem services. *Proceedings of the National Academy of Sciences*, *109*(45), 18619-18624. https://doi.org/10.1073/pnas.1215991109

Li, H., Liu, G., Yang, Z. i Hao, Y. (2016). Urban Gray Water Footprint Analysis Based on Input-Output Approach. *Energy Procedia*, *104*, 118-122. https://doi.org/10.1016/j.egypro.2016.12.021

Liu, J., Yang, H., Gosling, S.N., Kummu, M., Flörke, M., Pfister, S., Hanasaki, N., Wada, Y., Zhang, X., Zheng, C., Alcamo, J. i Oki, T. (2017). Water scarcity assessments in the past, present and future. *Earth's Future*, *5*(6), 545--559. https://doi.org/10.1002/2016EF000518

Martínez-Alcalá, I., Pellicer-Martínez, F. i Fernández-López, C. (2018). Pharmaceutical grey water footprint: Accounting, influence of wastewater treatment plants and implications of the reuse. *Water Research*, *135*, 278-287. https://doi.org/10.1016/j.watres.2018.02.033

Mekonnen, M.M. i Hoekstra, A.Y. (2016). Four billion people facing severe water scarcity. *Science Advances*, *2*(2), e1500323. https://doi.org/10.1126/sciadv.1500323

Międzynarodowa Komisja Ochrony Odry przed Zanieczyszczeniem [MKOO] (2015). *Aktualizacja Planu Gospodarowania Wodami dla Międzynarodowego Obszaru Dorzecza Odry na cykl planistyczny 2016–2021*. Pobrano z: http://mkoo.pl/Grf/MKOO2009/PGW/PGW_2015/MKOO_Plan_MOPO_2016_2021.pdf [dostęp 20.03.2020].

Morera, S., Corominas, Ll., Poch, M., Aldaya, M.M. i Comas, J. (2016). Water footprint assessment in wastewater treatment plants. *Journal of Cleaner Production*, *112*, 4741-4748. https://doi.org/10.1016/j.jclepro.2015.05.102

Mubako, S.T. (2018). Blue, green, and grey water quantification approaches: A bibliometric and literature review. *Journal of Contemporary Water Research & Education*, *165*(1), 4-19. https://doi.org/10.1111/j.1936-704X.2018.03289.x

Qin, X., Sun, C., Han, Q. i Zou, W. (2019). Grey Water Footprint Assessment from the Perspective of Water Pollution Sources: A Case Study of China. *Water Resources*, *46*(3), 454-465. https://doi.org/10.1134/S0097807819030187

Shao, L. i Chen, G.Q. (2013). Water Footprint Assessment for Wastewater Treatment: Method, Indicator, and Application. *Environmental Science & Technology*, *47*(14), 7787-7794. https://doi.org/10.1021/es402013t

Stejskalová, L., Ansorge, L., Kučera, J. i Vološinová, D. (2019). Využití indikátoru šedé vodní stopy k posouzení role ČOV v malém povodí. W 13. bienální konference Voda. 18––20.09.2019 Poděbrady.

Teodosiu, C., Barjoveanu, G., Sluser, B.R., Popa, S.A.E. i Trofin, O. (2016). Environmental assessment of municipal wastewater discharges: A comparative study of evaluation methods. *The International Journal of Life Cycle Assessment*, *21*(3), 395-411. https://doi.org/10.1007/s11367-016-1029-5

United Nations [UN] (2015). *Transforming Our World: The 2030 Agenda for Sustainable Development*. Pobrano z: https://sustainabledevelopment.un.org/post2015/transformingourworld/publication [dostęp dd.mm.rr].

Wada, Y., Flörke, M., Hanasaki, N., Eisner, S., Fischer, G., Tramberend, S., Satoh, Y., Vliet, M.T.H. van, Yillia, P., Ringler, C., Burek, P. i Wiberg, D. (2016). Modeling global water use for the 21st century: The Water Futures and Solutions (WFaS) initiative and its approaches. *Geoscientific Model Development*, *9*(1), 175-222. https://doi.org/10.5194/gmd-9-175-2016

Zhu, Y., Jiang, S., Han, X., Gao, X., He, G., Zhao, Y. i Li, H. (2019). A Bibliometrics Review of Water Footprint Research in China: 2003–2018. *Sustainability*, *11*(18), 5082. https://doi.org/10.3390/su11185082

Streszczenie

Wpływ oczyszczalni ścieków na redukcję zanieczyszczeń odprowadzanych w czeskiej części dorzecza Odry. Zanieczyszczenie wód powierzchniowych w całym dorzeczu Odry jest postrzegane jako poważny problem, na który znacząco wpływa niewystarczający stopień oczyszczania ścieków w zlewniach cząstkowych w stosunku do dostępnych najnowocześniejszych technologii i celów środowiskowych dyrektywy 2000/60/WE. Do określenia wpływu przemysłowych i komunalnych oczyszczalni ścieków na redukcję odprowadzanych zanieczyszczeń w czeskiej części międzynarodowego dorzecza Odry wykorzystano metodę oceny szarego śladu wodnego. W czeskiej części dorzecza Odry przeanalizowano dane z 391 oczyszczalni ścieków w latach 2004––2018. Uzyskane wyniki pokazują, że oczyszczalnie ścieków zmniejszają nawet o 92% szary ślad wodny, tj. ilość wody potrzebnej do rozcieńczenia zanieczyszczeń odprowadzanych do odbiornika w czeskiej części dorzecza Odry.

Summary

Effect of wastewater treatment plants to the reduction of pollution discharged in the Czech part of the Odra river basin. Surface water pollution is referred to be a problem in the entire Odra river basin. In sub-basins, an insufficient degree of wastewater treatment has been identified as a major problem – in relation to the best available technologies and environmental objectives of Directive 2000/60/EC. The grey water footprint indicator was used to express the influence of point sources of pollution (industrial and municipal wastewater treatment plants) on discharged pollution reduction in the Czech part of the international Odra river basin. The number of 391 records of wastewater treatment plants for the period 2004––2018 was analysed. The results show that the wastewater treatment plants reduce by up to 92% the potential water needs for dilution of pollution discharged into waters in the Czech part of the Odra river basin.

Authors' address:
Libor Ansorge
(https://orcid.org/0000-0003-3963-8290)
Lada Stejskalová
(https://orcid.org/0000-0003-2271-7574)
Jiří Dlabal
(https://orcid.org/0000-0002-2401-2917)
Elžbieta Čejka
Výzkumný ústav vodohospodářský
T. G. Masaryka, v. v. i.
Podbabská 2582/30, 160 00 Praha 6, Česká republika
e-mail: libor.ansorge@vuv.cz
lada.stejskalova@vuv.cz
jiri.dlabal@vuv.cz
alzbieta.cejka@vuv.cz

Scientific Review – Engineering and Environmental Sciences (2020), 29 (2), 136–144
Sci. Rev. Eng. Env. Sci. (2020), 29 (2)
Przegląd Naukowy – Inżynieria i Kształtowanie Środowiska (2020), 29 (2), 136–144
Prz. Nauk. Inż. Kszt. Środ. (2020), 29 (2)
http://iks.pn.sggw.pl
DOI 10.22630/PNIKS.2020.29.2.12

Salam Hussein EWAID[1], Bassam F. Al-FARHANI[2], Salwan Ali ABED[3], Nadhir Al-ANSARI[4]

[1] Southern Technical University, Technical Institute of Shatra
[2,3] University of Al Qadisiyah, College of Science
[4] Luleå University of Technology, Department of Civil, Environmental and Natural Resources Engineering

Modeling of trihalomethane compounds formation in Baghdad water supply network

Key words: trihalomethane, Baghdad, Tigris river, modeling

Introduction

Chlorination is the prevalent cleansing technique in Iraq and elsewhere. Nevertheless, scientific studies showed that chlorine interacts with natural organic materials (NOM) in raw water and produce harmful disinfection by-product materials (DBPs) such as the four trihalomethanes (THMs), chloroform ($CHCl_3$), bromodichloromethane ($CHBrCl_2$), chlorodibromomethane ($CHBr_2Cl$), and bromoform ($CHBr_3$), which have carcinogenic adverse pregnancy outcomes (Rook, 1974; Nikolaou & Lekkas, 2001).

Trihalomethanes formation varies depending on the properties of NOM in source water and increases by increasing bromide concentration, chlorine dose, contact time, temperature, and pH (Singer et al., 2002; Nikolaou, Golfinopoulos, Arhonditsis, Kolovoyiannis & Lekkas, 2004; Baribeau et al., 2006).

Tigris river only is the source of drinking water in Baghdad and other areas of Iraq. There are more than ten water-treated plants (WTPs) in Baghdad of all production ability is 2.5 million m^3 in a day. Each WTP utilizes chlorine to disinfect drinking water to keep a specific stage of remaining chlorine to prevent bacterial growth (Ewaid, Rabee & Al Naseri, 2018).

Many reviews recommended that the concentrations of THMs change seasonally, during warm months of year natural materials substances of surface water rises because of the quick rot of plant and draining through the rain in a water source, the rising in temperature and organic materials, as well as chlorine, leads to higher THMs formation (Rodriguez & Serodes, 2005; Chowdhury, Champagne & McLellan, 2009).

The seasonal variation of THMs concentrations was monitored during the distribution system of WTP in Istanbul according to a 30-week program of intensive sampling, highest THM stages stated in summer (117 $\mu g \cdot l^{-1}$), and lowest in spring (75 $\mu g \cdot l^{-1}$) (Toroz & Uyak, 2005).

Research in the Somas river basin in Romania approved that THMs concentration in four WTPs and distribution systems were below 100 $\mu g \cdot l^{-1}$ (Ristoiu et al., 2009).

The existence of THM in samples of tap water from 19 districts of Baghdad in summer was studied; the mean concentration of THM in summer was 81 $\mu g \cdot l^{-1}$ (Barbooti et al., 2010).

Numerous mathematical models for the prediction of THMs formation suggested previously in the literature that might be ordered in two fundamental sorts: models designed according to empirical relationships and models designed according to the kinetics participated in chlorine interactions (Di Cristo, Esposito & Leopardi, 2012).

Literature had been reviewed from 1974 to 2009 and found that more than 120 models for the prediction of DBPs fate published. Many variables are influencing the development of DBPs; these factors include disinfectant type, temperature, pH, NOM as total organic carbon (TOC), and others (Chowdhury, 2009).

Erispaha (2011) studied 40 prediction models and found that the prevailing variables faced in THM formation are TOC concentration, chlorine dose, temperature, pH, time, and bromide concentration.

There is little information about the concentrations of THMs and the relation with raw water properties in the drinking water of Baghdad. In addition, the seasonal diversity of THMs concentration is not well known. The aims of this research are to evaluate the seasonal diversity of THMs in raw and drinking water, to discover its relationship with many environmental parameters and to improve a mathematical predictive model that offers a simple means that may be readily used in the distribution system to assess the risk of THMs formation through expecting concentrations.

Material and methods

The city of Baghdad depends on the treatment of crude water from the Tigris river for drinkable water. In this research, the water tested took from seven WTPs using the conventional purification method; they are East Tigris, Wathba, Karama, Qadysia, Dura, Wahda, and Rasheed water treatment plant (Fig. 1). Samples as well as gathered from residential areas near to all plants.

Baghdad city has 7.5 million inhabitants (Burnham, Lafta, Doocy & Roberts, 2006), the city has 464 resident districts and its area is about 1,000 km^2. The styling abilities of the WTPs in Baghdad are 3,120,000 m^3 daily and the real production is 2,504,000 m^3 daily (CSO, 2013).

FIGURE 1. The study area in Baghdad

Sampling and water quality parameters measurement

Five samples from every plant took monthly from January 2017 to October 2017. The first sample was raw water from the river to define TOC and THM concentrations. The second sample was from treated water in the plant, the third, fourth, and fifth samples were taken immediately from used taps of neighborhoods at different distances from the plant.

The number of the gathered samples from the seven WTPs was 350 samples for the THM analyses and 70 samples for the TOC during 10 months of the study. Water samples were collected in 250 ml glass bottles fully full to obviate air bubbles and wastage of THM. Each bottle washed and cleaned in distilled and deionized water based on the standard procedure 1710B (APHA, 2012), each sample gathered in glass bottles closed in TFE-screw lined caps and put it in a cooler box, stocked at 4°C and analyzed during 2–3 h. Water temperature (Temp.) [°C], pH, and electrical conductivity (EC) [$\mu S \cdot cm^{-1}$] were determined *in situ* by a multi-meter model WTW Multi 340i. Turbidity (Tur.) [NTU] was measured *in situ* utilizing the portable turbidity meter model WTW TURB 355 IR/T. The residual chlorine (R. Cl_2) [$mg \cdot l^{-1}$] was measured *in situ* using Hach Pocket Colorimeter II.

The measurements of water parameters were by the $mg \cdot l^{-1}$ unit; alkalinity (Alk.), total solids (TS), and chlorine dose (Cl_2 dose) were obtained from the plant's administrations and laboratories.

Trihalomethane was measured utilizing gas chromatography model (DANI GC 1000, Dani Instrument SPA, Italy) with an electron capture detector (GC-ECD) according to standard method 6232B (APHA, 2012). TOC measured following the standard method 5310C (APHA, 2012) utilizing (multi N/C 3100 TOC analyzer, Analyticjena, Italy).

Modeling of THM formation

A log-linear multiple regression analyses utilized to develop a mathematical model which shows THMs concentration as the dependent variable with respect to other water quality parameters as independent variables utilizing field study measurements of areas close to seven WTPs by the Statistical Package of Social Scientists (SPSS) program (IBM Corporation, 2012).

The regression coefficient in predictive models is generally evaluated through log-transforming variables to have naturally distributed (Stow, Reckhow & Qian, 2006).

Results and discussion

To evaluate the relationship between the THMs formation with some water quality parameters, these parameters were measured in water samples from the seven 7WTPs, average values of all parameter: temperature (21.2°C), pH (7.96), total organic carbon (2.93 $mg \cdot l^{-1}$), alkalinity (148.3 $mg \cdot l^{-1}$), turbidity (212.9 NTU), total solids (604.6 $mg \cdot l^{-1}$) and electric conductivity (863 $\mu Sm \cdot cm^{-1}$) in raw water whereas residual chlorine (0.85 $mg \cdot l^{-1}$) and chlorine dose of (3.15 $mg \cdot l^{-1}$) in treated drinking water of seven WTPs. Concentrations of total trihalomethanes (TTHM) were measured in samples of raw water at the intake of each plant, treated water produced in the plants and from taps of consumers from the residential districts near those seven plants for 10 months between January and October 2014, the seasonal variations in TTHM concentrations is illustrated in Table 1.

There is a clear graduated increase within the annual average concentration of THM in raw, treated, and tap water. Seasonal diversity in river water quality is closed to alteration in climatic parameters such as temperature and rainfall. In warm months, natural organic materials content rising due to the quick dissolution of plants. Rains raise the content of the organic material through the filtering of natural materials into watersheds (Abdel Halim, 2013). This study found that there are concentrations of THMs in raw surface water and that might be because of naturally high levels of bromide ion in the Tigris river.

Pearson correlation coefficient (r) studied and utilized to measures correlation strength between all individual variables (independent factors) and THMs formation (dependent factor). The correlation matrix of tested variables parameters is presented in Table 2.

There was high significant positive correlation with chlorine dose ($sig.$ = = 0.00 < 0.02) and great relationship (r = = 0.82) THMs formation.

Adding chlorine to the water increases the formation of hypochlorous acid HOC1 and hypochlorite ion OC1, the formation of them relies on pH. The OCl is formed in alkaline medium and HOC1 dominates in acidic solutions

TABLE 1. Seasonal variations of TTHM among raw, treated, and tap water [$\mu g \cdot l^{-1}$]

WTP	River						
	East Tigris	Wathba	Karama	Qadysia	Dura	Wahda	Rasheed
Winter							
Raw water	3.5 ±2.1	4 ±1.4	4 ±1.4	4 ±2.8	5.5 ±0.7	9 ±1.4	6 ±0
Treated water	8.5 ±3.5	10.5 ±2.1	9.5 ±4.9	9.5 ±7.7	17 ±2.9	24 ±4.2	17.5 ±2
Tap water	12 ±5.6	14 ±3.5	15 ±4.2	13.5 ±10.6	22.5 ±2.1	33 ±5.6	23.5 ±2.1
Spring							
Raw water	10.3 ±5.5	12 ±7	31.3 ±33.5	12 ±2.6	9.3 ±4	14 ±1.5	13.6 ±3.2
Treated water	25.6 ±10.9	28.6 ±16.7	40 ±19.7	28.3 ±5.8	25 ±8.1	39.3 ±13	38 ±5.2
Tap water	36 ±16.3	40.6 ±23.7	33.3 ±15	40.3 ±8.3	24.3 ±12.2	53.3 ±18.5	51.6 ±8
Summer							
Raw water	25 ±3	28 ±6	28 ±2.6	22.6 ±4	25.6 ±8.9	30.3 ±2.5	23.6 ±2
Treated water	58 ±8.1	64.6 ±2	62.6 ±13	62.6 ±12.2	56.6 ±3.7	67 ±1.7	70.3 ±8.5
Tap water	83 ±11.1	89.6 ±4.7	90.6 ±15.6	86 ±16.5	79 ±16.3	97.3 ±4	94 ±6.9
Autumn							
Raw water	21.5 ±6.3	20.5 ±0.2	20.5 ±0.7	25 ±7	21.5 ±9.2	20 ±12.7	16.5 ±4.9
Treated water	53.5 ±7.7	54.5 ±0.1	51.5 ±16.2	51.5 ±17	50 ±18.3	53 ±32.5	61 ±24
Tap water	75 ±14.4	75 ±0.3	72 ±15.5	76.5 ±26.1	71.5 ±27.5	73 ±45.2	77.5 ±29

TABLE 2. The correlation matrix of the multiple regression analysis

×		THMs	TOC	pH	Temp.	Cl_2 dose	Alk.	Tur.	EC	TS	R. Cl_2
Pearson correlation	THMs	1									
	TOC	0.23	1								
	pH	–0.31	–0.29	1							
	Temp.	0.06	0.87	–0.24	1						
	Cl_2 dose	0.82	0.23	–0.35	0.04	1					
	Alk.	–0.29	–0.54	0.54	–0.44	–0.36	1				
	Tur.	–0.15	–0.85	0.25	–0.81	–0.09	0.47	1			
	EC	0.19	–0.09	–0.02	–0.37	0.31	–0.07	0.12	1		
	TS	–0.15	–0.05	0.11	–0.18	–0.01	–0.05	0.06	0.60	1	
	R. Cl_2	0.34	0.35	–0.3	0.35	0.52	–0.32	–0.20	–0.04	–0.2	1
p	THMs		0.02	0.00	0.30	0.00	0.00	0.10	0.04	0.10	0.0

(Uyak, Toroz & Meric, 2005). Generally, the THMs content increase with the ascent in water pH. In Tigris raw water, pH ranged from 7.72 to 8.25, OCI is the dominant chlorinated types, therefore, in charge of THMs formation. The release of THMs expands a comparable sum from OCI and the residual chlorine would diminish (Ye, Wang, Yang, Wei & Xueli, 2009).

Total organic carbon approved a significant correlation with the THMs formation (*sig.* = 0.02) and (r = 0.237), which is the expected situation since organic materials are the main precursor material for THM formation. It found that rising in both of content of soluble humic materials in natural water and rate of THMs formation similar to TOC consumption (Uyak et al., 2005).

Seasonal diversity in measure of NOM in crude water has been represented that it might play an essential part in the THMs formation (Chowdhury, Rodriquez & Serodes, 2010). As well as, the relative contribution of TOC to THMs product caused by hydrophilic NOM fraction than hydrophobic NOM fraction where hydrophilic NOM fraction interacts more easily with chlorine (Abdullah, Yew & Romli, 2003). Temperature shows non-significant positive correlation with THMs (r = 0.063, *sig.* = = 0.303) in all the WTPs. This may be explicated through the slow expansion in the rate of interaction between NOM and chlorine through expanding temperature. The expanded measure of THMs level through the expanding in temperature observed to be in the range of 25–50% (Ye et al., 2009).

On the contrary, the pH level in raw water proved a great negative linear correlation (r = –0.311, *sig.* = 0.004) with THM formation, that sudden state where THM forming is a base-catalyzed reaction, which may be foreseeable to reduce of pH in treatment water than raw. Many researchers stated a linear relation between THMs formation and pH water value (Uyak et al., 2005).

The THMs formation with the other tested parameters shows: Significant positive linear correlation with residual chlorine (*sig.* = 0.00, r = 0.343) and electrical conductivity (*sig.* = 0.049, r = = 0.199). Significant negative linear correlation with alkalinity (*sig.* = 0.007, r = –0.294) and non-significant negative linear correlation with turbidity (*sig.* = = 0.101, r = –0.154) and total solids (*sig.* = = 0.106, r = –0.151).

The reasons for the inconsistent situations with the expected relationships of THM with water parameters might be expected to the covariation in operational parameters or associated with the interaction among those parameters.

The obtained data from the monthly water parameters measurement of Tigris river raw water and the Baghdad water supply network were used to create a mathematical model to represent the concentrations of TTHM in the water supply network.

Statistical analysis of multiple regression was applied to develop this model which is a transformed power equation derived from multiple linear regression, parameters are converted to logarithm values (Sohn, Gate & Amy, 2001). The following data were obtained for 70 samples (N): correlation coefficient (R) equal 0.835, coefficient of determination (R^2) – 0.727, adjusted coefficient of determination (*adj.* R^2) – 0.686 and standard error (SE) – 0.38942.

The predictive mathematical model for statistical regression analysis may be explained as follow: TTHM equal 6.296, $(TOC)^{0.137}$, $(Temp.)^{-0.296}$, $(Tur.)^{-0.09}$, $(Alk.)^{0.126}$, $(pH)^{-0.214}$, $(EC)^{0.052}$, $(TS)^{-0.723}$, $(Cl_2\ dose)^{2.427}$, $(R.\ Cl_2)^{-0.246}$. Where THMs in $\mu g \cdot l^{-1}$, time in min, residual Cl_2 in $mg \cdot l^{-1}$, temperature in °C, TOC in $mg \cdot l^{-1}$, turbidity in NTU, alkalinity in $mg \cdot l^{-1}$, total solids in $mg \cdot l^{-1}$, electrical conductivity in $\mu Sm \cdot cm^{-1}$ and chlorine dose in $mg \cdot l^{-1}$.

The previous mathematical model can be simplified by using backward stepwise log-linear multiple regression analysis, which excludes the non-influential variables.

The results illustrated that the most important parameters are TOC, temperature, turbidity, total solids, chlorine dose. The following data were obtained for 70 samples (N): correlation coefficient (R) equal 0.842, coefficient of determination (R^2) – 0.709, adjusted coefficient of determination ($adj.\ R^2$) – 0.686 and standard error (SE) – 0.3894.

The mathematical equation for this correlation can be expressed as follows (R = 0.846): TTHM equal 7.533, $(TOC)^{0.119}$, $(Temp.)^{-0.553}$, $(Tur.)^{-0.130}$, $(TS)^{-0.625}$, $(Cl_2\ dose)^{2.169}$.

The calculated THMs concentrations for backward multiple regression analysis modes versus observed ones are presented in Figure 2.

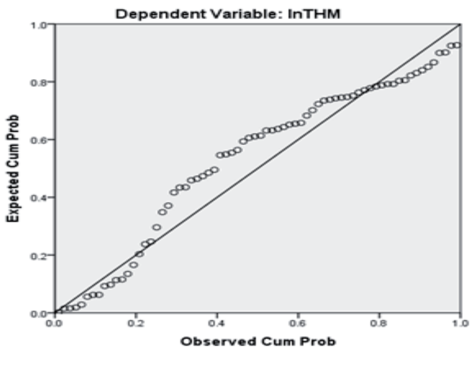

FIGURE 2. Comparison of observed and predictive THMs concentration

Conclusions

This research was directed to assess the relationship between water quality and THM formation coming about because of water chlorination at the Baghdad water supply network. Statistical regression analysis utilizing a gradual backward technique was utilized to build up a mathematical model for THM formation using field water samples. Correlation and regression analyses for study relation between independent variables and THM formation demonstrated guarantee and connection seemed, by all accounts, to be great. THM formation model could be valuable with the end goal of drinking water quality administration and operational administration of the treatment plant.

Likewise, the model may be utilized as a guideline in picking suitable procedures to decrease THM and chlorine utilization to enhance the disinfection procedure.

References

Abdel Halim, N.H. (2013). *The fate of natural organic matter and formation of disinfection byproducts in a conventional water treatment plant* (master's thesis, American University in Cairo, Cairo, Egypt).

Abdullah, M., Yew, C., & Ramli, M. (2003). Formation, modeling, and validation of THMs in Malaysian drinking water: a case study in the districts of Tampin, Negeri Sembilan and Sabak Bernam, Selangor, Malaysia. *Water Resources*, *37*(19), 4637-4644.

American Public Health Association [APHA] (2012). *Standard methods for the examination of water and wastewater*. Washington: APHA.

Barbooti, M., Bolzoni, G., Mirza, I., Pelosi, M., Barilli, L., Kadhum, R. & Peterlongo, G.

(2010). Evaluation of quality of drinking water from Baghdad, Iraq. *Science World Journal*, *5*(2), 35-46.

Baribeau, H., Boulos, L., Haileselassie, H., Crozes, G., Singer, P.C., Nichols, C., Schlesinger, S.A., Gullick, R.W., Williams, S.L., Williams, R.L., Fountleroy, L., Andrews, S.A. & Moffat, E. (2006). *Formation and decay of DBP in the distribution system*. Denver, CO: AWWA and IWA Publishing.

Burnham, G., Lafta, R., Doocy, S. & Roberts, L. (2006). Mortality after the invasion of Iraq: a cross-sectional cluster sample survey. *Lancet*, *368*, 1421-1428.

Chowdhury, S. (2009). *Modeling trihalomethane formation in drinking water with application to risk-based decision-making* (PhD thesis, Queen's University, Kingston, Canada).

Chowdhury, S., Champagne, P. & McLellan, P.J. (2009). Models for predicting disinfection byproduct (DBP) formation in drinking waters: a chronological review. *Science of the Total Environment*, *407*(14), 4189-4206.

Chowdhury, S., Rodriguez, M.J. & Serodes, J. (2010). Model development for predicting changes in DBP exposure concentrations during indoor handling of tap water. *Science of the Total Environment*, *408*(20), 4733-4743.

Central Statistical Organization [CSO] (2013). *Iraq environmental statistics report for the year 2012*. Baghdad: The Central Statistical Organization, Ministry of Planning.

Di Cristo, C., Esposito, G. & Leopardi, A. (2013). Modeling trihalomethanes formation in water supply systems. *Environmental Technology*, *34*(1-4), 61-70.

Ewaid, S.H., Rabee, A.M. & Al-Naseri, S.K. (2018). Carcinogenic risk assessment of trihalomethanes in major drinking water sources of Baghdad City. *Water Resources*, *45*(5), 803-812.

Erispaha, A. (2011). *Modeling of trihalomethane formation based on the consensus of existing empirical models* (master's thesis, Drexel University, Philadelphia, PA, USA).

IBM Corporation (2012). *SPSS Statistics for Windows. Version 21.0*. Armonk, NY: IBM Corp.

Nikolaou, A.D., Golfinopoulos, S.K., Arhonditsis, G.B., Kolovoyiannis, V. & Lekkas, T.D. (2004). Modeling the formation of chlorination by-products in river waters with different quality. *Chemosphere*, *55*, 409-420.

Nikolaou, A.D. & Lekkas, T.D. (2001). The role of natural organic matter during the formation of chlorination by-products: a review. *Acta Hydrochimica et Hydrobiologica*, *29*(2--3), 63-77.

Ristoiu, D., Gunten, U. von, Mocan, A., Chira, R., Siegfried, B., Kovacs, M. & Vancea, S. (2009). Trihalomethane formation during water disinfection in four water supplies in the Somes river basin in Romania. *Environmental Science and Pollution Research*, *16*(1), 55-65.

Rodriguez, M.J. & Serodes, J.B. (2005). Laboratory-scale chlorination to estimate the levels of halogenated DBPs in full-scale distribution systems. *Environmental Monitoring and Assessment*, *110*(1-3), 323-340.

Rook, J.J. (1974). Formation of haloforms during chlorination of natural waters. *Water Treatment Examination*, *23*, 234-243.

Singer, P.C., Weinberg, H.S., Brophy, K., Liang, L., Roberts, M. Grisstede, I., Krasner, S., Baribeau, H., Arora, H. & Najm, I. (2002). *Relative dominance of HAAs and THMs in treated drinking water.* Denver, CO: AWWA.

Sohn, J., Gate, D. & Amy, G. (2001). Monitoring and modeling of disinfection by-products (DBPs). *Environmental Monitoring and Assessment*, *70*(1-2), 211-222.

Stow, C.A., Reckhow, K.H. & Qian, S.S. (2006). A Bayesian approach to 362 retransformation bias in transformed regression. *Ecology*, *87*(6), 1472-1477.

Toroz, I. & Uyak, V. (2005). Seasonal variations of THMs in water distribution networks of Istanbul city. *Desalination*, *176*(1-3), 127--141.

Uyak, V., Toroz, I. & Meric, S. (2005). Monitoring and modeling of THMs for a water treatment plant in Istanbul. *Desalination*, *176*(1-3), 91-101.

Ye, B., Wang, W., Yang, L., Wei, J. & Xueli, E. (2009). Factors influencing disinfection by--products formation in drinking water of six cities in China. *Journal of Hazardous Materials*, *171*(1-3), 147-152.

Summary

Modeling of trihalomethane compounds formation in Baghdad water supply network. This study was conducted to measure the concentrations of four trihalomethane compounds (THMs) in raw, treated, and drinking water of seven water purification plants and the residential neighborhoods nearby in Baghdad. About 350 samples gathered between January and October 2017 and analyzed by the gas chromatography method. Results showed that THM annual levels in tap water ranged between 12 and 97.3 $\mu g \cdot l^{-1}$ in winter and summer consecutively, with a mean concentration of 60 $\mu g \cdot l^{-1}$, these concentrations did not exceed the level recommended by the WHO and the Iraqi standards. Statistical modeling by SPSS software for the formation of THM (the dependent factor) in the water supply network was undertaken using the measured water quality parameters (as independent factors) and utilizing multiple regression analysis. The model obtained has a high correlation (r = 0.842) and approved that the most affecting parameters on THM formation are total organic carbon, temperature, turbidity, total solids, and chlorine dose. The model that was derived may be used for the purposes of choosing appropriate THM-reduction procedures and the use of chlorine for improving the method of disinfection.

Authors' address:
Salwan Ali Abed
(https://orcid.org/0000-0001-7347-3843)
University of Al Qadisiyah
College of Science
P.O. Box 1895 Diwaniyah, Iraq
e-mail: Salwan.abed@qu.edu.iq

Scientific Review – Engineering and Environmental Sciences (2020), 29 (2), 145–154
Sci. Rev. Eng. Env. Sci. (2020), 29 (2)
Przegląd Naukowy – Inżynieria i Kształtowanie Środowiska (2020), 29 (2), 145–154
Prz. Nauk. Inż. Kszt. Środ. (2020), 29 (2)
http://iks.pn.sggw.pl
DOI 10.22630/PNIKS.2020.29.2.13

Nassrin Jassim Hussien Al-MANSORI, Thair Jabbar Mizhir Al-FATLAWI, Nariman Yahya OTHMAN
University of Babylon, Faculty of Engineering

Stochastic analysis for prediction of future performance of Mosul storage

Key words: reservoir system, simulation, hydropower generation, reliability

Introduction

Building a simulation model for a water storage system is vital to check the performance depending on the observed and received flows to the system. Modelling is also crucial in seeing the extent of dependence on the expected future performance of the system under average conditions. It is known that the observed and received flows that enter the units of a storage system represent only a limited part of the spectrum of data expected to occur in the future. A recent critical effort has created vigorous speculations and models for the portrayal of these flows over an assortment of execution stages. While these models are essential to empower repeatability, they do not use the captured data to its maximum capacity (Woodman, Hiden & Watson, 2017).

Accordingly, analysis requires the use of a particular type of exploratory model to prepare a hypothetical streaming flow line (stochastic models) to include the minimum of the spectrum of the fluctuating flow. The default outline will enable a system operator to study the reaction of the system in different scenarios for the expected inventory. It is necessary to consider that the hypothetical chains resulting from the developmental methods must maintain at least the statistical parameters of the first three heads of the desired stream, namely the rate, standard deviation and correlation coefficient between the two data parameters consecutively and vice versa. However, this type of stochastic model is hardly satisfactory and does not depend on the flowing energy produced (Abdel-Hameed, 2003).

Karapetyan and Mamikonyan (2005) expressed the strategy and consequences of dynamic parameter estimation for seismic soundness assurance in the working

Geghardalich water stockpiling dam in the Republic of Armenia. By trial hypothetical techniques, the epures of expected maximal horizontal accelerations (EMHA) were built on dam area height in its various profiles. The article's fundamental guidelines can be utilized in the observation of other hydropower developments and nuclear power plants.

A study by Heuts and Anderson (1976) discussed time series analysis in general and for overall forecasting, focussing on the Box–Jenkins method. The method features an autoregressive integrated moving average (ARIMA) and the rate autoregression (AR), which includes self-correlation and a moving average (MA). Anderson found that ARIMA can express well some hydrological activities, including the flow of water in a river, which is the subject of interest in the current research.

Howlett, Piantadosi and Pearce (2005) considered the administration of water stockpiling in two associated dams. The main dam is intended to catch storm water created by precipitation. Water is siphoned from the main dam to the subsequent dam and is in this manner provided to clients. There is no immediate admission of tempest water to the subsequent dam. We accept the irregular timings of precipitation as a known probability distribution and wish to discover functional siphoning arrangements from the catch dam to the inventory dam to limit flooding.

Pereira, Oliveira, Costa and Kelman (1984) developed a model for generating monthly flows for a hydroelectric generation system in Brazil, which is produced from a group of large reservoirs that have a high storage capacity. Kim and Heo (1997) studied the monthly operating rules for a water storage system located on the Han river in South Korea, which includes three main reservoirs that play an important role in preventing floods. The authors' research was referenced for this work to study the autoregressive moving average model – ARMA (1,1), data to generate monthly flow. Naggar (1999) used the Thomas–Fiering and ARMA (1,1) models to generate monthly flows for a time series covering about 700 years for five rivers in Iraq (Dajla, Al-Azb Al-Kabeer, Al-Azib Al-Sagheer, Al-Azim and Diyala). Naggar (1999) then used these data to simulate growth for the operating systems of the Euphrates and Tigris rivers.

Al-Mamosi (2007) used the Thomas–Fiering and ARIMA models to generate the flow for the two stations of Asakkalak and Mankoba on the Al-Azb, Al-Aalaa and the Khazir rivers, respectively, as examples of permanent flowing rivers. The author examined the al--Matheeq station on the Al-Azim river as an example of a seasonal river. There are many attempts that have been done for generating discharge data. These works, however, have not focussed on details indicating that the generating chains are descended from the statistical community itself as a product of the system. That is, the data for the observed chains was used in the generation of the data, which is why these generations do not refer to these parameters. The model must conform to the observed parameters of the chains if researchers want to rely on the outputs of these generation models.

In addition, this study confirms the relative conformity of the statistical features that have been calculated with the generated flow data. The results conform with their counterparts returning to the observed flow data, ensuring the model is appropriate and reliable in generating new flow data.

Bormann and Martinez (2014) investigated important attributes and distinguished appropriate markers to be used to appraise the appropriateness of existing dams and supplies for introducing an extra siphoned vitality stockpiling framework. The indicators incorporate physical and natural attributes. An impact investigation and a conflict examination for previously existing water employments for single or multipurpose dams altered the analysis. In light of the markers discovered as well as possible conflicts, an indicator-based system was created. The framework described a procedure to examine the appropriateness of existing dams for vitality stockpiling, measuring the physical possibilities of a site, considering the ecological limitations and establishing requirements regarding compromises among competing water employments.

Bormann, Ahlhorn and Klenke (2012) conducted a participatory investigation of network methods to handle provincial adjustments to environmental changes. Options for adapting water management in response to regional changes of climate were developed. Partners representing the Wesermarsch County in northern Germany participated in the study, which developed plans looking to 2050. Data on expected local environmental changes and a study modelling hydrological changes indicated that the adjustment of water management would be necessary until 2050. A provincial stakeholder discussion defined a vision of how the Wesermarsch should appear in 2050. Both regional partners and researchers took a dynamic part in the participatory learning process as required by European Union (EU) mandates.

Buenoa and Carta (2006) proposed the establishment on Gran Canaria island (Canarian Archipelago) of a suitably managed, wind-powered, siphoned hydro capacity framework. The findings from the use of an optimal financial model for such a framework demonstrated that influx of renewable energy could be expanded by 1.93% (52.55 GWh·year^{-1}) at a reasonable expense for the unit vitality provided. These outcomes assumed the use of the two most expansive reservoirs on the island (with a height difference of 281 m and a limit of around 5 million m^3 each) as capacity stores.

Anagnostopoulos and Papantonis (2008) presented a quantitative methodology for the ideal sizing of different segments of a reversible hydraulic system intended to recoup electric power from wind farms that have been dismissed because of limits to the power grid. The method was applied to formulate a functional case utilizing time-variance information of the dismissed force from various wind farms on the island of Crete, Greece. The outcomes indicated that an all-around upgraded configuration might be essential for the technical and financial suitability of the inspected framework.

Ding, Hu and Song (2012) proposed another coordination activity method for a wind farm (WF) and pumped-hydro storage plant (PHSP) in view of day-ahead wind power yield estimates. A deterministic, mixed-integer programming (MIP) definition was fabricated considering the imperatives of unit absolute start-up and shutdown frequencies, and also unit state rejection among generating and pumping. Moreover, the paper describes the chance--limited and situation-based streamlining formulations to manage errors in projected wind power. Sensitivity analyses and case studies showed that the coordination of WF and PHSP could ease the negative impact of wind power changes on the power network while raising profits.

This study was carried out on the Mosul reservoir to exploring the capability of the future system to generate hydroelectric power using a simulation by Simulink technique on the MATLAB platform.

Material and methods

Study area

The Mosul dam reservoir is located on the northern Tigris river, about 50 km from Mosul city. The area of the feeding basin in the upstream of the reservoir is 50,200 km^2, and the design of the dam is six units for generating hydroelectric power with a maximum capacity of 1,536 MW (Al-Gazzal, 2002). The reservoir can be considered as multipurpose, including developing the tourism sector in Iraq, generating hydropower, controlling floods, and feeding an irrigation area of about 2.26 million acres.

Model simulation

A model was built to simulate the northern storage system (Fig. 1), provided by Simulink software and using various simulation techniques on MATLAB systems. The technology is represented by a set of ready-made templates (icons). These templates are logically linked so that the model represents the system to be studied realistically. Note this technology is new in the application of water resources in general and the operation of storage systems in particular (Al-Mohsen, 2008). The model can take advantage of the capabilities of Simulink, which are mainly based on high-quality MATLAB software that focuses on processing mathematical vectors and matrices in a highly efficient manner.

To know more about the operation of this technology, one can refer to an attached Simulink library (MATLAB, 2004). The current research focuses on the topic of future performance of the system for hydroelectric generation, and not on the simulation model used to evaluate this performance for the purpose of identifying the details of a problem (Al--Ageli, 2009).

The simulation model has been in operation for a period of 30 months, from June 2015 to July 2018, representing the period for the actual operation of the Mosul reservoir (depending on operational data). To verify its results with the observed data, the simulation process was done as follows: operating the Mosul reservoir, depending on the observed data (incoming flow and the volume of releases from the reservoir), adding the water produced from the runoff surface from the bottom of the reservoir to the Al-Fattah region by adopting the one--way method that depends on unit runoff output (Kottagoda, 1980).

After the above operation and calibration process, the generation of monthly flow chains to the unit of the system was performed.

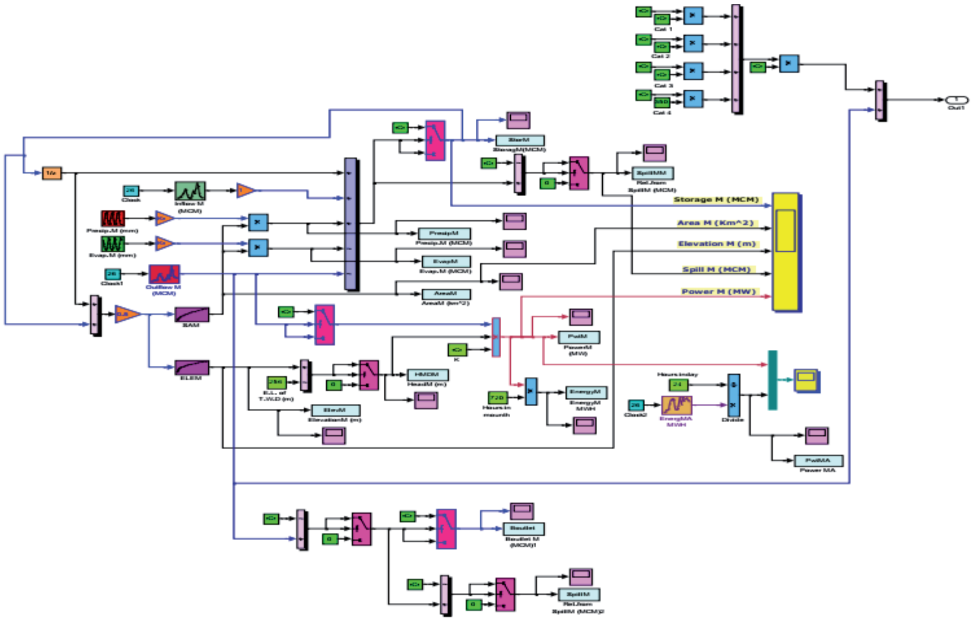

FIGURE 1. The storage system units using the technology (Simulink)

Stochastic model

Kottagoda (1980) declared many stochastic models, such as Markov, ARMA and ARIMA of different ranks. However, the difficulty in adopting and selecting any of these models lies in understanding the effectiveness of the product, that is, the time series to be modelled. The ARMA model is valid for a stationary time series model (non-change of the statistical parameters of effectiveness with time), whereas ARIMA models are successful in the non-stationary time series (changing the statistical parameters of effectiveness with time).

The Thomas–Fiering model has proven its high potential as a model for the monthly time flows for many rivers (Thomas & Feiring, 1962). The Thomas–Fiering model is considered one of the images of the Markov model from the first rank. Clarke (1984) has recommended using this method when modelling the time series in river flow and generating it when the model is in the middle of the month. Accordingly, the Thomas–Fiering model was chosen in this research to generate time series for the monthly flow coming into the units of the Mosul storage system, where Equation (1) shows the mathematical formula for this model.

$$Q_{i+1} = \bar{Q}_{j+1} + b_j(Q_i - \bar{Q}_j) + t_i \sigma_{j+1}(1 - r_j^2)^{0.5} \tag{1}$$

where:
Q_{i+1} – flow in month $i+1$,
$\bar{Q}_{j+1}$ – average of flow in month $j+1$,
b_j – gradient of line between the flow in month $j+1$ and the flow in month j,
Q_i – flow in month i,
$\bar{Q}_j$ – average of flows in month j,
t_i – normal random function,

σ_{j+1} – standard deviation for flows in month $j + 1$,
r_j^2 – correlation coefficient between flows of months j and $j + 1$.

Also, note that most (if not all) stochastic models used to generate flows are based on the hypothesis that observed flows used to build the model are subject to a normal distribution. Thus, this condition must be verified and guaranteed before initiating steps to build a reproductive model. If a normal distribution is not the case, resorting to the method of transformation as prepared by Box–Cox (see Eq. 2) is considered an approved method for converting the monitored flows into a distribution (Clarke, 1984). This transformation is used here and given by the following equation:

$$Y_t = \frac{(X_t^\lambda - 1)}{\lambda} \tag{2}$$

where:
Y_t – monthly flow after transforming to a normal distribution,
X_t^2 – observed monthly flow,
$\lambda - 1 \leq \lambda \leq 1$.

Observed and registered flows are available for each of the Tigris river at the Mosul station and the metering station in Askye-Klak on the top Al-Zab and the Mankoba station on the lower Zab for a period of 816 months from June 1931 to September 1999. A set of flow chains has been generated and is statistically compared with the chains monitored for the extent of knowledge of the validity of the approved model in generating monthly flow expenses.

Application of the Thomas–Fiering model

Depending on the values resulting from the transformation process and subject to the normal distribution, the SPSS program was used to calculate the statistical parameters used in the Thomas–Fiering model, which was formulated in Equation (1). This model includes both the mean and standard deviation for each month separately, and the correlation coefficient and regression coefficient between every two consecutive months. Simulink techniques were used for representing the Thomas–Fiering model de-

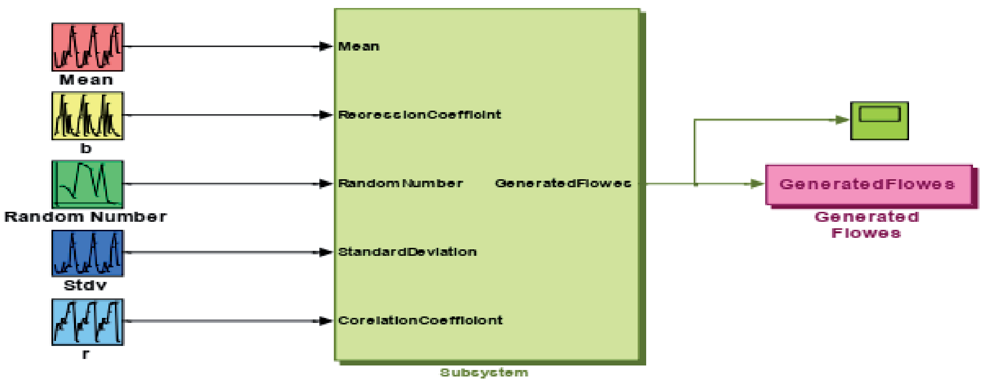

FIGURE 2. The general plan for the Thomas–Fiering model using Simulink

pending on the statistical data calculated to generate ten strings along the same observed string, which is 816 months. Figure 2 shows the general plan for the Thomas–Fiering model using Simulink.

Results and discussion

Testing the suitability of the proposed model

For testing the suitability of the proposed model and its fit in the generation of monthly flow strings, the SPSS.10 program was used to calculate the four main statistical parameters. The first was for the observed flow (average, standard deviation, the correlation coefficient between two consecutive months and the skewness coefficient). The same statistical parameters were then used for the ten generating chains. Table 1 lists the results obtained and compares the statistical parameters of the observatory and generator stream and the measuring station of the conductor discharge for clarification.

Based on these results, the model was deemed appropriate and could be to be reliable in generating monthly expenses for the flow.

Evaluating the performance of the system using the observed flows and generated chains

A simulation model of the storage system was used. At this stage, the reservoirs were operated virtually during a period of 84 years from October 1931 to September 2015. The simulation goal

TABLE 1. Statistical parameters of the observatory from 1931–2015 and the generator stream and Mosul measuring station

Month	R_1^2	R_2^2	SC_1	SC_2	ST_1	ST_2	AV_1	AV_2
Oct.	0.363	0.344	2.3379	1.3545	226.22	983.38	481.84	493 380
Nov	0.432	0.592	2.8357	2.6121	411.03	455.33	727.13	770 379
Dec.	0.412	0.636	2.7638	2.3848	794.95	803.37	1 152.59	933 68
June	0.677	0.585	1.7181	1.5779	875.96	887.37	1 464.26	1 440.34
Feb.	0.556	0.5	1.0486	0.8939	848.67	843.33	1 873.19	1 851.33
March	0.586	0.595	1.6432	1.6001	1489.44	3 793.86	3 146.29	3 159.31
April	0.808	0.771	0.8721	0.9183	1738.72	7 883.13	4 507.54	4 499.38
May	0.910	0.909	1.0220	1.0145	1834.65	8 533.71	4 072.24	4 173.38
June	0.951	0.951	0.7860	0.9374	721.77	734.31	1 754.59	1 756.39
July	0.926	0.926	0.6121	0.7296	278.26	886.30	772.47	770.31
Aug.	0.960	0.957	0.6792	0.5279	141.78	403.41	447.25	445.30
Sep.	0.081	0.173	0.8131	0.5418	104.34	103.51	362.66	361.39

R_1^2 – correlation coefficient between generated flow and the flow of next month; R_2^2 – correlation coefficient between observed flow and the flow of next month; SC_1 – skewness coefficient for generated flows; SC_2 – skewness coefficient for observed flows; ST_1 – standard deviation for generated flows; ST_2 – standard deviation for observed flows; AV_1 – average for generated flows; AV_2 – average for observed flows.

was to identify the capacity generated from the reservoir using the observed flow and the generated flow chains. The simulation model was run eleven times. In the first stage, the model was run using the observed incoming and outgoing flows to the Mosul reservoir. In the second phase, the form was run ten times using chains that were generated consecutively. Since the reservoir operates by default during this period, a volume has been determined that releases from the reservoir dependent on regularly providing the volume of monthly water requirements and ensuring the production of the highest possible hydropower.

By operating the simulation model in the manner described above, the average capacity generated per month for the observed flow was calculated. The chains as well as the average annual energy generated from the reservoir are shown in Table 2.

Depending on the results obtained, the generated chains have succeeded in efficiently generating the expected hydroelectric power from the system. The theoretical potential for generating hydroelectric power of the conductor reservoir is 2.4 × 106 MW·h^{-1} for one year. This figure was derived by observing the generation quantities calculated, either from the observed expenditures or the generated chains. Therefore, half of the capacity of the basin in hydroelectric generation can be obtained. It is well known that Iraq's need for electrical capacity as a whole is within the limits of (12,000 MW). This system can cover 1,500 MW, meaning it can meet about 12% of the country's electricity needs.

TABLE 2. Average annual energy from Mosul reservoir using observed flows from 1931–2015

Specification	Flow [MW·h^{-1}]
Observed	2 370 588
1st generation chain	2 308 676
2nd generation chain	2 312 353
3rd generation chain	2 280 735
4th generation chain	2 501 470
5th generation chain	2 388 529
6th generation chain	2 375 147
7th generation chain	2 386 323
8th generation chain	2 328 970
9th generation chain	2 363 382
10th generation chain	2 330 147
Average of all	2 357 573

Conclusions

1. Simulink technologies provided by MATLAB software are considered modern technologies, successfully used in many different engineering fields. The model performed well in simulating the water storage system as well as in building the Thomas–Fiering Model for generating expected flow data.
2. Findings revealed that the flow lines generated using the Thomas–Fiering model maintained major statistical parameters of the observed data used in the generation, and thus can be relied upon in extrapolating future performance of the storage system for generating hydroelectric power.
3. At 1.5 GW, the storage system of the Mosul reservoir covers a significant percentage of the overall electricity supply in Iraq, particularly at the present time.

References

Abdel-Hameed, M. (2003). Optimal control of dams using $P\lambda,\tau M$ policies and penalty cost. *Mathematical and Computer Modeling*, *38*(11-13), 1119-1123. https://doi.org/10.1016/s0895-7177(03)90112-9

Al-Ageli, Y.H. (2009). A *simulation model for a storage system on the river Dijma* (master's degree, Water Resources Division, Quantity of Engineering, University of Mosul, Mosul, Iraq).

Al-Gazzal, A.M.Y. (2002). *Optimal water utilization from Tigris basin reservoirs north of Fatha for hydroelectric power generation* (PhD thesis, University of Mosul, Mosul, Iraq).

Al-Mamousi, F. (2007). *Evaluation of some disease developmental outcomes in generating expenses for seasonal and permanent rivers* (master's thesis, University of Mosul, Mosul, Iraq).

Al-Mohseen, K.A. (2008). A Mathematical Model for Azizya Evaporating Pond Operation Using SIMULINK Techniques. Al-Rafidain Engineering Journal, 16(3) 14-24. https://doi.org/10.33899/rengj.2008.44692

Anagnostopoulos, J.S. & Papantonis, D.E. (2008). Simulation and size optimization of a pumped–storage power plant for the recovery of wind-farms rejected energy. *Renewable Energy*, *33*(7), 1685-1694. https://doi.org/10.1016/j.renene.2007.08.001

Bormann, H., Ahlhorn, F. & Klenke, T. (2012). Adaptation of water management to regional climate change in a coastal region – hydrological change vs. community perception and strategies. *Journal of Hydrology*, *454-455*, 64-75. https://doi.org/10.1016/j.jhydrol.2012.05.063

Bormann, H. & Martinez, I.M.A. (2014). Towards an indicator based framework analyzing the suitability of existing dams for energy storage. *Water Resource Management*, *28*(6), 1613-1630. https://doi.org/10.1007/s11269-014-0569-3

Buenoa, C. & Carta, J.A. (2006). Wind powered pumped hydro storage systems, a means of increasing the penetration of renewable energy in the Canary Islands. *Renewable and Sustainable Energy Reviews*, *10*(4), 312-340. https://doi.org/10.1016/j.rser.2004.09.005

Clarke, R.T. (1984). Mathematical models in hydrology. *FAO Irrigation and Drainage Paper*, *19*, 54-59.

Ding, H., Hu Z. & Song, H. (2012). Stochastic optimization of the daily operation of wind farm and pumped-hydro-storage plant. *Renewable Energy*, *48*, 571-578. https://doi.org/10.1016/j.renene.2012.06.008

Heuts, R.M.J. & Anderson, O.D. (1976). Time series analysis and forecasting: the Box-Jenkins approach. *Journal of the Royal Statistical Society. Series D (The Statistician)*, *25*(4), 310-314. https://doi.org/10.2307/2988092

Howlett, P., Piantadosi J. & Pearce, C. (2005). Analysis of a practical control policy for water storage in two connected dams. In V. Jeyakumar, A. Rubinov (ed.), *Continuous optimization. Applied optimization*. Vol. 99 (pp. 435-450). Boston, MA: Springer. https://doi.org/10.1007/0-387-26771-9_16

Karapetyan, S.S. & Mamikonyan, B.M. (2005). The measuring of dynamic parameters of functioning water storage dams. In *Proceedings of 2005 International Conference Physics and Control*. Saint Petersburg, Russia, 24--26.08.2005 (pp. 853-858). IEEE. https://doi.org/10.1109/phycon.2005.1514108

Kim, T. & Heo, J.H. Application of implicit stochastic optimization in the Han river basin. In Proceedings of the 4th International Conference on Hydro-Science & Engineering, Seoul, South Korea, 26-29.09.2000. Seoul: Korea Water Resources Associates.

Kottagoda, N.T. (1980). Linear stochastic models. In *Stochastic water resources technology* (pp. 111-127). New York: John Wiley and Sons. https://doi.org/10.1007/978-1-349-03467-3_4

MATLAB (2004). *MATLAB manual*. Natick, MA: MathWorks.

Naggar, O.M. (1999). *Development of decision support systems in water resources* (PhD thesis, University of Baghdad, Baghdad, Iraq).

Pereira, M.V.F., Oliveira, G.C., Costa, C.C.G. & Kelman, J. (1984). Stochastic streamflow models for hydroelectric systems. *Water Resources Research*, *20*(3), 379-390. https://doi.org/10.1029/wr020i003p00379

Thomas, H.A. & Feiring, M.B. (1962). Mathematical synthesis of streamflow sequences for the analysis of river basins by simulation

In A. Mass (ed.), *Design of water resources systems* (pp. 459-493). Cambridge: Harvard University Press. https://doi.org/10.4159/harvard.9780674421042.c15

Woodman, S., Hiden, H. & Watson, P. (2017). Applications of provenance in performance prediction and data storage optimization. *Future Generation Computer Systems*, *75*, 299-309. https://doi.org/10.1016/j.future.2017.01.003

Summary

Stochastic analysis for prediction of future performance of Mosul storage. An investigation of the Mosul reservoir system within the Tigris river basin in Iraq was conducted to determine the ability of the system to generate hydroelectric power. A reproduction model utilizing the Simulink environment on the MATLAB platform was used to imitate the Mosul reservoir system. The reliability of the system under various future scenarios of data sources was also examined by employing a stochastic model used to create an inflow time series. The Thomas–Fiering model was chosen for this reason, which provided a wide range of data sources (inflows) to generate hydropower from the reservoir system under examination. Generally, the annual potential capacity of the Mosul basin for energy generation reaches 20,000 $GW \cdot h^{-1}$. Realizing that Iraq's energy requirements are approximately 12 GW of power, and the integrating power production of the basin under examination is about 1.5 GW, this would cover around 12% of the total demand, which is significant.

Authors' address:
Nassrin J.H. Al-Mansori – corresponding author
(https://orcid.org/0000-0002-8921-7868)
Nariman Yahya Othman
(https://orcid.org/0000-0002-1908-2080)
University of Babylon
Faculty of Engineering
Department of Environmental Engineering
00964, 80 Street, Babylon, Iraq
e-mail: Eng.nassrin.jassim@uobabylon.edu.iq

Thair Jabbar Mizhir Al-Fatlawi
(https://orcid.org/0000-0001-8427-0400)
University of Babylon
Faculty of Engineering
Department of Civil Engineering
00964, 80 Street, Babylon, Iraq

Scientific Review – Engineering and Environmental Sciences (2020), 29 (2), 155–171
Sci. Rev. Eng. Env. Sci. (2020), 29 (2)
Przegląd Naukowy – Inżynieria i Kształtowanie Środowiska (2020), 29 (2), 155–171
Prz. Nauk. Inż. Kszt. Środ. (2020), 29 (2)
http://iks.pn.sggw.pl
DOI 10.22630/PNIKS.2020.29.2.14

Sarah Mustafa AHMED[1], Omer Muhie Eldeen TAHA[2], Mohamed A. NAJEMALDEN[3], Rehab T. AHMED[3], Ali A. ABEDULWAHAB[3]

[1] University of Kirkuk, Environmental Research Unit
[2] University of Kirkuk, College of Engineering
[3] Iraqi Ministry of Health and Environment

Assessment of Lower Zab river water quality using both Canadian Water Quality Index Method and NSF Water Quality Index Method

Key words: NSF Water Quality Index, Canadian Water Quality Index, Lower Zab river, physicochemical parameters, dissolved oxygen, biochemical oxygen demand

Introduction

Water is well known as the main constituent of Earth's streams, lakes, and oceans, and the fluids of most of earth organisms. It is essential for all known forms of life. During the last decades of the 20th century polluted water has started to become a universal grave issue and surface water quality is becoming a real global concern (Witek & Jarosiewicz, 2009). Human existence, development and well-being have always been linked to water (Eulisse, 2010; Reza & Singh, 2010). Over two thirds of Earth's surface are covered by water, which represent about 71% of the Earth's surface, and more than 96% of this water is saline. Over 68% of freshwater is in ice and glaciers and 30% is confined in the ground. The rest (about 1.2%) represent the fresh surface-water sources, such as rivers and lakes (Shiklomanov, 1993). Rivers are considered the most important sources of surface water on Earth. They are play a significant role in all human activities, like agriculture, drinking, irrigation, industry, and domestic work. Many industries rely in their processes on water, and about 40% of food supply around the world is grown under irrigation (BCAS, 2000). However, all these activities have posed a major threat to the quality of the river's water in many countries around the world particularly in developing countries and some drinking water supplies have become contaminated (Akoto & Adiyiah, 2007). The United Nations reports pointed that a child dies every 8 second as a result of a water-related illness (Al-Adawi, 2005). As noted by the World Health Organization (WHO), 3.4 million people, mostly children, die annually from water-related diseases (WHO, 2001). Beside the anthropogenic influences such as urban, industrial, and agricultural activities, there are many factors that affect water quality characteristics such as natural processes like climate, precipitation inputs and catchment area, tectonic, erosion of crustal materials and bedrock geology, in combine with the influence of the environment (Glińska-Lewczuk, 2006; Nas, Bayram, Nas & Bulut, 2008; Kašiarová & Feszterová, 2010).

Therefore, many studies conducted to evaluate water quality index in different rivers and water bodies around the world. The importance of the water quality index is emerged through providing data base about quality of the water source, and explain the change in the water quality over a period of time, as well as finding the degree of pollution of a water body (Al-Heety, Turki & Al--Othman, 2011; Phadatare & Gawande, 2016). The pollution of Iraqi waters is one of the major problems that have started to appear and have increased. This necessitates serious thinking to find ways to combat and minimize the water pollution, especially as the rivers and lakes attract human communities and often most of the villages and cities in Iraq are located on the edges of rivers and lakes (Shahin, 2007). As the river was a source of all the requirements of people from water in return were dumping waste and wastewater to this river, which led to pollution of river.

Thus, the current study involved determination of physicochemical and biological parameters of Lower Zab river in Kirkuk city at different points. This study aims to evaluate the water quality of Lower Zab river by analyzing of some selected water quality parameters like: pH, total dissolved solids, biochemical oxygen demand, dissolved oxygen, turbidity, electrical conductivity, alkalinity, and salinity etc., and compare the results with the Canadian Council of Ministers of the Environment (CCME) and the National Sanitation Foundation (NSF) water quality index (CCME, 2001).

Material and methods

Study area

In Iraq there are two main rivers considered the lifeline of the country. Tigris is the eastern of the two great rivers that define Mesopotamia, the other being the Euphrates (Frenken, 2009). Flowing into the Tigris river, within the borders of Iraq, a large group of tributaries supplying more than half of the Tigris in the flood season, scattered in the territory of Turkey, Iran and Iraq, the most important Khabur, Great Zab, Lower Zab, Al--Adhaim, and Diyala. Lower Zab river (also named as Little Zab) is one of the five main catchments in Northern Iraq (Frenken, 2009; Saeedrashed & Guven, 2013). The Lower Zab begins in Iran in a mountainous range which is part of the Zagros mountains (Kliot, 2005; Frenken, 2009). Its equipped with the Dukan Dam (6.8 km^3) in Sulaymaniyah city in Iraq (Frenken, 2009). The river basin of

21,475 km^2 generates about 7.17 km^3, of which 5.07 km^3 of annual safe yield after buildup Dokan Dam (Frenken, 2009). The total length of the river is 400 km (Kassim, Sabri & Salman, 2007; Shahin, 2007; Jabar, 2008). The Lower Zab river is lying between the geographic coordinates of SN latitude 35.16° to 36.79° and WE longitude 43.39° to 46.26°, and it is going over within the administrative boundaries of the governorates: Erbil, Sulaymaniyah, and Kirkuk (Saeedrashed & Guven, 2013). About 30 km north of Fatha, the Lower Zab joins the river Tigris (Al-Ansari, 2016). The river water depends on the melting of snow in the mountains and the amount of rainfall, which fluctuates from year to year according to climatic conditions, where the water level is the highest level in the spring because of melting snow and less in the summer. The Lower Zab river is the major source for drinking water in Kirkuk Governorate, as well as for agriculture and irrigation in the region.

The study of the water quality index of the Lower Zab river within the administrative boundaries of Kirkuk Governorate, where two monitoring points are adopted for the purpose of modeling. These points approved by the Ministry of health and environment in Iraq – Directorate of Protection and Improvement of the Environment of the Northern Region. The monitoring stations were adopted within the geographical area of the province of Kirkuk, which is LZ2 (Lower Zab station 2) and LZ3 (Lower Zab station 3). The first monitoring point (LZ2) is located in Alton Kobri (GPS coordinates 35.76053 N, 44.14189 E) which is a small town located northwest of Kirkuk city and it is about 40-kilometer distance. The second monitoring point (LZ3) located in Dibs District (GPS coordinates 35.68447 N, 44.07072 E) about 35 km northwestern Kirkuk city (Fig. 1).

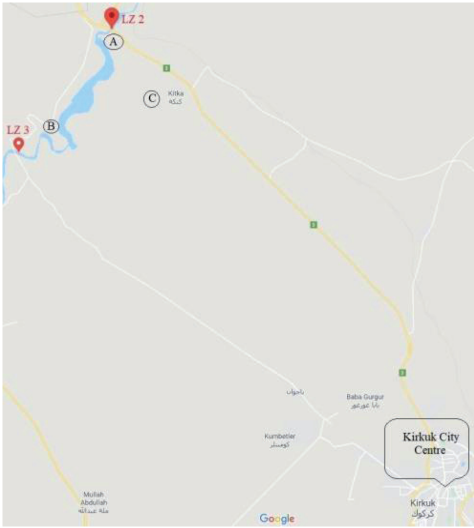

FIGURE 1. Location of stations on the Lower Zab river

Many human and industrial activities taking place near the Lower Zab river and along the riverbed, like the discharges of the power plant of Dibs and the residues of stone quarries and block factories are considered threats to the quality of water in the Zab river. Also, the existence of agricultural fields near the riverbed which affects the increase of pollution by returning the water used for irrigation to the riverbed, which is loaded with pollutants of fertilizers and salts. In addition, there is a discharge of Karwanchi Beverage Factory (Soft drink factory), which is disposed to the Lower Zab river in the area confined between LZ2 and LZ3. The main problem that cause pollution in the Lower Zab river are from the

TABLE 1. Location and name of the polluting activity of the Lower Zab river

Location	Waste type	Symbol
Kirkuk – Alton Kubri	untreated sewage water of residential houses	A
Kirkuk – Dibs	untreated sewage water of residential houses	B
Kirkuk – Karwanchi Group Company for Soft Drink Juices Water	− treated sewage water − untreated industrial wastewater	C

discharging the sewage water of Hawija, Debs, Alton Kubri and Zab areas directly into the river body. All these places do not have sanitation projects. All the polluting activity between the LZ2 and LZ3 are listed in Table 1.

Sample collection

Raw water samples were collected from the Lower Zab river twice a month by one sample every 15 days from each station. The samples collected from January 2013 to March 2019. Water samples were taken from about 3 to 4 m from the edge of the river at a depth of 20–30 cm from the water surface of the river. The water quality data include 16 parameters: pH, dissolved oxygen (DO), biochemical oxygen demand (BOD), phosphates (PO_4), nitrate (NO_3), calcium (Ca), magnesium (Mg), total hardness (TH), potassium (K), sodium (Na), sulfates (SO_4), chlorides (Cl), total dissolved solids (TDS), electrical conductivity (EC), alkalinity (ALK), and turbidity (TRUB). The data of the sixteen parameters included in this study was obtained from Directorate of Protection and Improvement of the Environment – Northern Region (Kirkuk, Iraq). The standard used here was the Canadian Drinking Water Guidelines and if there was no Canadian standard, Iraqi standard for drinking water or the World Health Organization guidelines are used (IQS 417, 2009; WHO, 2017). Collected samples were taken by sterilized bottles from the middle of the stream. Tests were carried out following the American Public Health Association (APHA, 1995) standard methods.

Water quality indices calculations

A number of water quality indices have been formulated over the last five decades. First formulated of WQI was by Horton (1965). It is commonly used for the detection and estimating of water pollution based on several quality parameters (Horton, 1965). This index provides a single number which expresses overall water quality at a certain location and time by simplify complex data into simple information that is easy to understand and usable by the public (Schultz, 2001). Many WQI studies have been conducted all over the world in different countries, they were reported in literature by many researchers (Brown, McClelland, Deininger & Tozer, 1970; Fulazzaky, 2009; Tyagi, Sharma, Singh & Dobhal, 2013; Gupta, Pandey & Hussain, 2017). Many studies developed numerous water quality indicators to provide a convenient way to summarize water quality data, each using different group of analytes (House & Ellis, 1987). In this study two water quality methods used to assess the quality of Lower Zab river (NFS Method and CCME Method).

National Sanitation Foundation (NFS)

The NFS WQI is a commonly-used water quality index developed by the National Sanitation Foundation in 1970 to provide a standardized way to compare the water quality of different water bodies. In this method, weight was assigned for each parameter where the sum of the weights is equal to one (Brown et al., 1970). The water quality results can be reported using descriptive words to summarize the data into one of five classes, ranging from "very bad" to "excellent" (Ott, 1978). This type of WQI ignores the type of water consumption, therefore it can be used for various water bodies types (Ott, 1978). It is useful for estimating spatial and temporal changes and classify the quality of river water (Reza & Singh, 2010), and groundwater source (Rajankar, Gulhane, Tambekar, Ramteke & Wate, 2009).

The NFS WQI is designed to include nine parameters, they are dissolved oxygen (DO), five-day biochemical oxygen demand (BOD_5), nitrate, total phosphate, temperature, turbidity, fecal coliform, and total solids (Brown et al., 1970). It can still be calculated if there are some missing parameters (Srivastava & Kumar, 2013), or further parameters more than nine (Kumar & Alappat, 2009; Ewaid, Abed & Kadhum, 2018). When it is difficult to find the concentration of all nine quality parameters, the weight of the missing parameters will be distributed over other parameters based on the weight of each parameter in the index.

The result of WQI with missing parameters will be different from the real result if all the nine parameters adopted, but the difference is very low that made the classification of quality index still in the same class (Srivastava & Kumar, 2013). However, it is clear that choosing a small number of water quality parameters are not met the objectives well, while if a large number of parameters are used a different picture will be provide (CCME, 2001). In the literature some researchers used fewer than nine variables in water quality studies (Al-Mutairi, Abahussain & El-Battay, 2014; Gupta et al., 2017; Ebuete & Ebuete, 2018). While others used more variables to obtain a more comprehensive picture of water quality (Alobaidy, Abid & Maulood, 2010; Ewaid et al., 2018). The parameters and their corresponding weights are listed in Table 2 (Kumar & Alappat, 2009; Ewaid et al., 2018).

The mathematical equations for WQI are given as follows:

$$Q_i = \left(\frac{Q_{\text{actual}} - Q_{\text{ideal}}}{Q_{\text{standard}} - Q_{\text{ideal}}} \right) 100 \qquad (1)$$

$$NSF\ WQI = \sum_{i=1}^{n} W_i Q_i \qquad (2)$$

where:
Q_i – sub-index for i^{th} water quality parameter,
n – number of water quality parameter,
W_i – weight (in terms of importance) associated with i^{th} water quality parameter.

The Canadian Council of Ministers of the Environment (CCME)

The CCME WAI Method is a widely used and globally accepted model for assessing the water quality (Khan, Pa-

TABLE 2. NSF WQI parameters and weights (Ott, 1978; Kumar & Alappat, 2009; Batabyal & Chakraborty, 2015; Ewaid et al., 2018)

Parameter	Unit	Assigned weight (w_i)	Relative weight $W_i = \frac{w_i}{\sum_1^n w_i}$	Standard	Reference
pH	–	4.33	0.0894	6.5–8.5	–
Dissolved oxygen (DO)	$mg \cdot l^{-1}$	4.59	0.0947	4.0–6.5	–
Five-day biochemical oxygen demand (BOD_5)		3.88	0.0801	3	WHO, 2017
Phosphates (PO_4) concentration		3.89	0.0803	0.4	IQS 417, 2009
Nitrate (NO_3) concentration		3.8	0.0784	1	–
Calcium (Ca) concentration		1.96	0.0405	25	–
Magnesium (Mg) concentration		1.76	0.0363	50	–
Total hardness (TH)		2.84	0.0586	250	–
Potassium (K) concentration		0.94	0.0194	8	–
Sodium (Na) concentration		0.94	0.0194	20	–
Sulfates (SO_4) concentration		2.64	0.0545	250	IQS 417, 2009
Chlorides (Cl) concentration		3.43	0.0708	250	–
Total dissolved solids (TDS)		3.63	0.0749	450	–
Electrical conductivity (EC)	$\mu S \cdot cm^{-1}$	3.22	0.0665	1 600	–
Alkalinity (ALK)	$mg \cdot l^{-1}$	3.13	0.0646	250	WHO, 2017
Turbidity (TRUB)	NTU	3.47	0.0716	5	–

TABLE 3. Water Quality Index (WQI) ranges (Batabyal & Chakraborty, 2015)

Criteria	WQI range
Excellent	0–50
Good	50–100
Poor	100–200
Very poor	200–300
Unsuitable for drinking	> 300

terson & Khan, 2004). It is based on a formula developed by the British Columbia Ministry of Environment, Lands and Parks and modified by Alberta Environment (CCME, 2001). This index has been extensively used in water quality studies because its flexibility in terms of the type and number of variables selected for testing quality of water and the type of water body, also the time period of application. Another advantage of this model is enabling the researchers to use the national standards for water quality (A.A. Khan, Tobin, Paterson, Khan & Warren, 2005). Many studies have been conducted to determine water quality in different countries (Khan et al., 2004; Lumb, Halliwell & Sharma, 2006; Damo & Icka, 2013; Munna, Chowdhury, Ahmed, Chowdhury & Alom, 2013; Mahagamage & Manage, 2014; Gupta et al., 2017). The CCME WQI model consists of three factors:

1. Scope: represents the number of variables that do not meet their objectives.
2. Frequency: represents the number of times these objectives are not met.
3. Amplitude: represents the amount by which the objectives are not met.

These factors produce a number value (from 0 to 100) refers to the total water quality for the water body, where 0 represents the "worst" and 100 represents the "best" value for water quality (CCME, 2001; H. Khan, Khan & Hall, 2005; Lumb et al., 2006; Panduranga Murthy & Hosmani, 2009). The formulation of the WQI as described in the Canadian Water Quality Index 1.0 – Technical Report, is shown in the following equations (Munna et al., 2013): The measure for scope is F_1. This represents the number of variables whose value does not match the objectives over the study time period.

$$F_1 = \left(\frac{number\ of\ failed\ variables}{total\ number\ of\ variables} \right) 100 \tag{3}$$

The measure for frequency is F_2. This represents the failed tests which is the percentage of individual tests that do not meet objectives.

$$F_2 = \left(\frac{number\ of\ failed\ tests}{total\ number\ of\ tests} \right) 100 \tag{4}$$

The measure for amplitude is F_3. This represents the number of failed test values that do not meet their objectives. This step consists of several phases. Initially calculation of Excursion, the number of times by which the test value is greater than the objective, the excursion calculated from the following equation

$$excursion = \left(\frac{failed\ test\ value}{guideline\ value} \right) 100 \tag{5}$$

For the cases in which the test value is less than the objective, formula (6) is used

$$excursion = \left(\frac{guideline\ value}{failed\ test\ value} \right) - 1 \tag{6}$$

The normalized sum of excursions (*nse*) can be calcalated by equation (7)

$$nse = \frac{\sum_{i=1}^{n} excursion}{number\ of\ tests} \tag{7}$$

Finally, the amplitude (F_3) can be found from equation (8)

$$F_3 = \frac{nse}{0.01 nse + 0.01} \tag{8}$$

The CCME WQI is then calculated as shown in the following equation

$$WQI = 100 - \left(\frac{\sqrt{F_1^2 + F_2^2 + F_3^2}}{1.732} \right) \tag{9}$$

then the value of water quality can be ranked by relating it to one of the five categories set out in Table 4.

The main pollution parameters that considered for surface water quality management in this work include 16 parameters: turbidity (TRUB), pH, dissolved oxygen (DO), five-day biochemical oxygen demand (BOD_5), total dissolved solids (TDS), total hardness (TH), electrical conductivity (EC), alkalinity

TABLE 4. CCME WQI categorization schema (CCME, 2001; H. Khan et al., 2005)

Category	WQI	Status
1	95–100	excellent
2	80–94	good
3	65–79	fair
4	45–64	marginal
5	0–44	poor

(ALK), concentration of: nitrate (NO_3), phosphorus (PO_4), calcium (Ca), magnesium (Mg), sulfates (SO_4), potassium (K), sodium (Na), and chlorides (Cl).

Result and discussion

The results for the descriptive data of the 16 water quality variables (pH, DO, BOD, TDS, EC, ALK, TH, TRUB, concentration of PO_4, NO_3, Ca, Mg, K, Na, SO_4, Cl), which were measured twice a month during sampling period of seven years (from 2013 to 2019) at two stations on the Lower Zab river, were analyzed and presented in Figures 2, 3, 4, and 5. The investigation of the physical and chemical parameters results gives a broad understanding for water quality

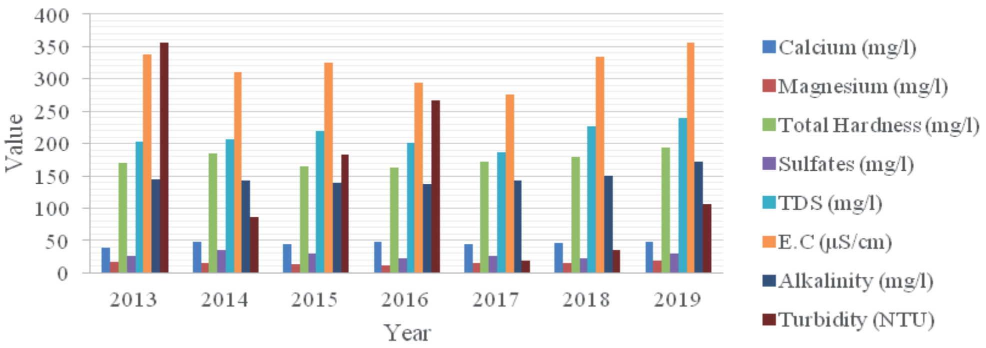

FIGURE 2. Trend of calcium, magnesium, total hardness, sulfates, TDS, EC, alkalinity, and turbidity for LZ2 station

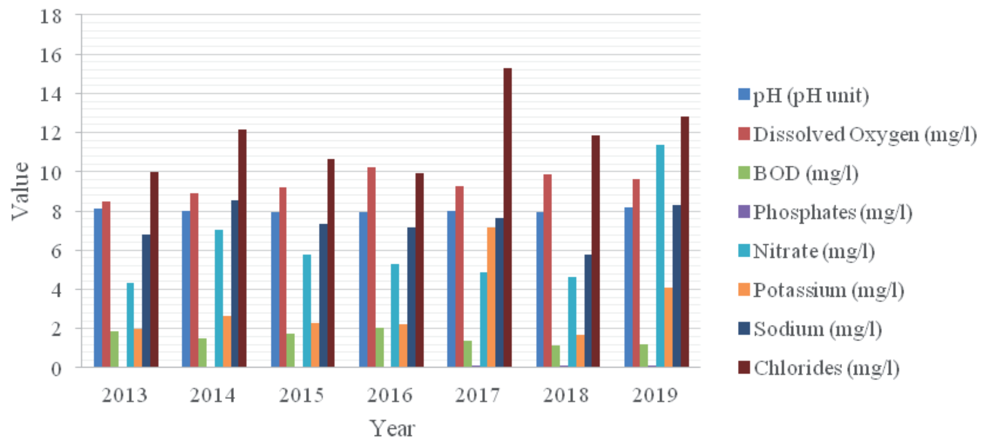

FIGURE 3. Trend of pH, dissolved oxygen, BOD, phosphates, nitrate, potassium, sodium, and chlorides for LZ2 station

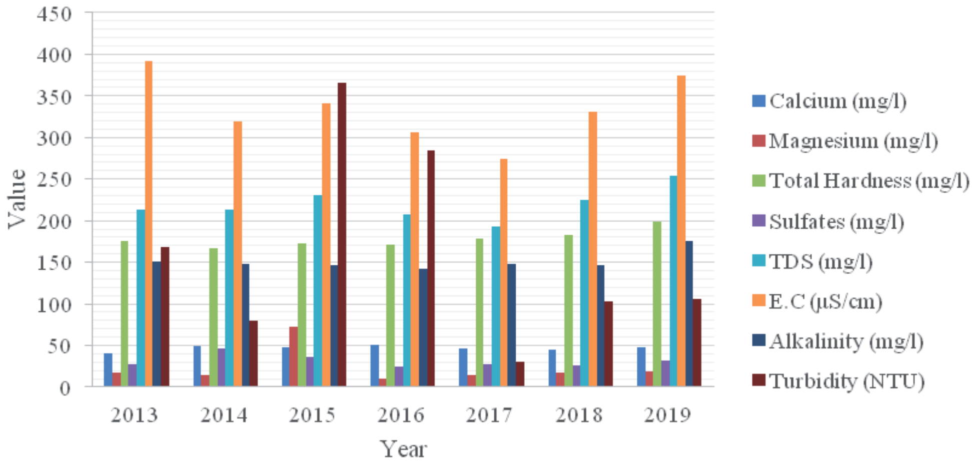

FIGURE 4. Trend of calcium, magnesium, total hardness, sulfates, TDS, EC, alkalinity, and turbidity LZ3 station

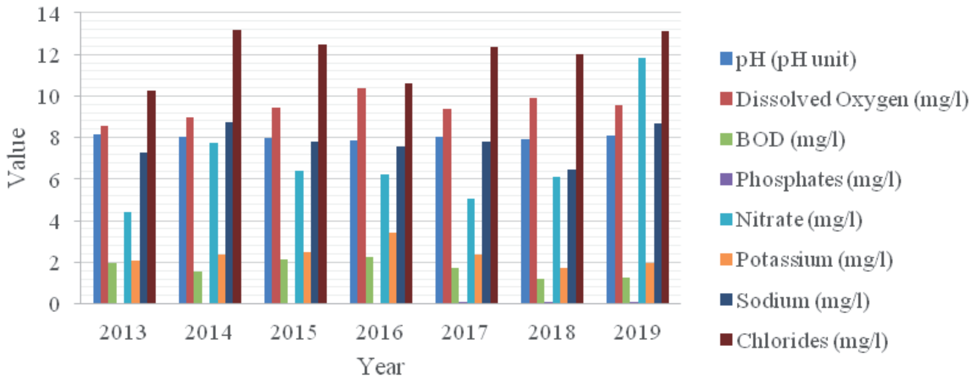

FIGURE 5. Trend of pH, dissolved oxygen, BOD, phosphates, nitrate, potassium, sodium, and chlorides for LZ3 station

of the river by finding out the parameters responsible for detraction the water quality.

The results show that all parameters values were within the standards of drinking water proposed by the CCME standards (2001), Iraqi standards (IQS 417, 2009), and the WHO standards (WHO, 2017) for drinking purpose, except turbidity, dissolved oxygen, concentration of nitrate and calcium, which were mostly higher than the standards and occasionally biochemical oxygen demand and concentration of potassium.

The pH measure reflects the acid content of the water source. According to the standards produced by the CCME, the WHO, and Iraq standards for drinking water (IQS 417, 2009), the range of pH lies between 6.5 and 8.5. Alkaline water with pH level higher than 8.5 is produce salty taste for water and caused eye irritation. If the pH is less than 6.5 water produce sour taste and classified as acidic water. Acidity water does not have useful minerals for human body (Nollet, 2004; Kumari, Sudhakar, Sri, & Sree, 2011). In this study, the pH values ranged from 7.7 to 8.38 which follow the standards given by the CCME, the WHO, and the Central Organization for Standardization and Quality Control (COSQC). That narrow range of pH variation of pH indicates a slightly alkaline water (Rabee, Abdul-Kareem & Al-Dhamin, 2011).

Dissolved oxygen is an important parameter in calculation of water quality, it reveals the amount of free oxygen (O_2) dissolved in water which is necessary for sustaining and support aquatic life, so is human life (Chang, 2005). The dissolve oxygen standard requisites for aquatic life is 4 $mg \cdot l^{-1}$, and for drinking purposes it is 6 $mg \cdot l^{-1}$ (Alam, Islam, Muyen, Mamun & Islam, 2007). The maximum and minimum values for DO in the current study were between 7.57 and 10.8 $mg \cdot l^{-1}$, which means that all values of DO in water samples are above the recommended permissible limits. Generally, a higher DO level indicates better water quality.

Biochemical oxygen demand levels measured were between 0.33 and 8.37 $mg \cdot l^{-1}$. BOD is the amount of oxygen required to dismantle domestic and industrial pollutants present in the water source (De, 2003). According to WHO drinking water standard, BOD level of 3 $mg \cdot l^{-1}$ is accepted and should not exceed 6 $mg \cdot l^{-1}$. In the current study all the values of BOD were within the standards except in July (2013) were 8.37 and 8.22 for both monitoring stations (LZ2 and LZ3). Also, in November the BOD value was 4.3 for LZ3 for the same year. The high values of BOD attributed to the existence of untreated wastewater flowing into river body.

Total hardness values were all in the range of the permissible limits, the minimum value of (150 $mg \cdot l^{-1}$) recorded in December (2013) and the maximum (235 $mg \cdot l^{-1}$) was in March (2018).

Total dissolved solids is the measure of the solid materials dissolved in the water sample. High levels of TDS causes harm effect to the public health as well as fish and aquatic plants. A serious danger can infect the nervous system of the human body by causing paralysis of the tongue, lips, face (Chang, 2005). In this study the range of TDS falls between 292 and 151 $mg \cdot l^{-1}$, which is within the recommended value of 500 $mg \cdot l^{-1}$ by the CCME (2001) and the WHO (2017) standards for water quality and specification limit for drinking water.

The electrical conductivity varies from 221.5 to 432 $\mu S \cdot cm^{-1}$; and it is lies within the standards of drinking water.

The total alkalinity of water in this study ranged from 117 to 210 $mg \cdot l^{-1}$, which is within the CCME (2001) standards of drinking water quality.

The TDS, TH, TA and EC parameters indicate the status of inorganic pollution, and represent the concentration of soluble salts in water (Turner & Rabalais, 2003; Gupta, Vishvakarma & Rawtani, 2009).

The minimum and maximum turbidity values of water in Lower Zab river were 4.9 NTU and 4,000 NTU, respectively. The maximum value for turbidity (4,000 and 1,100 NTU) recorded in November 2013 at the both stations LZ2 and LZ3. The reason for the high value of turbidity due to the end of the dry seasons (summer and autumn) and rainfall in the beginning of the rainy season. The increase of turbidity values results due to the high concentration of suspended matter in the water column, and subsequently increase dispersion of light. Which in turn causes in deterioration of the water quality, also will damage the aquatic life (Verma et al., 1984). For this purpose, the WHO, the CCME, and the IQS proposed a maximum range for turbidity of 5 NTU based on the processes used to treat wastewater (De, 2003).

The nitrate results obtained from the two sampled stations were higher than the maximum permissible limits proposed by the CCME (2001) for drinking water. The minimum and maximum values for nitrate were 0.147 and 16.44 $mg \cdot l^{-1}$. High nitrate levels in drinking water can be harmful to humans and cause serious illnesses such as "blue baby syndrome", cancer risks, and hemorrhaging of the spleen (Michalski & Kurzyca, 2006; Aydin, 2007; Gupta et al., 2009; Yang & Wang, 2010). Nitrites can also affect the aquatic life, plants and algae by decreased oxygen level when its concentrations rise in water (Davie & Quinn, 2019).

Calcium concentrations in water samples were varying between 30 to 57 $mg \cdot l^{-1}$. All the data does not within the objective values suggested by the CCME (2001) for drinking water which is 25 $mg \cdot l^{-1}$. Approach results were obtained by Ewaid et al. (2018) in a study to assess the quality of water for the Tigris river. These results are due to the nature of the surrounding soil.

The potassium levels varying across the range of 1.02–40.8 $mg \cdot l^{-1}$. In general, all the potassium levels were found to be within the accepted limits for drinking water quality standards. Except one value (40.8 $mg \cdot l^{-1}$) recorded higher than the standards during winter in January 2017.

The results of the water quality index (WQI) at LZ2 station are shown in Figure 6. Both Canadian and NSF methods were used to calculate the WQI. It was noted that the WQI from 2013 to 2019 between marginal and fair status according to the CCME (Table 5). While the WQI are classified for the years 2013, 2015, 2016 as unsuitable for drinking and for 2014, 2019 as poor water and for 2017, 2018 as a good water according to Table 4.

For LZ3 station, the results showed that the WQI from 2013 to 2019 are between marginal and fair status according to the CCME (Table 5). The results are same as the LZ2 station with some marginal decrease in the WQI. The decrease in the WQI possibly due to the polluting activity of the Lower Zab river mentioned in Table 2. In accordance to Table 4, the results showed that the WQI for 2013, 2015, 2016 years are unsuitable for drinking and for 2014, 2018, 2019 years are poor water and for the year of 2017 is good water. Also, it was noting that some marginal increase in the WQI value in which decreases the subtility of the water for drinking use (Fig. 7).

For the years 2014, 2015, and 2016, the water quality was degraded due to the ISIS war. Moreover, it was noted in the 2013 year that the water quality almost stable and have a constant value during spring and summer. A high decease in the water quality (high increase in WQI according to NSF Method) in the fall and winter seasons. This degradation in

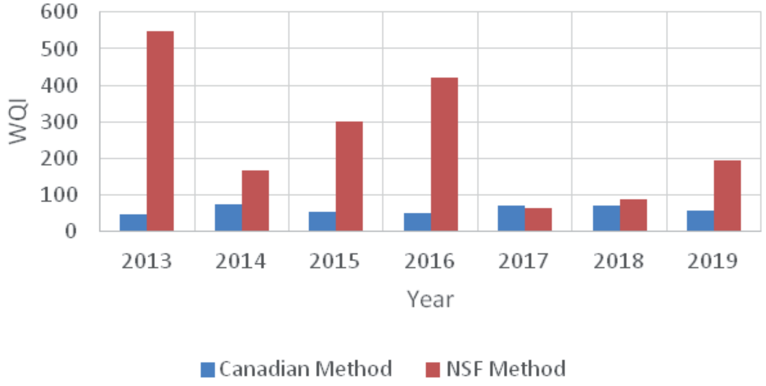

FIGURE 6. Water Quality Index (WQI) at LZ2 station

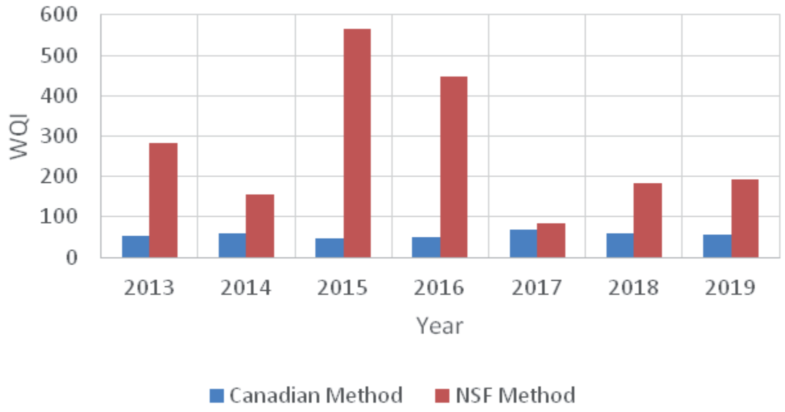

FIGURE 7. Water Quality Index (WQI) at LZ3 station

the water quality is due to that the earth has exposed to the long-dried season and then suddenly exposed to a high rainfall season which in turns leads to increase some parameters very high, i.e. turbidity (Fig. 8). Finally, the Lower Zab river water cannot be use for drinking directly. However, a pretreatment is needed before drinking use.

However, a recent research was noted that the quality of water are highly affected by seasons (Mena-Rivera, Salgado-Silva, Benavides-Benavides, Coto--Campos & Swinscoe, 2017). Also it was noted previosuly that the quality of water in the spring is more better than other seasons (Ameen, 2019). Especially when the turbidity parameter is not included which gave good drinking water (Ewaid & Abed, 2017). And this interpreted the varation in the WQI during seasons.

Conclusions

This research focused on the assessment of Lower Zab river water quality using both methods – Canadian Water

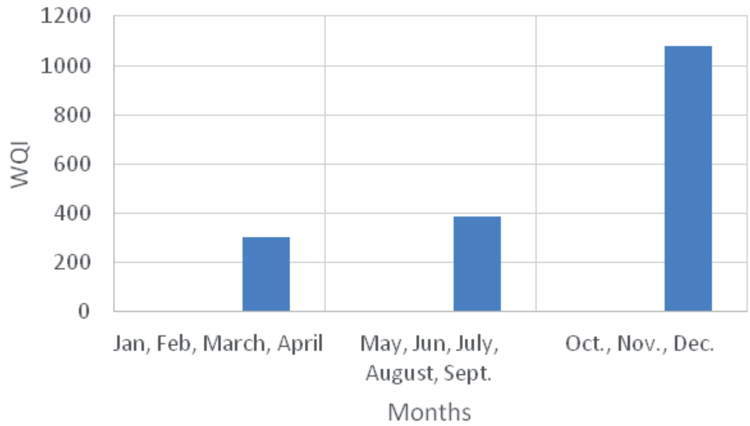

FIGURE 8. Water Quality Index (WQI) variation during year of 2013

Quality Index and NSF Water Quality Index. Two different stations LZ2 and LZ3 were selected for this study. The results show that all parameters values were within the standards of drinking water proposed by the CCME standards (2001), Iraqi standards (IQS 417, 2009), and the WHO standards (2017) for drinking purpose, except turbidity, DO, nitrate, calcium, which were mostly higher than the standards and occasionally BOD and potassium. Also, the results of WQI showed that the quality of water at LZ3 station is lower than the quality of water in the LZ2 station. This degradation in the quality of water is due to the polluting activity of the Lower Zab river (Table 2). Moreover, for the years 2014, 2015, and 2016, the water quality was degraded due to the ISIS war. However, the quality of the water is degraded in winter season more than summer season due to that the earth has exposed to the long-dried season and then suddenly exposed to a high rainfall season which in turns leads to increase some parameters very high (i.e. turbidity). Finally, the Lower Zab river water cannot be use for drinking directly. However, a pre-treatment is needed before the drinking use.

References

Akoto, O. & Adiyiah, J. (2007). Chemical analysis of drinking water from some communities in the Brong Ahafo region. *International Journal of Environmental Science & Technology*, *4*(2), 211-214.

Al-Adawi, M.S. (2005). *Water supply engineering*. Alexandria: Alexandaria University Engineering College.

Alam, Md.J.B., Islam, M.R., Muyen, Z., Mamun, M. & Islam, S. (2007). Water quality parameters along rivers. *International Journal of Environmental Science & Technology*, *4*(1), 159-167. https://doi.org/10.1007/bf03325974

Al-Ansari, N. (2016). Hydro-politics of the Tigris and Euphrates basins. *Engineering*, *8*(3), 140--172. https://doi.org/10.4236/eng.2016.83015

Al-Heety, E.A.M., Turki, A.M. & Al-Othman, E.M. (2011). Assessment of the water quality index of Euphrates river between Heet and Ramadi cities, Iraq. *International Journal of Basic & Applied Sciences*, *11*(6), 38-47.

Al-Mutairi, N., Abahussain, A. & El-Battay, A. (2014). Application of Water Quality Index to assess the environmental quality of Kuwait Bay. In *AABES-2014: International Confer-*

ence on Advances in Agricultural, Biological and Environmental Sciences. Dubai, UAE, 15-16.10.2014. Dubai: AABES-2014.

Alobaidy, A.H.M.J, Abid, H.S. & Maulood, B.K. (2010). Application of Water Quality Index for assessment of Dokan lake ecosystem, Kurdistan Region, Iraq. *Journal of Water Resource and Protection*, *2*(9), 792-798. https://doi.org/10.4236/jwarp.2010.29093

Ameen, H.A. (2019). Spring water quality assessment using water quality index in villages of Barwari Bala, Duhok, Kurdistan Region, Iraq. *Applied Water Science*, *9*(8), 176. https://doi.org/10.1007/s13201-019-1080-z

American Public Health Association [APHA] (1995). *Standard Methods for the Examination of Water and Wastewater*. 19th ed. New York: APHA.

Aydin, A. (2007). The microbiological and physico-chemical quality of groundwater in West Thrace, Turkey. *Polish Journal of Environmental Studies*, *16*(3), 377-383.

Bangladesh Center for Advance Studies [BCAS] (2000). *Pollution study, management of aquatic ecosystem through community husbandry (MACH)*. Dhaka, Bangladesh: Bangladesh Center for Advance Studies.

Batabyal, A.K. & Chakraborty, S. (2015). Hydrogeochemistry and Water Quality Index in the assessment of groundwater quality for drinking uses. *Water Environment Research*, *87*(7), 607-617. https://doi.org/10.2175/106143015x14212658613956

Brown, R.M., McClelland, N.I., Deininger, R.A. & Tozer, R.G. (1970). A water quality index: do we dare? *Water and Sewage Works*, *117*, 339-343.

Canadian Council of Ministers of the Environment [CCME] (2001). *Canadian water quality guidelines for the protection of aquatic life: CCME Water Quality Index 1.0*. User's Manual. Winnipeg: CCME.

Chang, H. (2005). Spatial and temporal variations of water quality in the Han river and its tributaries, Seoul, Korea, 1993–2002. *Water, Air, and Soil Pollution*, *161*(1), 267-284. https://doi.org/10.1007/s11270-005-4286-7

Damo, R. & Icka, P. (2013). Evaluation of Water Quality Index for drinking water. *Polish Journal of Environmental Studies*, *22*(4), 1045-1051.

Davie, T. & Quinn, N.W. (2019). *Fundamentals of hydrology*. Abingdon: Routledge.

De, A.K. (2003). *Environmental chemistry*. New Delhi: New Age International.

Ebuete, A.W. & Ebuete, I.Y. (2018). Water quality of Kolo Creek in Bayelsa State by means of Water Quality Index for missing parameters. *International Journal of Innovative Research and Advanced Studies*, *5*(8), 53-60.

Eulisse, E. (2010). *Challenges in water resources management*. Venezia, Italy: Marie Curie Training Course.

Ewaid, S.H. & Abed, S.A. (2017). Water quality index for Al-Gharraf river, southern Iraq. *The Egyptian Journal of Aquatic Research*, *43*(2), 117-122. https://doi.org/10.1016/j.ejar.2017.03.001

Ewaid, S.H., Abed, S.A. & Kadhum, S.A. (2018). Predicting the Tigris river water quality within Baghdad, Iraq by using water quality index and regression analysis. *Environmental Technology & Innovation*, *11*, 390-398. https://doi.org/10.1016/j.eti.2018.06.013

Frenken, K. (2009). *Irrigation in the Middle East region in figures*. Rome: FAO Water Reports.

Fulazzaky, M.A. (2009). Water quality evaluation system to assess the Brantas river water. *Water Resources Management*, *23*(14), 3019-3033. https://doi.org/10.1007/s11269-009-9421-6

Glińska-Lewczuk, K. (2006). Effect of land use and lake presence on chemical diversity of the Łyna river system. *Polish Journal of Environmental Studies*, *15*(2), 259-269.

Gupta, N., Pandey, P. & Hussain, J. (2017). Effect of physicochemical and biological parameters on the quality of river water of Narmada, Madhya Pradesh, India. *Water Science*, *31*(1), 11-23. https://doi.org/10.1016/j.wsj.2017.03.002

Gupta, P., Vishvakarma, M. & Rawtani, P.M. (2009). Assesment of water quality parameters of Kerwa Dam for drinking suitability. *International Journal of Theoretical & Applied Sciences*, *1*(2), 53-55.

Horton, R.K. (1965). An index number system for rating water quality. *Journal of the Water Pollution Control Federation*, *37*(3), 300--305.

House, M.A. & Ellis, J.B. (1987). The development of water quality indices for operational management. *Water Science and Technology*, *19*(9), 145-154. https://doi.org/10.2166/wst.1987.0076

IQS 417 (2009). Iraqi criteria and standards for drinking water, chemical limits. In ICS 13.060.20. Drinking water.

Jabar, R.A.A. (2008). Effects of some physical and chemical factors of Lower Zab water on Tigris river. *Tikrit Journal of Pure Science*, *13*(1), 132-142.

Kašiarová, S. & Feszterová, M. (2010). Changes in stream water contamination in select Slovakian settlements. *Polish Journal of Environmental Studies*, *19*(2), 343-349.

Kassim, T.I., Sabri, A.W. & Salman, M.S. (2007). The limnological effects of river lesser-Zab on Tigris river, Iraq. *Um-Salama Science Journal*, *4*(3), 452-457.

Khan, A.A., Paterson, R. & Khan, H. (2004). Modification and application of the Canadian Council of Ministers of the Environment Water Quality Index (CCME WQI) for the communication of drinking water quality data in Newfoundland and Labrador. *Water Quality Research Journal*, *39*(3), 285-293. https://doi.org/10.2166/wqrj.2004.039

Khan, A.A., Tobin, A., Paterson, R., Khan, H. & Warren, R. (2005). Application of CCME procedures for deriving site-specific water quality guidelines for the CCME Water Quality Index. *Water Quality Research Journal*, *40*(4), 448-456. https://doi.org/10.2166/wqrj.2005.047

Khan, H., Khan, A.A. & Hall, S. (2005). The Canadian Water Quality Index: a tool for water resources management. In *MTERM International Conference*. Bangkok, Thailand, 6-10.06.2005. Thailand. Bangkok: AIT.

Kliot, N. (2005). *Water resources and conflict in the Middle East*. Abington: Routledge.

Kumar, D. & Alappat, B.J. (2009). NSF-Water Quality Index: does it represent the experts' opinion? *Practice Periodical of Hazardous, Toxic, and Radioactive Waste Management*, *13*(1), 75-79. https://doi.org/10.1061/(ASCE)1090-025X(2009)13:1(75)

Kumari, B.L., Sudhakar, P., Sri, M.H. & Sree, K.P.N.V.S. (2011). Analysis of physico-chemical parameters of water quality in and around Saltpans of Prakasam (Dt.) A.P. *Journal of Ecobiotechnology*, *3*(10), 1-6.

Lumb, A., Halliwell, D. & Sharma, T. (2006). Application of CCME Water Quality Index to monitor water quality: a case study of the Mackenzie river basin, Canada. *Environmental Monitoring and Assessment*, *113*(1), 411-429. https://doi.org/10.1007/s10661-005-9092-6

Mahagamage, M.G.Y.L. & Manage, P.M. (2014). *Water Quality Index (CCME-WQI) based assessment study of water quality in Kelani river basin, Sri Lanka*. The 1st Environment and Natural Resources International Conference. Bangkok, Thailand, 6-7.11.2014.

Mena-Rivera, L., Salgado-Silva, V., Benavides--Benavides, C., Coto-Campos, J.M. & Swinscoe, T.H.A. (2017). Spatial and seasonal surface water quality assessment in a tropical urban catchment: Burío River, Costa Rica. *Water*, *9*(8), 558. https://doi.org/10.3390/w9080558

Michalski, R. & Kurzyca, I. (2006). Determination of nitrogen species (nitrate, nitrite and ammonia ions) in environmental samples by ion chromatography. *Polish Journal of Environmental Studies*, *15*(1), 5-18.

Munna, Md.G., Chowdhury, M., Ahmed, A.A., Chowdhury, S. & Alom, Md.M. (2013). A Canadian Water Quality Guideline-Water Quality Index (CCME-WQI) based assessment study of water quality in Surma river. *Journal of Civil Engineering and Construction Technology*, *4*(3), 81-89. https://doi.org/10.5897/JCECT12.074

Nas, S.S., Bayram, A., Nas, E. & Bulut, V.N. (2008). Effects of some water quality parameters on the dissolved oxygen balance of streams. *Polish Journal of Environmental Studies*, *17*(4), 531-538.

Nollet, L.M.L. (ed.) (2004). *Handbook of water analysis*. Boca Raton: CRC Press.

Ott, W.R. (1978). *Water Quality Index. A survey of indices used in the United States*. Washington: Environmental Protection Agency.

Panduranga Murthy, G., & Hosmani, S.P. (2009). *Water Quality Index (WQI) to evaluate surface water quality for protection of aquatic life: a case study: Bherya Lake, Mysore, Karnataka State, India*. 13th World Lake Conference. Wuhan, China, 01-05.11.2009.

Phadatare, S.S. & Gawande, S. (2016). Review paper on development of Water Quality

Index. *International Journal of Engineering and Technical Research*, *5*(5), 765-767.
Rabee, A.M., Abdul-Kareem, B.M. & Al-Dhamin, A.S. (2011). Seasonal variations of some ecological parameters in Tigris river water at Baghdad Region, Iraq. *Journal of Water Resource and Protection*, *3*(4), 262-267.
Rajankar, P.N., Gulhane, S.R., Tambekar, D.H., Ramteke, D.S. & Wate, S.R. (2009). Water quality assessment of groundwater resources in Nagpur Region (India) Based on WQI. *E--Journal of Chemistry*, *6*(3), 905-908. https://doi.org/10.1155/2009/971242
Reza, R. & Singh, G. (2010). Assessment of ground water quality status by using Water Quality Index Method in Orissa, India. *World Applied Sciences Journal*, *9*(12), 1392-1397.
Saeedrashed, Y. & Guven, A. (2013). Estimation of geomorphological parameters of lower Zab river-basin by using GIS-based remotely sensed image. *Journal of Water Resource Management*, *27*(1), 209-2019.
Schultz, M.T. (2001). A critique of EPA's index of watershed indicators. *Journal of Environmental Management*, *62*(4), 429-442. https://doi.org/10.1006/jema.2001.0451
Shahin, M. (2007). *Water resources and hydrometeorology of the Arab Region*. Dordrecht: Springer Netherlands.
Shiklomanov, I. (1993). World fresh water resources. In P. Gleick (ed.), *Water in crisis: a guide to the world's fresh water resources* (pp. 13-24). Oxford: Oxford University Press.
Srivastava, G. & Kumar, P.R. (2013). Water Quality Index with missing parameters. *International Journal of Research in Engineering and Technology*, *2*(4), 609-614. https://doi.org/10.15623/ijret.2013.0204035
Turner, R.E. & Rabalais, N.N. (2003). Linking landscape and water quality in the Mississippi river basin for 200 years. *BioScience*, *53*(6), 563-572. https://doi.org/10.1641/0006-3568(2003)053[0563:llawqi]2.0.co;2
Tyagi, S., Sharma, B., Singh, P. & Dobhal, R. (2013). Water quality assessment in terms of Water Quality Index. *American Journal of Water Resources*, *1*(3), 34-38.
Verma, S.R., Sharma, P., Tyagi, A., Rani, S., Gupta, A.K. & Dalela, R.C. (1984). Pollution and saprobic status of Eastern Kalinadi. *Limnologia (Berlin)*, *15*, 69-133.
Witek, Z. & Jarosiewicz, A. (2009). Long-term changes in nutrient status of river water. *Polish Journal of Environmental Studies*, *18*(6), 1177-1184.
World Health Organization [WHO] (2001). *WHO World Water Day Report*. Geneva: WHO.
World Health Organization [WHO] (2017). *Guidelines for drinking water quality*. Geneva: WHO.
Yang, Y.S. & Wang, L. (2010). Catchment-scale vulnerability assessment of groundwater pollution from diffuse sources using the DRASTIC method: a case study. *Hydrological Sciences Journal*, *55*(7), 1206-1216. https://doi.org/10.1080/02626667.2010.508872

Summary

Assessment of Lower Zab river water quality using both Canadian Water Quality Index Method and NSF Water Quality Index Method. Rivers are considered the most important sources of surface water on Earth. They are play a significant role in all human activities and the quality of river water is needed. Therefore, the importance of the water quality index is arising through providing data base about quality of the water source, and explain the change in the water quality over a period of time continually. This study involved determination of physicochemical and biological parameters of Lower Zab river in Kirkuk city at two different points. The objectives of the study are to assess the present water quality, through analysis of some selected water quality parameters like pH, TDS, BOD, dissolved oxygen, turbidity, EC, alkalinity, and salinity etc. and to compare the results with the Canadian Council of Ministers of the Environment and National Sanitation Foundation Water Quality Indices. Raw water samples were collected from the Lower Zab river twice a month by one sample every 15 days from each station. The water quality data include 16 different parameters. Tests were carried out following the American Public Health Association standard methods. The results

show that all parameters values were within the standards of drinking water proposed by the CCME standards and Iraqi standards or the World Health Organization standards for drinking purpose, except turbidity, DO, nitrate, calcium, which were mostly higher than the standards and sometimes BOD and potassium. The results of WQI showed that the water quality at LZ3 station is lower than LZ2 station due to the polluting activity of the Lower Zab river. Furthermore, for the years 2014, 2015, and 2016, the water quality was degraded due to the ISIS war. Also, it was noted in the 2013 year that the water quality degraded more in fall and winter seasons due to that the earth has exposed to the long-dried season and then suddenly exposed to a high rainfall season which in turns leads to increase some parameters very high (i.e. turbidity). Finally, the Lower Zab river water cannot be use for drinking directly. However, a pretreatment is needed before the drinking use.

Authors' address:
Sarah Mustafa Ahmed
(https://orcid.org/0000-0002-0965-3433)
University of Kirkuk
Environmental Research Unit
36013, Kirkuk, Iraq
e-mail: sarahmustafa@uokirkuk.edu.iq

Omer Muhie Eldeen Taha
(https://orcid.org/0000-0003-4922-7778)
University of Kirkuk
Department of Civil Engineering
36013, Kirkuk, Iraq
e-mail: omer.muhie@uokirkuk.edu.iq

Scientific Review – Engineering and Environmental Sciences (2020), 29 (2), 172–183
Sci. Rev. Eng. Env. Sci. (2020), 29 (2)
Przegląd Naukowy – Inżynieria i Kształtowanie Środowiska (2020), 29 (2), 172–183
Prz. Nauk. Inż. Kszt. Środ. (2020), 29 (2)
http://iks.pn.sggw.pl
DOI 10.22630/PNIKS.2020.29.2.15

Mohammed Fakhraldeen AHMED, Raid Mahmood FAISAL
Mosul University, Collage of Environmental Sciences and Technology

GIS based modeling of GWQ assessment at Al-Shekhan area using AHP and SAW techniques

Key words: AHP, SAW, GWQ, Al-Shekhan area, GIS based model

Introduction

Groundwater Quality (GWQ) determination of human consumption is necessary for a healthy living (Ishaku, 2011). There is a shortage of papers published in regard of GWQ at Nineveh governorate, Iraq, nevertheless a rapid review of research concerning similar cases studying GWQ in other areas.

Al-Hayali (2010) studied GWQ of 16 wells distributed in Mosul city, Iraq during 2008 along four months. The results show that GWQ of the wells were unsuitable for drinking purposes but it was suitable only for plants resistant to saline water.

Mukheef, Al-Kubaisi and Rasool (2019) assessed the GWQ in Baghdad Province for irrigation purposes by using WQI. The results show that there is an increase of Cl, K, and Ca ions in water samples, and that GWQ is very poor in the middle part of the studied area while it is moderate in the western part for the irrigation purpose.

Gorgij, Kisi, Moghaddam and Taghipour (2017) assessed GWQ of 21 samples at Azarshahr Plain, Iran for drinking purposes by using the entropy technique which extracts the weights needed in determining the Water Quality Index (WQI). The results show that the GW samples are classified as good to poor, and bicarbonate ion is the most effective parameter.

Rao, Venkatesch and Ahmed (2018) studied GWQ of 30 wells in Guntur District Andhra Pradesh-India. Inverse Distance Weighted IDA technique was used to determine the spatial distribution of the GW parameters. The results show that most of GWQ which is located in the western parts of the district is not suitable for drinking purposes, while the eastern part of the district had the most suitability zones for different purposes.

Al-Ozeer and Ahmed (2019) assessed 18 shallow wells for different purposes at east side of Mosul city using SAW technique. The research included an application of Groundwater Modeling System (GMS 10.1) to create the studied area sub-layers as three dimension map. The results show that GWQ is suitable for livestock purposes.

Ochungo, Ouma, Obiero and Odero (2019) studied samples of 39 wells to assess their suitability for drinking purpose in Langata, Kenya. The research concluded that there is no indication of surface water percolation due to low concentrations of SO_4 and Cl ions.

Minh et al. (2019) developed WQI by founding the weight of parameters depends on fuzzy-AHP techniques of shallow wells during 10 years in Giang Province, Vietnam. The research concluded that GWQ in areas located in the Northeast of Giang had very bad quality because of both human activities and natural reasons.

Ibe, Aigbedion, Marcellinus, Okoli and Sola (2019) studied the physical and chemical properties of GW samples from 45 wells for drinking purposes at Ado-Ekiti State, Nigeria, using WQI and Arc GIS. The results show that 34 wells were suitable, while the rest were unsuitable. The research ranked WQ in the studied area as best in the north-west, fair in south east, and very poor in the south.

This study aims to assess GWQ of Al-Shekhan area by the help of AHP, SAW techniques and Arc GIS version 10.5 to build a model which serves this aim, and can be a raw model to be applied to assess GWQ in any other area after inserting the values of their parameters.

Material and techniques

The studied area

Al-Shekhan area is located in the north eastern of Mosul city, Iraq between 36°44′57″ to 36°29′6″ N latitudes and between 43°12′28″ to 43°31′10″ E longitude with 30 wells to be examined, as in Figure 1.

Data analysis

Eleven parameters are experimentally analyzed based on APHA, AWWA, WEF (2005) measurements and compared with international standards (WHO, 2003; EPA, 2004), as in Table 1. Data of parameters is tabulated in Table 2.

The used techniques

Analytical Hierarchical Process

AHP technique was firstly developed by (Saaty, 1980, 2008). This technique can be used in different applications (Faisal & Ahmed, 2018). This technique uses pair wise comparison to derive the relative weights of parameters. Three steps are used in this technique; the extracted parameters are organized and given certain importance degree in the first step. Then, a matrix of the selected relative weights is adopted in the second step. At last, the consistency ratio (CR) is applied to check the importance degree. If CR $\leq$ 0.1, there is no need for reweighting. The scale of relative importance for pair wise comparison is arranged as a scale from 1 to 9, where 1 represents equal importance while 9 represents extreme importance.

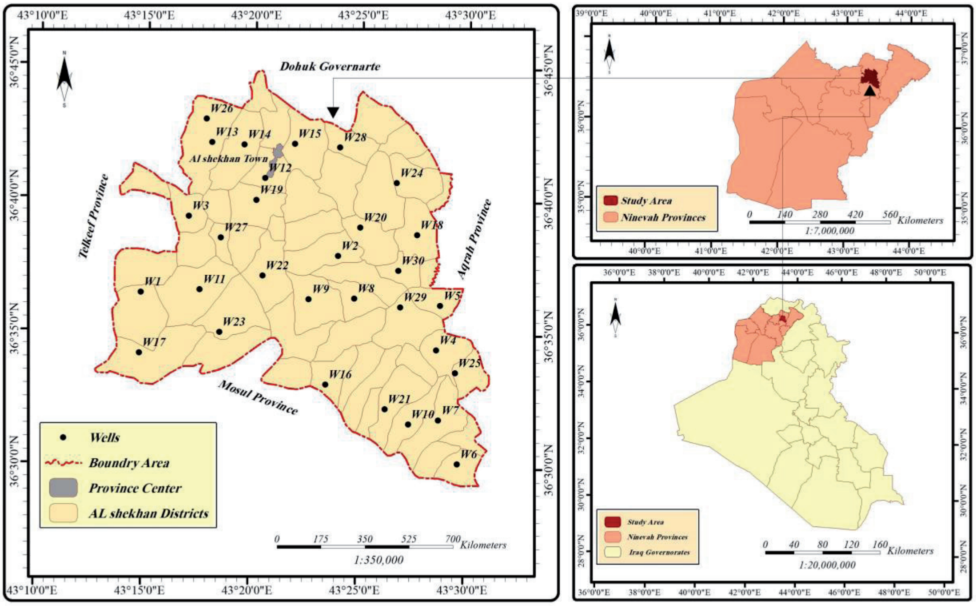

FIGURE 1. Location of the studied area

TABLE 1. Parameters international standards

Drinking parameters	Drinking standards (EPA, 2004)	Irrigation parameters	Irrigation standards (EPA, 2004)	Livestock parameters	Livestock standards (WHO, 2003)
Ca^{2+}	75 $mg \cdot l^{-1}$	Na^{+}	200 $mg \cdot l^{-1}$	TDS	10 000 $mg \cdot l^{-1}$
Mg^{2+}	100 $mg \cdot l^{-1}$	HCO_3^{-}	350 $mg \cdot l^{-1}$	EC	12 500 $mg \cdot l^{-1}$
Na^{+}	200 $mg \cdot l^{-1}$	SAR	15 $meq \cdot l^{-1}$	pH	6.5–8.5
HCO_3^{-}	400 $mg \cdot l^{-1}$	Cl^{-}	250 $mg \cdot l^{-1}$	NO_3^{-}	440 $mg \cdot l^{-1}$
SO_4^{2-}	250 $mg \cdot l^{-1}$	B	0.7 $mg \cdot l^{-1}$	SO_4^{2-}	250 $mg \cdot l^{-1}$
Cl^{-}	250 $mg \cdot l^{-1}$	TDS	1 750 $mg \cdot l^{-1}$	×	×
NO_3^{-}	10 $mg \cdot l^{-1}$	pH	6.5–8.5 $mg \cdot l^{-1}$	×	×
TDS	500 $mg \cdot l^{-1}$	EC	2 700 $\mu hos \cdot cm^{-1}$	×	×
pH	6.5–8.5	×	×	×	×
EC	2 000 $\mu hos \cdot cm^{-1}$	×	×	×	×

TABLE 2. Studied wells parameter’s data

Well	Depth	Ca	Mg	Cl	Na	SAR	SO_4	HCO_3	NO_3	TDS	EC	pH
	m	$mg \cdot l^{-1}$				$meq \cdot l^{-1}$	$mg \cdot l^{-1}$				$\mu hos \cdot cm^{-1}$	-
1	100	18.0	4.0	37.0	20.0	1.11	10.0	50	0.3	226	550	8.6
2	203	135.0	73.0	280.0	175.0	3.02	160.0	370	2.4	1 890	3 270	8.0
3	144	28.0	8.0	60.0	30.0	1.29	23.0	70	0.3	276	475	8.6
4	200	24.0	28.2	17.0	94.0	3.1	285.0	147	176.0	494	761	8.9
5	120	19.2	25.3	15.0	13.0	0.46	225.0	288	152.0	228	305	8.8
6	183	30.9	3.9	19.9	200.0	9.05	76.9	319	6.6	450	603	7.2
7	156	48.0	23.0	5.0	22.0	0.64	28.0	280	2.0	260	425	8.1
8	185	24.0	42.9	31.0	92.0	2.59	97.5	241	1.2	356	571	8.2
9	200	19.3	38.0	17.0	66.0	2.00	76.0	292	1.9	592	703	7.5
10	156	27.3	32.2	5.0	7.8	0.24	21.8	226	3.1	355	468	7.0
11	156	32.1	24.3	18.9	52.0	1.68	35.4	273	2.7	455	577	7.8
12	168	90.0	52.6	40.0	26.0	0.53	44.2	478	3.14	769	863	7.1
13	160	46.5	12.6	2.0	14.0	0.46	6.0	219	3.89	334	353	6.9
14	150	62.6	4.87	3.0	15.0	0.48	10.3	224	2.75	326	335	7.1
15	150	27.3	34.1	3.0	21.0	0.63	11.7	258	2.19	368	393	7.2
16	150	57.8	21.4	3.0	6.0	0.17	21.2	258	1.50	387	446	8.1
17	180	59.4	61.4	20.0	17.0	0.32	157.0	253	1.10	610	945	7.3
18	149	321.0	117.0	26.0	17.0	0.20	954.0	219	0.36	1 663	1 890	7.6
19	152	35.3	41.4	12.0	11.0	0.29	55.7	248	1.59	405	527	7.8
20	123	32.0	28.0	18.0	34.0	5.01	40.0	170	50.0	335	608	8.1
21	49	40.0	28.0	11.0	56.0	7.62	48.0	246	10.0	285	480	7.1
22	134	44.0	33.0	15.0	48.0	0.00	43.0	322	0.0	376	620	8.1
23	47	19.0	11.0	66.0	100.0	20.20	24.0	290	0.0	334	650	8.0
24	75	47.0	38.0	20.0	46.0	5.66	91.0	251	2.0	424	677	8.2
25	61	52.0	23.0	9.0	21.0	2.63	34.0	254	2.0	272	377	7.8
26	104	28.0	29.0	4.0	2.0	0.30	19.0	159	18.0	199	294	8.3
27	55	48.0	29.0	15.0	58.0	7.33	99.0	230	8.0	392	597	8.0
28	104	132.0	76.0	19.0	35.0	2.68	238.0	299	34.0	769	1 450	6.8
29	73	24.0	34.0	23.0	18.0	2.81	10.0	250	0.0	221	430	7.6
30	76	44.0	34.0	14.0	28.0	3.58	38.0	311	19.0	331	490	7.7

Tripych worksheet

Tripych is an Excel add-in tool that is part of the Statistical Design Institute (StatDesign, 2018) which is used to prioritize items by performing AHP matrix of the parameters. The yielded results are tabulated in Tables 3, 4, and 5.

Simple Additive Weighting technique

Simple Additive Weighting technique is used firstly by McDuffie and Haney in 1973 to summarize the huge data into one index. In this simple technique, relative weights which are extracted from AHP are multiplied by quality rating scale to calculate the sub-index for each parameter. The following equation illustrates the calculation of quality rating (Qr) which is computed by dividing the concentration of each parameter (Ci) to its standard value (S), as follows: $Qr = Ci / S$. Summation of the sun-indices gives the final index. This final index classifies water quality into five categories: 0–25 excellent, 26–50 good, 51–75 poor, 76–100 very poor, and unsuitable if the index is more than 100. The indices' results of the three purposes are tabulated in Table 6.

Geographic Information System

ARC GIS 10.5 is used to create all the suitability maps for each purpose, then building a model through applying multiple tools and finally extracting the final map (Esri, 2016). Maps of each purpose were created by ArcGIS, as in Figures 2, 3 and 4.

TABLE 3. Tripych drinking water results, CR = 0.0479

		TDS	EC	SO_4	NO_3	Ca	Mg	Na	HCO_3	Cl	pH	Row total	Relative importance	Scaled importance
1	TDS	1	2	3	3	4	5	5	4	5	5	37.00	21.11%	5.00
2	EC	1/2	1	2	2	3	4	4	3	4	4	27.50	15.69%	3.87
3	SO_4	1/3	1/2	1	2	3	4	4	3	5	6	28.83	16.45%	4.03
4	NO_3	1/3	1/2	1/2	1	2	3	4	3	5	6	25.33	14.45%	3.61
5	Ca	1/4	1/3	1/3	1/2	1	2	2	2	3	4	15.42	8.80%	2.43
6	Mg	1/5	1/4	1/4	1/3	1/2	1	2	0.5	3	4	12.03	6.87%	2.02
7	Na	1/5	1/4	1/4	1/4	1/2	1/2	1	0.5	2	3	8.45	4.82%	1.60
8	HCO_3	1/4	1/3	1/3	1/3	1/2	2	2	1	2	3	11.75	6.70%	1.99
9	Cl	1/5	1/4	1/5	1/5	1/3	1/3	1/2	1/2	1	2	5.52	3.15%	1.25
10	pH	1/5	1/4	1/6	1/6	1/4	1/4	1/3	1/3	1/2	1	3.45	1.97%	1.00

TABLE 4. Tripych irrigation results, CR = 0.0763

		TDS	EC	Na	HCO_3	Cl	pH	B	SAR	Row total	Relative importance	Scaled importance
1	TDS	1	2	4	4	3	4	3	2	23.00	24.78%	5.00
2	EC	1/2	1	3	4	3	3	2	2	18.50	19.93%	4.07
3	Na	1/4	1/3	1	2	2	3	2	1	11.58	12.48%	2.65
4	HCO_3	1/4	1/4	1/2	1	2	3	2	0.5	9.50	10.23%	2.22
5	Cl	1/3	1/3	1/2	1/2	1	2	2	3	9.67	10.41%	2.25
6	pH	1/4	1/3	1/3	1/3	1/2	1	0.5	0.33	3.58	3.86%	1.00
7	B	1/3	1/2	1/2	1/2	1/2	2	1	0.33	5.67	6.10%	1.43
8	SAR	1/2	1/2	1	2	1/3	3	3	1	11.33	12.21%	2.60

The results

Figure 2 illustrates the suitability of drinking water purpose where the higher class ranges between 19.27 and 25, which is located in the north western part of the studied area, and lower class is 87.5–100, which is located in the north eastern part of the studied area. Figure 3 shows the suitability of irrigation purpose where the higher class ranges between 16 and 20, which is located in the north western part of the studied area and lower class is 40–45, which is located in the south eastern part of the studied area. Figure 4 illustrates the suitability of livestock purpose where the higher class ranges between 9.2 and 15 including the whole studied area except the eastern part which is considered as the lower class with 25–30. All relative weights and indices extracted from AHP and SAW respectively, in addition to Figures 2, 3, and 4 are utilized to build a model.

Model building

A model is built using ArcGIS and its primary tools as "Add field", "Calculated field", and "Kernel"; while the secondary tools are: "Reclassify", "Raster to vector", "Clip", "Union overlay", and "Select by attribute", as in Figure 5. This model utilizes the importance scale of parameters, the relative weights indices, and area suitability maps to create the final map which represents an overall reference combining the suitability of water for the three purposes.

Final map

The final map is created by using union tool within GIS overlay mapping tools, as clarified in Figures 5 and 6.

TABLE 5. Tripych livestock results, CR = 0.0204

		TDS	EC	pH	NO_3	SO_4	Row total	Relative importance	Scaled importance
1	TDS	1	2	4	3	3	13.00	37.96%	5.00
2	EC	1/2	1	3	2	2	8.50	24.82%	3.27
3	PH	1/4	1/3	1	0.5	0.5	2.58	7.54%	1.00
4	NO_3	1/3	1/2	2	1	0.5	4.33	12.65%	1.67
5	SO_4	1/3	1/2	2	2	1	5.83	17.03%	2.25

TABLE 6. GWQIs of each purpose

Well	Drinking Index	DGWQ	Irrigation Index	IGWQ	Livestock Index	LGWQ
1	19.2	excellent	18	excellent	10.7	excellent
2	137.3	unsuitable	92.7	very poor	25	excellent
3	22.7	excellent	21.7	excellent	11	excellent
4	50	good	32	good	22.2	excellent
5	36	good	21.2	excellent	18.5	excellent
6	39.6	good	45.3	good	11.6	excellent
7	26.5	good	23.5	excellent	10.5	excellent
8	36.2	good	30.7	good	12.4	excellent
9	45.1	good	32.3	good	12.5	excellent
10	28	good	19.8	excellent	9.7	excellent
11	36.3	good	29	good	11.4	excellent
12	59.1	poor	38	good	12.6	excellent
13	26.6	good	19.8	excellent	9.2	excellent
14	26.5	good	18.9	excellent	9.2	excellent
15	29.1	good	22.4	excellent	9.6	excellent
16	31.2	good	21.1	excellent	10.9	excellent
17	50.6	good	29	good	14.2	excellent
18	150	unsuitable	51.5	poor	33.6	good
19	34	good	24.3	excellent	11.4	excellent
20	32.6	good	25	good	12.7	excellent
21	34.6	good	28.7	good	10.2	excellent
22	34.6	good	27.8	good	11.5	excellent
23	31.3	good	34.5	good	11	excellent
24	38.8	good	30.6	good	12.8	excellent
25	26.5	good	20.7	excellent	10.2	excellent
26	23.4	excellent	16	excellent	10.5	excellent

TABLE 6 cont.

Well	Drinking Index	DGWQ	Irrigation Index	IGWQ	Livestock Index	LGWQ
27	38.3	good	26.4	good	12.6	excellent
28	80.4	very poor	38.8	good	17.6	excellent
29	22.5	excellent	22	excellent	9.5	excellent
30	36.6	good	27.4	good	11.1	excellent

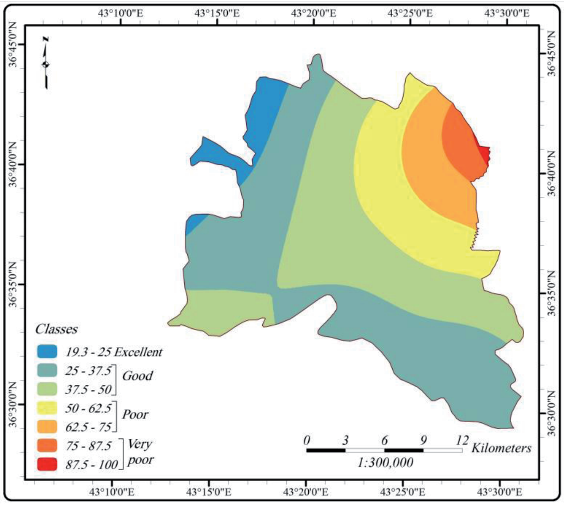

FIGURE 2. Drinking water suitability classes

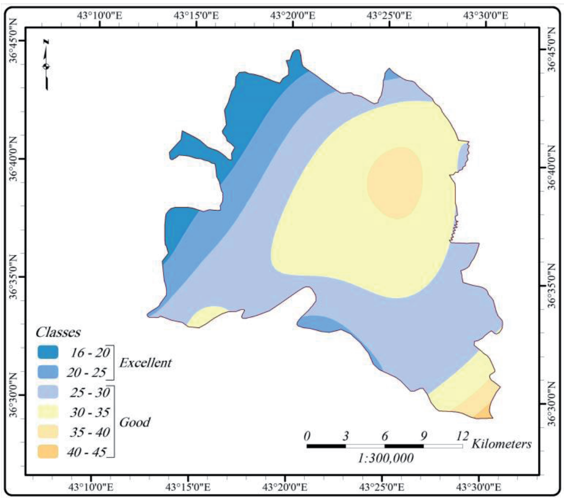

FIGURE 3. Irrigation water suitability classes

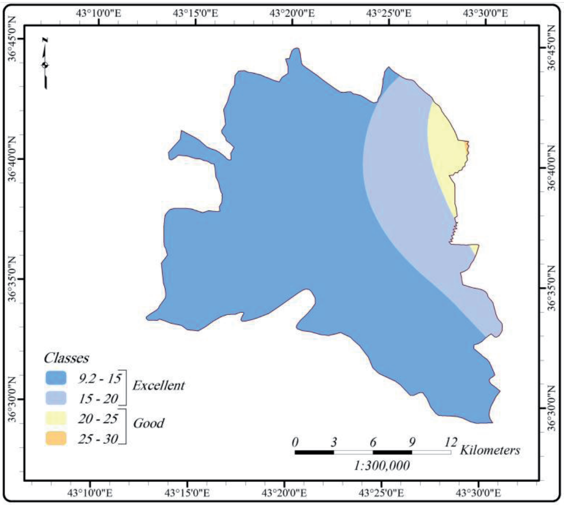

FIGURE 4. Livestock suitability classes

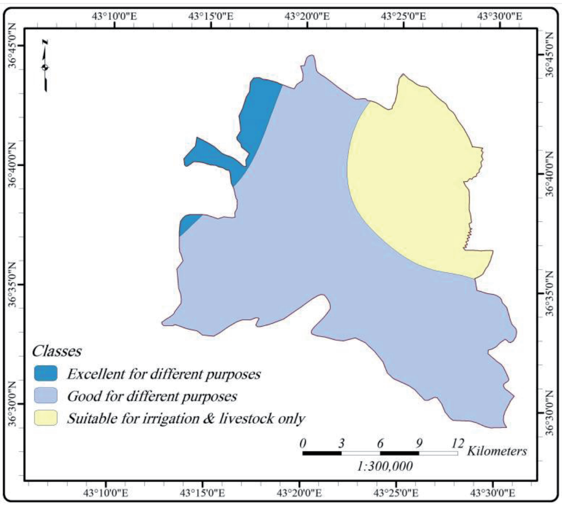

FIGURE 6. The final map

This map shows that the first part 4.6% of the study area which is located in the western part is excellent for the three purposes. The central large part which represents 70% of the study area is good for the three purposes. The eastern part of the studied area occupies the last class which represents 25.4% of the study area which is only suitable for irrigation and livestock purposes.

The discussion

To the best of the knowledge of the authors of this study, there is no previous work that build a model based on both

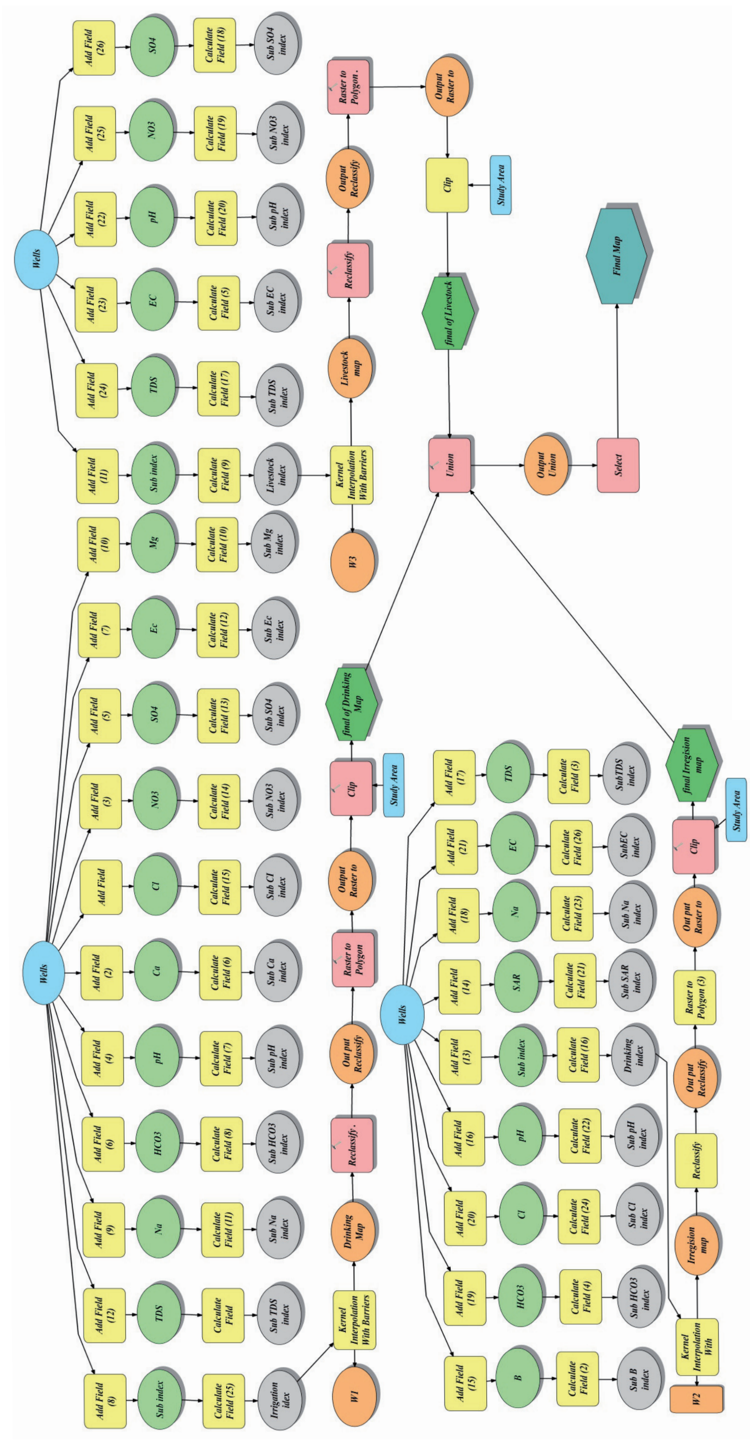

FIGURE 5. The model building

ArcGIS and AHP to assess groundwater quality. Therefore, the concluded model can be conducted to create a detailed map of classes of water suitability after applying the relevant parameters.

Conclusions

The use of AHP and SAW are useful to determine the relative weights and indices of the parameters. ArcGIS utilizes the combination of the relative weights and indices in addition to water suitability maps to create a model. The model identifies water quality in the study area and is considered as a database for future agricultural and developmental projects. The final map illustrates that GWQ can be classified according to its indices, where all wells are suitable for multipurposes except wells (18, 24, and 28), as in Figure 1, which are appropriate for irrigation and livestock only.

Acknowledgements

The authors are very grateful to the College of Environmental Sciences and Technology of the University of Mosul for their provided facilities, which helped to improve the quality of this work.

References

Al-Hayali, A.K. (2010). Studying groundwater quality in Mosul City and its suburb and its suitability for drinking and irrigation. *Journal of Education and Science*, *23*(3), 48-67.

Al-Ozeer, A.Z. & Ahmed, M.F. (2019). Groundwater assessment at east side of Mosul City during 2014–2017. *Scientific Review – Engineering and Environmental Sciences*, *28*(1), 35-48. DOI 10.22630/PNIKS.2019.28.1.4

American Public Health Association [APHA], American Water Works Association [AWWA], Water Environment Federation [WEF] (2005). *Standard methods for the examination of water and wastewaters*. Washington, DC: APHA.

Environmental Protection Agency [EPA] (2004). *Guidelines for water reuse*. Washington, DC: Environmental Protection Agency and U.S. Agency for International Development.

Esri (2016). *Arc GIS 10.5.0.6491*. Retrieved from: www.esri.com

Faisal, R.M. & Ahmed, M.F. (2018). GIS and AHP based modeling for landfill site selection (case study: west side of Mosul city). *Scientific Review – Engineering and Environmental Sciences*, *27*(4), 425-437.

Gorgij, A.D., Kisi, O., Moghaddam, A.A., Taghipour, A. (2017). Groundwater quality ranking for drinking purposes, using the entropy technique and the spatial autocorrelation index. *Environmental Earth Science*, *76*(7), 269. DOI 10.1007/s12665-017-6589-6

Ibe, P.I., Aigbedion, I.P., Marcellinus, M., Okoli, F.U. & Sola, A.B. (2019). Assessment of water quality index for groundwater in Ado Ekiti, Nigeria. *Journal of World News of Natural Sciences (WNOFNS)*, *22*, 93-101.

Ishaku, J.M. (2011). Assessment of groundwater quality index for Jimeta-yola area, north eastern Nigeria. *Journal of Geology and Mining Research*, *3*(4), 219-231.

McDuffie, B. & Haney, J.T. (1973). *A proposed river pollution index*. Spring 1973 Meeting of the American Chemical Society, Division of Water, Air and Waste Chemistry.

Minh, H.V., Avtar, R., Kumar, P., Tran, D.Q., Ty, T.V., Behera, H.C. & Kurasaki, M. (2019). Groundwater quality assessment using fuzzy--AHP in An Giang Province of Vietnam. *Journal of Geosciences*, *9*(8), 330. DOI 10.3390/ geosciences 9080330

Mukheef, R.A., Al-Kubaisi, A.A. & Rasool, M.H. (2019). Evaluating the groundwater suitability for a number of wells in Baghdad province for irrigation. *International Journal of Civil Engineering and Technology*, *10*(1), 1186-1204.

Ochungo, E.A., Ouma, G.O., Obiero, J.P.O. & Odero, N.A. (2019). Water Quality Index for assessment of potability of groundwater resource in Langata Sub County, Nairobi-Kenya. *American Journal of Water Resources*, *7*(2), 62-75.

Rao, K.T.V.S., Venkatesh, D.V. & Ahmed, S.F. (2018). Assessment and comparison of ground water quality in Guntur District, Andhra Pradesh by using ARC GIS. *International Journal of Innovative Science and Research Technology*, *3*(4), 201-213.

Saaty, T.L. (1980). *The analytic hierarchy process*. New York: McGraw-Hill.

Saaty, T.L. (2008). Decision making with the analytic hierarchy process. *International Journal of Sciences*, *1*(1), 83-98.

StatDesign (2018). *SDI tools 4.11.1*. Retrieved from: https//stat-design.com

World Health Organization [WHO]. (2003). *Guideline for drinking-water quality*. Geneva: WHO.

Summary

GIS based modeling of GWQ assessment at Al-Shekhan area using AHP and SAW techniques. There is a continuous need to assess Groundwater Quality (GWQ) for human beneficial uses especially in areas suffering a shortage of nearby surface water. This study aims to assess GWQ of 56 wells located at Al-Shekhan area for drinking, irrigation, and livestock purposes. Analytical Hierarchical Process (AHP) technique is used to extract weights of parameters that are needed in the calculation of Simple Additive Weighting (SAW) technique. Maps are created using Geographical Information Systems (GIS), and these maps shows the classes of suitable areas for each purpose depending upon the calculated indices which are extracted from SAW technique. The results show that the final map classifies the suitable parts according to the drinking, irrigation and livestock purposes, and it shows that the north eastern part of the studied area is suitable for irrigation and livestock only. A model of GIS and AHP is built to assess the suitability of GWQ in Al-Shekhan area, and can be a raw model to be applied to assess GWQ in any other area after inserting the values of their parameters.

Authors' address:
Mohammed Fakhraldeen Ahmed
(https://orcid.org/0000-0003-0414-0509)
Raid Mahmood Faisal al-Moula
Mosul University
Collage of Environmental Sciences
and Technology
Department of Environmental Technology
42001, Mosul, Iraq
e-mail: mfakher1962@gmail.com
raidalfaisal2017@yahoo.com

Scientific Review – Engineering and Environmental Sciences (2020), 29 (2), 184–195
Sci. Rev. Eng. Env. Sci. (2020), 29 (2)
Przegląd Naukowy – Inżynieria i Kształtowanie Środowiska (2020), 29 (2), 184–195
Prz. Nauk. Inż. Kszt. Środ. (2020), 29 (2)
http://iks.pn.sggw.pl
DOI 10.22630/PNIKS.2020.29.2.16

Ibtihaj S. ABDULFATTAH[1], Jasim M. RAJAB[2, 3], Ali M. Al-SALIHI[2], Aha SULIMAN[3], Hwee San LIM[4]

[1] Mustansiriyah University Presidency, Division of Human resources
[2] Mustansiriyah University, College of Science
[3] University of Al-Hamdaniya, Laser and Photonics Research Center
[4] Universiti Sains Malaysia, School of Physics

Observed vertical distribution of tropospheric carbon monoxide during 2012 over Iraq

Key words: AIRS, remote sensing, pollution, carbone monoxide, Iraq

Introduction

Both as an air pollutant and as a significant in atmospheric chemistry, the CO is an efficient research topic entails accurate representation of the magnitude and location of CO surface emissions (Fortems-Cheiney et al., 2011). The CO is regulated as the Environmental Protection Agency (EPA) specification pollutant due to of its lineal adverse effectiveness on human health. It emitted by incomplete combustion of hydrocarbons and industrial operations to the atmosphere such as iron smelting (Al-Bayati & Al-Salihi, 2019). It importantly affects the OH budget, and thus secondarily impacts the ozone (O_3) and methane (CH_4) concentrations. The CO affecting air quality and climate, and acts as a serious indirect greenhouse gases (GHGs) because of it does not absorb terrestrial thermal infrared (IR) from the Earth. These is due to the CO distinctive by indirect radiative forcing raises and effect the troposphere CH_4 and O_3 measurements through chemical reactions with other atmospheric constituents (Rajab, Jafri, Lim & Abdullah, 2011; Herron-Thorpe et al., 2012; Faten, 2018). The two largest surface sources of CO are the fossil fuel and combustion of biomass. In general, agreed the biomass burning accounts almost one quarter of CO emission to the atmosphere (Pétron et al., 2004). Carbone monoxide molecular have a global-average lifetime of about two months and it weight is close to that of air. Unpredictability in the CO budget are still rightly large due to distress in quantify the variability of CO sources and sinks, because of the lack of emissions statistics and quantification used to derive emissions inventories (Drori et al., 2012).

Although the aircraft-mounted and ground-based devices are able to make precise observations of CO measurements in the troposphere, they are not able to provide large-scale global or regional coverage. Only the space observations allow such measurements (in the absence of cloud) to be made over a rationally short time period. Over the past decade IMG (Interferometer Monitor for Greenhouse Gases) (Kobayashi et al., 1999), MOPITT (Measurements of Pollution in the Troposphere) (Deeter et al., 2010), TES (Tropospheric Emission Spectrometer) (Bowman et al., 2006; Luo et al., 2007) and AIRS (Automated Import Reference System) (McMillan et al., 2003). Sensors have all successfully implemented measurements in the 4.7 μm spectral band to increase the vertical information content of profiles and also global coverage as well as cost so much money and arduous efforts (Illingworth et al., 2011).

The satellite remote sensing provide good global coverage and quantitatively data with crucial temporal or spatial resolution, and boost the researcher ability to understand the impact of human activities on the chemical composition of the atmosphere and climate change. Also, the free download satellite information provided by AIRS website. Therefore, the scientists have explored its use in studying fire emission and biomass burning. Parameters deduced from satellite data include aerosol index, fire counts, biomass density, and fire counts. Using these parameters from satellite data, the CO emission has been indirectly estimated from vegetation fires (Rajab, Jafri, Lim & Abdullah, 2012). The Aqua satellite put to space aboard Aqua satellite by the NASA on 4 May 2002 provide vertical profiles of the atmosphere with a nadir 45 km field-of--regard (FOR) across a 1650 km swath. The AIRS have wide spectral coverage (3.7–16 μm with 2,378 channels) comprises spectral features of O_3, CH_4, CO, and CO_2. The AIRS observe the CO total column by 36 channels with vertical encasement 1,000–1 mb. The troposphere CO multitude is restore in the 4.58–4.50 μm (2,180–2,220 cm^{-1}) area from AIRS observed radiances of IR spectrum (Chahine et al., 2006; Rajab, Hassan, Kadhum, Al-Salihi & Hwee, 2020).

In this study we present the AIRS vertical (seven levels CO) profile observations of troposphere CO obtained during the year 2012. The restored AIRS monthly L3 product V5 measurements were utilized. We show the temporal and vertical distribution of troposphere CO across Iraq for five locations; Baghdad, Basra Mosul, Al Fakka, and Maysan, in study period. The seven layers monthly CO MVR was produced using kriging interpolation technique to analyses its allocation over study area during 2012. With AIRS observations, spatial and temporal differences of CO emission able are examined directly and separately from other approaches over various areas.

Material and methods

Study area and climate features

Iraq, located in the western part of Asia and mainly occupies the Mesopotamian Plain, located, between 39° and 49° E longitudes (a small area lies west of 39°) and 29° and 38° N latitudes. At the north, Iraq borders by Turkey, Kuwait and Saudi Arabia at south, Syria at northwest, Iran at east, and Jordan at southwest. Iraq country involves of 437,072 km^2 by 18 states; it is the 58^{th} biggest country in the world (Faten, 2018; Al-Salihi, Rajab & Salih, 2019).

The Iraqi Meteorological and Seismology Organization (IMSO) divide Iraq into four regions according to geological, meteorological and hydrological characteristics as follows:

a) Northern Region bounded by longitudes 43.09 and 43.50° E, and latitudes 34.11 and 36.19° N.
b) Southern Region bounded by the longitudes of 44.45 and 48.50° E and latitudes 30.11 and 32.30° N.
c) Western Region bounded by longitudes 43.19 and 44.32° E and latitudes 30.30 and 33.15° N.
d) Central Region bounded by longitudes of 45.20 and 45.19° E, and latitudes 31.81 and 34.18° N.

Acquisition and specification

The data used in this study was acquired from AIRS Level-3 (L3) ascending data (NASA Earthdata, 2019). Generally, ascending granules L3 data downloaded for 12 months (January–December) to get the required output. The data are covering Iraq as a grid of 132 points extends from 28.5–49.5° N latitudes and 38.5–49.5° E longitudes with a uniform grid interval of 1° in longitude and 1° in latitude. In previous papers, we discussed the distribution of CO

FIGURE 1. The geographical attribute of study area (Rajab, Ahmed, & Moussa, 2013)

for different periods (2003–2016) over Iraq using spatial, temporal, and trends (Rajab et al., 2013; Salih, Al-Salihi & Rajab, 2018; Al-Salihi et al., 2019). To preferable exam the vertical distribution of CO VMR above Iraq for the study period the cross section, time–pressure of CO, mole fraction in air (daytime/ /ascending) monthly 1° (AIRS AIRX-3STM v006) over January–December 2012, Region 49E, 28N, 38E, and 49N map obtained from the NASA-operated GIOVANNI website. Seven atmospheric layers CO data used in this work with height and pressures are summarized in Table 1, for vertical analysis. In addition, surface CO values for time series distribution and comparison. The difficulty in obtaining the monthly ground CO data, due to Iraq circumstances, only Baghdad station CO data were collected from Iraqi Meteorological Office for compression and regression analysis with AIRS data during the period 2012. The simple linear regression is utilized to model the relationship between two singles, response and exploratory, variables y and x. The SigmaPlot software were used for this model between the ground and AIRS monthly CO values over Baghdad station; the model is

$$y_i = \hat{A}_0 + \hat{A}_1 x_i + \varepsilon_i$$

where:
(x_i, y_i), $i = 1, \dots, n$ – response and exploratory variables sample values,
$\hat{A}_0$ – intercept parameter,
$\hat{A}_1$ – slope parameter,
ε_i – random disturbance terms (Landau & Everitt, 2004).

In order to evaluate and investigate the seasonal change in troposphere CO emission, two steps were used to analyze the data. The first step is monthly basis file data, including the identical location and time in a HDF (hierarchical data format) format from AIRS website, and set out in table using MS Excel. In the second step the five dispersed locations were selected across Iraq (Baghdad, Mosul, Basra, Al Fakka and Maysan), as summarized in Table 1. Two graphs between CO with altitude, and troposphere CO with months for 2012, respectively, were designed to detect the seasonal change in CO values for the study period.

Results and discussion

The first analysis for the data showed that there is significant increase of maximum values of the troposphere CO in

TABLE 1. Height and pressure of the layers (left) and stations GMD (right)

Layer	Height [m]	Pressure [hPa]
0	13 500	155.625
1	11 000	253.5
2	8 500	351
3	5 820	505.25
4	3 100	706
5	1 450	850
6	750	930

Station	Longitude	Latitude
Baghdad	44.36 E	33.31 N
Mosul	43.16 E	36.35 N
Basra	47.78 E	30.50 N
Al Fakka	47.30 E	32.10 N
Maysan	47.10 E	31.50 N

March over all five locations. Figure 2 illustrates monthly troposphere CO from January to December 2012 for five locations; Baghdad, Basrah, Maysan, Al Fakka, and Mosul. The standard deviation of monthly troposphere CO was (107.15 ±18.75 ppbv) for the whole period. Elevation in troposphere CO observed along study period over the manufacturing and crowded urban zones, i.e. Baghdad, Mosul and Basra. The CO exposure differences seasonal alterations depend on whether circumstance and topography. The seasonal variations undulate between winters and summer seasons. A more certain inspections illustrate a spatial pattern subtle differences in the CO values for each season. A minimum value of the CO occurs in October. The seasonal differences are observable, but none are as declared during the study period.

The nominal summit of troposphere CO amount and sensitivity observed from seasonal variations. Record the variation between the seasons with maximum values in the winter and minimum values in the autumn. The seasonal photochemical cycle of hydroxyl radical (OH) in the troposphere cased the seasonal dichotomy of CO variations. In the Northern Hemisphere, reduction of OH concentrations coincides with the elevation CO values concentrations during winter and early spring (McMillan et al., 2003).

From Figure 2, the highest value of CO raised through the winter and early spring seasons as a results of the increased of partial product by burning of thermal heaters, were used excessively for heating throughout the cold season. In March CO raised to its maximum values throughout the year, though it a bit decreases to medium in April, compare to prior months. Extensive sources are evident in both north and southeast of Iraq with subsequent plumes contributed to CO concentrations are from Turkey bring by northwesterly wind (winter shamal) driven by the passage of a strong synoptically forced cold front. This variation in the CO values throughout the period (December–May)

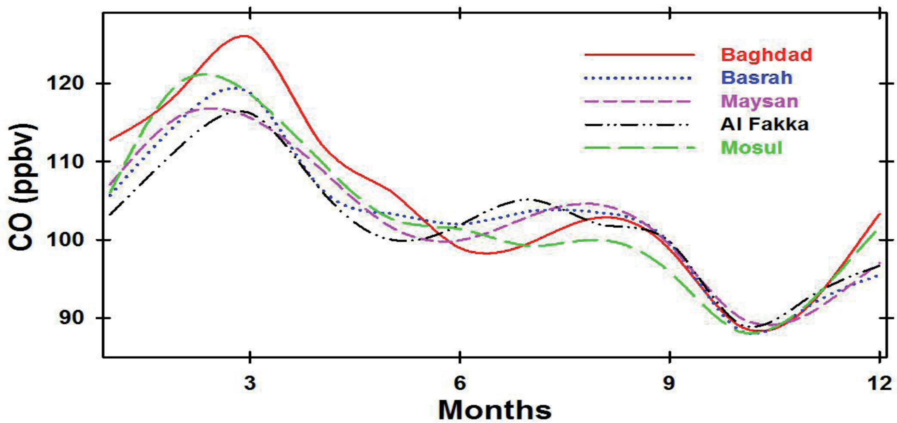

FIGURE 2. Monthly troposphere CO VMR for January to December 2012 for the locations: Baghdad, Basrah, Maysan, Al Fakka, and Mosul

was also due to the human activity, geographic nature and climatic changes (Salih et al., 2018).

In contrast, during the summer and autumn seasons the troposphere CO decreases, whereas a bit rise to medium values of CO in August. The summer season is near the lack of the CO sources, anthropogenic sources have very small variability, and the CO emissions from Turkey have very small contribution (Drori et al., 2012). The summer Gasus (shamal) or "wind of 120 days" blows nearly daily through the summer months (June–September) and has great vertical motion over a large natural flat area, which able to diminish the CO values (Rajab et al., 2013). Elevation of CO concentrations during this period over the southeastern districts compared to its values over the rest areas. All these because of the pollutions released from oil prospecting and extraction, and paddy fields by burning residuals of agricultural (Salih et al., 2018). In this period, the best high value happened on November over Maysan state, and on October was the lowest value.

A slight variation is plainly evident in the comparison between AIRS (dotted line) values of CO with the *in situ* (solid line) measurements, plotted against months for Baghdad station, as presented in Figure 3. The ground values curve has fluctuations and parallel to the AIRS curve throughout the year. There was a small phase delay between AIRS and ground CO values. The amplitude of the CO seasonal cycle generally increased to a natural peak in the late autumn season till early spring season between mid-October and March, and there were disparities between the ground and AIRS CO values resulting from increased its emissions by using fuel heating sources, especially in winter, when temperature and hours of sunshine were at their minimum.

The ground CO was plotted against the AIRS value, and the results are presented in Figure 4. The agreements between both are fairly good, with a mean deviation not exceeding 4% between these two sets data. Another indication of the regression was the points tended to cluster along the 45 tangent lines, and

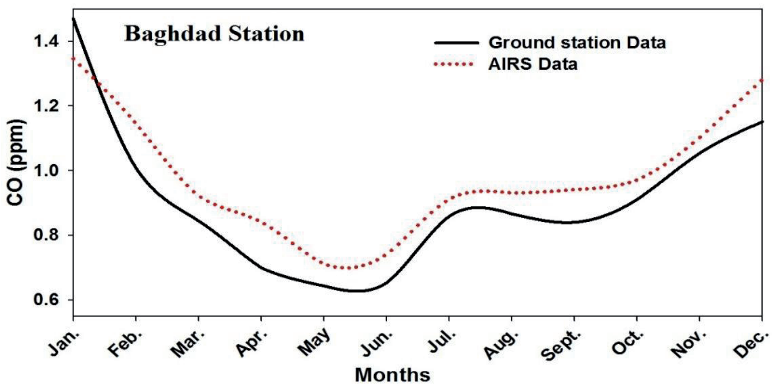

FIGURE 3. The ground station CO (solid line) and AIRS CO values (dotted line) in 2012 for the Baghdad stations

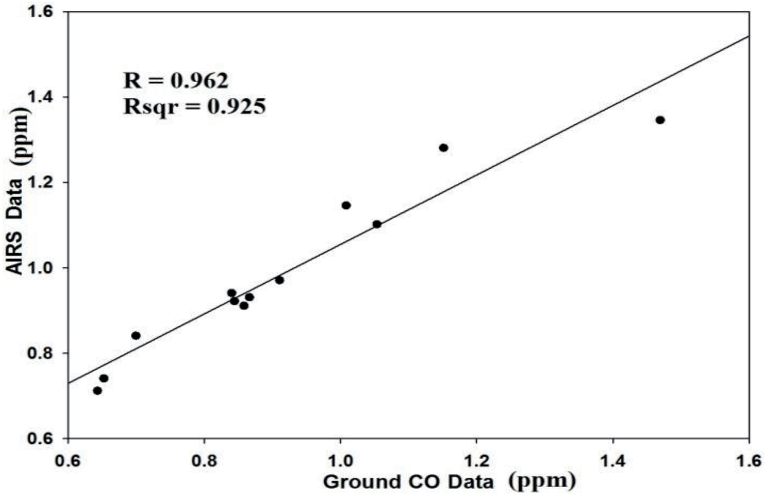

FIGURE 4. The ground station CO *versus* AIRS CO values for 2012 over Baghdad

yielded the strong correlation coefficient (R) with AIRS for 2012 represented by values 0.962. Observed largest differences between terrestrial and satellite data at January and December due to clouds cover affects to satellite efficiency during winter season (Xiong et al., 2008). In addition, the asset values of R^2 was 0.925, and the coefficient of the regressions was statistically highly significant ($p < 0.001$). The agreement shows that AIRS is very useful to perform the CO measurements.

An example of CO values variation with height over study area is illustrated in Figure 5 for 2012 over cross section, Region 49E, 28N, 38E, and 49N. The CO VMR was close to 125 ppbv on De-

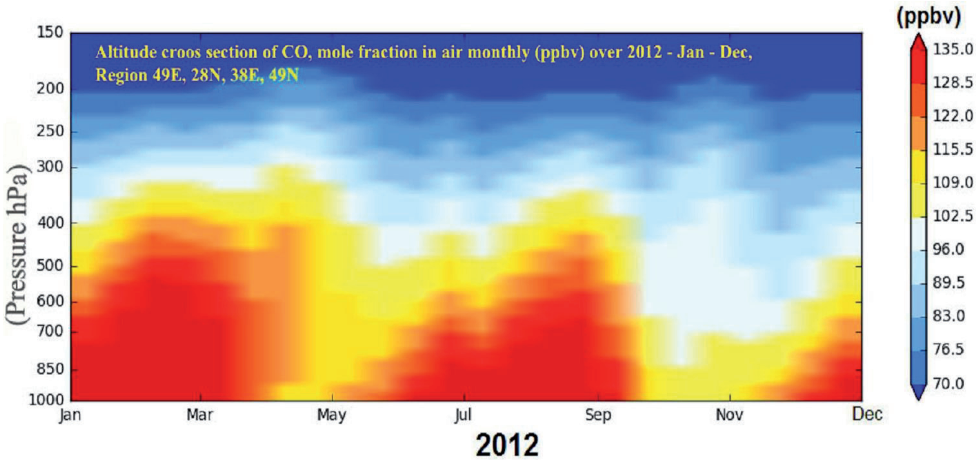

FIGURE 5. Cross section, time–pressure of CO, mole fraction in air ascending monthly over January–December 2012, Region 49E, 28N, 38E, and 49N

cember–March and July–September at altitude of 850 hPa. The magnified CO values was transported vertically up to 500 hPa on February, and up to 600 hPa during February, March and August. The CO values were closed to 105 ppbv on February–April at altitude of 350 hPa. The lowest CO values closed to surface was 90 ppbv observed during October at altitude of 800 hPa. In addition, Figure 6 displayed a comparison for different levels of mean vertical CO profiles of 12 sets observed by AIRS between 0.75 and 13.5 km altitude for the locations: Baghdad (solid line), Basrah (dotted line), Maysan (dashed line), Al Fakka (solid--dotted line), and Mosul (long-dashed line) during 2012. All data have been interpolated to a latitudinal grid of 1°. For the clean case (June–November), note how most of the CO values have similar shapes and peak between 8 and 10 km altitude and at surface are as significant as any other CO values, especially in August and September. Near the surface, there are clear inequality and different between the CO measurements descending from north to south in March, April, May and September, while less difference in other months.

The vertical distribution of CO shown in Figures 6 is characterized by enhanced abundances of CO, with values that can exceed 120 ppbv at approximately 4 km altitude over Baghdad and Mosul. This enhanced layer of CO is present in February, March and April, and begins to dissipate by May. This is due to the moderate and low influence of the northward and eastward winds during this period, which bring favorable CO from Europe, coincides with moderate influence of northward winds over northern Iraq (Drori et al., 2012; Rajab et al., 2013; Faten, 2018). The substantial contribution of anthropogenic from Turkey and Europe carried by eastward wind tag to the local emissions affect the CO values (Drori et al., 2012), so the troposphere CO values were have considerable values. The prevailing northeast wind transported favorable CO plume from the northwest regions of Arab Gulf to the southern Iraq (Badarinath et al., 2010). The lower CO amounts were observed of approximately 88–90 ppbv at 253 mb (altitude 11 km) during October. The vertical CO observation by AIRS is providing meaningful information for different altitude layers closer to the troposphere.

Conclusions

We present new observations from the AIRS instrument of the vertical distributions of troposphere CO over Iraq. We had started to scrutinize the wealth of CO information for the 2012. The AIRS IR and AMSU (without-HSB) L3 monthly CO retrieval Standard V5 data were used to evaluate and analyses the monthly troposphere CO spatial and vertical distributions over study area, and quality of the satellite measurements. The CO concentrations are virtually correlated with weather circumstance and nature of areas geography. The foreseeable variation of monthly CO was 107.15 ±18.75 ppbv for the entire study duration. The seasonal differences of CO surface oscillated significantly observed between two seasons, the winter and summer. The lowest CO measurements observed of approximately 88–90 ppbv at 253 mb

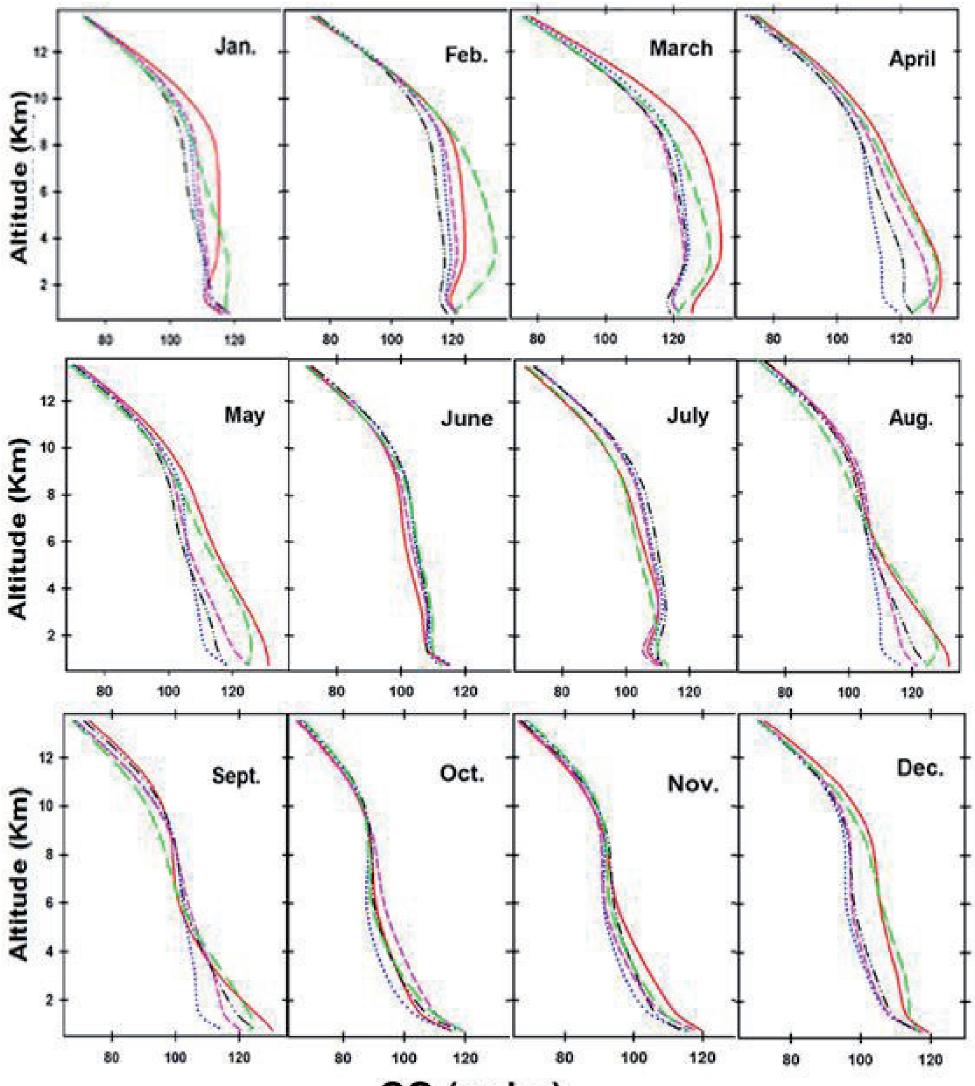

FIGURE 6. Monthly mean January to December 2012 CO vertical profiles over five locations: Baghdad (solid line), Basrah (dotted line), Maysan (dashed line), Al Fakka (solid-dotted line), and Mosul (long--dashed line)

(altitude 11 km) during the autumn season, and the highest CO occurred during spring season on March. Also, the increases in CO concentrations can be spotted along the year over the manufacturing and crowded urban districts.

The variations in the CO values from December to May duration were caused by the human actions, geographic regions nature and climatic changes. While the raises of CO measurements along the June–November duration over south-eastern districts compared to its values over the rest areas, was caused by the pollutions released from the oil drilling and extraction, and the paddy fields by burning residuals of crops. Winter shamal bring subsequent plumes from Turkey are contributed to CO concentrations, and summer shamal have very small contribution to CO concentrations. Combined ground based and satellite measurements of CO play a crucial role in obtaining better satellite validate data set. The results show that AIRS are strong candidates in order to improve our knowledge of vertical atmospheric CO. The capability of AIRS information and the satellite observations could enable the researchers in future studies to measure the elevation of the troposphere CO values over various districts and altitudes, and long periods.

Acknowledgements

The authors expressed their gratitude to the National Aeronautics and Space Administration (NASA) Goddard Earth Sciences Data Information and Services Centre (DISC) and the NASA-operated GIOVANNI for providing of AIRS data utilized in present research.

References

Al-Bayati, R.M. & Al-Salihi, A.M. (2019). Monitoring carbon dioxide from (AIRS) over Iraq during 2003-2016. *AIP Conference Proceedings*, *2144*(1), 030007. DOI 10.1063/1.5123077

Al-Salihi, A.M., Rajab, J.M., & Salih, Z.Q. (2019). Satellite monitoring for Outgoing Longwave Radiation and Water Vapor during 2003-2016 in Iraq. *Journal of Physics: Conference Series*, *1234*(1), 012009. DOI 10.1088/1742-6596/1234/1/012009

Badarinath, K., Kharol, S.K., Kaskaoutis, D., Sharma, A.R., Ramaswamy, V. & Kambezidis, H. (2010). Long-range transport of dust aerosols over the Arabian Sea and Indian region – a case study using satellite data and ground-based measurements. *Global and Planetary Change*, *72*(3), 164-181.

Bowman, K.W., Rodgers, C.D., Kulawik, S.S., Worden, J., Sarkissian, E., Osterman, G., Steck, T., Ming, L., Eldering, A., Shephard, M., Worden, H., Lampel, M., Clough, S., Brown, P., Rinsland, C., Gunson, M. & Beer, R. (2006). Tropospheric emission spectrometer: Retrieval method and error analysis. *IEEE Transactions on Geoscience and Remote Sensing*, *44*(5), 1297-1307.

Chahine, M.T., Pagano, T.S., Aumann, H.H., Atlas, R., Barnet, C., Blaisdell, J., Chen, L., Divakarla, M., Fetzer E.J., Goldberg, M., Gautier, C., Granger, S., Hannon, S., Irion, F.W., Kakar, R., Kalnay, E., Lambrigtsen, B.H., Lee, S.Y., Marshall, J.L., McMillan, W.W., McMillin, L., Olsen, E.T., Revercomb, H., Rosenkranz, P., Smith, W.L., Staelin, D., Strow, L.L., Susskind, J., Tobin, D., Wolf, D. & Zhou, L. (2006). AIRS: Improving weather forecasting and providing new data on greenhouse gases. *Bulletin of the American Meteorological Society*, *87*(7), 911-926.

Deeter, M., Edwards, D., Gille, J., Emmons, L., Francis, G., Ho, S.P., Mao, D., Masters, D., Worden, H., Drummond, J.R., Novelli, P.C. (2010). The MOPITT version 4 CO product: Algorithm enhancements, validation, and long-term stability. *Journal of Geophysical Research: Atmospheres*, *115*(D7). DOI 10.1029/2009JD013005

Drori, R., Dayan, U., Edwards, D., Emmons, L., Erlick, C. & Kanakidou, M. (2012). Attributing and quantifying carbon monoxide sources affecting the Eastern Mediterranean: a combined satellite, modelling, and synoptic analysis study. *Atmospheric Chemistry & Physics*, *12*(2), 1067-1082.

Faten, G.A., Al-Salihi, A.M. & Rajab, J.M. (2018). Spatiotemporal Monitoring of Methane Over Iraq During 2003-2015: Retrieved From Atmospheric Infrared Sounder (Airs). *ARPN*

Journal of Engeneering and Applied Science, *13*(22), 3650-3663.

Fortems-Cheiney, A., Chevallier, F., Pison, I., Bousquet, P., Szopa, S., Deeter, M. & Clerbaux, C. (2011). Ten years of CO emissions as seen from Measurements of Pollution in the Troposphere (MOPITT). *Journal of Geophysical Research: Atmospheres*, *116*(D5). DOI 10.1029/2010JD014416

Herron-Thorpe, F.L., Mount, G.H., Emmons, L.K., Lamb, B.K., Chung, S.H. & Vaughan, J.K. (2012). Regional air-quality forecasting for the Pacific Northwest using MOPITT//TERRA assimilated carbon monoxide MOZART-4 forecasts as a near real-time boundary condition. *Atmospheric Chemistry and Physics*, *12*(12), 5603-5615.

Illingworth, S.M., Remedios, J.J., Boesch, H., Ho, S.P., Edwards, D., Palmer, P. & Gonzi, S. (2011). A comparison of OEM CO retrieval from the IASI and MOPITT instruments. *Atmospheric Measurement Techniques*, *4*(5), 775-793.

Kobayashi, H., Shimota, A., Kondo, K., Okumura, E., Kameda, Y., Shimoda, H. & Ogawa, T. (1999). Development and evaluation of the interferometric monitor for greenhouse gases: a high-throughput Fourier-transform infrared radiometer for nadir Earth observation. *Applied Optics*, *38*(33), 6801-6807.

Landau, S. & Everitt, B.S. (2004). *A handbook of statistical analyses using SPSS*. New York: CRC Press Company.

Luo, M., Rinsland, C., Fisher, B., Sachse, G., Diskin, G., Logan, J., Worden, H., Kulawik, S., Osterman, G., Eldering, A., Herman, R. & Shephard, M. (2007). TES carbon monoxide validation with DACOM aircraft measurements during INTEX-B 2006. *Journal of Geophysical Research: Atmospheres*, *112*(D24). DOI 10.1029/2007JD008803

McMillan, W., McCourt, M., Revercomb, H., Knuteson, R., Christian, T. J., Doddridge, B., Hobbs, P.V., Lukovich, J.V., Novelli, P.C., Piketh, S., Sparling, L., Stein, D., Swap, R.J. & Yokelson, R.J. (2003). Tropospheric carbon monoxide measurements from the Scanning High-Resolution Interferometer Sounder on 7 September 2000 in southern Africa during SAFARI 2000. *Journal of Geophysical Research: Atmospheres*, *108*(D13). DOI 10.1029/2002JD002335

NASA Earthdata (2019). *Data collections*. Retrieved from: http://disc.sci.gsfc.nasa.gov/AIRS

Pétron, G., Granier, C., Khattatov, B., Yudin, V., Lamarque, J.F., Emmons, L., Gille, J. & Edwards, D.P. (2004). Monthly CO surface sources inventory based on the 2000–2001 MOPITT satellite data. *Geophysical Research Letters*, *31*(21), 1-5.

Rajab, J.M., Jafri, M.M., Lim, H.S. & Abdullah, K. (2011). Monthly distribution map of carbon monoxide (CO) from AIRS over Peninsular Malaysia, Sabah and Sarawak for the year 2003. *Pertanika Journal of Science and Technology*, *19*, 89-96.

Rajab, J.M., Jafri, M.M., Lim, H.S. & Abdullah, K. (2012). Regression analysis in modeling of air surface temperature and factors affecting its value in Peninsular Malaysia. *Optical Engineering*, *51*(10), 101702. DOI 10.1117/1.OE.51.10.101702

Rajab, J.M., Ahmed, H.S. & Moussa, H.A. (2013). Monthly carbone monoxide (CO) distribution based on the 2010 MOPITT satellite data in Iraq. *Iraqi Journal of Science*, *54*(5), 1183-1192.

Rajab, J.M., Hassan, A.S., Kadhum, J.H., Al--Salihi, A.M. & Hwee, S. (2020). Analysis of tropospheric NO2 over Iraq using OMI satellite measurements. *Scientific Review – Engineering and Environmental Sciences*, *29*(1), 3-16.

Salih, Z.Q., Al-Salihi, A.M. & Rajab, J.M. (2018). Assessment of troposphere carbon monoxide variability and trend in Iraq using atmospheric infrared sounder during 2003-2016. *Journal of Environmental Science and Technology*, *11*, 39-48.

Xiong, X., Barnet, C., Maddy, E., Sweeney, C., Liu, X., Zhou, L. & Goldberg, M. (2008). Characterization and validation of methane products from the Atmospheric Infrared Sounder (AIRS). *Journal of Geophysical Research: Biogeosciences*, *113*(G3). DOI 10.1029/2007JG000500

Summary

Observed vertical distribution of tropospheric carbon monoxide during 2012 over Iraq. The atmospheric parameters observations enable to made continental and global scales by remote sensing devices existent in space. One of these instruments is the Atmospheric InfraRed Sounder (AIRS) onboard Aqua satellite. We characterize the vertical distribution of troposphere carbon monoxide (CO) measured by AIRS over IRAQ. This study presents one year data. Results shown standard deviation of monthly troposphere CO for five locations: Baghdad, Basrah, Maysan, Al Fakka, and Mosul, from January to December 2012, was 107.15 ±18.75 ppbv for entire period depend on whether circumstance and topography. The seasonal differences undulate between winter and summer seasons, with higher values CO in the winter than in the summer and autumn seasons. In addition, the rising in troposphere CO values can be measured during year over the manufacturing and crowded urbanized zones. AIRS observations reveal enhanced abundances of CO, with values that can exceed 120 ppbv at approximately 4 km altitude over Baghdad and Mosul. The lower CO amounts observed of approximately 88–90 ppbv at 253 mb (altitude 11 km) during October. Comparisons over Baghdad station in 2012 showed close agreement between the ground CO data and the observed CO from AIRS, and regression result showed high correlation coefficient (R = 0.962). The vertical CO observation by AIRS is providing meaningful information for different altitude layers closer to the troposphere, and the satellite measurements are able to measure the increase of the atmosphere CO concentrations over varied regions.

Authors' address:
Ibtihaj S. Abdulfattah
(https://orcid.org/0000-0001-8543-4112)

Ali M. Al-Salihi – corresponding author
(https://orcid.org/0000-0002-6945-767X)
Mustansiriyah University
College of Science
Department of Atmospheric Sciences
Palestine street, 46131, Baghdad, Iraq
e-mail: alialsalihi.atmsc@uomustansiriyah.edu.iq
salihi72@yahoo.com

Hwee San Lim
(https://orcid.org/0000-0002-4835-8015)

Scientific Review – Engineering and Environmental Sciences (2020), 29 (2), 196–211
Sci. Rev. Eng. Env. Sci. (2020), 29 (2)
Przegląd Naukowy – Inżynieria i Kształtowanie Środowiska (2020), 29 (2), 196–211
Prz. Nauk. Inż. Kszt. Środ. (2020), 29 (2)
http://iks.pn.sggw.pl
DOI 10.22630/PNIKS.2020.29.2.17

Osama T. Al-TAAI, Zainab M. ABBOOD
Mustansiriyah University, College of Science

Analysis of the convective available potential energy by precipitation over Iraq using ECMWF data for the period of 1989–2018

Key words: convective precipitation, total precipitation, Spearman rho test, CAPE, ECMWF, Iraq

Introduction

The rain is the most common type of precipitation in our atmosphere and when liquid droplet falls to the earth surface. The source of precipitation is water vapor, which is always present in the atmosphere in varying amounts; there are three major types of rain can be distinguished depending on the different factors that cause the airlifting and formation of clouds and rain falling as well as meteorology factors (Niwas, Singh, Singh, Khichar & Singh, 2006):

– Convectional rainfall: this type of rainfall occurs due to the ground surface heating. When the land warms up, it heats the air above it. This causes the air to expand and rise. As the air rises it cools and condenses. If this process continues then rain will fall. Convectional rainfall occurs for a very short duration but occurs in the form of heavy showers. This type of rain is often accompanied by lightning and thunder. It is called ascending/rising rain because it is the result of a rising process of the atmosphere, which is exposed to thermal heating and clouds resulting from this type cumulus and cumulonimbus (Saxena & Gupta, 2017).
– Cyclonic/Frontal rainfall: this type of rainfall occurs when a warm and moist air mass (warm front) meets a cold and dry air mass (cold front). When both masses come together, warmer air is forced to rise over cold air. The moist warm air condenses as it cool, which causes cloud and rain. When there are condensation nuclei and when the atmosphere arrives at saturation

ratio. Frontal rain produces a variety of clouds, which bring moderate to heavy rainfall. They are called with this name because they are formed by the collision of two air masses and clouds resulting from this type stratus, altostratus, cirrus, and cumulus (Goyal, 2016).

– Orographic rainfall: this type of rainfall occurs when moisture-laden air encounters a mountain range, the air is forced to rise. It cools off at the higher elevation and this condenses water out of the air and creates clouds and rains. If the temperature is cold enough, the precipitation falls as snow. It is called orographic rain because it is influenced by the terrain when falling. Clouds forms and precipitation occurs on the windward side of the mountain and another side of the mountain is called the leeward side, it receives very little precipitation and clouds resulting from this type stratus, altostratus and cumulus and occurs in the northern and northeastern regions (Ahrens, 2013; Lackmann, 2013), as shown in Figure 1 (Gabler, Petersen, Trapasso & Sack, 2009).

Literature review

There many from studies to find the effect of rainfall on soil erosion for the selected station in Iraq and found when analyzing the monthly total rainfall for 18 years that rainfall varies according to the station height and geographic location as well as by months.

Where northern stations recorded the highest loss of the rain while south stations recorded the lowest loss of the rain and was the higher loss of rain during winter months (December, January and February) and was the lower loss of rain during summer months (Al-Obeidi, 2008). Some research showed that the highest rainfall was in the northern regions, especially in Sulaymaniyah station. The lowest rainfall was in Babil station for the period of 2000–2013. The amount of rainfall began to fluctuate and decrease during 2007 due to temperature variation (Salman, 2015). However, there a seasonal study of convective available potential energy (CAPE) is done using 6-h ERA-Interim data over West Africa during 35 years (1979–2014).

Climatology of CAPE presented in terms of seasonal means, variances and

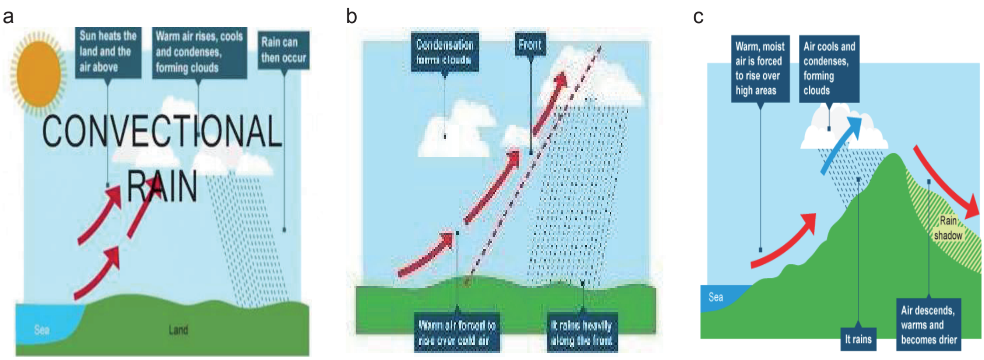

FIGURE 1. Rainfall: a – convectional, b – cyclonic/frontal, c – cyclonic (Gabler et al., 2009)

trends shows large values toward 12°––16° N with maxima during summer, according to higher relative humidity due to the arrival of monsoon in West Africa (Meukaleuni, Lenouo & Monkam, 2016). Also, their synoptic study of the role of convective available potential energy on formation rainstorm over Iraq and resulted in convectional precipitation coincides convective available potential energy this due to Low Mediterranean Sea and Low Sudanese and the northern regions of Iraq have the highest CAPE, followed by the central regions and southern regions, accompanied by the highest rainfall values (Namdar, 2017).

Convective available potential energy (CAPE)

CAPE is the amount of energy a given parcel of air would have if lifted a certain distance vertically through the atmosphere. CAPE is effectively the positive buoyancy of an air parcel and is an indicator of atmospheric instability, which makes it very valuable in predicting severe weather. It is a form of fluid instability found in thermally stratified atmospheres in which a colder fluid overlies a warmer one. An air mass will rise if it is less dense than the surrounding air (its buoyant force is greater than its weight). This can create vertically developed clouds due to the rising motion, which could lead to thunderstorms. It could also be created by other phenomena, such as a cold front. Even if the air is cooler on the surface, there is still warmer air in the mid-levels that can rise into the upper levels. However, if there is not enough water vapor present, there is no ability for condensation, thus storms, clouds, and rain will not form (Schultz, 1989; Riemann-Campe, Fraedrich & Lunkeit, 2009). CAPE exists within the conditionally unstable layer of the troposphere, the free convective layer (FCL), where an ascending air parcel is warmer than the ambient air.

CAPE is measured in joules per kilogram of air. Any value greater than 0 $J \cdot kg^{-1}$ indicates instability and an increasing possibility of thunderstorms and hail. Often exceed the potential energy values in the thunderstorms 1,000 $J \cdot kg^{-1}$ and in extreme cases may exceed 5,000 $J \cdot kg^{-1}$. Generic CAPE is calculated by integrating vertically the local buoyancy of a parcel from the level of free convection (LFC) to the equilibrium level (EL):

$$CAPE = \int_{Z_f}^{Z_n} g \left(\frac{T_{v_{par}} - T_{v_{env}}}{T_{v_{env}}} \right) dz \qquad (1)$$

whereas:
Z_n – height of the equilibrium level,
Z_f – height of the level of free convection,
g – acceleration due to gravity,
$T_{v_{par}}$ – virtual temperature of the specific parcel [°K],
$T_{v_{env}}$ – virtual temperature of the environment [°K] (Doswell III & Rasmussen, 1994; Gettelman, Seidel, Wheeler & Ross, 2002).

Convective precipitation (C_p)

Convective precipitation is also known as thermodynamic precipitation. While dynamic precipitation only needs saturated air and lift, convective precipitation requires an additional component called instability (Wang, 2013). Uplift due to instability release occurs when the air rises on its own after being lifted to a certain point in the troposphere. Instability is commonly assessed by examining the Lifted Index (LI) and CAPE. Both these indices can be used to assess the acceleration rate of air once air from the lower troposphere is brought to a level in the troposphere where it will rise on its own due to positive buoyancy. Instability causes the air to rise much faster than it would be forced lifting alone (Abbood & Al-Taai, 2018a). Think of convective precipitation as falling from thunderstorms with strong updrafts while dynamic precipitation falls from a deck of stratus clouds. Convective precipitation tends to have lighting, thunder and heavy rain while dynamic precipitation is more of a gentle long-lasting rain with no lightning and thunder (Abbood & Al-Taai, 2018b).

Data and methodology

Study stations and location

Data were taken from the European Center for Medium-range Weather Forecasts for monthly CAPE, C_p and T_p for 30 years, from 1989 to 2018 over Iraq. As Iraq is located within the arid and semi-arid region, it is characterized by variance rainfall between one year and another and this variation in the amount of rain has made there are years characterized by high quantities of general levels it is a wet year, and other decreases in the amount of rain it is a dry year (Zakaria, Al-Ansari, Ezz-Aldeen & Knutsson, 2012). Iraq is located within the southwestern part of the continent of Asia. The northeastern part of the Arab world and extends between the two latitudes 29.5°–37.22° N and longitudes 48.45°––38.45° E; it includes the following stations as in Table 1 (Al-Timimi, 2012), see Figure 2.

TABLE 1. The geographical locations of Iraqi stations (Al-Timimi, 2012)

Station	Longitude [°]	Latitude [°]	Elevation [m]
Emadiyah	43.3	37.05	1236
Salahaddin	44.2	36.38	1075
Sulaymaniyah	45.45	35.53	843
Sinjar	41.83	36.32	583
Dohook	43	36.87	554
Zakho	42.72	37.13	433
Arbil	44	36.15	420
Rabiah	42.1	36.8	382
Taleafer	42.48	36.37	373
Kirkuk	44.35	35.47	331
Nukheb	42.28	32.03	305
Dukcan	44.95	35.95	276
Sumeel	42.75	36.87	250

TABLE 1 cont.

Station	Longitude [°]	Latitude [°]	Elevation [m]
Mosul	43.15	36.31	223
Rutba	40.28	33.03	222
Tuz	44.65	34.88	220
Khanqin	45.38	34.35	202
Qaim	41.02	34.38	178
Anah	41.95	34.37	175
Biji	43.53	34.9	116
Hadithah	42.35	34.13	108
Tikrit	43.7	34.57	107
Samaraa	43.88	34.18	75
Heet	42.75	33.63	58
Najaf	44.32	31.95	53
Ramadi	43.32	33.45	48
Kahalis	44.53	33.83	44
Baghdad	44.4	33.3	32
Kerbela	44.05	32.57	29
Hella	44.45	32.45	27
Makoor	43.6	35.75	22
Kut	45.75	32.49	21
Diwaniya	44.95	31.95	20
Hai	46.03	32.13	17
Samawa	45.27	31.27	11
Amara	47.17	31.83	9
Nasiriya	46.23	31.02	5
Basrah	47.78	30.52	2

Statistical used

There were several statistical tests but selected Spearman rho tests for the order of this work has been selected regression analysis. In particular, the simple linear regression to predict the relationship between CAPE, C_p and T_p (Bolboaca & Jäntschi, 2006; Hron, Filzmoser & Thompson, 2012). Where used statistical program Sigma plot to calculate the value of the slope of the regression (b) and the value of *p*-value simple linear regression way and Surfer program to graph total yearly mean of CAPE, C_p and T_p over Iraq and GIS to graph Iraq map (Padua, 2000; York, Evensen, Martinez & Delgado, 2004) and statistical used represents in following equations:

– simple linear regression (SLR)

$$\overline{Y} = a + b\overline{X} \tag{2}$$

– Spearman rho test (SRT)

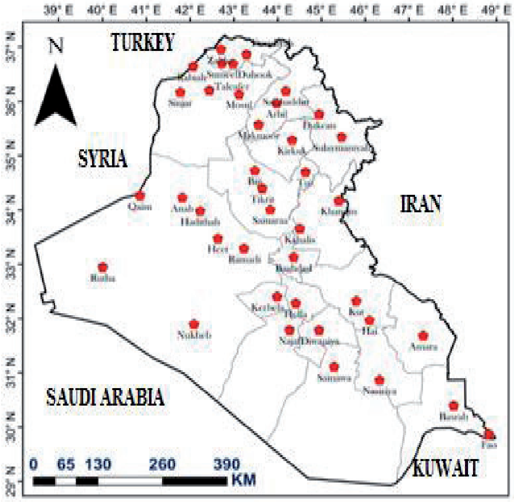

FIGURE 2. Locations of Iraqi stations

$$rs = 1 - \frac{6\sum_{i=1}^{n} di^2}{n(n^2 - 1)} \tag{3}$$

– probability value (p-value)

Then calculating the amount of (d_i) through ($d_i = k_i - i$) where (i) value ranging I = 1, 2, 3, …, n. Where n is the number of measurements in each of the two varieties in the correlation, d_i is the ranked difference between the i^{th} measurements for the two varieties. In a statistical hypothesis test, the p-value is the level of marginal significance representing a given event's probability of occurrence. To calculate p-values, you can use p-value tables or spreadsheet/ /statistical software (Al-jaf & Al-Taai, 2019a). A smaller p-value indicates that there is stronger evidence favoring the alternative hypothesis (Al-jaf & Al-Taai, 2019b).

Results and discussion

The total yearly mean of CAPE, C_p and T_p over Iraq

Figure 3 shows the highest total yearly mean of CAPE, C_p and T_p over Iraq including northern stations as Dohook, Zakho, etc. This is due to meteorological factors, which include low temperatures, high humidity and low solar radiation. Which leads to the formation of many clouds and rain, which are accompanied by many different weather phenomena such as lightning, thunder, storms and hurricane. While the central and southern stations are characterized by high temperature and low humidity and the amount of solar radiation high, which leads to a decrease in the number of clouds and lack of rain as well as nature of the surface and to the nature of

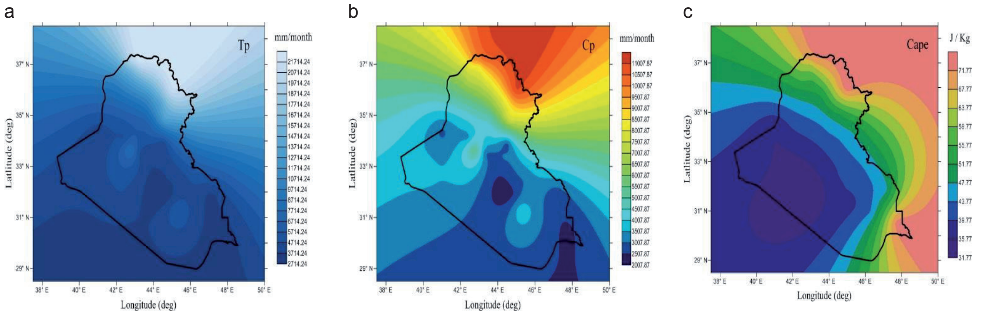

FIGURE 3. Total yearly mean of T_p (a), C_p (b) and CAPE (c) over Iraq for 30-year period, from 1989 to 2018

the various air masses that are blowing on the country, climate changes, air pressure systems, jet streams, the Mediterranean sea cyclone and the Sudanese cyclone. Which have an important role in the formation and rainfall? The amount of rain is important to improve weather and climate forecasting.

The total monthly mean of CAPE, C_p and T_p over Iraq

Figure 4 shows the total monthly mean of CAPE, C_p and T_p over the Dohook station. It is seen that the behavior of rainfall with months oscillates between increase and decrease. Where the highest average 30-year of the CAPE coefficient was during April and the lowest in July and August months.

The highest total 30-year of the C_p coefficient was during March month and the lowest in July and August months. The highest total 30-year of the T_p coefficient was during January month and the lowest in July and August months. Increased rainfall in winter and early spring and autumn this due to increased frequency of medium atmospheric depressions and Sudanese cyclone, there is light rain at the early summer returning to the season Indian cyclone (thermal cyclone) and it dissolves in mid-summer.

Figure 5 shows the total monthly mean of CAPE, C_p and T_p over the Mosul station. It is seen that the behavior of rainfall with months oscillates between increase and decrease where the highest average 30-year of the CAPE coefficient was during April and the lowest in July and August months. The highest total 30-year of the C_p coefficient was during March month and the lowest in July and August months.

The highest total 30-year of the T_p coefficient was during January month and the lowest in July and August months. Increased rainfall in winter and early spring and autumn this due to increased frequency of medium atmospheric depressions and Sudanese cyclone, there is light rain at the early summer returning to the season Indian cyclone (thermal cyclone) and it dissolves in mid-summer.

Figure 6 shows the total monthly mean of CAPE, C_p and T_p over the Rabiah station. It is seen that the behavior of rainfall with months oscillates between increase and decrease where the highest average 30-year of the CAPE coefficient was during April and May while the lowest in July and August months. The high-

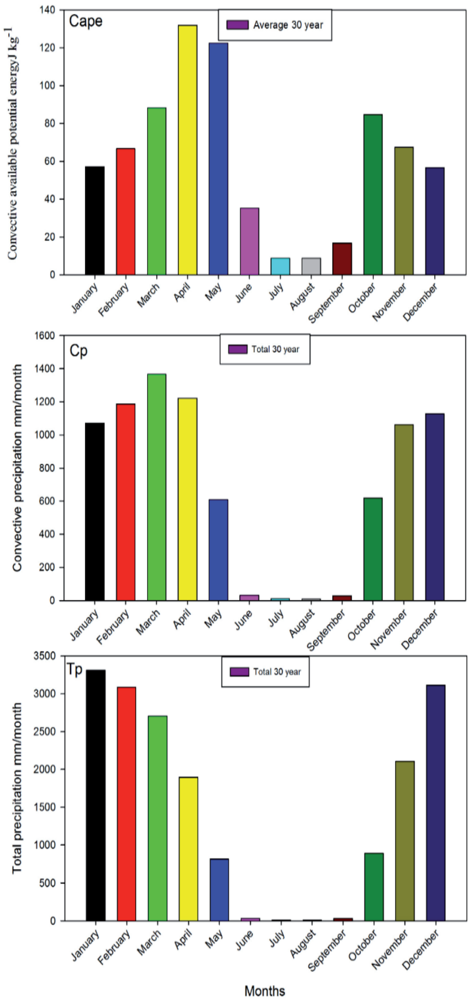

FIGURE 4. The total monthly mean of convective available potential energy (J·kg^{-1}), monthly convective precipitation (mm) and total monthly precipitation (mm) respectively by CAPE, C_p and T_p for Dohook station

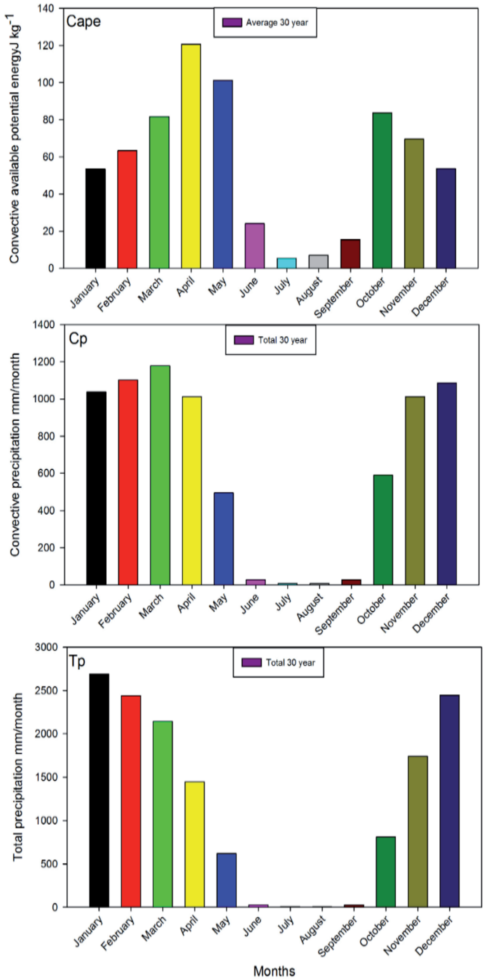

FIGURE 5. The total monthly mean of convective available potential energy (J·kg^{-1}), monthly convective precipitation (mm) and total monthly precipitation (mm) respectively by CAPE, C_p and T_p for Mosul station

est total 30-year of the C_p coefficient was during March and December months and the lowest in July and August months. The highest total 30-year of the T_p coefficient was during January and December months while the lowest in July and August months. Increased rainfall in winter and early spring and autumn this due to increased frequency of medium atmospheric depressions and Sudanese cyclone, there is light rain at the early summer returning the season Indian cyclone (thermal cyclone) and it dissolves in mid-summer. Figure 7 shows the total

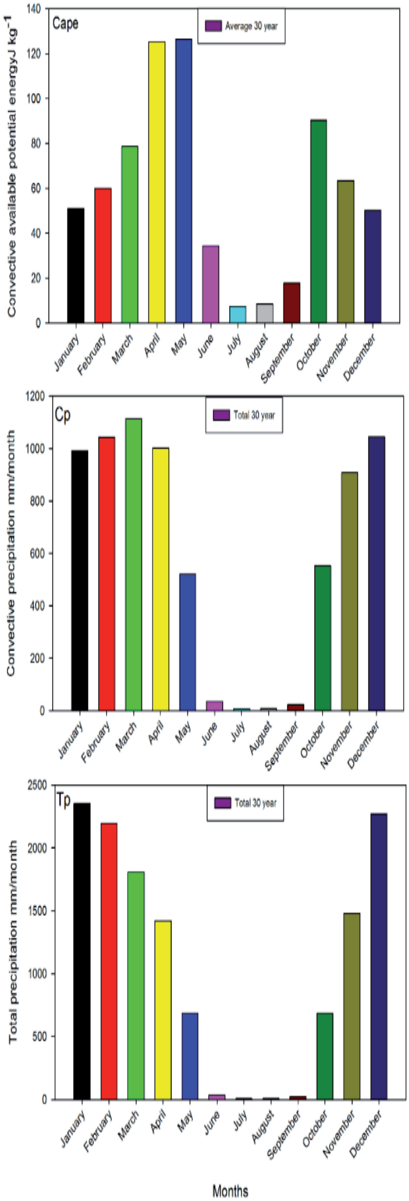

FIGURE 6. The total monthly mean of convective available potential energy ($J \cdot kg^{-1}$), monthly convective precipitation (mm) and total monthly precipitation (mm) respectively by CAPE, C_p and T_p for Rabiah station

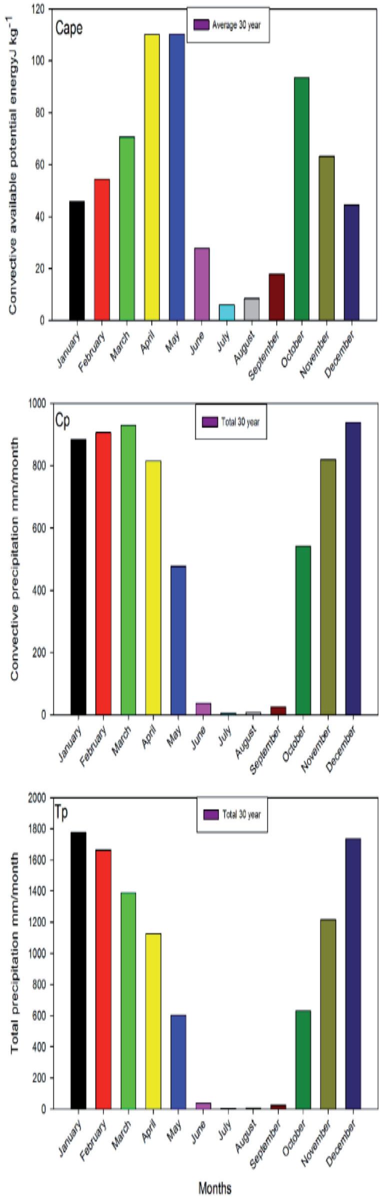

FIGURE 7. The total monthly mean of convective available potential energy ($J \cdot kg^{-1}$), monthly convective precipitation (mm) and total monthly precipitation (mm) respectively by CAPE, Cp and T_p for Sinjar station

monthly mean of CAPE, C_p and T_p over the Sinjar station. It is seen that the behavior of rainfall with months oscillates between increase and decrease where the highest average 30-year of the CAPE coefficient was during April and May while the lowest in July and August months.

The highest total 30-year of the C_p coefficient was during March and December months and the lowest in July and August months. The highest total 30-year of the T_p coefficient was during January and December months while the lowest in July and August months. Increased rainfall in winter and early spring and autumn this due to increased frequency of medium atmospheric depressions and Sudanese cyclone, there is light rain at the early summer returning to the season Indian cyclone (thermal cyclone) and it dissolves in mid-summer. Figure 8 shows the total monthly mean of CAPE, C_p and T_p over the Zakho station. It is seen that the behavior of rainfall with months oscillates between increase and decrease where the highest average 30-year of the CAPE coefficient was during April and may while the lowest in July and August months. The highest total 30-year of the C_p coefficient was during March and April months and the lowest in July and August and September months. The highest total 30-year of the T_p coefficient was during January and December months and the lowest in July and August months. Increased rainfall in winter and early spring and autumn this due to increased frequency of medium atmospheric depressions and Sudanese cyclone, there is light rain at the early summer returning to the season Indian cyclone (thermal cyclone) and it dissolves in mid-summer.

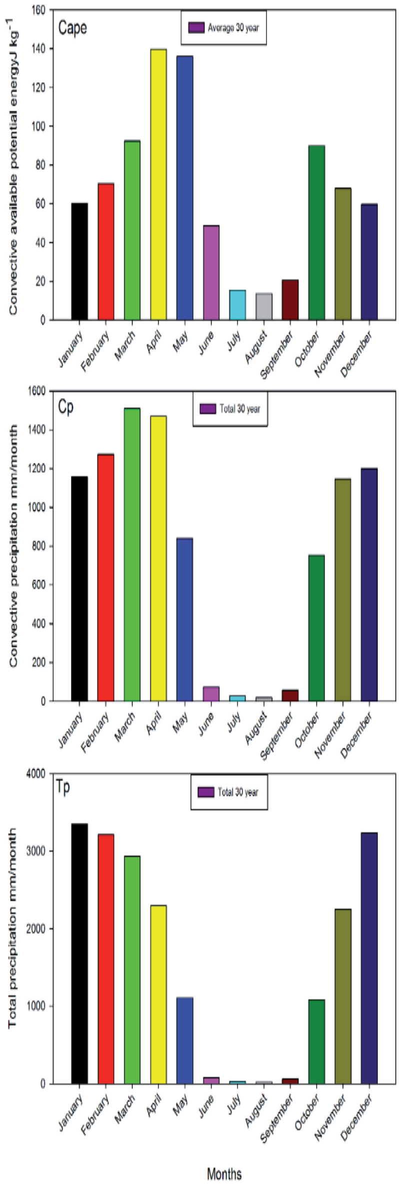

FIGURE 8. The total monthly mean of convective available potential energy (J·kg^{-1}), monthly convective precipitation (mm) and total monthly precipitation (mm) respectively by CAPE, C_p and T_p for Zakho station

The total yearly mean of CAPE, C_p and T_p for the selected station over Iraq

Figure 9 shows the maximum yearly mean of CAPE, C_p and T_p over Dohook station respectively 101.9047 $J \cdot kg^{-1}$ for the 2006 year, 434.2045 mm for the 2018 year, 908.7591 mm for the 1992 year. The maximum yearly mean of CAPE, C_p and T_p over Mosul station respectively 96.84094 $J \cdot kg^{-1}$, 410.1414 mm, 718.0172 mm for the 2018 year. The maximum yearly mean of CAPE, C_p and T_p over Rabiah station respectively 106.2608 $J \cdot kg^{-1}$ for the year 2006, 400.8977 mm, 692.3379 mm for the 2018 year. The maximum yearly mean of CAPE, C_p and T_p over Sinjar station respectively 100.6505 $J \cdot kg^{-1}$ for 2006 year, 377.1396 mm, 605.5202 mm for the 2018 year. The maximum yearly mean of CAPE, C_p and T_p over Zakho station respectively 106.8305 $J \cdot kg^{-1}$ for the 2006 year, 479.4777 mm for the 2018 year, 935.4565 mm for the 1992 year. Iraq is affected by the cyclone arrival of the Mediterranean Sea (rain is concentrated in northern regions) and the Sudanese cyclone (rain is concentrated in central and southern regions) this leading to precipitation, thunderstorms and changes in wind speed and direction, atmospheric pressure, temperature and humidity.

The relationship between CAPE, C_p and T_p for the selected station over Iraq

Figure 10 shows the type of relationship and the strength of the correlation between meteorological parameters for

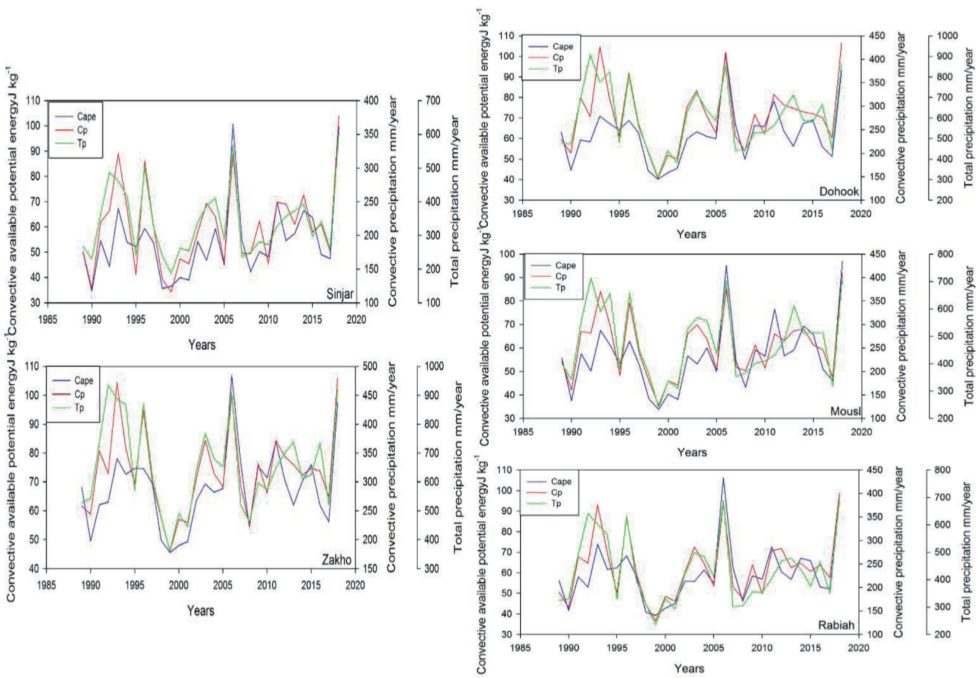

FIGURE 9. The yearly mean of CAPE, C_p and T_p data for selected stations

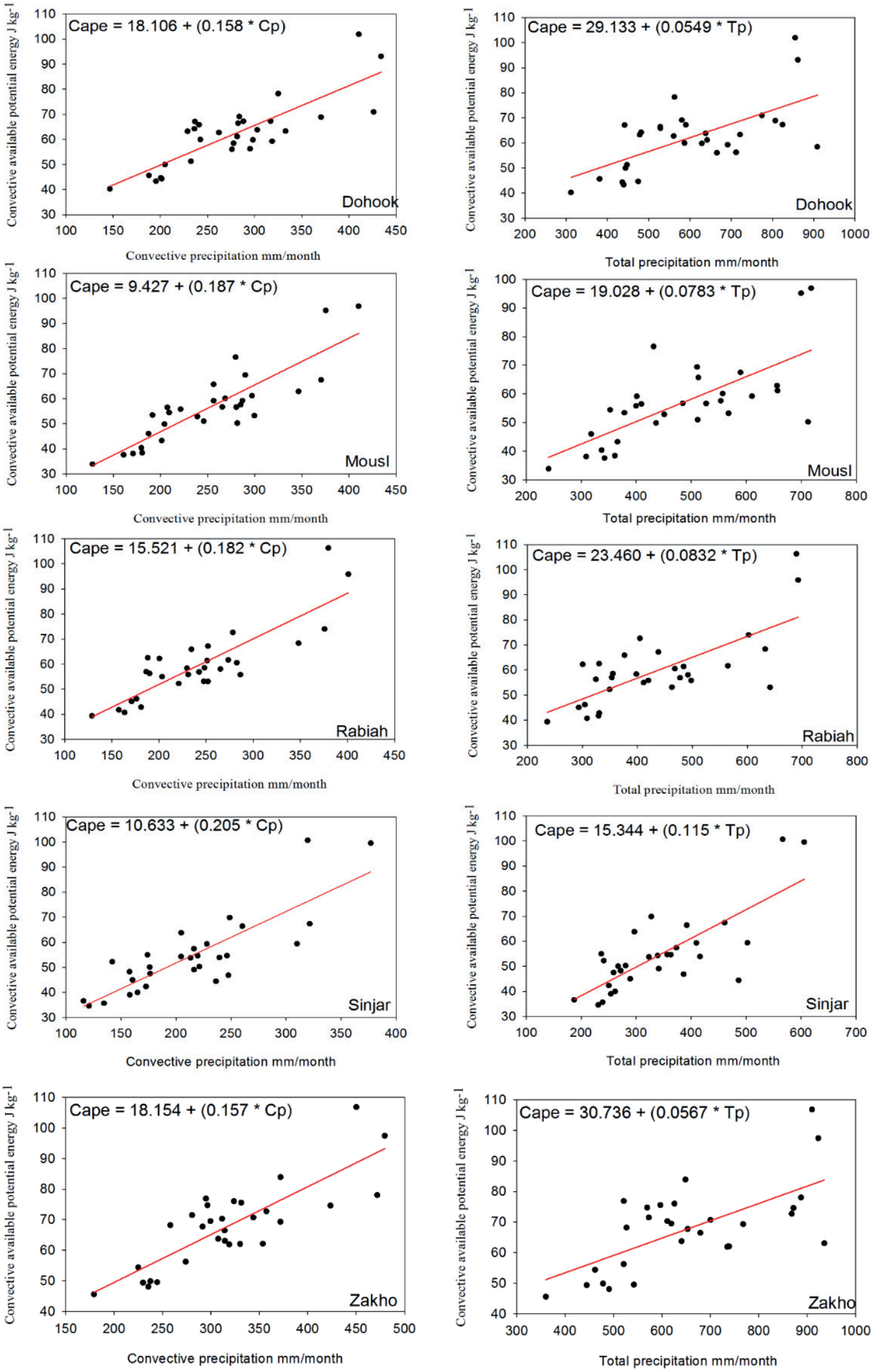

FIGURE 10. The relationship between CAPE, C_p and T_p data for selected stations

selected station Dohook, Mosul, Rabiah, Sinjar and Zakho. Where the relationship between the convective available potential energy and the convective precipitation is positive and the relationship between the convective available potential energy and the total precipitation is positive too at all station but Mosul station represents very high correlation while Zakho station represents low correlation. This due to heating of ground surface when the land warms up, it heats the air above it. This causes the air to expand and rise. As the air rises, it cools and condenses this lead to form clouds and convective rainfall is often accompanied by lightning and thunder. Which makes the high correlation. However, Mosul has high heating but weak condensation, leading to fewer clouds and rains, thus rainfall depends on geographical location and nature of the region. Table 2 shows relationship between CAPE with C_p and T_p for the 30 years over Iraq.

Conclusions

- Iraq is characterized by a lack of rainfall and limited to winter mainly and the beginning of spring and autumn less degree this due to the increased frequency of medium atmospheric depressions but in spring and autumn are less rainy because the Mediterranean declines are losing their impact on Iraq and the region is under the influence of tropical continental air, which is characterized by drought. Thus, lead to increased drought and high evaporation due to the amount of solar radiation high especially in summer.
- Rain is increasing in the northern stations more than in the southern stations, where it gradually takes shape in the north. Rain falls more than the central stations where the central stations have more rain than the southern stations. This difference is due to

TABLE 2. The relationship between CAPE with C_p and T_p for the 30 years over Iraq

Simple linear regression		Spearman rho test			Station
Interpretation of relationship	p	Correlation degree	R_s	relation	
linear relation	< 0.001	high positive correlation	0.8	CAPE vs C_p	Dohook
linear relation	< 0.001	high positive correlation	0.8	CAPE vs T_p	
linear relation	< 0.001	high positive correlation	0.9	CAPE vs C_p	Mosul
linear relation	< 0.001	high positive correlation	0.7	CAPE vs T_p	
linear relation	< 0.001	high positive correlation	0.8	CAPE vs C_p	Rabiah
linear relation	< 0.001	high positive correlation	0.6	CAPE vs T_p	
linear relation	< 0.001	very high positive correlation	0.8	CAPE vs C_p	Sinjar
linear relation	< 0.001	high positive correlation	0.7	CAPE vs T_p	
linear relation	< 0.001	middle positive correlation	0.7	CAPE vs C_p	Zakho
linear relation	< 0.001	low positive correlation	0.5	CAPE vs T_p	

the nature of the Earth's surface and the different air masses blowing on the country.

- The main reason for Iraq's rains during winter and spring is the Mediterranean Sea cyclone, Sudanese cyclone, convective clouds, instability, the pressure systems, meteorological factor, and airlifting mechanism, nature of the surface, various air masses, terrain and jet streams.
- The relationship between CAPE and C_p is positive and the relationship between CAPE and T_p is positive too at all station but Mosul station represents very high correlation while Zakho station represents low correlation this due to the nature of the region, airlifting mechanism, condensation and the meteorological factors.
- The Dohook station the maximum yearly mean of CAPE, C_p and T_p respectively 101.9047 J·kg^{-1} for the 2006 year, 434.2045 mm for the 2018 year, 908.7591 mm for the 1992 year.
- The Mosul station the maximum yearly mean of CAPE, C_p and T_p respectively 96.84094 J·kg^{-1}, 410.1414 mm, 718.0172 mm for the 2018 year.
- The Rabiah station the maximum yearly mean of CAPE, C_p and T_p respectively 106.2608 J·kg^{-1} for the 2006 year, 400.8977 mm, 692.3379 mm for the 2018 year.
- The Sinjar station the maximum yearly mean of CAPE, Cp and T_p respectively 100.6505 J·kg^{-1} for 2006 year, 377.1396 mm, 605.5202 mm for the 2018 year.
- The Zakho station the maximum yearly mean of CAPE, C_p and T_p respectively 106.8305 J·kg^{-1} for the 2006 year, 479.4777 mm for the 2018 year, 935.4565 mm for the 1992 year.
- The Zakho station of Iraq has the highest total monthly mean of CAPE accompanied by the highest convective and total precipitation.

Acknowledgements

An acknowledgement to the European Center Medium Weather Forecasts (ECMWF) on the data used in this study as well as an acknowledgement to the Mustansiriyha University.

References

Abbood, Z.M. & Al-Taai, O.T. (2018a). Calculation of absorption and emission of thermal radiation by clouds cover. *ARPN Journal of Engineering and Applied Sciences*, *13*(24), 9446-9456.

Abbood, Z.M. & Al-Taai, O.T. (2018b). Study of absorbance and emissivity solar radiation by clouds, aerosols and some atmospheric gases. *Journal of Applied and Advanced Research*, *3*(5), 128-134.

Ahrens, C.D. (2013). *Meteorology today: an introduction to weather, climate and the environment*. 10th ed. Belmont, CA: Brooks/Cole.

Al-jaf, S.J. & Al-Taai, O.T. (2019a). Impact of nitrous oxide (N_2O) concentrations on atmospheric air temperature changes over Iraq and some neighboring regions. *Journal of the University of Garmian*, *6*(1), 338-343.

Al-jaf, S.J. & Al-Taai, O.T. (2019b). Impact of carbon dioxide concentrations on atmospheric temperature changes over Iraq and some neighboring countries. *Plant Archives*, *19*(2), 1450-1456.

Al-Obeidi, A.M. (2008). *The effect of rainfall on soil erosion for selected station in Iraq* (PhD thesis, Mustansiriyah University Baghdad, Iraq).

Al-Timimi, Y.K. (2012). *Assessment of drought in Iraq using Standardized Precipitation Index*

(SPI) and satellite data (PhD thesis, Mustansiriyah University Baghdad, Iraq).
Bolboaca, S.D. & Jäntschi, L. (2006). Pearson versus Spearman, Kendall's tau correlation analysis on structure-activity relationships of biologic active compounds. *Leonardo Journal of Sciences*, *5*(9), 179-200.
Doswell III, C.A. & Rasmussen, E.N. (1994). The effect of neglecting the virtual temperature correction on CAPE calculations. *Weather and Forecasting*, *9*(4), 625-629. DOI 10.1175/1520-0434(1994)009<0625:TEONTV>2.0.CO;2
Gabler, R.E., Petersen, J.F., Trapasso, L.M. & Sack, D. (2009). *Physical geography*. 9th ed. Belmont, CA: Brooks/Cole.
Gettelman, A. Seidel, D. Wheeler, M. & Ross, R. (2002). Multidecadal trends in tropical convective available potential energy. *Journal of Geophysical Research Atmospheres*, *107*(D--21), ACL-17. DOI 10.1029/2001JD001082
Goyal, M.K. (2016). Engineering hydrology. Delhi: PHI Learning.
Hron, K., Filzmoser, P. & Thompson, K. (2012). Linear regression with compositional explanatory variables. *Journal of Applied Statistics*, *39*(5), 1115-1128.
Lackmann, G. (2013). *Midlatitude synoptic meteorology*. Chicago: The University of Chicago Press.
Meukaleuni, C., Lenouo, A. & Monkam, D. (2016). Climatology of convective available potential energy (CAPE) in ERA – interim reanalysis over West Africa. *Atmospheric Science Letters*, *17*(1), 65-70.
Namdar, K.H. (2017). *Synoptic study of role of convective available potential energy on formation rainstorm over Iraq* (master's thesis, Mustansiriyah University Baghdad, Iraq).
Niwas, R., Singh, S., Singh, D., Khichar, M.L. & Singh, R. (2006). *A textbook on agricultural meteorology*. Research Gate.
Padua, D. (2000). The Fortran I compiler. *Computing in Science and Engineering*, *2*(1), 70-75.
Riemann-Campe, K., Fraedrich, K. & Lunkeit, F. (2009). Global climatology of convective available potential energy (CAPE) and convective inhibition (CIN) in ERA-40 reanalysis. *Atmospheric Research*, *93*(1-3), 534-545.
Salman, A.D. (2015). *The effect of temperature and rainfall on crop productivity of wheat and barley in some governorates of Iraq* (master's thesis, Mustansiriyah University Baghdad, Iraq).
Saxena, R.N. & Gupta, D.C. (2017). *Elements of hydrology and groundwater*. Delhi: PHI Learning.
Schultz, P. (1989). Relationships of several stability indices to convective weather events in northeast Colorado. *Weather and Forecasting*, *4*(1), 73-80.
Wang, P.K. (2013). *Physics and dynamics of clouds and precipitation*. Cambridge: Cambridge University Press.
York, D., Evensen, N.M., Martýnez, M.L. & Delgado, J.D. (2004). Unified equations for the slope, intercept, and standard errors of the best straight line. *American Journal of Physics*, *72*(3), 367-375.
Zakaria, S., Al-Ansari, N., Ezz-Aldeen, M. & Knutsson, S. (2012). Rainwater harvesting at eastern Sinjar Mountain, Iraq. *Geoscience Research*, *3*(2), 100-108.

Summary

Analysis of the convective available potential energy by precipitation over Iraq using ECMWF data for the period of 1989–2018. The Convective Available Potential Energy (CAPE) represents the amount of energy for a sample of air. The sample departs vertically within the atmosphere and through these values the potential energy to predict the extreme weather conditions such as storms, hurricanes, lightning and thunder. Data are taken by CAPE, convective precipitation (C_p) and total precipitation (T_p) from satellites recorded by the European Centre for Medium-Range Weather Forecasts (ECMWF). The choice of 30 years (1989–2018) over Iraq station between two latitudes (29.5°–37.22° N) and two longitudes (48.45°–38.45° E). Otherwise, we have studied total yearly mean of CAPE, C_p and T_p over Iraq, the total monthly mean of CAPE, C_p and T_p for the selected station, as well as the relationship between of CAPE, C_p and T_p for the selected station. The results showed that the highest total yearly mean of CAPE, C_p and T_p over Iraq was included northern stations and lowest was included central and southern stations. The highest total monthly mean of CAPE, C_p and T_p for Zakho station. The relationship between the CAPE and C_p is positive and the relationship between CAPE and T_p is positive too at five stations but Mosul station represents very high correlation while Zakho station represents the low correlation.

Authors' address:
Osama T. Al-Taai
(http://orcid.org/0000-0002-4747-214X)
Zainab M. Abbood
(https://orcid.org/0000-0003-4005-2510)
Mustansiriyah University
College of Science
Atmospheric Science Department
Baghdad, Iraq
e-mail: osamaaltaai77@uomustansiriyah.edu.iq
zainabatmo@uomustansiriyah.edu.iq

Scientific Review – Engineering and Environmental Sciences (2020), 29 (2), 212–222
Sci. Rev. Eng. Env. Sci. (2020), 29 (2)
Przegląd Naukowy – Inżynieria i Kształtowanie Środowiska (2020), 29 (2), 212–222
Prz. Nauk. Inż. Kszt. Środ. (2020), 29 (2)
http://iks.pn.sggw.pl and Environment
DOI 10.22630/PNIKS.2020.29.2.18

Zahraa M. HASSAN[1, 2], Monim H. Al-JIBOORI[2], Hazima M. Al-ABASSI[3]

[1] Iraqi Ministry of Health and Environment
[2] Mustansiriyah University, College of Science
[3] University of Baghdad, Ibn al-Haytham College of Education

Heat waves and health impact on human in Baghdad

Key words: heat wave, max air temperature, CBC analysis, Baghdad

Introduction

Global climate change would affect human health via pathways of varying complexity, scale and directness and with different timing. Similarly, impacts would vary geographically as a function both of environment and topography and of the vulnerability of the local population (Michael, 2007; Mogil, 2007). Impacts would be both positive and negative (although expert scientific reviews anticipate predominantly negative). This is no surprise since climatic change would disrupt or otherwise alter a large range of natural ecological and physical systems that are an integral part of Earth's life support system (NWS-NOAA, 2014). Via climate change humans are contributing to a change in the conditions of life on earth. The main pathways and categories of health impact of climate change are shown in Figure 1.

The more direct impacts on health include those due to changes in exposure to weather extremes (heat waves, winter cold); decreases in winter mortality due to milder winters may compensate for increases in summer mortality due to the increased frequency of heat waves (Sessler, 2009). In countries with a high level of excess winter mortality, such as the United Kingdom (Langford & Bentham, 1995; Roony, McMichael, Kovats & Coleman, 1998). The health impacts of climate variability are, in general, likely to be more pronounced over the near term than are those of climate change. For example, large anomalies in temperature and rainfall in a particular season could cause a number of vector-borne and water-borne epidemics, thereafter the weather could return to normal. Extremes of heat can cause heat exhaustion, cardiovascular disease (heart attacks and

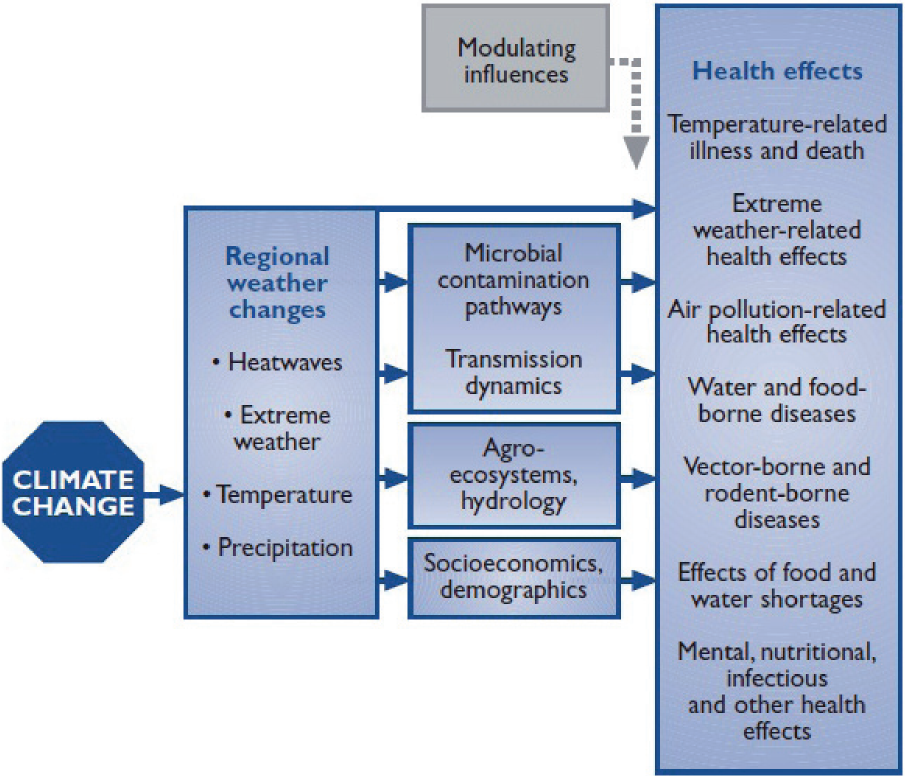

FIGURE 1. Pathways by which climate change affects human health, including local modulating influences and the feedback influence of adaptation measures (Patz et al., 2000)

strokes) while cold spells can lead to hypothermia and increase morbidity and mortality from cardiovascular disease (Lindsay & Martens, 2000).

In this research, 40 blood samples were taken from the individual exposure heat wave and the necessary laboratory tests were performed. Most of the tests were conducted by specialized doctors, where these readings were taken from the laboratories of hospitals (medical city), Ibn al-Baladi Children's Hospital, Kadhimiya and Sheikh Zayed hospital by age groups (10–60 years) and for both genders. This study is the first study of its kind in the Department of Atmospheric Sciences, but for laboratory tests, it gives basic and basic laboratory indicators to monitor human health and reveals the presence of disorders in the vital functions of the human body; these tests include: ESR, CRP, HB, PL, PCV.

Erythrocyte sedimentation rate (ESR) is a blood sedimentation test, which is a laboratory test, in which the blood components are deposited and calculates the time taken for sedimentation. Level of erythrocyte sedimentation for inflammation in the body. Infections generally cause the proteins in the blood cells to change, causing them to bind in mass, becoming denser than proteins in normal blood cells. The ESR test simply measures the rate of deposition in the cells. The lower the test tube, the faster it falls down, the more inflammatory it is in the body (Michael, 2015). Table 1 presents normal values according to the Westergren method.

TABLE 1. The Westergren method standards for ESR according to age and sex

Specification	Normal value [$mm \cdot h^{-1}$]
Newborn	0–2
Children	1–10
Males in total	0–25
aged 0–50	< 15
aged 51–85	< 20
aged > 85	< 30
Females in total	0–30
aged 0–50	< 20
aged 51–85	< 30
aged > 85	< 42

C-reactive protein (CRP) is an analysis done to determine the amount of protein in the blood in the human body and is an abbreviation of the medical term C-reactive protein. If this protein is found to increase in blood, it means that the person has acute inflammation, which helps the doctor to diagnose and treat some diseases (Chen et al., 2006). There are two types of CRP test: (1) regular CRP: protein test found in very high blood between 10 and 1,000. This test is used to determine the presence of inflammation or infection in the body; (2) high sensitivity CRP: high-sensitivity protein test, which helps in measuring the proportion of light color protein in the blood between 0.05 and 10 $mg \cdot l^{-1}$. It is used in normal people to determine the extent of coronary insufficiency or some heart disease.

Hemoglobin (HB) analysis is useful to know the patient's blood status in case of anemia (anemia, bleeding, infection or allergy), depending on the height of each component of the blood or low.

Platelet counts (PL) are part of the CBC analysis to determine the triglycerides and the standard and percentage of each.

Packed cell volume (PCV) is one of the CBC tests, which is the ratio of the size used by red blood cells, and is a way to determine whether the number of red blood cells is high or low or normal.

TABLE 2. Reference values unit normal the Westergren CBC value range for male and female

Factor	Value
WBC	$5.00 \cdot 10^3$ iu
HB	11.0–14.0 $g \cdot dl^{-1}$
PCV	11.6–14.0
PL	$150 \cdot 10^3$ iu

Climate of Baghdad

Baghdad is the capital of Republic of Iraq and is located in the middle of it along the Tigris river. It splits Baghdad in half, with the eastern half being called Risafa and the western half known as Karkh (Fig. 2). Geographically, Baghdad is situated at latitude 33.6–33.5° N, longitude 44.25–44.5° E and 30–38 m above mean sea level (msl). It covers an area of 857.3 km^2 and forms 0.2% of an overall Iraq area and is in the heart

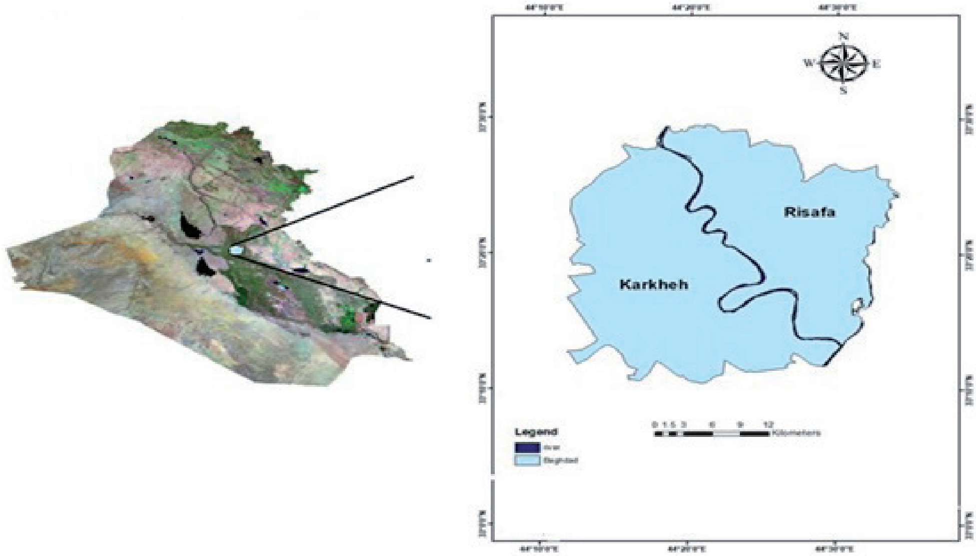

FIGURE 2. Map of Baghdad

of ancient Mesopotamia. The land is almost entirely flat and low-lying. The climate of Baghdad has a subtropical desert climate (Köppen climate classification BWH) featuring extremely hot, dry summer and mild, damp winter (Roth, 2007). The mean annual range of air temperature over a whole gear is 15–34°C with the mean of 25°C, while annual range of the mean daily sunshine duration is about 10–14–14 h with mean of 7.5 h.

Material and methods

Study group

The study was conducted for the period of June, July and August 2019, it included 40 blood samples for patients exposed to heat waves who attended to Medical City, Ibn Al-Baladi, Sheikh Zayed, Kadhimiya Educational with male and female ages 10–60 years, CBC analysis was performed.

Blood sample

Blood venous (5 ml) was withdrawn from 40 patient's by using sterile medical syringe and placed in clean, dry plastic tubes free of anticoagulants and let it coagulate at room temperature and then placed in a centrifuged for 10 min (3,000 rpm) to separate serum.

Statistical analysis

Statistical analysis of the data was carried out using (SigmaPlot) software to analyze the results and conclude the variance. The significant values of the analyses were calculated (CRP, ESR, WBC, PL, PCV). The mean values were calculated for each age group which divided in to five sub-groups, each group comprising (10 years) shown in Table 3, as well as calculated the deviation and percentage for each group.

TABLE 3. Number of patients exposed to heat wave

Age group	Numbers of cases
10–19	8
20–29	6
30–39	14
40–49	6
50–60	6
Total	40

Result and discussion

Daily average of maximum air temperature

The air temperature is one of the important atmospheric elements because of its wide effects on climate variables. Baghdad's climate was described using maximum temperatures in the summer. The monthly trend data for the three months of the summer (June, July and August) and the results showed that the general trend of temperature has increased over time clearly over the monthly averages despite the variation in these rates as shown in Table 4. Where the average temperature for the month of June (42.72) was the standard deviation for it (3.314), the average temperature for July (47.53) and the standard deviation was (1.816), the average temperature for the month of August (47.4) and the standard deviation for it (2).

TABLE 4. Average and standard deviation for three summer months for the year 2019

Month	*AVG*	*SD*
June	42.72	3.314
July	47.53	1.816
August	47.4	2

Figure 3 shows the daily air max temperatures for the three summer months (June, July and August) for the year 2019, where we notice through these forms that the general trend of temperatures indicates an increase despite the presence of fluctuations ranging from increase and decrease, and that the summer months (June, July and August) are distinguished by the fact that it has an increasing trend of temperatures as shown in Figure 3.

As shown in Table 5 which illustrated the mean and percent value for CRP, ESR and CBC analyze for patients (male). Table 5 also shows the average temperature of three months of summer (June, July, August) for the year 2019.

The result for CRP was (mean and percent) for all age group (10–60 years) the mean were (12, 14.5, 17, 15.5, 17) respectively and the percent were (92%, 99%, 100%, 100%, 100%) respectively we observe a highly percent was in age group (30–39, 40–49 and 50–60). This result was in a concordance with performed by (Chen et al., 2006).

CRP was elevated after exposure to infectious agent and consider as a biomarker for detecting of acute inflammation but there is no explanation for their elevation after exposing to heat wave because there is no previous studies focus in this field.

The result for ESR was (mean and percent) for all age group (10–60 years)

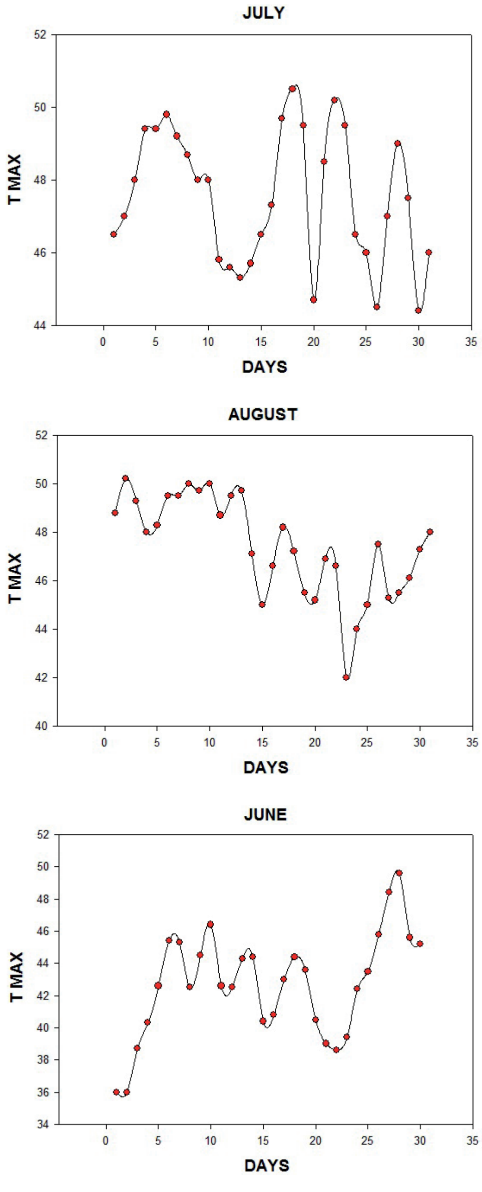

FIGURE 3. Daily air max temperature for three months (June, July and August) for 2019

the mean were (43, 40.5, 53.5, 43, 49) respectively, the percent were (99%, 101%, 100%, 100%, 100%) respectively, we observe a highly percent was in age groups (30–39 and 50–60). This result was in an agreement which performed by Michael (2015).

The increased rate of erythrocyte sedimentation is only an indication of inflammation or disease in the human body as it interacts with acute conditions in the body that lead to a rise in the level of ESR in the blood (MedlinePlus, 2012).

The result for CBC analyze (WBC, PCV, PL) (mean and percent) for all age groups (10–60 years) were WBC (10.5, 14.15, 11.35, 11.55, 11) respectively (99%, 101%, 100%, 100%, 99%) respectively we observe a highly percent was in age groups (20–29). PCV (27, 36, 28, 28.5, 32) respectively (100%, 100%, 100%, 100%, 100%) respectively, we observe a highly percent in age groups (20–29, 50–60) and PL (215, 268.5, 182.5, 215.5, 215) respectively, (101%, 101%, 100%, 100%, 100%) respectively, we observe a highly percent in age groups (10–19, 20–29, 30–39, 40–49, 50–60). This result was in an agreement which performed by Reiser (1981) and Brewer (2006).

As shown in Table 6 which illustrated the mean and percent value for CRP, ESR and CBC analyze for patients (female). Table 6 also shows the average max air temperature of three months of summer (June, July, August) for the year 2019 which was (45.8). The result for CRP (mean and percent) for all age groups (10–60 years) were (14, 17, 15, 15, 12) respectively (99%, 100%, 100%, 101%, 100%) respectively, we observe a highly percents was in age groups 20–29, 30–39 and 40–49.

The result for ESR (mean and percent) for all age groups (10–60 years) were 46, 31.5, 43.5, 47.5, 31) respectively (100%, 100%, 101%, 100%, 99%) re-

TABLE 5. Result of CBC analyses for male for three summer months (June, July and August) for 2019

Age	Mean CRP	CRP%	Mean ESR	ESR%	Mean WBC	WBC%	Mean PCV	PCV%	Mean PL	PL%	T_{max} [°C]
10–19	12	92	43	99	10.5	99	27	100	215	101	45.8
20–29	14.5	99	40.5	101	14.15	101	36	100	268.5	101	
30–39	17	100	53.5	100	11.35	100	28	100	182.5	100	
40–49	15.5	100	43	100	11.55	100	28.5	100	215.5	100	
50–60	17	100	49	100	11	99	32	100	215	100	
Total	15.5	100	43	100	11.35	100	28.5	100	215	100	

TABLE 6. Result of CBC analyses for female for three summer months (June, July and August) for 2019

Age	Mean CRP	CRP%	Mean ESR	ESR%	Mean WBC	WBC%	Mean PCV	PCV%	Mean PL	PL%	T_{max} [°C]
10–19	14	99	46	100	11.9	100	33	100	131	100	45.8
20–29	17	100	31.5	100	10.85	100	30	100	220.5	100	
30–39	15	100	43.5	101	11.35	99	29	100	190.5	99	
40–49	15	101	47.5	100	11.9	101	32.5	100	291	101	
50–60	12	100	31	99	7.6	101	31	100	245	100	
Total	15	100	43.5	100	11.35	100	31	100	220.5	100	

spectively, we observe a highly percents was in age groups (10–19, 30–39, 30–39 and 40–49).

The result for CBC analyze (WBC, PCV, PL) (mean and percent) for all age groups (10–60 years) were WBC (11.9, 10.85, 11.35, 11.9, 7.6) respectively (100%, 100%, 99%, 101%, 101%, 99%) respectively, we observe a highly percents in age groups (10–19, 20–29, 30–39, 40–49). PCV (33, 30, 29, 32.5, 31) respectively, (100%, 100%, 100%, 100%, 100%) respectively, we observe a highly percent in age groups (10–19, 20–29, 30–39, 40–49, 50–60) and PL (131, 220.5, 190.5, 291, 245) respectively (100%, 100%, 99%, 101%, 100%) respectively, we observe a highly percents in age groups (20–29, 30–39, 40–49, 50–60).

Figures 4 and 5 show the number of high levels of CBC values for all age groups from (10–60 years) this rise appears clear in males more than females and due to the increase in diseases in males more than females due to the fact that the immune factor in men is lower than the immune factor in women because of the high estrogen in women which strengthens the immune system (MedlinePlus, 2012).

This study showed that platelets have a high count. The platelets that control levels of liquidity and blood clotting, if the medical results of more than 100,000 plates, this indicates a defect in

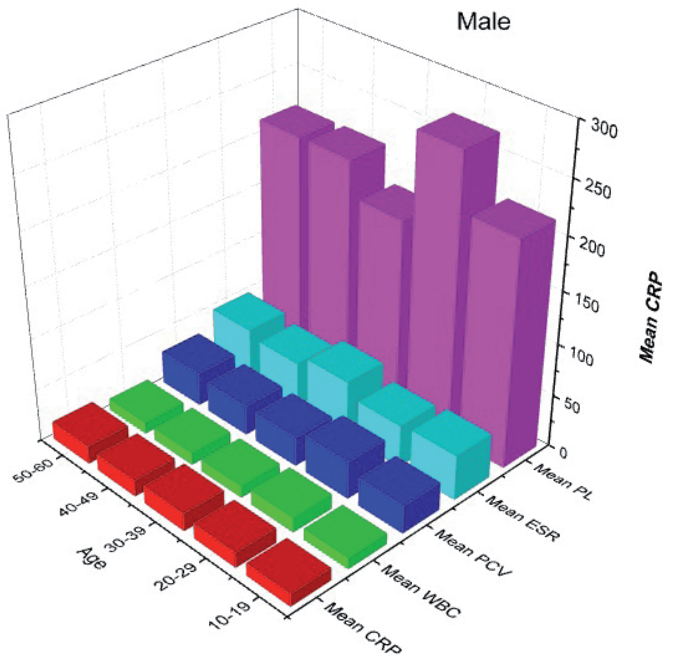

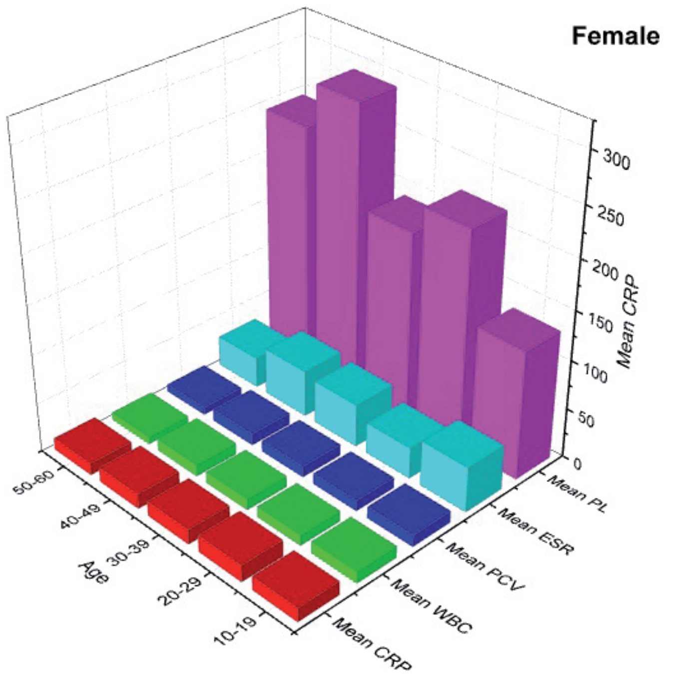

FIGURE 4. The mean of males and females exposed to heat waves for the period of June, July and August 2019

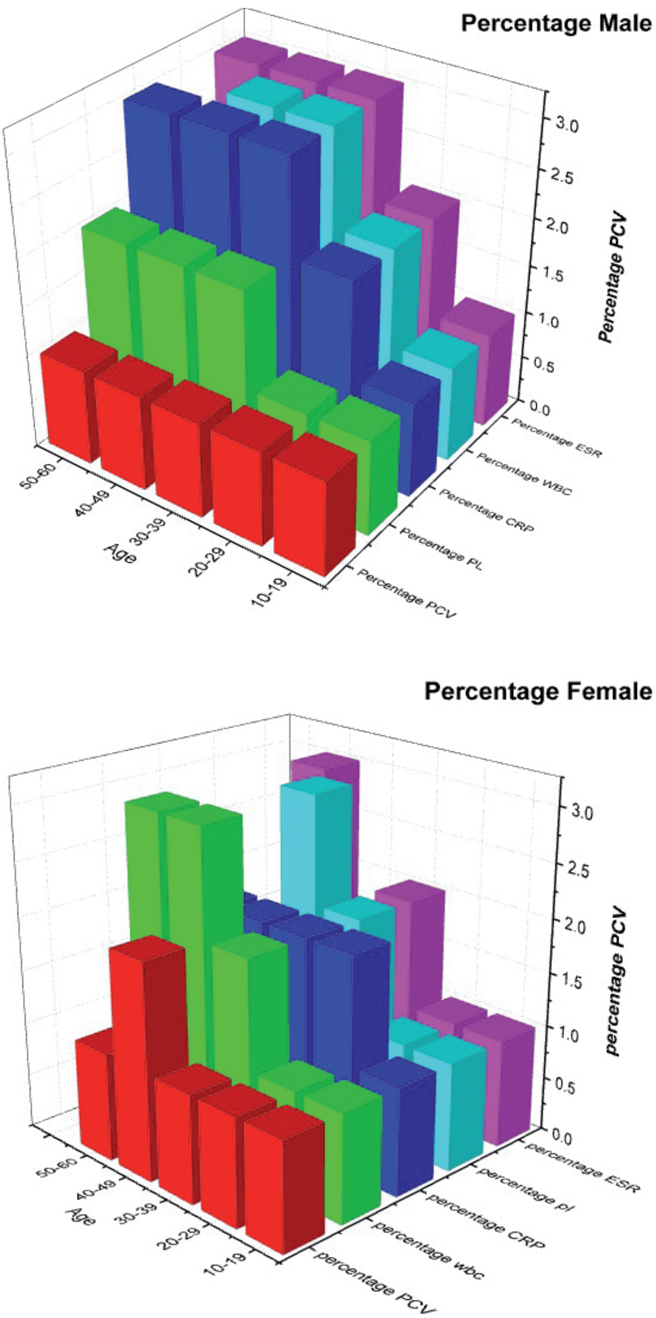

FIGURE 5. The percent of males and females exposed to heat waves for the period of June, July and August 2019

blood fluid and this explains the injury of patients exposed to heat waves of heart clots and angina.

Hyperthermia is distinct from a fever heat stroke generally present with a hyperthermia of greater than 40.6°C, combination with disorientation before when body exposure to high temperature and heat stroke keratinocytes can produces (IL-1) which interleukin induce hypothalamus to produce prostaglandin (PGE_2) with through interaction with the (GP_3) receptor stimulates neurotransmitters such as cyclic adenosine monophosphate and increase body temperature.

Also this cytokines stimulate production of inducible cycloxygenase (arachidonic acid metabolite) and through this pathway thromboxane A_2 (TXA_2) will produce which causes vasoconstriction and promote platelet aggregation, as a consequence dissemination clotted will occur and multiorgan failure is the main cause of death.

Conclusion

According to the result of present study we can conclude that all people who exposed for heat wave are under risk to initiate heart attack that may occur due to the highly significant increasing in their platelet count and CRP level.

References

Brewer, D.B. (2006). Max Schultze (1865), G. Bizzozero (1882) and the discovery of the platelet. *British Journal of Haematology*, *133*(3), 251–58.

Chen, C.M., Hou, C.C., Cheng, K.C., Tian, R.L., Chang, C.P. & Lin, M.T. (2006). Activated protein C therapy in a rat heat stroke model. *Critical Care Medicine*, *34*(7), 1960-1966.

Langford, I.H. & Bentham, G. (1995). The potential effects of climate change on winter mortality in England and Wales. *International Journal of Biometeorology*, *38*(3), 141-147.

Lindsay, S. & Martens, W.J.M. (1998). Malaria in the African Highlands: past, present and future. *Bulletin of the World Health Organization*, *76*(1), 33-45.

Michael, H. (2015). Erythrocyte sedimentation rate and C-reactive protein. *Australian Prescriber*, *38*(3), 93-94.

Mogil, H.M. (2007). *Extreme weather*. New York: Black Dog & Leventhal Publishers.

National Weather Service – National Oceanic and Atmospheric Administration [NWS-NOAA] (2014-06-16). *Heat*: *a major killer*. Retrieved from: https://www.weather.gov/grb/heat

Patz, J., McGeehin, M.A., Bernard, S.M., Ebi, K.L., Epstein, P.R., Grambsch, A., Gubler, D.J., Reither, P., Romieu, I., Rose, J.B., Samet J.M. & Trtanj, J. (2000). The potential health impacts of climate variability and change for the United States: executive summary of the report of the health sector of the US National Assessment. *Environmental Health Perspectives*, *108*(4), 367-376.

Reiser, S.J. (1981). *Medicine and the reign of technology*. Cambridge: Cambridge University Press.

Rooney, C., McMichael, A.J., Kovats, R.S. & Coleman, M.P. (1998). Excess mortality in England and Wales, and in Greater London, during the 1995 heatwave. *Journal of Epidemiology & Community Health*, *52*(8), 482-486.

Roth, M. (2007). Review of urban climate research in (sub) tropical regions. *International Journal of Climatology: A Journal of the Royal Meteorological Society*, *27*(14), 1859-1873.

MedlinePlus (2014-08-14). *Medical Encyclopedia – ESR*. Retrieved from: http://www.nlm.nih.gov/medlineplus/ency/article/003638.htm [access 14.08.2014].

Sessler, D. (2009). Thermoregulatory defense mechanisms. *Critical Care Medicine*, *37*(7), 203-210.

World Meteorological Organisation [WMO] (2016). *Provisional WMO statement on the status of the global climate in 2016*. Retrieved from: https://public.wmo.int/en/media/press-release/provisional-wmo-statement-status-of-global-climate-2016

Summary

Heat waves and health impact on human in Baghdad. This investigation aim to evaluate the effect of heat wave on health of human, so to achieve this 40 blood samples for person exposed to heat wave were drawn most patients were attend to specialists in hospital laboratories (Medical City, Ibn al--Baladi, Sheikh Zayed, Kadhimiya Educational). The patients aged 10–60 years, male (20) and female (20). CBC analyzes was performed. The result of the presents study recorded a highly significant difference in total (mean and percent) as compared with the normal value of the CBC analyze the result for total (mean and percent) for male the factors CRP, ESR, WBC, PCV, PL (15.5, 43, 11.35, 28.5, 215) respectively (100%, 100%, 100%, 100%, 100%) and the result for total (mean and percent) for female the factors CRP, ESR, WBC, PCV, PL (15, 43.5, 11.35, 31, 220.5) respectively (100%, 100%, 100%, 100%, 100%). According to the result we can conclude that there was a highly significant deferent in mean value for patient compared with the normal value which is the mean cause of hard attack which lead to death. The study is the first of its kind in the Department of Atmospheric Sciences in Iraq.

Authors' address:
Zahraa M. Hassan
Ministry of Health, Bab-Al-Muadum, Baghdad, Iraq
22, 8 Baghdad
Iraq
e-mail: zahraamousa86@gmail.com

Scientific Review – Engineering and Environmental Sciences (2020), 29 (2), 223–233
Sci. Rev. Eng. Env. Sci. (2020), 29 (2)
Przegląd Naukowy – Inżynieria i Kształtowanie Środowiska (2020), 29 (2), 223–233
Prz. Nauk. Inż. Kszt. Środ. (2020), 29 (2)
http://iks.pn.sggw.pl
DOI 10.22630/PNIKS.2020.29.2.19

Ewa FIGIEL, Dorota LECIEJ-PIRCZEWSKA
West Pomeranian University of Technology, Faculty of Civil and Architecture

Outer wall with thermal barrier. Impact of the barrier on heat losses and CO_2 emissions

Key words: thermo-active-wall-barrier, CO_2 impact, heat loss, energy consumption

Introduction

The building sector's large contribution to the total energy use in the EU, estimated to be 40% (Directive 2010/31//UE) simultaneously creates a potential for reducing its power consumption as well as the emission of greenhouse gasses by implementing pertinent solutions. Current Polish and EU research confirms, that efforts to improve the energy efficiency of the building sector have led to a significant impact on the reduction of greenhouse gas emissions and are consequently mitigating the effects of climate change (Report COM(2017) 56). They also decrease the low-stack emissions, which pose significant harm to the public and the environment. The requirements and laws to reduce the energy consumption and to up the share of renewable energy sources employed in buildings are becoming stricter, which forces the inception of new, innovative technologies. One of them is a thermal barrier in the exterior wall creating a nonstandard thermal insulation (Xu, Wang, Wanga & Xiao, 2010). Buildings with an active thermal barrier are categorized as thermo-active building systems (TABS). A thermal barrier is achieved by maintaining a constant flow of a low temperature medium, most commonly a solar fluid, through a conduit properly spaced out within the layer of the exterior wall. During the heating period this medium has a lower temperature compared to the conditions inside the building, but a higher temperature compared to conditions inside the same wall layer had the pipes not been installed. This way heat loss due to transmission is minimized. Energy supplied this way to the outer wall interior is most commonly derived from solar and geothermal energy accumulated in a special thermal energy storage. The active thermal barrier can be used not only for heating, but also for the cooling of the building. In such a case, the temperature of the medium is lower compared to the temperature of the same wall interior layer had the pipes not been installed.

Such an application of a relatively low-temperature medium is intended to limit heat loss due to transmission in new buildings as well as thermo-modernised buildings using one of various systems, including: ISOMAX, ISOACTIVE-3D, BT&SONS Kft system.

Active thermal insulation

Walls with active thermal insulation can have different constructions. However, they always have coils that generate a thermal barrier for heat transfer through the wall. One of the first systems using this solution was the ISOMAX system. In this system an external wall is built from 12.5 cm foamed polystyrene board connected by means of patented concrete fins to another 12.5 cm foamed polystyrene board. Between them PP pipes in form of meanders are placed. The space between these foamed polystyrene boards is filled with BIO-POR concrete. The construction of such a wall is based on a core in which a constant temperature is maintained, and which is thermally well insulated on both sides. A thermal barrier is achieved by providing a constant flow of a low-parameter medium through pipes appropriately placed in the core. The application of a partition with a thermal barrier prevents vapour from escaping and significantly reduces the loss of heat by transmission from a building interior by creating blockades preventing heat flow from the areas of higher energy levels into the lower ones. Figure 1 presents the scheme of such a partition.

Walls with active thermal insulation of slightly different construction are used in Hungary. In ISOACTIVE-3D technology, the external wall is made of foamed polystyrene board: 5 cm thick (external) and 15 cm connected by means of a special metal mesh embedded in lightweight concrete. The PP pipes are placed in the outer layer of the concrete. Similar to the ISOMAX system, the thermal barrier is achieved due to the constant flow of a low-temperature medium through the coils. The scheme of such a partition is

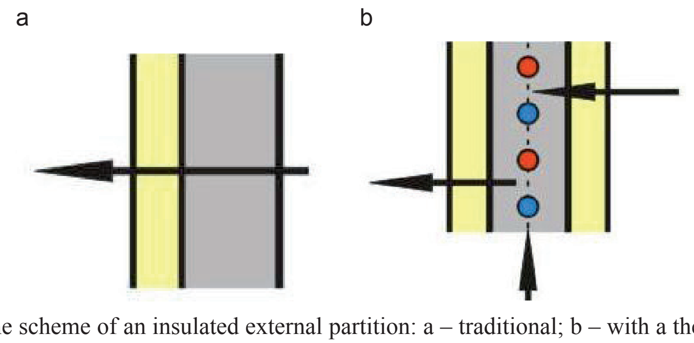

FIGURE 1. The scheme of an insulated external partition: a – traditional; b – with a thermal barrier in the ISOMAX system (12.5 cm of foamed polystyrene, 15 cm of BIO-POR – concrete with PP pipes, 12.5 cm of foamed polystyrene)

shown in Figure 2. Walls with active thermal insulation from BT&SONSKft have different constructions shown in Figure 3.

As observed the coils can be located in different layers of the wall cross-section. The effectiveness of the coil's operation as a thermal barrier depends largely

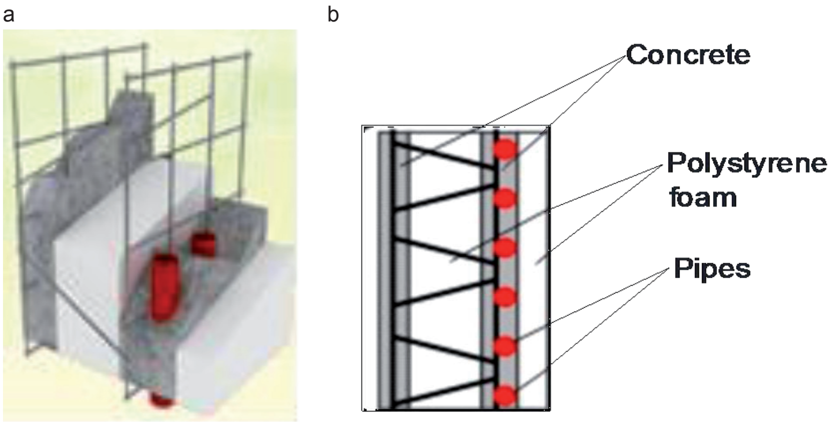

FIGURE 2. The view and the scheme of the external partition with a thermal barrier in the ISOACTIVE-3D system (5 cm of foamed polystyrene from the outside, lightweight concrete with PP pipes, 15 cm of foamed polystyrene, lightweight concrete, all connected with a metal mesh embedded in concrete)

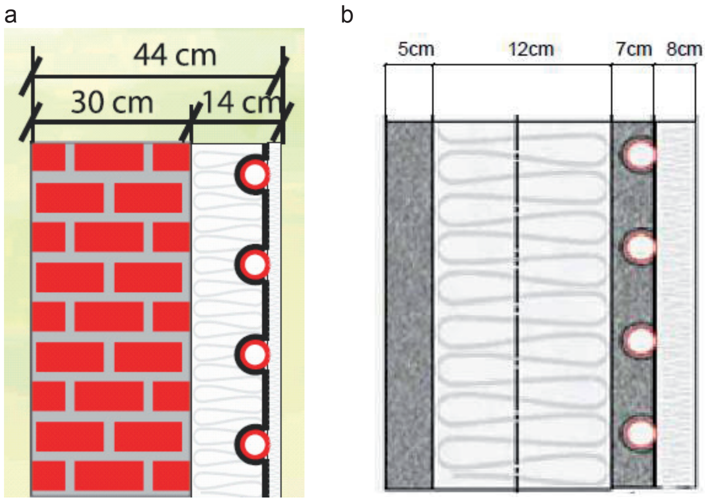

FIGURE 3. The scheme of the external partition with an active thermal insulation BT&SONS Kft: a – a partition made of 30 cm Porotherm, insulated with 14 cm thick foamed polystyrene with PE pipes with a low parameter measure on the outside; b – a partition made of 5 cm Porotherm, 12 cm of foamed polystyrene, 7 cm of Porotherm with PE pipes on the outside and external layer of 8 cm foamed polystyrene

FIGURE 4. The external partition with an active thermal insulation (photo by BT&SONS Kft, 15 April 2017)

on its position as well as on the temperature level of the medium that supplies it.

The building's heating in the above-mentioned technologies using an active thermal insulation is realised through a combination of passive solar energy use within the roof and outer walls as well as geothermal energy. There is a solar absorber in the building's roof. It consists of a system of thin polypropylene or polyethylene pipes located directly under the roof, but above the insulation layer of the roof structure (between roofing and roof insulation). The system of polypropylene pipes is also in the core of the external walls (Fig. 4). Under the building there is a foundation – a floor plate. It also has a polypropylene pipe system insulated with foamed polystyrene and it performs the function of an underground heat storage system (energy reservoir) – Figure 5. The principle of the system's operation is as follows (Fig. 6).

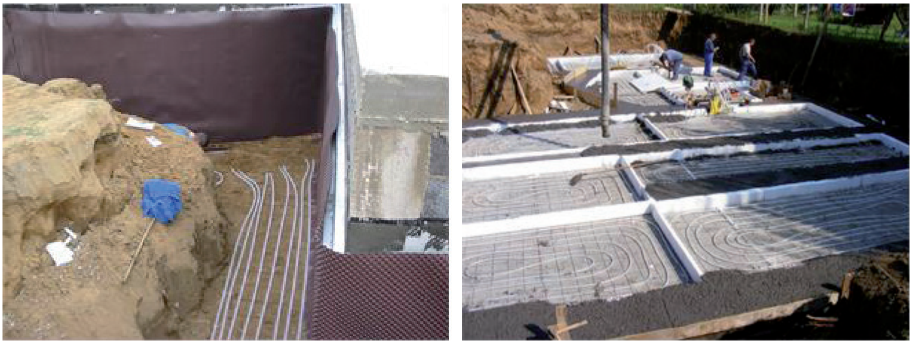

FIGURE 5. Heat storage under the foundation plate and outside the building (photo by BT&SONS Kft, 15 April 2017)

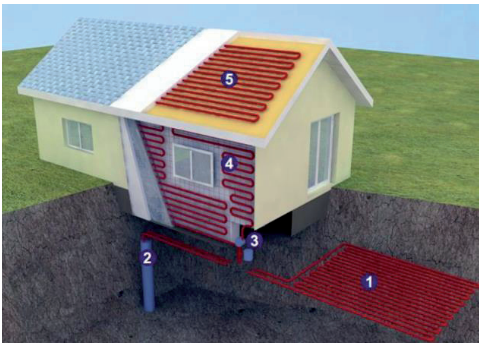

FIGURE 6. The scheme of the building with an active thermal insulation in external partitions (illustration by BT&SONS Kft system, 15 April 2017): 1, 2 – heat storage under the foundation plate or next to the building; 3 – circulating pump; 4 – coils in external walls; 5 – roof absorber

Solar energy is absorbed by the solar absorber below the roof and is transmitted to the external walls. The excess of energy, which is not used for the building's heating is accumulated in the underground storage system. As the needs arise this energy is consumed. Energy obtained from the sun, stored under the foundation plate is returned to the wall's core from cellular concrete and it also indirectly heats the soil under the building. For the sake of high air tightness of the building the mechanical ventilation with heat recovery is used additionally.

The influence of thermal barrier position on its effectiveness

The outer walls with a thermal barrier limit heat transmission losses from heated rooms. In the ISOMAX system polypropylene pipes with heating medium are located exactly in the centre of the wall's core. In reality they can be in any place inside the wall. In the partitions used in Hungary, the coils are located on the outside of the wall. Therefore, the following section shows how the location of the pipes influences heat transmission losses from heated rooms. For this purpose, the model of an outer wall with thermal barrier presented in earlier works was used (Leciej-Pirczewska & Szaflik, 2006, 2010). It is based on the balance of energy supplied and discharged from the partition. Based on this the heat fluxes $\dot{Q}_1$, $\dot{Q}_2$ and $\dot{Q}_3$ were determined (Fig. 7).

The heat fluxes $\dot{Q}_1$, $\dot{Q}_2$ and $\dot{Q}_3$ were made dependent on R_1 – the thermal resistance of the internal courses of the external wall (these which are between pipes and the room), in order to better display this problem.

The calculations were conducted for the walls made of the same materials as presented in the above section about active thermal insulation. The results of calculations for a partition in the ISOMAX system are introduced in Figure 7 for three different locations of thermal barrier and for the wall without this barrier. The following data was used in the calculations:

– internal temperature $T_i = 20°C$,
– external temperature $T_e = -16°C$,
– initial medium temperature $T_p = 10°C$,
– medium thermal capacity $W = 104.8$ $W \cdot K^{-1}$.

Heat fluxes $\dot{Q}_1 / \dot{Q}$, $\dot{Q}_2 / \dot{Q}$ and $\dot{Q}_3 / \dot{Q}$ relative as a function of thermal resistance R_1 established for such conditions are introduced in Figure 8.

The heat flux transmission from the room $\dot{Q}_1$ decreases when the thermal barrier moves along the outside. The heat flux transmission outside the building $\dot{Q}_2$ and the heat flux given out during medium flow $\dot{Q}_3$ grows when the thermal barrier moves along outside.

The use of a thermal barrier considerably limits the heat losses from the room. The heat flux transmitted from the inside when the outer wall has a thermal barrier decreased compared with the wall without thermal barrier by:

– 41.09% for the outer wall in IZOMAX system with thermal barrier located inside the core,
– 44.75% for the outer wall in IZOMAX system with thermal barrier located in the centre of the core,
– 47.32% for the outer wall in IZOMAX system with thermal barrier located outside the core,
– 57.32% for the outer wall in BT&SONS Kft system with thermal barrier on the outside (Fig. 3b),
– 59.22% for the outer wall in BT&SONS Kft system with thermal barrier on the outside (Fig. 3a).

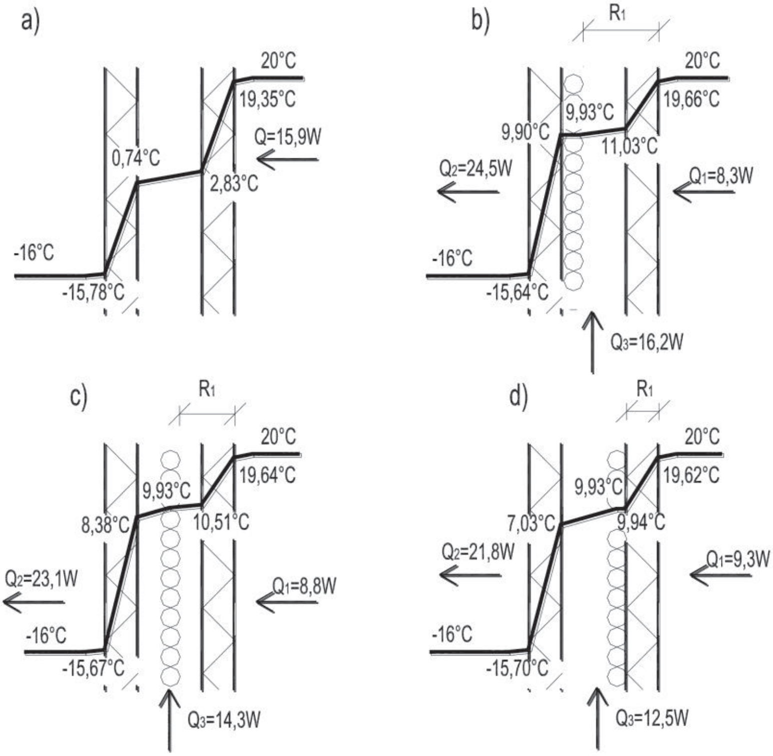

$\dot{Q}_1$ – heat flux penetrated from the room, $\dot{Q}_2$ – heat flux penetrated outside, $\dot{Q}_3$ – heat flux given up during medium flow, $\dot{Q}$ – heat flux penetrated from the room with traditional wall without thermal barrier.

FIGURE 7. Possible solutions of outer wall and wall's temperature distribution: a – traditional, highly--insulated outer wall without thermal barrier; b – outer wall with thermal barrier – PP pipes are close to outside the core; c – outer wall with thermal barrier – PP pipes are in the centre of the wall's core; d – outer wall with thermal barrier – PP pipes are close to inside the core

Resulting from this analysis, the highest reduction of heat losses is achieved with the thermal barrier positioned on the outside of the core. Such a position of the thermal barrier inside the wall is usually encountered in newly thermo-renovated buildings. This instance of the barrier placement has been thus assumed for further energy analysis below.

Thermal barrier influence on the energy performance of a typical single-family house and CO_2 emission

It is interesting, to what degree the thermal barrier can contribute to improvement of the building's energy

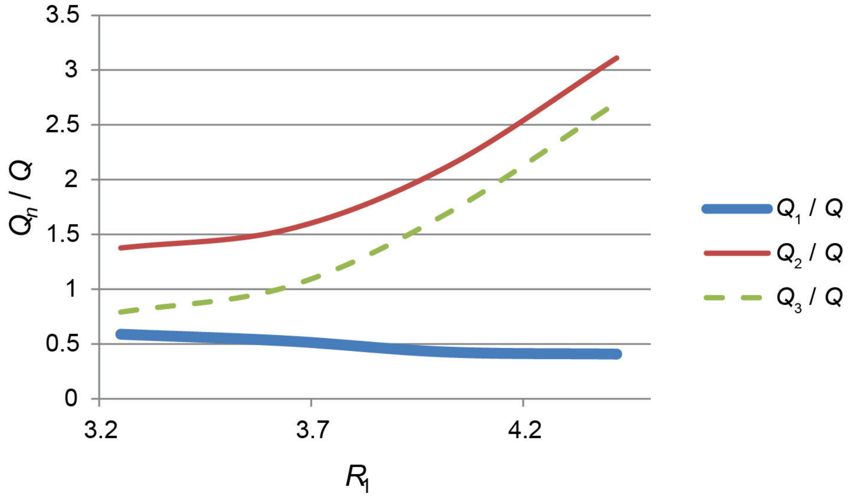

FIGURE 8. Diagram of relative heat fluxes $\dot{Q}_1 / \dot{Q}$, $\dot{Q}_2 / \dot{Q}$ and $\dot{Q}_3 / \dot{Q}$ depending on thermal resistance of the internal courses of the external wall R_1 [$m^2 \cdot K \cdot W^{-1}$]

performance and the reduction of CO_2 emissions. To arrive at an answer to this question an analysis of the influence of the energy consumption on a typical single-family building after thermo-modernisation was conducted. It was important to determine the following quantities for the selected building:

- the index of annual demand for final energy (EK),
- the index of annual energy needs (EU).

Methodology of research

Calculations were performed using current procedures for evaluating building energy performance, using the monthly method, according to 2016 Regulation of the Minister of Infrastructure and Construction methodology. The general calculations of the energy demand for heating, cooling and ventilation are based on methods from CEN standards (ISO 13790:2008). The energy demand for heating and ventilation in the building has been determined, excluding heating of domestic hot water. The general calculations are based on methods from CEN standards (ISO 13790:2008). Emission factors for electricity are taken from the report of the Polish National Centre for Emissions Management (KOBiZE, 2018). On that basis, CO_2 emissions were calculated.

Case study

The target building for this case study is a typical single-family household. It is a semi-detached building with three floors, a garage and a complete basement. The attic is not utilized. The basement, porch and attic are regarded as non-heated spaces.

The buildings parameters are:

- total surface area 170.8 m^2,
- utility surface area 92.6 m^2,
- ceiling height 2.8 m.

The thermal barrier is assumed to be constructed on the outer side of the core of the exterior wall analogous to the proposed thermo-modernisation solution of the ISOMAX system. A barrier temperature of 10°C was assumed.

Compared variants:

– before modernisation,
– after thermo-modernisation with the use of an active thermal barrier on the exterior side of the wall directly behind a 12 cm thick layer of insulation.

When it comes to the construction of the walls, the two variants differ from each other only on the basis, that after modernisation cement lime plaster to embed the wall barrier PP pipes has been added to the wall.

In the variant before thermo-modernisation the central heating installation is equipped with floor heating elements. The building possesses a mechanical ventilation unit with heat recovery of φ = = 80%. The source of heat is a brine/water heat pump (*SCOP* = 4.0).

In the variant after thermo-modernisation, the foundation slab serves as a heat storage unit as a result of the renovation of the basement. The accumulated thermal energy is provided to the thermal barrier made from PP pipes. The installation is equipped also with floor heating elements as before thermo-modernisation. The same conditions were assumed for ventilation and the heat source as for the building before renovation. Figure 9 presents the calculated values for the EU and EK index of annual demand for useable and final energy for heating and ventilation.

TABLE 1. The multilayer wall construction with thermal barrier for building after thermo-modernisation

Envelope element	Material	s	λ	R	ΣR	Rsi	Rse	R_1
		m	$W \cdot m^{-1} \cdot K^{-1}$	$m^2 \cdot K \cdot W^{-1}$				
Exterior wall	porous ceramic bricks Porotherm 38 P+W	0.38	–	2.690	2.73	0.13	–	2.86
	gypsum plaster	0.015	0.35	0.043				

R_1 – the thermal resistance of the internal courses of the external wall (those between pipes and the room).

TABLE 2. The multilayer wall construction with thermal barrier (TB)

Envelope element	Material	s	λ	R	ΣR	Rsi	Rse	R_2
		m	$W \cdot m^{-1} \cdot K^{-1}$	$m^2 \cdot K \cdot W^{-1}$				
Exterior wall	gypsum plaster	0.01	0.35	0.029	3.06	–	0.04	3.10
	polystyrene EPS 70-040 12 cm thickness	0.12	0.04	3.000				
	cement-lime plaster coat to embed the wall barrier PP pipes	0.025	0.82	0.030				

R_2 – the thermal resistance of the external courses of the external wall (those between pipes and the outdoor air).

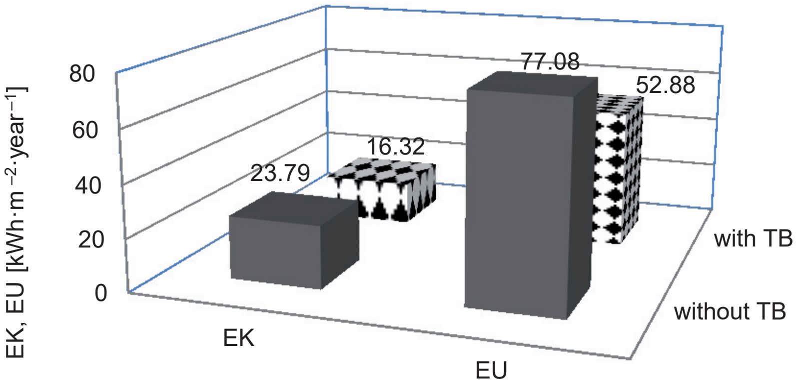

	EK	EU
without TB	23.79	77.08
with TB	16.32	52.88

FIGURE 9. Value o indexes EU, EK before (without thermal barrier TB) and after thermorenovation (with TB)

	kg•year−1	kg•year−1
before renovation	2 176	
after renovation		1 743

FIGURE 10. CO_2 emission in the analyzed building before (without TB) and after thermorenovation (with TB)

Results

The improvement of the energy performance due to the renovation concerning the application of a thermal barrier results in a reduction of about 31% of the building's energy demand referring to both final and usable energy for heating and ventilation in the modernised building. It was calculated by KOBiZE (2018), that the average CO_2 emissions for electricity in Poland are approximately 778 g of CO_2 per 1 kWh. Using this specific CO_2-factor for electricity needed to operate the heat pump and auxillary equipment in the analyzed building, savings from the thermal barrier installation amount to 433 kg of CO_2 annually (Fig. 10).

Conclusions

From the example of a typical single-family house it can be concluded, that the energy performance and CO_2 emission responsible for global warming can be significantly improved by using a thermo active barrier in the external wall. The application of a thermal barrier results in a reduction of the heat lost from the inside. A barrier placement near to the outside is beneficial, and installing it during thermorenovation can yield significant energetic improvements and be more enviromentally friendly. Even though in the article the values of energy demand and CO_2 emission relate only to the analysed building and our assumptions, it can be expected, that the results generalize further.

References

BT&SONS Kft system (2017-04-15). Retrieved from: www.btandsons.hu [access 15.04.2017].

Directive 2010/31/UE of the European Parliament and the Council of 19 May 2010 on the energy performance of buildings (recast). OJ L 153 of 18.06.2010.

ISO 13790:2008. Energy performance of buildings. Calculation of energy use for space heating and cooling.

ISOACTIVE-3D system (2019). *ISOACTIVE-3D system*. Retrieved from: www.isoactive-3d.hu [access 09.09.2019].

ISOMAX system (2019a). *ISOMAX system*. Retrieved from: http://isomax.isodom.pl/budownictwo,abc_systemu_isomax.html [access 09.09.2019].

ISOMAX system (2019b). *ISOMAX system*. Retrieved from: http://www.isomaxterrasol.eu/technologie.html [access 09.09.2019].

Krajowy Ośrodek Bilansowania i Zarządzania Emisjami [KOBiZE] (2018). *Wskaźniki emisyjności CO_2, SO_2, NO_x, CO i pyłu całkowitego dla energii elektrycznej na podstawie informacji zawartych w Krajowej bazie o emisjach gazów cieplarnianych i innych substancji za 2017 rok* [*Emission factors of CO_2, SO_2, NO_x, CO and TSP for electricity on the basis of information contained in the National Base on Emissions greenhouse gases and other substances for 2017*]. Warszawa: KOBiZE.

Krzaczek, M., Florczuk, J. & Tejchman J. (2019). Improved energy management technique in pipe-embedded wall heating/cooling system in residential buildings. *Applied Energy*, *254*, 113711-113738.

Leciej-Pirczewska, D. & Szaflik, W. (2006). Uses of outer wall with permanent thermal barrier in building engineering. In *XI International Symposium on heat transfer and renewable sources of energy*. Międzyzdroje 2006 (pp. 321-328). Szczecin: Wydawnictwo Uczelniane Politechniki Szczecińskiej.

Leciej-Pirczewska, D. & Szaflik, W. (2010). Wykorzystanie niskotemperaturowego czynnika w ogrzewaniu ściennym [Application of low-temperature medium in wall heating]. *Ciepłownictwo, Ogrzewnictwo, Wentylacja*, *41*(5), 168-172.

Report from the Commission to the European Parliament and the Council. 2016 assessment of the progress made by Member States in 2014 towards the national energy efficiency targets for 2020 and towards the implementation of the Energy Efficiency Directive 2012/27/EU as required by Article 24 (3) of the Energy Efficiency Directive 2012/27/EU. COM(2017) 56 final of 01.02.2017. Brussels: European Commission.

Rozporządzenie Ministra Infrastruktury i Budownictwa z dnia 20 grudnia 2016 r. zmieniające Rozporządzenie w sprawie metodologii wyznaczania charakterystyki energetycznej budynku lub części budynku oraz świadectw charakterystyki energetycznej. Dz.U. 2017, poz. 22 [Regulation of the Minister of Infrastructure and Construction of 20 December 2016 on the methodology of determining the energy performance of a building or part of a building and energy performance certificates. Journal of Laws 2017, item 22].

Xu, Xh., Wang, S., Wanga, J. & Xiao, F. (2010). Active pipe-embedded structures in buildings for utilizing low-grade energy sources: a review. *Energy and Buildings*, *42*(10), 1567-1581.

Summary

Outer wall with thermal barrier. Impact of the barrier on heat losses and CO_2 emissions. New demands for lowering energy consumption of buildings lead to many new solutions including, amongst others, the introduction of an outer wall thermal barrier for both heating and cooling effect. The analysed thermo-active-wall-barrier is a water-based system, where the pipes are embedded in the wall construction. It enables the use of a low-temperature barrier medium for space heating, thereby increasing the efficiency of all potential energy supply systems using renewable energy sources. The pipes form an active thermal barrier for heat transfer between the outer and the heated space. There are many possibilities to place the pipes in the wall for example in the case of energetic thermo-modernisation. Our research and calculations have shown that thermo-active-wall-barrier is sensitive to the location of pipes. The following paper also provides a study of the impact of thermal barrier on a building's energy performance. The analysis was conducted for a single-family house in a temperate climate based on parameters taken from one of the Polish meteorological data-bases. Calculations using current procedure of evaluating building energy performance show, that the thermal barrier can contribute to significant reduction of transmission energy loss thus lowering the environmental impact.

Authors' address:
Ewa Figiel
Dorota Leciej-Pirczewska
Zachodniopomorski Uniwersytet Technologiczny w Szczecinie
Wydział Budownictwa i Architektury
al. Piastów 50, 70-311 Szczecin
Poland
e-mail: figiel@zut.edu.pl
dlp@zut.edu.pl

Scientific Review – Engineering and Environmental Sciences (2020), 29 (2), 234–243
Sci. Rev. Eng. Env. Sci. (2020), 29 (2)
Przegląd Naukowy – Inżynieria i Kształtowanie Środowiska (2020), 29 (2), 234–243
Prz. Nauk. Inż. Kszt. Środ. (2020), 29 (2)
http://iks.pn.sggw.pl
DOI 10.22630/PNIKS.2020.29.2.20

Firas Kh. JABER[1], Nidal A. JASIM[2], Faiq M.S. Al-ZWAINY[3]

[1] Middle Technical University, Electrical Engineering Technical College
[2] University of Diyala, College of Engineering
[3] Al-Nahrain University, College of Engineering

Forecasting techniques in construction industry: earned value indicators and performance models

Key words: Machine Learning Regression Techniques (MLRT), earned value indexes, SPI, CPI, and TCPI

Introduction

The construction industry is an important industry for any government due to its direct association with the implementation of the goals and policies of the government in various fields of concern to the citizen in terms of education, health, housing and other facilities and services. The construction industry is also one of the broad and important sectors of any country's economy, and it is one of the main engines that governments resort to move the economy and create jobs and reduce unemployment. And the construction industry has unique characteristics, which made it an industry that is distinguished from the rest of the other industries by its many risks, and its projects always suffer from the problems of delay in implementation and increase in cost in most countries of the world. Among the most important characteristics of the construction industry (Myers, 2005):

1. The nature of its product is unique, each project differs from the other, and the temporary of each project is limited in duration and location, with the completion of the project, the equipment and labor will be transferred to another project in another place.
2. The nature of work within a single project is fragmented, as several different parties separate and separate to complete the project.
3. The industry's heavy dependence on manpower and its lack of research and development in methods and methods of implementation.

4. The criterion of competition for bidding in most cases is the lower price, which reduces the profit margin and thus reduces the desire of the companies executing in research, development and creativity.

The increasing demand for tall buildings represents a huge opportunity to reconstruct the construction industry and create value through joint action. According to research prepared by the McKinsey Global Institute, the industry can boost the productivity of its workers by up to 60% if changes are made in seven key areas: regulations, design operations, contracts, supply and supply chain management, and on-site implementation (Granskog, Guttman & Sjödin, 2016).

Tall buildings since the 1990s and during the first decade of the 21st century are considered civilization and urbanization facilities, not only that, but tall buildings have become symbols of countries. Tall buildings are defined as those buildings whose height is not less than 40 m or 13 floors. In most cases, the management of tall projects is not a simple matter, as success in such projects requires good coordination as well as a comprehensive integrated operating system for the project, so that all project participants can understand their roles and agree on key performance indicators (Al-Zwainy & Edan, 2017).

Earned value management system (EVMS) is a useful management technique available for tall buildings projects managers to monitor and control projects; a technique that combines the work scope, schedule and the cost elements of a project and facilitates the integrated reporting of a project's progress and the cost status. Earned value management system in effect integrates time management and cost management which are essential elements of tall buildings projects management (Al-Zwainy, Mohammed & Mohsen, 2015).

Review of the literature related to earned value management system with Forecasting techniques such as Machine Learning Regression Techniques (MLRT) was in top management journals such as International Journal of Project Management. Where, various researchers have used Machine Learning Regression Techniques (MLRT) as a tool for prediction and optimization in different project management areas are also reviewed, including earned value management. The great majority of project management applications of Multiple Linear Regression are based on the inter algorithm. The previous studies are among the most important scientific foundations on which the current study is based. The researcher begins with research, examination and analysis in the previous studies; this is because the research processes are cumulative processes that depend on the previous ones. In the next paragraph, the previous studies on the earned value management will be addressed and techniques used for forecasting purposes.

During the last few years or so, the use of EVM has increased in many construction engineering projects and has demonstrated some degree of success. The following literature review reveals that EVM have been used successfully in modelling of the earned value management. Pajares and Lopez-Paredes (2011) proposed two new metrics that combine earned value management and project risk management for construction project controlling and monitoring. Elshaer (2013) studied the impact of the activities sensitivity information on the forecasting accuracy of the Earned Schedule Method (ESM). Czemplik (2014) applied schedule forecast Indicator (SFI) to support site managerial decision concerning variation orders. Khamooshi and Golafshani (2014) provided a new approach to decouple the schedule and cost dimensions in EVM by adding earned duration while maintaining the unique interaction of the three major project management elements of scope, cost, and time similar to EVM. Chen, Chen and Lin (2016) improved the predictive power of Planned Value (PV) before executing construction project. Jaber, Hachem and Al-Zwainy (2019) applied the value management methodology acquired in the waste water treatment plant projects to measure performance by predicting performance indicators such as CPI, SPI and TCPI.

The following literature review reveals that Machine Learning Regression Techniques (MLRT) have been used successfully in construction project management (Al-Zwainy et al., 2015) developing EAC model for bridges projects using Multifactor Linear Regression Technique (MLRT). Bilal and Oyedele (2020) presented guidelines for Applied Machine Learning (AML) in the construction industry from training to operationalizing models, which are drawn from our experience of working with construction folks to deliver Construction Simulation Tool (CST). Sabahi and Parast (2020) used predictive analytics by proposing a machine learning approach to predict individuals' project performance based on measures of several aspects of entrepreneurial orientation and entrepreneurial attitude of the individuals.

The researchers did not found any study that is exactly the same as the current study while searching in international libraries and discreet periodicals such as Scopus, Springer, Taylor France and others, as this current study is almost unique of its kind that deals with predicting the value indicators gained using Machine Learning Regression Techniques (MLRT) in tall building projects, despite the existence of multiple studies dealing with a topic prediction in construction projects. Based on the above discussion the contribution of this study are as follows.

Firstly, in this study, the main target is on using associate Forecasting techniques for the aim of earned value prediction, meant as a decision-support aid to project manager, contractors and planners. The contribution of this study is to spot the most effective activity in terms of model structure and parameters on an earned value prediction. Applied interest of this study may well be use machine intelligence techniques such as Machine Learning Regression Techniques (MLRT) as an acceptable tool for earned value estimating, where, Project managers in Iraq; typically have to be compelled to estimate the earned value of construction projects at construction stage quickly and around to supply funding or to get the adoption of the budget from decision-makers. Therefore, it's necessary to search out the simplest way to understand the earned value of the construction projects in a very short time with acceptable accuracy.

In summary, the application EVM in tall building projects would be specifically helpful for a state like Iraq which suffers from shortage of a high number of severe tall buildings. The main objective of this study is to develop Machine Learning Regression Techniques (MLRT) to predict the earned value indicators at early stage of tall buildings projects in Iraq to reduce the percentage error of estimation. This will facilitate the project practitioners to the further use of EVA for the schedule and cost control of their construction projects. To achieve this, there is a need to identify the factors that affect the performance of residential buildings projects that can be available at early stages. Therefore, the specialists researchers in this study are endeavoring improvement and assessment earned value models through the below stages:

1. Choose the appropriate statistics software.
2. Identification of MLRT variables that have an effect on the earned value index in tall buildings projects.
3. Building a numerical model to foresee of the earned value indexes (SPI, SPI and TCPI).
4. Check the confirmation and approval of the scientific models.

Choose the appropriate statistics software

Several applications that support the establishment of statistics analysis like Microsoft Excel, Statistica, MINITAB, and MATLAB, but this study was selected SPSS Program, where SPSS is the premier statistics analysis environment. The SPSS range provides an easy--to-use, visual, object-oriented approach to problem solving using intelligent technologies.

SPSS is short for Statistical Package for the Social Sciences, and it's utilized by different sorts of analysts for complex measurable information investigation. The SPSS programming bundle was made for the administration and factual examination information in different sciences. Long produced by SPSS Inc., it was acquired by IBM in 2009. The current versions are named IBM SPSS Statistics.

Identification ANN Models variables

The Bismayah City Project is the first of its kind and the largest in the history of Iraq in terms of size and level of services and infrastructure provided in it, and Hanwha Engineering and Construction Company is proud to be the first company to implement such a strategic project in Iraq. The new city of Basmaya is an integrated residential complex located 10 km southeast of the capital, Baghdad, Iraq, on the international road No 6 linking the capital Baghdad and Wasit Governorate, and on an area of 1,830 ha, and consists of 100,000 housing units, and also includes a network Integrated infrastructure of water and electricity, as well as schools and recreational and commercial complexes. The cost of constructing the complex amounts to $7.75 billion, the project is implemented by the Korean Hanwha Engineering and Construction Company, which works in the field of construction and construction around the world, with a duration of implementation of up to seven years. The new Basmaya city represents a new modern lifestyle that may be characterized by a high level of services and an ideal environment suitable for the development of new generations. The aerial photos show the level of progress of work and completion of other residential and service buildings, as shown in Figure 1.

FIGURE 1. The new city of Basmaya in Iraq

Machine Learning Regression Techniques (MLRT) requires a lot of data. Therefore, a lot of historical tall buildings projects were collected which were done between 2012 and 2018 as shown in Table 1. There are two types of variables that affected on the earned value in tall buildings projects in Republic of Iraq which are dependent variables and independent variables. Cost Performance Index (CPI), Schedule Performance Index (SPI) and To Complete Cost Performance Indicator (TCPI) are defined as the dependent variables. There are many variables as an independent variable such as: Budget at Completion (BAC), Actual Cost (AC), Actual Percentage (A%), Earned Value (EV), Planning Percentage (P%), and Planning Value (PV).

TABLE 1. Summary of historical data for Bismayah City Project

Parameter	Max.	Min.	Range	*AVG*
BAC	950	800	150	865
AC	600	200	400	375
A%	60	25	35	39
EV	510	237.5	272.5	339.8
P%	60	25	35	42
PV	510	237.5	272.5	358
SPI	1.11	0.75	0.36	0.95
CPI	1.18	0.80	0.38	0.93
TCPI	0.80	1.19	0.80	0.39

Building Machine Learning Regression (MLR) Models

The factors that were recognized at the information distinguishing proof stage were utilized to build up the Machine Learning Regression Techniques (MLRT). Three numerical models were created in this examination by utilizing Machine Learning Regression Techniques (MLRT). It was utilized on the grounds that it is probably the most kind that broadly utilized in this field of study. What's more, the venture qualities or parameters in a numerical model were utilized to foresee earned value indexes. The Statistical Product and Solutions Services (SPSS) programming forms 26 are utilized as a tool to build up the three models, as following:

1. Schedule Performance Index (SPI).
2. Cost Performance Index (CPI).
3. To Complete Cost Performance Indicator (TCPI).

First: Schedule Performance Index Model

Table 2 expounds multiple linear regression estimates, such as coefficients of standardized, coefficients of unstandardized, standardized errors, t-test and

TABLE 2. Coefficients of SPI-Model (dependent variable: $Y1$)

Model	Unstandardized coefficients		Standardized coefficients	t	$sig.$
	B	SE	$ß$		
Constant	–14.393	8.593	–	–1.675	0.193
$X1$	0.018	0.010	3.253	1.784	0.172
$X2$	0.007	0.005	2.684	1.255	0.298
$X3$	–0.076	52.969	–0.026	–0.001	0.999
$X4$	–0.013	0.066	–3.922	–0.197	0.857
$X5$	33.633	50.328	10.067	0.668	0.552
$X6$	–0.034	0.057	–8.747	–0.590	0.597

testing the significant of every autonomous factors or independent variable.

The regression statistics of Schedule Performance Index Model (SPI-Model) are set in Table 1, which can be formed as Equation (1):

$$Y1 = SPI = -14.393 + (0.018X1) + (0.007X2) - (0.076X3) - (0.013X4) + (33.633X5) - (0.034X6) \quad (1)$$

Second: Cost Performance Index Model

The regression statistics of Cost Performance Index Model (CPI-Model) are set in Table 3.

Statistics of regression for model CPI are set in Table 3, which can be formed as Equation (2):

$$Y2 = CPI = -12.405 + (0.015X1) + (0.002X2) - (22.344X3) + (0.016X4) + (50.059X5) - (0.05X6) \quad (2)$$

Third: Complete Cost Performance Indicator

The regression statistics of To Complete Cost Performance Indicator (TCPI-Model) are set in Table 4.

TABLE 3. Coefficients of CPI-Model (dependent variable: $Y2$)

Model	Unstandardized coefficients		Standardized coefficients	t	$sig.$
	B	SE	$ß$		
Constant	–12.405	7.813	–	–1.588	0.211
$X1$	0.015	0.009	2.609	1.641	0.199
$X2$	0.002	0.005	0.881	0.472	0.669
$X3$	–22.344	48.16	–7.317	–0.464	0.674
$X4$	0.016	0.060	4.731	0.272	0.803
$X5$	50.059	45.75	14.372	1.094	0.354
$X6$	–0.050	0.052	–12.444	–0.963	0.407

TABLE 4. Coefficients of CPI-Model (dependent variable: *Y*3)

Model	Unstandardized coefficients		Standardized coefficients	*t*	*sig.*
	B	*SE*	*ß*		
Constant	–1.436	8.477	–	–0.169	0.876
*X*1	0.001	0.010	0.164	0.092	0.932
*X*2	–0.002	0.005	–0.789	–0.378	0.731
*X*3	–31.521	52.258	–10.647	–0.603	0.589
*X*4	0.036	0.065	10.635	0.547	0.623
*X*5	31.441	49.653	9.311	0.633	0.572
*X*6	–0.030	0.057	–7.538	–0.521	0.638

Statistics of regression for model TCPI are set in Table 4, which can be formed as Equation (3):

$$Y3 = TCPI = -1.436 + (0.001X1) - (0.002X2) - (31.521X3) + (0.036X4) + (31.441X5) - (0.03X6) \quad (3)$$

Check the Confirmation and Approval of the Scientific Models

Below is the model's summary, which has some important statistics. It provides us correlation coefficient (*R*) with determination coefficient (R^2) and the estimation of standard error. This statistical analysis was bring about for the MLR models (SPI, CPI, and TCPI) between output (earned value indexes) and input (BAC, Budget at Completion – *X*1; AC, Actual Cost – *X*2; A%, Actual Percentage – *X*3; EV, Earned Value – *X*4; P%, Planning Percentage – *X*5; PV, Planning Value – *X*6). On the other hand, the *R*-values for SPI, CPI, and TCPI models are equal to 85.5%, 89.2%, and 86.3% respectively, which is viewed as extremely aloft correlation. In addition, the determination coefficient shows the extent of the variety in input variable from an output variables, and that models have

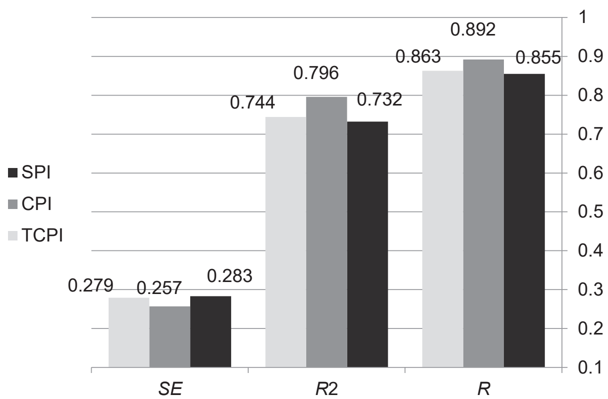

FIGURE 1. Summary statistics of models

R^2 values equal to 73.2%, 79.6%, and 74.4% respectively.

From Figure 1, it can be seen that model (SPI), model (CPI), model (TCPI) verification have pretty performance in order that offered high correlation of coefficient (R) 85.5%, 89.2% and 86.3%, respectively. Figures 2–4 illustrate the capability of MLR models (SPI-model, CPI-model, TCPI-model), where, the coefficient of determination (R^2) is 73.2%,

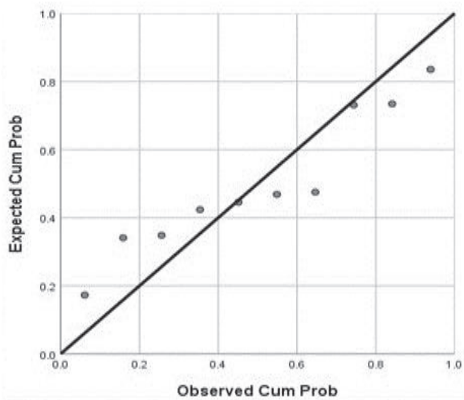

FIGURE 2. Relationship between observed SPI and expected SPI

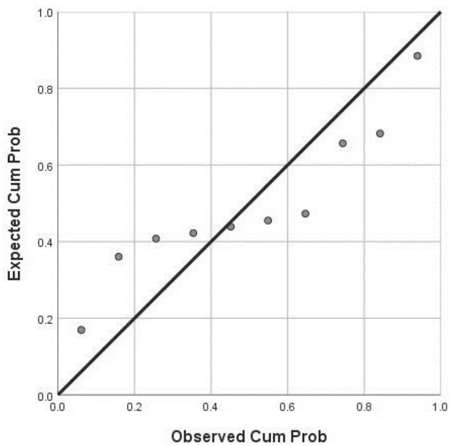

FIGURE 3. Relationship between observed CPI and expected CPI

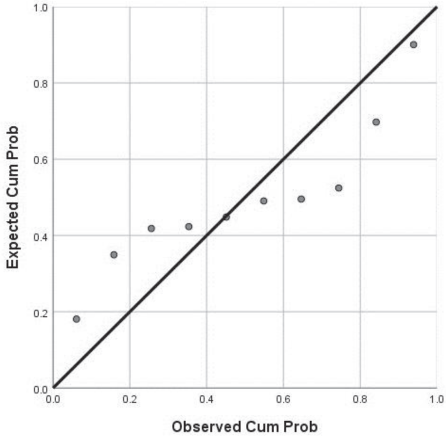

FIGURE 4. Relationship between observed TCPI and expected TCPI

79.6% and 74.4%, therefore, it can be concluded that these models shows an excellent agreement with the actual measurements.

Conclusions

In this study, a depiction of models factors, information assortment strategy and factual determination of verifiable information has been clarified. Bismayah New City was selected as a case study, six variables were adopts as independent variables (BAC, Budget at Completion – $X1$; AC, Actual Cost – $X2$; A%, Actual Percentage – $X3$; EV, Earned Value – $X4$; P%, Planning Percentage – $X5$; PV, Planning Value – $X6$), and three variables were (Cost Performance Index – CPI; Schedule Performance Index – SPI; To Complete Cost Performance Indicator – TCPI) are defined as the dependent variables. In addition, Machine Learning Regression Techniques (MLRT) has been used to build prediction model for earned value indexes by using SPSS-26 statistically software. It was found that the MLRT showed good results of estimation in terms of correlation coefficient (R) generated by MLR models for SPI and CPI and TCPI where the R were 85.5%, 89.2%, and 86.3% respectively. At long last, a result tends to be presumed that these models show a brilliant concurrence with the genuine estimations.

The availability of data

The study discoveries which were bolstered by the information, are realistic by the relating's essayist can be obtained on demands.

Conflicts of interest

The authors asserted that they hadn't interest clashes and conflicts.

Acknowledgements

Authors would like to thank those respected persons who have helped and guided us to achieve this paper; they really deserve all respect and gratitude. Then, we'd like to thank all the staff of the Al-Nahrain University, Middle Technical University, Baghdad, and the University of Diyala in Iraq to help us to get guideline for our paper by providing us lots of consultations. As well as, we also want to thank and give our gratitude to everyone who has guided or advised us in submitting or writing this paper.

Author contributions

Firas Kh. Jaber conceived of the presented idea and contributed to sample preparation and wrote the manuscript. Faiq M.S. Al-Zwainy developed the MLR models and performed the computations. Nidal A. Jasim confirmed the logical techniques and regulated the discoveries of this work. All researchers talked about the outcomes and writting to the last composition of manuscript.

References

Al-Zwainy, F.M.S. & Edan, I.A. (2017). *Information technology in construction project management*. Amman, Jordan: Darghaidaa for Publishing [translated from Arabic].

Al-Zwainy, F.M.S., Mohammed, I. & Mohsen, D.S. (2015). *Earned value management in construction project.* Saarbrűcken: LAP LAMBERT Academic Publishing.

Bilal, M. & Oyedele, L.O. (2020). Guidelines for applied machine learning in construction industry – a case of profit margins estimation. *Advanced Engineering Informatics*, *43*, 101013. DOI 10.1016/j.aei.2019.101013

Chen, H.L., Chen, W.T. & Lin, Y.L. (2016). Earned value project management: improving the predictive power of planned value. *International Journal of Project Management*, *34*(1), 22-29.

Czemplik, A. (2014). Application of earned value method to progress control of construction projects, *Procedia Engineering*, *91*(1), 424-428.

Elshaer, R. (2013). Impact of sensitivity information on the prediction of project's duration using earned schedule method. *International Journal of Project Management*, *31*(4), 579-588.

Granskog, A., Guttman, B. & Sjödin, E. (2016). *Toward a customer-centric construction-equipment industry*. McKinsey & Company. Retrieved from: https://www.mckinsey.com/industries/automotive-and-assembly/our-insights/toward-a-customer-centric-construction-equipment-industry

Jaber, F.K., Hachem, S.W. & Al-Zwainy, F.M. (2019). Calculating the indexes of earned value for assessment the performance of waste water treatment plant. *ARPN Journal of Engineering and Applied Sciences*, *14*(4), 792-802.

Khamooshi, H. & Golafshani, H. (2014), EDM: Earned Duration Management, a new approach to schedule performance management and measurement. *International Journal of Project Management*, *32*(6), 1019-1041.

Myers, D. (2005). *Construction economics: a new approach*. London: Spon Press.

Pajares, J. & Lopez-Paredes, A. (2011). An extension of the EVM analysis for project monitoring: The Cost Control Index and the Schedule Control Index. *International Journal of Project Management*, *29*(5), 615-621.

Sabahi, S. & Parast, M.M. (2020). The impact of entrepreneurship orientation on project performance: a machine learning approach. *International Journal of Production Economics*, 107621. DOI 10.1016/j.ijpe.2020.107621

Summary

Forecasting techniques in construction industry: earned value indicators and performance models. Machine Learning Regression Techniques (MLRT) as a shrewd method can be utilized in this study being exceptionally fruitful in demonstrating non--linear and the interrelationships among them in problems of construction projects such as the earned value indexes for tall buildings projects in Republic of Iraq. Three forecasting models were developed to foresee Schedule Performance Index (SPI) as first model, Cost Performance Index (CPI) as a second model, and the third model is To Complete Cost Performance Indicator (TCPI) in Bismayah New City was chosen as a case study. The methodology is mainly impacted by the deciding various components (variables) which impact on the earned value analysis, six free factors (*X*1: BAC, Budget at Completion; *X*2: AC, Actual Cost; *X*3: A%, Actual Percentage; *X*4: EV, Earned Value; *X*5: P%, Planning Percentage, and *X*6: PV, Planning Value) were self-assertively assigned and agreeably depicted for per tall buildings projects. It was found that the MLRT showed good results of estimation in terms of correlation coefficient (*R*) generated by MLR models for SPI and CPI and TCPI where the *R* were 85.5%, 89.2%, and 86.3% respectively. At long last, a result tends to be presumed that these models show a brilliant concurrence with the genuine estimations.

Authors' address:
Faiq M. S. Al-Zwainy
(https://orcid.org/0000-0002-9948-6594)
Al-Nahrain University
College of Engineering
Department of Civil Engineering
10072 Al-Jadryia, Baghdad, Iraq
e-mail: faiq.al-zwainy@eng.nahrainuniv.edu.iq

Scientific Review – Engineering and Environmental Sciences (2020), 29 (2), 244–258
Sci. Rev. Eng. Env. Sci. (2020), 29 (2)
Przegląd Naukowy – Inżynieria i Kształtowanie Środowiska (2020), 29 (2), 244–258
Prz. Nauk. Inż. Kszt. Środ. (2020), 29 (2)
http://iks.pn.sggw.pl
DOI 10.22630/PNIKS.2020.29.2.21

Maciej MALARSKI, Marek KALENIK
Warsaw University of Life Sciences – SGGW, Institute of Environmental Engineering

Purpose of the housing double stage polypropylene-carbon cartridges filters usage in bath gray water treatment

Key words: gray water, filtration, cartridge filter, water and wastewater quality, gray water turbidity

Introduction

In Poland, water resources are limited. Considering water consumption for industry and agriculture, the amount of water that can be used for communal purposes is only approx. 365 $m^3 \cdot M^{-1} \cdot year^{-1}$ (Kundzewicz, Zalewski, Kędziora & Pierzgalski, 2010). Such a quantity of water should theoretically be enough to meet the needs of human consumption. Water consumption in households is around 36.5–54.75 $m^3 \cdot M^{-1} \cdot year^{-1}$ (Chudzicki & Sosnowski, 2011b). However, it is necessary to consider the periods of drought occurring in Poland that contribute to lowering the level of groundwater and drinking water shortages.

Water quality in recent years in Poland is improving, but the amount of drinking water in the rivers is still unsatisfactory. Kundzewicz et al. (2010) determined the good condition of waters only for 7% of the Vistula and Odra river basins. Additionally, it should be remembered that the occurring floods also do not improve the situation (Kundzewicz et al., 2010). They cause pollution of surface waters. This, in turn, adversely affects the drinking water resources.

Analyzing the water usage in a typical household (Chudzicki, 2010; Chudzicki & Sosnowski, 2011b), it turns out that nearly 30% is used to flush toilet bowls. Usually tap water is used here. The question arises whether water needs to be used for this purpose with the parameters of drinking water quality that meets the 2017 Regulation of the Minister of Health on water quality for human consumption. It is believed that gray water may be used to the toilet after pre-treatment (Abdel-Shafy & Al-Sulaiman, 2014; Gross, Maimon, Alfiya & Friedler, 2015; Vuppaladadiyam et al., 2019). Considering the amount of gray sewage generated in homes (about 51% of the total amount of sewage), one can notice enough of them to rinse the toilet bowls. Currently in Poland, sewage in households is entirely discharged into collective sewage systems (Kalenik, 2015; Bugajski, Chmielowski & Kaczor, 2016) or are cleaned in household wastewater treatment plants (Kalenik, 2014; Spychała, 2016).

Gray water reuse gives the possibility of economic management of drinking water. It is estimated that re-use of gray water can bring savings of 30–50% (Mucha & Jodłowski, 2010). The problem, however, is their quality. Gray water (sewage from the bath – approx. 26% of sewage, body wash – approx. 10%, laundry – approx. 15%) are considered as contaminated water without faeces. However, these wastewater often contain various types of soaps, washing powders and liquids, fats of human origin, solid impurities (Christowa-Boal, Eden & McFarlane, 1996; Mucha & Jodłowski, 2010; Boyjoo, Pareek & Ang, 2013). This is the reason for the reluctance of potential users to use them even in toilets. Gray water frequently contributes to excessive deposition of contaminants on the surfaces of ceramic sanitary facilities (Chudzicki & Sosnowski, 2011b). They can also cause the production of dangerous aerosols when flushing the toilet bowls (Mucha & Jodłowski, 2010; Chudzicki & Sosnowski, 2011a).

In Poland, there are currently no legal regulations regarding the quality of water used in households for other purposes than consumption or bathing. The literature specifies that this water should be safe for life and health, it should not be a habitat for flies, it cannot pose a threat to the environment, it should look aesthetically. These guidelines, presented in the work of Mucha and Jodłowski (2010), are the basic parameters of the quality of liquid used for economic purposes. The authors also present gray water to be used for this purpose, citing various solutions using gray water in toilets without prior pre-treatment. However, such installations may be used only in the case of direct use of gray water to rinse the toilet bowls without holding them longer time and when the appearance and smell are acceptable.

The gray water system should be easy and friendly to use. If it is necessary to keep gray water before their secondary use, it is advisable to clean them up to a level that does not endanger human health and life. In addition, this installation should minimize the possibility of deposition of contaminants on sanitary ceramics (Malarski, 2013).

The pre-treatment of gray water can be carried out in many ways. Christowa-Boal, Eden and McFarlane (1996), March, Gual and Orozco (2004), Gual, Moia and March (2008), Abudi (2011), Khalaphallah (2012), Abdel-Shafy, El-Khateeb and Shehata (2013), Ushijima, Ito, Ito and Funamizu (2013), Charchalac Ochoa, Ushijima, Hijikata and Funamizu (2015) propose the use of a system based on filtration of gray water through polypropylene mesh filters, sand filters and chlorine disinfection. The literature also refers to systems based on biofiltration system with swamp plants (Masi et al., 2010; Abdel-Shafy & Dewedar, 2012; Abdel-Shafy & El-Khateeb, 2013), and RBC type devices (rotating biological contactor), UASB (upflow anaerobic sludge blanket) or membrane reactors (Hourlier et al., 2010; James, Surendran, Ifelebuegu, Ganjian & Kinuthia, 2016; Huelgas-Orbecido & Funamizu, 2019; Wu, 2019). These devices are proposed for installation in collective use buildings, multi-family residential buildings, housing estates or their surroundings. They are often large devices used to treat wastewater from the entire household. Unfortunately, this often results in a high price and a significant reduction in applicability in a single sanitary point in the household.

The aim of the research was to determine the suitability of using double stage cartridge filters for pre-treatment of bathing gray water for possible secondary use of it. The possibilities of using double stage polypropylene-carbon cartridge filter FCCA-STO, as well as polypropylene FCPS10 and carbon FCCA cartridges filter, constituting single stages of a double stage cartridge were determined.

Material and research methodology

Analyzed gray water contained pollution coming from washing and bathing sources of a typical two-family building used by seven people. The effluent for tests was collected at the outflow from sanitary facilities. The effluent were collected in a septic tank and then passed through cartridge filter with a fixed initial capacity of 0.1 $dm^3 \cdot s^{-1}$. This value corresponds to the normative outflow of water into the toilet bowl from the water supply system (PN-92/B-01706, PN-EN 806-3:2006). Performing filtration on the cartridge filter, it was attempted to determine the possibility of using a selected cartridge filter for pre-treatment of bath gray water. The characteristics of gray water are shown in Table 1.

Housing cartridge filters are small devices (Aquafilter 2016, BWT 2016), with a standard height of approx. 30 cm and a diameter of approx. 12 cm. Filter element with a height of 10" and a diameter of 2.5" can be replaced alone without the participation of specialized service. In the case of drinking water purification, the filter cartridge should be replaced every 6 months (Aquafilter 2016, BWT 2016). However, for the pretreatment of gray water, the "lifetime" of cartridges is not estimated.

The research was divided into three experiments that differ in the type of filter cartridge used. In the first experiment, a double stage polypropylene-carbon cartridge filter FCCA-STO was used. However, the other two experiments that examined individual filtration stages were made on a single polypropylene cartridge FCPS10 with a filtration accuracy of 10 μm (the second experiment) and on a single carbon cartridge filter FCCA (third experiment).

During the tests, samples of raw gray water and filtrate were collected for analytical tests of their quality. The samples were tested for the following parameters:

- pH – electrometric measurement (PN-EN ISO 10523:2012) using the Hach Lange Sension 4 pH meter and Elmetron EPP-3 electrode,
- suspended and dissolved solids – measurement by weight in relation to the procedure included in the PN-78/C-04541 standard,

– turbidity – measurement by nephelometric method (PN-EN ISO 7027:2003. Chapter 6) with the use of turbidimeter 2100N IS Turbidimeter,
– conductivity – conductometric measurement (PN-EN 27888:1999),
– biochemical oxygen demand (BOD_5) – measurement using the WTW bottle method, in accordance with the PN-EN 1899-1:2002, 2:2002 standard,
– decay – measurement by visual method (PN-C-04626:1976),
– chemical oxygen demand (COD) – measurement by means of a titration method (PN-ISO 15705:2005).

The research focused mainly on the results of turbidity and decay of the investigated gray water. These parameters show the time of possible liquid retention before its secondary use, e.g. for flushing the toilet bowls and organoleptic acceptance by the potential user. The results of the tests were compared for each measurement series separately.

Results and discussion

Bathing gray water is characterized by high variability of quality parameters. Their composition depends mainly on the contamination of the person taking a bath, as well as on the amount and type of detergent (Malarski, 2013, 2016; Malarski, Matusiak & Cybula, 2016). Table 1 presents the results of testing the quality of gray water from the bath. Samples of gray water from baths of a two-family building inhabited by seven people were tested. Limit values of obtained results as well as average values, standard deviation and median of individual quality parameters are presented.

According to Dixon et al. (1999) and Boyjoo et al. (2013) gray water should not last longer than 48 h without treatment. It results from biodegradability of gray water. In the Malarski study (2013) carried out on gray water from the bathtub, the results of decay were obtained at the level of 170 h. In the own research, however, a different time of gray water is noticeable, average 74 h. This proves a significant diversity of gray water depending on their origin. At the same time, it shows the need for an individual approach to the possible use or treatment of gray water. Often forcing them to purify almost immediately, which is consistent with the guidelines for using gray water in many countries (Yu, Rahardianto, De Shazo, Stenstrom & Cohen, 2013; Oron et al., 2014; James et al., 2016).

Tested gray water was characterized by a similar turbidity value (average 74.9 NTU) to the Jabornig and Favero (2013) tests results about 133 NTU, Oron et al. (2014) tests results about 50–250 NTU, Šostar-Turk, Petrinić and Simonič (2005) tests results about 35 NTU, Gual et al. (2008) tests results about 38.8 NTU, Jamrah, Al-Futaisi, Prathapar and Harrasi (2008) tests results about 279 NTU, March et al. (2004) tests results about 20 NTU. In the author's own research, studies were carried out on gray water from bath, as in the presented literature. The turbidity of gray water after bathing can be set at different levels depending on the "soiling" of the person taking a bath and the consumption of washing agent.

Analyzing the obtained results of the gray water quality tests an increased concentration of COD and BOD values

TABLE 1. Ranges of values of selected indicator of pollutants in bath gray water testing (own studies)

Indicator	Unit	Values	*AVG*	*M*	*SD*
Turbidity	NTU	28–156	74.9	71.9	29
pH	–	7.12–9.39	8.21	8.33	0.60
Conductivity	$\mu s \cdot cm^{-1}$	1 234–2 900	1 752	1 687	483
Decay	h	64–90	74	75	8
COD	mg $O_2 \cdot dm^{-3}$	182–273	224	224	25
BOD_5	mg $O_2 \cdot dm^{-3}$	71–180	118	115	25
Total suspended solids (TSS)	$mg \cdot dm^{-3}$	74–892	482	476	233
Fixed suspended solids (FSS)	$mg \cdot dm^{-3}$	48–445	227	202	100
Volatile suspended solids (VSS)	$mg \cdot dm^{-3}$	26–640	255	280	162
Total dissolved solids (TDS)	$mg \cdot dm^{-3}$	854–3 715	2 452	2 281	829
Total fixed solids (TFS)	$mg \cdot dm^{-3}$	315–2 285	1 325	1 327	496
Total volatile solids (TVS)	$mg \cdot dm^{-3}$	539–1 768	1 127	1 054	404

is noticeable. Values exceed the limit set out in the 2014 Regulation of the Minister of Environment on conditions of sewage and substances particularly harmful to water environment for wastewater that may be introduced into waters or into the ground.

High turbidity, variable value of decay, and often also the color of gray water may cause reluctance to their possible re-use. Therefore, in determining the efficiency of operation of selected filter cartridges in each research series, the quality of raw gray water was tested.

Experiment 1. Filtration on a filter with a double stage polypropylene--carbon FCCA-STO cartridge

In series 1 of tests, the filtration of bath gray water was carried out using a double stage polypropylene carbon filter cartridge FCCA-STO. For this purpose, baths gray water from the two-family building was stored in the tank – about 300 dm^3. Then, 80 dm^3 of averaged gray water was filtered on the prepared test stand, without getting a full colmatation of the filter cartridge. Five filtrate samples and one raw gray water sample were collected. The remaining gray water was used to carry out experiments 2 and 3. The experiments were carried out twice at an interval of two weeks.

As a result of the tests, parameters of the filter cartridge were determined in terms of selected quality parameters. Table 2 presents the average values of the parameters from two conducted experiments.

As a result of filtration, the quality indicators of gray water underwent slight changes. The best effect was obtained for suspensions. After filtering 40 dm^3 of gray water, a reduction of 80% was obtained. The remaining tested quality indicators showed a smaller reduction. The turbidity reduction was 44% in the samples taken after filtration of 20 dm^3 gray water, for COD reduction by 13%, BOD_5 by 30%, TDS by 14% in samples of 10 dm^3. The remaining analyzed indicators of the quality of the liquid practi-

TABLE 2. Characteristics of bath gray water raw and treated on the housing double-stage polypropylene-carbon cartridge filter FCCA-STO (own studies)

Indicator	Unit	Raw gray water	Volume of filtrate [dm^3]				
			10	20	40	60	80
Turbidity	NTU	45.6	26.1	25.4	27.1	28.2	27.5
pH	–	7.58	7.80	7.81	7.79	7.75	7.82
Conductivity	$\mu s \cdot cm^{-1}$	1 386	1 296	1 310	1 356	1 341	1 330
Decay	h	70	70	70	70	70	70
COD	mg $O_2 \cdot dm^{-3}$	224	195	214	205	205	200
BOD_5	mg $O_2 \cdot dm^{-3}$	103	72	80	92	85	95
Total suspended solids (TSS)	$mg \cdot dm^{-3}$	706	185	162	141	165	148
Fixed suspended solids (FSS)	$mg \cdot dm^{-3}$	75	65	60	52	63	58
Volatile suspended solids (VSS)	$mg \cdot dm^{-3}$	631	120	102	89	102	90
Total dissolved solids (TDS)	$mg \cdot dm^{-3}$	1 078	932	968	970	954	972
Total fixed solids (TFS)	$mg \cdot dm^{-3}$	754	654	676	679	666	678
Total volatile solids (TVS)	$mg \cdot dm^{-3}$	324	278	290	291	288	294

cally showed no major changes. The test results are presented in Table 2.

In the research, a double stage filter cartridge was used, obtaining the results of reduction of pollutants at a level similar to the reduction values of the investigated pollutants obtained by March et al. (2004) and Gual et al. (2008) in studies based on filtration of gray water from hotel rooms through a nylon filter. Similarly to own research, the researchers conducted studies on bath gray water coming from bathrooms, for which the initial concentrations and as well as values obtained after the filtration process on the used cartridge are still high, significantly exceeding the permissible values for waste water introduced into water or soil in accordance with the 2014 Regulation of the Minister of Environment.

On the basis of the obtained results, it can be only assume the legitimacy of the use of housing cartridge filters in the tests of treating gray water from the bath at least in the first stage of treating. The use of a carbon element in the filter for the purification of this type of gray water is not a good solution at this stage of treating. The carbon filter should provide sorption processes. In the case analyzed in the experiment, most likely the pores in the carbon element of the filter cartridge were quickly blocked by impurities contained in the gray water and the filter acted as a normal filter with mechanical removal of impurities. Therefore, it seems necessary to determine the effectiveness of the individual fractions of the filter cartridge used.

A double stage polypropylene-carbon filter was used for testing without the possibility of sampling between individual stages. Hence, to determine the effect of individual filter stages on wastewater treatment, tests were carried out on single polypropylene filter cartridges FCPS10 (experiment 2) and carbon FCCA (experiment 3). These cartridges are made of filter material used to build the FCCA-STO cartridge used in experiment 1.

Experiment 2. Filtration on a filter with a polypropylene cartridge with a filtration accuracy of 10 μm – FCPS10

In the second experiment, filtration of bath gray water through a filter with a polypropylene cartridge with a filtration accuracy of 10 μm FCPS10. The research was carried out in the same way as in experiment 1, using gray water remaining in the tank. Amount of 80 dm^3 of gray water were filtered. During the tests samples of the filtered liquid were collected. Five samples of filtrate were taken during the experiment. Analogously to the experiment 1, tests were carried out twice at an interval of two weeks. The results of laboratory tests on the concentrations of selected quality parameters of collected samples are presented in Table 3, as mean values from tests. During the filtration, no full colmatation of the deposit was obtained.

The filtration of bath gray water through the analyzed filter cartridge did not significantly change the parameters of their quality. Individual quality indicators did not change much. Maximum recorded average reductions of ratios from duplicate tests were obtained for samples collected after filtration of 20 dm^3 of sewage: for turbidity – reduction by 65%; TSS – by 81%; TDS – by 22%; COD – by 13%; BOD_5 – by 41%.

There is a noticeable fluctuation in the concentration of COD in individual

TABLE 3. Characteristics of bath gray water raw and treated on the housing polypropylene cartridge filter FCPS10 (own studies)

Indicator	Unit	Raw gray water	Volume of filtrate [dm^3]				
			10	20	40	60	80
Turbidity	NTU	45.6	16.0	15.8	16.1	16.3	16.5
pH	–	7.58	7.63	7.67	7.59	7.55	7.69
Conductivity	$\mu s \cdot cm^{-1}$	1 386	1 389	1 366	1 376	1 381	1 379
Decay	h	70	77	77	77	77	77
COD	mg $O_2 \cdot dm^{-3}$	224	214	195	200	205	200
BOD_5	mg $O_2 \cdot dm^{-3}$	103	70	61	65	69	65
Total suspended solids (TSS)	$mg \cdot dm^{-3}$	706	140	131	155	163	147
Fixed suspended solids (FSS)	$mg \cdot dm^{-3}$	75	15	17	19	18	18
Volatile suspended solids (VSS)	$mg \cdot dm^{-3}$	631	125	114	136	145	129
Total dissolved solids (TDS)	$mg \cdot dm^{-3}$	1 078	831	843	862	851	854
Total fixed solids (TFS)	$mg \cdot dm^{-3}$	754	582	592	601	602	595
Total volatile solids (TVS)	$mg \cdot dm^{-3}$	324	249	251	261	249	259

samples of filtered liquid. However, considering their small reduction relative to the raw gray water, at the same time relatively low value compared to industrial wastes (Malarski, Czajkowska & Nowak, 2018), these changes should be considered as the result of measurement error.

Compared to the obtained values of squashing with the Dixon et al. study (1999), a longer time was obtained. However, as in Malarski's research (2013), this index has not improved significantly during filtration.

For the potential user of gray water an important parameter of their quality is decay. This indicator for raw gray water was 70 h. During filtration the value of this parameter slightly improved to 77 h. Some of indicators, which case decay decrease during filtration, that is confirm by other parameters tested.

Experiment 3. Filtration on a filter with a carbon cartridge – FCCA

In the third experiment, filtration of bath gray water through a carbon cartridge filter FCCA was carried out. The aim of the conducted research in the experiment was to determine the impact of the second stage of the FCCA-STO filter on the filtration of bath gray water. The research was carried out in the same way as in experiments 1 and 2, using the remaining gray water from the bath accumulated in the tank. The experiment was completed after filtering 80 dm^3 of gray water. The filter cartridge has not been fully colmatated. During the tests, five samples of filtered gray water were collected. The tests were carried out twice at an interval of two weeks. The tests results of the analyzed quality parameters at taken samples were presented as mean values from the tests in Table 4.

TABLE 4. Characteristics of bath gray water raw and treated on the housing carbon cartridge filter FCCA (own studies)

Indicator	Unit	Raw gray water	Volume of filtrate [dm^3]				
			10	20	40	60	80
Turbidity	NTU	45.6	33.2	35.1	35.9	35.9	36.0
pH	–	7.58	7.66	7.71	7.65	7.68	7.71
Conductivity	$\mu s \cdot cm^{-1}$	1 386	1 355	1 368	1 380	1 369	1 372
Decay	h	70	72	72	72	72	72
COD	mg $O_2 \cdot dm^{-3}$	224	200	200	205	214	205
BOD_5	mg $O_2 \cdot dm^{-3}$	103	85	81	88	91	88
Total suspended solids (TSS)	$mg \cdot dm^{-3}$	706	146	141	133	150	148
Fixed suspended solids (FSS)	$mg \cdot dm^{-3}$	75	37	36	35	39	38
Volatile suspended solids (VSS)	$mg \cdot dm^{-3}$	631	109	105	98	111	110
Total dissolved solids (TDS)	$mg \cdot dm^{-3}$	1 078	916	905	925	909	891
Total fixed solids (TFS)	$mg \cdot dm^{-3}$	754	641	633	648	630	625
Total volatile solids (TVS)	$mg \cdot dm^{-3}$	324	375	372	277	279	266

The filtration of bath gray water through the analyzed filter cartridge did not significantly affect the quality parameters of liquid. They have improved to a small extent, but the analyzed liquid quality indicators have not changed significantly.

The obtained results showed lower efficiency of the carbon cartridge in the gray water pretreatment process as compared to experiments 1 and 2. Considering that the analyzed filter cartridge is a carbon cartridge used mainly as a sorption cartridge for removing dissolved pollutants, its lower efficiency in treating gray water containing a series of impurities in a suspended form is justified.

Based on the results of the research, it can be assumed that the used filter cartridge in the case of gray water filtration on it acted like an ordinary mechanical filter with low filtration efficiency.

Because of filtration, the following quality parameters have slightly changed: turbidity (up to approx. 27% in the first sample), COD (up to approx. 11% in samples 1 and 2), TDS (up to 17% in sample 5), BOD_5 (up to about 21% in sample 2). Higher reduction was obtained for the TSS (up to about 81% in sample 3).

Based on the test results, it can be assumed that the sorption capacity of the filter cartridge was quickly exhausted with the first portion of gray water as a result of clogging of the pores of the filter bed. After that the cartridge still worked only as a bed of mechanical filtration. This is confirmed by a greater reduction of turbidity and TSS in the analyzed filtrate samples.

The tests on single FCPS10 and FCCA filtration cartridges confirm the assumption that follows the first series of tests (experiment 1) with a double stage polypropylene-carbon filter. The amount of pollution reduction on the FCPS10 filter is at the same level as on the filter with the FCCA-STO cartridge, while the use of the FCCA cartridge (carbon cartridge) showed worse results. Hence it can be concluded that the carbon filter, which is a sorption filter, under these conditions in the experiment does not work properly. Using it for the treatment of bath gray water acts as an ordinary mechanical filter with low efficiency of removing impurities. For comparison, in studies conducted by Šostar-Turk et al. (2005) on bath gray water, the obtained pollution reduction was at the level of 85–95% using a coagulation process in combination with filtration on a 1 m filter column filled with sand and filtration through a 1m column with granular activated carbon.

For the potential user of recycled gray water, an important parameter of wastewater quality is their appearance. This parameter can be determined by wastewater turbidity. In order to determine the effectiveness of individual tested filter cartridges, their effectiveness in terms of turbidity reduction was analyzed.

The analysis of gray water treatment efficiency in terms of turbidity was conducted for all experiments performed using the values of the turbidity parameter presented in Tables 2–4. To minimize the impact of analytical errors, an attempt was made to approximate the measurement points with different functions. The best reflection of the points was obtained using the hyperbolic function. For this reason, the diagrams shown in Figure 1 were constructed, where the vertical axis is turbidity (S) and the horizontal filtered volume of sewage. The determination coefficients (R^2) have been determined for the presented functions. It was assumed that the function with the highest value of the R^2 coefficient would be a good fit of the function. Linear functions and their R^2 determination coefficients are shown in Figure 1.

efficiency are decreasing. This means that the analyzed cartridges, together with the amount of filtered gray water, have less ability to remove turbidity. At the same time, a faster decrease in the turbidity reduction efficiency in the filtrate is noticeable by using a contribution with activated carbon content relative to the polypropylene cartridge. Comparing

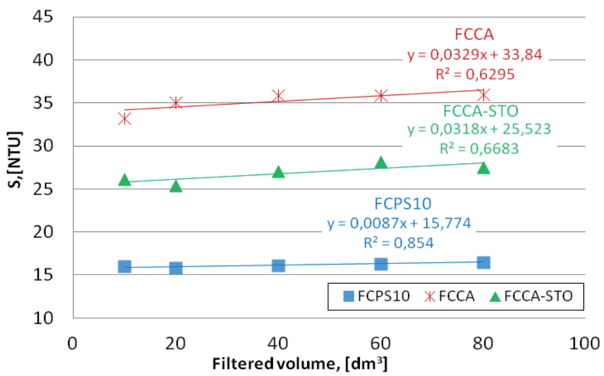

FIGURE 1. Hyperbolic dependence of turbidity as a function of gray water flow (own studies)

The functions presented in Figure 1 were used to calculate the effectiveness of gray water treatment using the following formula

$$\eta = \frac{S_p - S_i}{S_p}$$

where:
η – efficiency of decreasing wastewater turbidity,
S_p – initial turbidity of gray water,
S_i – turbidity after filtering a given volume.

Effectiveness of gray water treatment on individual filter cartridges is shown in Figure 2. As can be seen there, the functions of the turbidity reduction the method of pollution reduction applied in the own research with a double stage filter cartridge, for example with the Vakil, Sharma, Bhatia, Kazmi and Sarkar (2014), using the electrocoagulation processes, the obtained effect is minimal. The researchers obtained the turbidity reduction effect at the level of 85%, where in the authors' own research the effect was obtained at only 40% for a double stage cartridge.

Used FCCA carbon cartridges, FCPS10 polypropylene cartridges and FCCA-STO polypropylene carbon cartridges were not blocked during the tests. Only 80 dm^3 of gray water were filtered each time, and then the experiments were stopped. Based on the assumption of FCCA-STO and FCCA filters operation

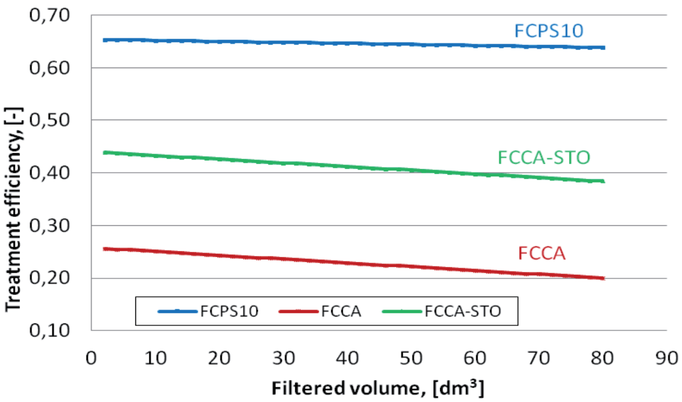

FIGURE 2. Effectiveness of turbidity decomposition according to gray water flow filtration (own studies)

as ordinary mechanical cartridge filters instead of sorption filters and a straight decrease in their efficiency, their turbidity removal capacity will run out after filtering about 630 dm^3 of gray water with an FCCA-STO cartridge, 360 dm^3 with an FCCA cartridge and 3,400 dm^3 with a FCPS cartridge.

It may seem to be problematic why filtration using the double stage polypropylene carbon cartridge FCCA-STO showed lower efficiency of turbidity reduction from gray water relative to the single stage filtration system on the FCPS10 polypropylene cartridge and at the same time higher relative to the system using the single stage FCCA carbon cartridge. The carbon cartridge, which is a sorption filter, under the given conditions works most likely like an ordinary mechanical filter after the rapid exhaustion of its sorption capacity. It should be noted that for the FCCA-STO and FCPS10 cartridge, the contact time of gray water with a polypropylene bed at the same flow will be different due to the twice the bed layer for the FCPS10 cartridge.

Conclusions

The filtration of natural bath gray water through the cartridge filters did not show significant improvement in the quality of the liquid. The filter cartridges used only contribute to the reduction of turbidity in the treated gray water. The remaining quality parameters after gray water filtration remained at a similar level to the initial values.

The carbon cartridge, which is a sorption filter, in the case of filtration of gray water, most likely acts as a filter for mechanical removal of pollutants. Its sorption capacity is exhausted very quickly. And the quality parameters of gray water are practically not improved.

The used filter cartridges for gray water treatment can be used as preliminary stages of purification. However, the use of a carbon refill at this stage of purification is not recommended due to the minimal efficiency and, at the same time, unnecessary increase in the costs of potential gray water treatment.

Decay and turbidity can be important parameters for a potential user of a gray water recycling plant. The values of these parameters obtained in the tests can be accepted by the user. Relatively low turbidity (FCPS10 – 16 NTU, FCCA-STO – 27 NTU, FCCA – 35 NTU) and long time of decay (three days) give the possibility of their reuse in the household. However, it should be remembered that gray water from the bath is characterized by high variability. The obtained parameters from gray water filtration may be significantly worse in bath gray water with a higher degree of biodegradability (higher BOD_5, lower decay, higher turbidity, etc.). Therefore, the filtration of gray water from the bath, even through a double stage filter cartridge, is not recommended as the only way to prepare them.

References

Abdel-Shafy, H.I. & Al-Sulaiman, A.M. (2014). Assessment of physic-chemical processes for treatment and reuse of greywater. *Egyptian Journal of Chemistry*, *57*(3), 215-231.

Abdel-Shafy, H.I. & Dewedar, A. (2012). Constructed wetlands for urban wastewater treatment in Egypt. *Journal Sustainable Sanitation Practice*, *12*, 27-32.

Abdel-Shafy, H.I. & El-Khateeb, M.A. (2013). Integration of septic tank and constructed wetland for the treatment of wastewater in Egypt. *Desalination and Water Treatment*, *51*(16-18), 3539-3546.

Abdel-Shafy, H.I., El-Khateeb, M.A. & Shehata, M. (2013). Grey water treatment using different designs of sand filters. *Desalination and Water Treatment*, *52*(28-30), 5237-5242.

Abudi, Z.N. (2011). The effect of sand filter characteristics on removal efficiency of organic matter from grey water. *Al-Qadisiya Journal for Engineering Sciences*, *4*(2), 143-155.

Aquafilter (2016-04-10). *Materiały techniczne Aquafilter INC* [*Technical materials – Aquafilter INC*]. Retrieved from: https://www.aquafilter.com [access 10.04.2016].

BWT Polska (2015-06-15). *Materiały techniczne Best Water Technology* [*Technical materials – Best Water Technology*]. Retrieved from: https://www.bwt.pl [access 15.06.2015].

Boyjoo, Y., Pareek, V.K. & Ang, M. (2013). A review of grey water characteristics and treatment processes. *Water Science and Technology*, *67*(7), 1403-1424.

Bugajski, P., Chmielowski, K. & Kaczor, G. (2016). Wpływ wielkości dopływu wód opadowych na skład ścieków surowych w małym systemie kanalizacyjnym. *Acta Scientiarum Polonorum – Formatio Circumiectus*, *15*(2), 3-11.

Charchalac Ochoa, S.I., Ushijima, K., Hijikata, N. & Funamizu, N. (2015). Treatment of domestic greywater by geotextile filter and intermittent sand filtration bioreactor. *Journal of Water Reuse and Desalination*, *5*(1), 39-49.

Christowa-Boal, D., Eden, R.E. & McFarlane, S. (1996). An investigation into grey water reuse for urban residential properties. *Desalination*, *106*(1-3), 391-197.

Chudzicki, J. (2010). *Oszczędzanie wody bez rezygnacji z komfortu* [*Saving water without sacrificing comfort*]. Ładny Dom. Retrieved from: http://ladnydom.pl/budowa/1,106590,6719177,Oszczedzanie_wody_bez_rezygnacji_z_komfortu___Druga.html [access 10.12.2019].

Chudzicki, J. & Sosnowski, S. (2011a). *Instalacje kanalizacyjne. Projektowanie, wykonawstwo, eksploatacja* [*Sewage installation. Design, execution, operation*]. Józefosław: Wydawnictwo Seidel-Przywecki.

Chudzicki, J. & Sosnowski, S. (2011b). *Instalacje wodociągowe. Projektowanie, wykonawstwo, eksploatacja* [*Water installation. Design, execution, operation*]. Józefosław: Wydawnictwo Seidel-Przywecki.

Dixon, A.M., Butler, D., Fewkes, A. (1999). Guidelines for Greywater Re-Use: Health Issues. *Water and Environment Journal*, *13*(5), 322-326.

Gross, A., Maimon, A., Alfiya, Y. & Friedler, E. (2015). *Grey water reuse*. Boca Raton: CRC Press, Taylor & Francis Group.

Gual, M., Moia, A. & March, J.G. (2008). Monitoring of an indoor pilot plant for osmosis rejection and greywater reuse to flush toilets in a hotel. *Desalination*, *219*(1-3), 81-88.

Hourlier, F., Massé, A., Jaouen, P., Lakel, A., Gerente, C., Faur, C. & Le Cloirec, P. (2010). Membrane process treatment for greywater recycling: Investigations on direct tubular nanofiltration. *Water Science & Technology*, *62*(7), 1544-1550.

Huelgas-Orbecido A. & Funamizu N. (2019). Membrane system for gray water. In: N. Funamizu (ed.), *Resource-oriented agro-sanitation systems* (pp. 185-193). Tokyo: Springer.

Jabornig, S. & Favero, E. (2013). Single household grey water treatment with a moving bed biofilm membrane reactor (MBBMR). *Journal of Membrane Science*, *446*, 277-285.

James, D.T.K., Surendran, S., Ifelebuegu, A.O., Ganjian, E. & Kinuthia, J. (2016). *Grey water reclamation for urban non-potable reuse challenges and solutions: A review.* The 7th International Conference on Sustainable Built Environment. Kandy, Sri Lanka, 16-18.12.2016.

Jamrah, A., Al-Futaisi, A., Prathapar, S. & Al Harrasi, A. (2008). Evaluating grey water reuse potential for sustainable water resources management in Oman. *Environmental Monitoring and Assessment*, *137*, 315-327. DOI 10.1007/s10661-007-9767-2

Kalenik, M. (2014). Skuteczność oczyszczania ścieków w gruncie piaszczystym z warstwą naturalnego klinoptylolitu [Sewage treatment efficacy of sandy soil bed with natural clinoptiolite assist layer]. *Ochrona Środowiska*, *36*(3), 43-48.

Kalenik, M. (2015). Empirical formulas for calculation of negative pressure difference in vacuum pipelines. *Water*, 7(10), 5284-5304.

Khalaphallah, R. (2012). *Greywater treatment or reuse by slow sand filtration: study of pathogenicmicroorganisms and phage survival* (doctoral thesis, Ecole des Mines de Nantes, Nantes).

Kundzewicz, Z.W., Zalewski, M., Kędziora, A. & Pierzgalski, E. (2010). Zagrożenia związane z wodą [Water-related hazards]. *Nauka*, *4*, 87-96.

Malarski, M. (2013). Treatment of bath grey water using cartridge filters as a way to reduce water consumption in households. *Annals of Warsaw University of Life Sciences – SGGW. Land Reclamation*, *45*(1), 49-59.

Malarski M. (2016). Jakość ścieków szarych zawierających płynne środki chemii gospodarczej [The quality of grey waters containing liquid household chemicals]. *Scientific Review – Engineering and Environmental*, *25*(4), 433-443.

Malarski, M., Czajkowska, J. & Nowak, P. (2018). Preliminary studies on the use of Fenton reagent to reduce pollution from wastewater from the production of household chemicals. *Annals of Warsaw University of Life Sciences – SGGW. Land Reclamation*, *50*(4), 301-312.

Malarski, M., Matusiak, K. & Cybula, J. (2016). Wpływ wybranych produktów chemii gospodarczej na jakość ścieków szarych [The influence of selected household chemical products on the quality of greywater]. *Scientific Review – Engineering and Environmental*, *25*(1), 61-71.

March, J.G., Gual, M. & Orozco, F. (2004). Experiences on grey water re-use for toilet flushing in a hotel (Mallorca Island, Spain). *Desalination*, *164*(3), 241-247.

Masi, F., El Hamouri, B., Abdel, Shafi, H., Baban, A., Ghrabi, A. & Regelsberger, M. (2010). Treatment of segregated black/grey domestic wastewater using constructed wetlands in the Mediterranean basin: the Zer0-m Experience. *Water Science and Technology*, *61*(1), 97-105. DOI 10.2166/wst. 2010.780

Mucha, J. & Jodłowski, A. (2010). Ocena możliwości wykorzystania wody szarej [Evaluation of possibility of using gray water]. *Gaz, Woda i Technika Sanitarna*, *7-8*, 24-27.

PN-78/C-04541. Woda i ścieki. Oznaczanie suchej pozostałości, pozostałości po prażeniu, straty przy prażeniu oraz substancji rozpuszczonych, substancji rozpuszczonych mineralnych i substancji rozpuszczonych lotnych [Water and sewages. Determination of the dry residue, residue on ignition, loss on ignition and solute substances, mineral solute substances and volatile solute substances].

PN-92/B-01706. Norma polska. Instalacje wodociągowe. Wymagania w projektowaniu [PN--92/B-01706. *Installations* for water supply. Design].

PN-C-04626:1976. Woda i ścieki. Oznaczenie zagniwalności i względnej trwałości [Water and sewages. Determination of the putrescibility and relative durability].
PN-EN 27888:1999. Jakość wody. Oznaczanie przewodności elektrycznej właściwej [Water quality. Determination of the specific electrical conductivity].
PN-EN 1899-1:2002. Biochemiczne zapotrzebowanie tlenu BZTn. Jakość wody. Oznaczanie biochemicznego zapotrzebowania tlenu po n dniach (BZTn). Część 1: Metoda rozcieńczania i szczepienia z dodatkiem allilotiomocznika [Biochemical oxygen demand BODn. Water quality. Determination of biochemical oxygen demand after n days (BODn). Part 1: Dilution and seeding method with allylthiourea addition].
PN-EN 1899-2:2002. Biochemiczne zapotrzebowanie tlenu BZTn. Jakość wody. Oznaczanie biochemicznego zapotrzebowania tlenu po n dniach (BZTn). Część 2: Metoda próbek nierozcieńczonych [Biochemical oxygen demand BODn. Water quality. Determination of biochemical oxygen demand after n days (BODn). Part 2: Method for indiluted samples].
PN-EN ISO 7027:2003. Jakość wody. Oznaczanie mętności [Water quality. Determination of the turbidity].
PN-ISO 15705:2005. Chemiczne zapotrzebowanie tlenu ChZT. Jakość wody. Oznaczanie indeksu chemicznego zapotrzebowania tlenu (SP-ChZT). Metoda zminiaturyzowana z zastosowaniem szczelnych probówek [Chemical oxygen demand COD. Water quality. Determination of the chemical oxygen demand index (ST-COD). Small-scale sealed-tube *method*].
PN-EN 806-3:2006. Wymagania dotyczące wewnętrznych instalacji wodociągowych do przesyłu wody przeznaczonej do spożycia przez ludzi. Część 3: Wymiarowanie przewodów. Metody uproszczone [PN-EN 806-3:2006. Specifications for installations inside buildings conveying water for human consumption – Part 3: Pipe sizing – simplified method].
PN-EN ISO 10523:2012. Jakość wody. Oznaczanie pH [Water quality. Determination of pH].
Oron, G., Adel, M., Agmon, V., Friedler, E., Halperin, R., Leshem, E. & Weinberg, D. (2014). Grey water use in Israel and worldwide: standards and prospects. *Water Research*, *58*, 92-101.
Rozporządzenie Ministra Środowiska z dnia 18 listopada 2014 r. w sprawie warunków, jakie należy spełnić przy wprowadzaniu ścieków do wód lub do ziemi, oraz w sprawie substancji szczególnie szkodliwych dla środowiska wodnego. Dz.U. 2014 poz. 1800 [Regulation of the Minister of Environment of 18 November 2014 on conditions for the introduction of sewage into water or soil and on the list of substances particularly harmful to water environment. Journal of Laws 2014, item 1800].
Rozporządzenie Ministra Zdrowia z dnia 7 grudnia 2017 r. w sprawie jakości wody przeznaczonej do spożycia przez ludzi. Dz.U. 2017 poz. 2294 [Regulation of the Minister of Health of 7 December 2017 on the quality of water intended for human consumption. Journal of Laws 2017, item 2294].
Šostar-Turk, S., Petrinić, I. & Simonič, M. (2005). Laundry wastewater treatment using coagulation and membrane filtration. *Resources, Conservation and Recycling*, *44*, 185-196.
Spychała, M. (2016). Skuteczność filtrów włókninowych do oczyszczania ścieków w warunkach stałego poziomu piętrzenia [Efficiency of textile filters for wastewater treatment in condition of stable wastewater table]. *Acta Scientiarum Polonorum – Formatio Circumiectus*, *15*(1), 19-34.
Ushijima, K., Ito, K., Ito, R. & Funamizu, N. (2013). Grey water treatment by slanted soil system. *Ecological Engineering*, *50*, 62-68.
Vakil, K.A., Sharma, M.K., Bhatia, A., Kazmi, A.A. & Sarkar, S. (2014). Characterization of greywater in an Indian middle-class household andinvestigation of physicochemical treatment using electrocoagulation. *Separation and Purification Technology*, *130*, 160--166.
Vuppaladadiyam, A.K., Merayo, N., Prinsen, P., Luque, R., Blanco, A. & Zhao, M. (2019). A review on grey water reuse: quality, risks, barriers and global scenarios. *Reviews in Environmental Science and Bio/Technology*, *18*(1) 77-99.

Wu, B. (2019). Membrane-based technology in greywater reclamation: A review. *Science of The Total Environment*, *656*, 184-200.
Yu, Z.L.T., Rahardianto, A., DeShazo, J.R., Stenstrom, M.K. & Cohen, Y. (2013). Critical review: regulatory incentives and impediments for onsite grey water reuse in the United States. *Water Environment Research*, *85*(7), 650-661.

Summary

Purpose of the housing double stage polypropylene-carbon cartridges filters usage in bath gray water treatment. Bath gray water organoleptically did not appear to be significantly contaminated liquid. However, in order to re-use them, they need proper treatment. When recirculated in a household, they cannot pose a threat to human life. Based on their appearance, it seems that the solution to the problem is the use of cartridges filter. The article presents the results of the filtration of gray water from the bath through the filtration system with a housing double stage polypropylene-carbon filter FCCA-STO and to determine the impact of individual filter layers on wastewater treatment, tests were carried out on a single polypropylene FCPS10 and carbon FCCA filtration cartridge. The aim of the study was to determine the suitability of the selected housing filter cartridges for the treatment of bathing gray water for their reuse. For the tests were used natural bathing gray water from a two-family building inhabited by seven people. Wastewater were fed to the filter with a constant flow rate of 0.1 $dm^3 \cdot s^{-1}$. The assessment of the work of the filters based on parameters such as: COD, BOD_5, suspension, dry residue, decay and turbidity. The conducted tests have shown a slight improvement in most of the quality parameters of gray water after filtration through selected housing cartridge filters. Only for turbidity, the reduction in the value of the pollution indicator was noticeable. The cartridge filters used in tests, acted like ordinary mechanical filtration cartridges. For the considered gray water, the use of analyzed cartridge filters can only be used for their initial purification.

Authors' address:
Maciej Malarski
(https://orcid.org/0000-0002-9731-7092)
Marek Kalenik
(https://orcid.org/0000-0001-6184-1899)
Szkoła Główna Gospodarstwa Wiejskiego
w Warszawie
Instytut Inżynierii Środowiska
Wydział Budownictwa i Inżynierii Środowiska
Katedra Hydrauliki i Inżynierii Sanitarnej
ul. Nowoursynowska 159, 02-776 Warszawa
Poland
e-mail: maciej_malarski@sggw.pl
marek_kalenik@sggw.pl

Scientific Review – Engineering and Environmental Sciences (2020), 29 (2), 259–272
Sci. Rev. Eng. Env. Sci. (2020), 29 (2)
Przegląd Naukowy – Inżynieria i Kształtowanie Środowiska (2020), 29 (2), 259–272
Prz. Nauk. Inż. Kszt. Środ. (2020), 29 (2)
http://iks.pn.sggw.pl
DOI 10.22630/PNIKS.2020.29.2.22

Hary SUDJONO[1], PRATIKTO[1], SURACHMAN[2], Sugiono SUGIONO[1]

[1] Brawijaya University, Faculty of Engineering
[2] Brawijaya University, Faculty of Economics

The product strength analysis of woven bag made from recycled mineral water plastic cups based on the polypropylene content

Key words: woven bag, green manufacturing, tenacity, plastic wastes

Introduction

Since the first time it was discovered, the use of plastic wastes has been having a gradual increase. It is influenced by technological development, industrial development as well as the rising number of population. The global use of plastic in 2007 had reached 260 million t (Asmita, Shubbamsingh, Tejashree & Road, 2015). Other than as the biggest contributor of solid wastes in the terrestrial environment, it is also noted that from the 260 million t of plastic produced, around 8 t of plastic wastes were carried by the stream and ended up in the high seas (Eriksen et al., 2014). The source of plastic wastes is dominated by packaging (38%), followed by buildings and constructions (21%), automotive (7%), electricity and electronics (6%) and other sectors (28%) the likes of medical and recreations (European Commission, 2009; Plastics Europe, 2009). The plastic wastes that can be managed by the Indonesian government are only around 20–30%. The rest of it will be dumped into the wastes disposal areas. The solid wastes removal and extermination by burying them under the ground are also typically done. Some researchers in their researches argue that the residual monomer consisted of the plastic polymer can be dangerous (Lithner, Larsson & Dave, 2011; Galloway, 2015; Comăniță, Hlihor, Ghinea & Gavrilescu, 2016). Besides, the chemical compounds used in the production of plastic as an additive, especially plasticizer, are dangerous to the human and environment's health, along with the degradation products which might be emitted during the life cycle of plastic.

Furthermore, Verma, Vinoda, Papireddy and Gowda (2016) added that the burning of poly vinyl chloride (PVC) will release the halogen which is dangerous and pollutes the air, leading to climate change. The toxic substances released that way are a thorough threat to the vegetation, health, and environment of human and animals. The polystyrene is destructive to the central nerves system. The dangerous brominated compounds act as a carcinogen and mutagen. The dioxin sediments in the plants and waterways, therefore it is dangerous to the human when consuming that food and water.

Based on that condition, the 3R (reuse, reduce, recycle) methods of plastic wastes management, as Visvanathan, Adhikari and Ananth (2007) explained in their research, are developed. Reuse is the repeated use of plastic products. Reduce is lowering the purchase or usage of plastic stuff, especially the disposable ones. Recycle is reprocessing the plastic products. By implementing this management system, the wastes will be transformed back to the initial cycle as raw materials for the other more useful products. The heightened global attention and awareness toward the environmental aspects enhance the industry to implement green manufacturing (GM) concept in their business practices (NPCS Board of Consultants & Engineers, 2014). The idea of green manufacturing (GM) is basically a process/system which has a minimum impact or negative influence on the environment. Some countries in the world have committed to pay more attention to the environmental aspects of their agendas. The implementation of GM can lower the material cost since it uses wastes as the raw materials, avoids aggravating the environmental damage, and positively influences the institutions' reputation (Webb, Arnott, Crawford & Ivanova, 2013).

The implementation of GM in manufacturing companies consider the thoroughness and links of their current business practices in woven bag production. The core phase in the process of using the raw materials made from recycled wastes is implementing the planning of GM principles by producing woven bag in accordance with the specifications determined by the companies and the consumers' demands, referring to Standard National Indonesia (SNI) and the positive impacts to the environment. The primary quality parameter of the woven bag is the tenacity of plastic threads. This tenacity is the main factor of strength quality of woven bag in carrying weights. To achieve the quality of thread tenacity qualified to the specifications, the experiments in the factors of machines setup and plastic raw materials' components are influential. This research will examine the influence of operational temperature in the extraction machines and the adding of plastic wastes as the raw materials of the woven bag. The temperature factor becomes an essential component in structuring microplastics. Ariff, Ariffin, Rahim and Jikan (2012) in their research explains that the viscosity of ore plastic liquids is strongly influenced by the operational temperature.

Research materials

To be able to explain the role of plastic cup wastes in becoming the raw materials of the woven bag within the concept of green manufacturing, there will be discussions on some theoretical framework, such as plastic wastes, green manufacturing concept, and the production process of the woven bag.

Plastic wastes

Plastic is an artificial material which molecular structure has a complicated composition, which also purposely set to fulfill the specific applications demanded by plastic constructed by many monomers, which eventually constructs a polymer. The characteristic of plastic depends on the constructive monomer. In general, plastics have a low density, are electrically insulating, have varying mechanical strength, limited temperature resistance, and vary chemical resistance. In addition, plastic is also lightweight, easy to design, and low-cost manufacturing. Unfortunately, behind all these advantages, plastic waste creates problems for the environment. The plastic polymer is composed upon elements of carbon, oxygen, and hydrogen. The plastic molecules can be formed through the organic condensation or polymer addition and can also consist of other substances to improve the performance or economic values. Plastic classification based on its chemical structure is divided into two types, i.e. linear and three-dimensional network. When the monomer forms a polymer chain straight (linear), thermoplastic plastic will be formed which has properties melts at a certain temperature, attached to changes in temperature and can reversible to its nature, i.e. re-harden when cooled. When three-dimensional monomers due to chain polymerization will form thermosetting plastics with properties cannot keep up with changes in temperature. When once hardening has occurred, the material cannot be softened again. Plastic has various boiling and melting points, this is based on the formation monomers. Monomers are often used in plastic manufacturing is propene (C_3H_6), ethane (C_2H_4), vinyl chloride (CH_2), nylon, carbonate (CO_3), and styrene (C_8H_8). Generally, there are seven types of plastics which we often used in our daily lives, as seen in the table.

The mixed raw materials used in the woven bag production is polypropylene (PP) and the transparent plastic cup wastes (Fig. 1a), which is also come from PP. The raw materials are the type of plastic often used to wrap food or beverage type 5 (see the table). This type is also used as a food container and baby drink bottle. This product is considered as a disposable product which can only be used once and then becomes a solid wastes or recycled. The PP plastics consist of the crystalline polymer formed through the process of propylene gas polymerization. Propylene has a lower specific gravity compared to other types of plastics (Maddah, 2016). Polypropylene is a thermoplastic polymer. Polyolefin is ready to be formed by the process of propylene polymerizing with a suitable catalyst, such as aluminum alkyl and titanium tetrachloride. Therefore, it is light and suitable as a wrapper material. A polypropylene has a pretty high melting point (190–200°C), while its crystallization point is around 130–135°C. Polypropylene has a high chemical resistance, yet low impact strength.

A plastic can be degraded by the environment through four mechanisms, which are photodegradation, thermal oxidation degradation, hydrolytic degra-

TABLE. Seven types of plastics based on the danger levels toward the environment and human (Ryedale District Council, n.d.)

Symbol	Acronym	Information
	PET	For mineral water and ready to drink bottles. Not to be refilled, especially with hot water.
	HDPE	Milky white bottles. Usually for mineral water galoon, plastic chairs, or milk packaging for food. This bottle is also disposable.
	PVC	Hardly recyclable plastics, such as plastic wrap or bottles. The components of this plastic can melt and diffuse to the food in the temperature of < 15°
	LDPE	Usually for food, plastic packaging have soft or flexible texture. Food plastic wraps or bottles with this symbols is quite safe to be used.
	PP	Safe to be used as food or beverage wraps. Usually this plastic is used as food container and baby drink bottles. The plastic is transparent.
	PS	Disposable sterofoam packaging for food/beverage. This material can mix with the food under high temperature. Dangerous to the brain and nerves.
	other	SAN (styrine acrylonitrile), ABS (acrynitrile butadiene styrene), PC (polycarbonate), nylon. Usually for food/beverage, household appliances, computer, etc. Plastic with code 7 SAN and ABS is good and safe to be used for food/beverage. Meanwhile, PC is dangerous for the body.

a b

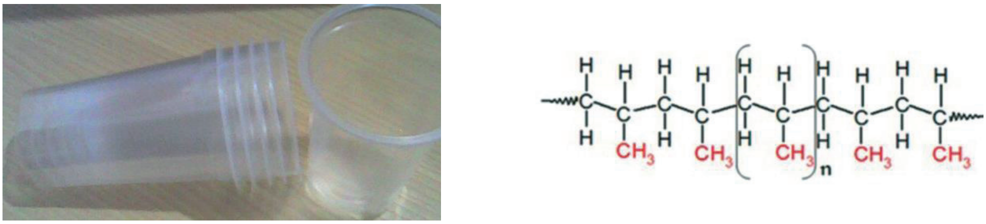

FIGURE 1. a – woven bag mixed raw materials of plastic cup wastes, b – polypropylene chemical structure

dation, and biodegradation by the microorganisms. Through these mechanisms, the plastic can be degraded perfectly within at least 50 years (Webb, Arnott, Crawford & Ivanova, 2013). Because of such a long time, there is a technology developed which can recycle plastic materials so that the environmental impacts can be reduced. Recycling processes of plastics can be divided into four ways category for primary, secondary, tertiary, and sometimes quaternary recycling. The primary category plastic processing is defined as a process without changing the type of product. This process category is characterized by simple, low-cost stages (Grigore, 2017). In addition, this process does not change the chemical structure of plastic (Singh, Hui, Singh, Ahuja, Feo & Fraternali, 2017). The secondary category of plastic processing is to change the shape of the product for use in other functions, for example beverage bottles are cut to be used as plant pots. Both of primary and secondary category processes are identical to mechanical changes (Stewart, 2009). Processing of tertiary recycling plastic waste is to break down plastic products into molecules chemically and then as the basis for making new products. Quaternary recycling is turning plastic waste into an energy source. The recycling process which is conducted when the product has been used by the consumers and re-processed into its polymer form is called mechanical, yet the transformation to the monomer form is called chemical. The method of energy recovery refers to the restoration of plastic energy composition, yet it has a negative impact on the health risks upon toxic substances in the air. Among those recycling methods, the chemical is the best because it leads to its construction of monomer, where the polymer is generated.

Some general steps in the process of chemical recycling of PP plastic are (Harron & Gilbert, 2014):

1. Collection: plastic wastes are collected from different locations.
2. Cleaning: The cleaning step consists of wastes washing and drying.
3. Sorting: In this step, not only separating the polymer from foreign substances, but also from other polymers.
4. Size reduction: This step is aimed to reduce the size of the wastes as well as separating the different polymer. The final product of shredding can be in a form of ragged plastic pieces.

Green manufacturing

Green manufacturing includes a number of activities aimed to prevent pollution, to reduce the use of toxic substances, and to implement Reduce, Reuse, and Recycle (3R). The pollution prevention focuses on how to avoid and minimalize the wastes by reducing the wastes resources or doing on the spot recycling. Reducing the resources of wastes can be achieved through ways related to the process or the products (Dornfield, Yuan, Diaz, Zhang & Vijayaraghavan, 2013; Seth, Rehman & Shrivastava, 2018), such as the modification of product by changing the shape and the composition of the product's raw materials; substituting the input so that the use of raw materials and additive substances, which cause pollution and require process aids (such as lubricant and cooler), can be reduced; modifying the technology by involving an improvement in the automation process, optimation process, redesign of the tools and process substitution; as well as changing the operational procedure and management to decrease or removing the wastes and emission. The green concept includes the manufacturing process by using minimal materials and a process which minimalizes the negative impacts toward the environment, low energy and natural resources, safe for the employees, people, and consumers, but also protecting the economic values (Al Shayeb, 2013; Duić, Urbaniec & Huisingh, 2015).

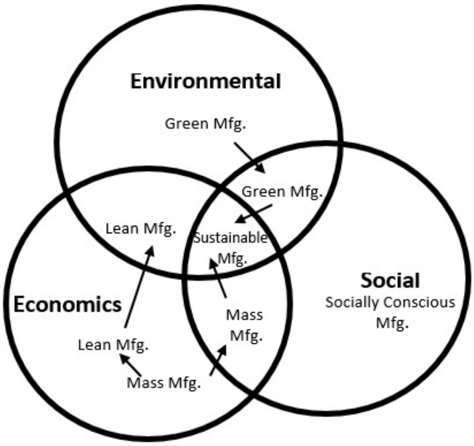

FIGURE 2. The linkages of green manufacturing with the economy, social, and environment

Green manufacturing (GM) has a significant role in enhancing sustainability in plastic use through plastic wastes recycle. The need for the green environment has reinforced the emergence of GM so that plastic sustainability can be achieved. The existence of sustainable manufacturing will be influential to the social, economy, and environment (Fig. 2). A sustainable manufacture refers to a manufacturing system or process that fulfills these three important factors – which are discussing its impacts toward the environment, economy, and society (Teodorescu, 2012; Astuti, Prawoto, Irawan & Sugiono, 2018). Considering the definition of the US Trade Department upon the sustainable manufacture that includes "minimalizing the negative impacts toward the environment, save energy and natural resources, safe for the employee, society, and consumers as well as being economically healthy" – the three underlined! A company cannot sustain if those three, at least, is not balanced with the financial.

Generally, the management of plastic wastes includes collecting, sorting, crushing, washing, and manufacturing into the product. The production process of PP woven bag involves the mixing of raw materials started from the pellet of PP or HDPE and other additives, extrusion of raw materials into the PP resin thread heated with $CaCO_3$ and pigment, melted and extruded as a flat film (Ain & Panchal, 2017). Meanwhile, the production process of the woven bag with the mixture of plastic bottle wastes includes several activities, such as:

– Recycle. The plastic as a wastes of packaged mineral water is recycled into the form of beans to be able to be used as a raw material by using a shredder machine to crush the plastics and shaped it into plastics beans.
– Mixing the raw materials in the mixer. The raw materials, which have been mixed using mixer machine with a certain composition to generate a finished material, are sheets of plastics with a quality-adjusted with SNI's requirements (4–6 g per 1 denier).
– Plastic extrusion process. The raw materials mixed with other materials using mixer are then inserted into a plastic extrusion machine to generate the plastic sheets.
– The cooling of the finished materials (plastic sheets). The cooling treatment to the plastic sheets is done by dipping it into cold water, where the temperature should not exceed

30°C. The objective is so that the PP plastics generated can have a strong crystal structure of PP plastics.

- The plastic sheets cutting process. The stretching process of plastic ribbons is done on a plate with certain temperatures so that the plastic ribbons have a strong tenacity due to the stretching. In this step, the ribbons will have a weaker tenacity.
- Annealing (heating without stretching). In this step, the plastic sheets are heated through a hot plate without any stretching so that the plastic sheets can recover its tenacity.
- Rolling. In this step, the plastic ribbons which have been cut are then rolled in a rolling machine consisted of many rolls moving back and forth in accordance with the arrangement set automatically so that the movement of the rolls would not overlap each other. The changing of the full rolls is done gradually in accordance with the rolls' position order and it can be done manually. The rolls changing should be done wearing gloves so that the plastic ribbons would not tear apart and harm the hands.
- Weaving the plastic rolls. This process is the knitting or spinning of the plastic ribbons/threads. It requires many rolls and it should be monitored by a supervisor because it is often that during the process, there are plastic rolls that break.
- Cutting. After the bag is cut, the lower part of the bag is sewn up and ready to be a woven bag.
- Final products. The final products of woven bags are ready to be delivered to the customers.

Research methodology

This section discusses the theoretical framework and research design. This research is conducted in order to implement the green manufacturing concept within the manufacturing process of the woven bag by utilizing the raw materials made of mineral bottle plastic wastes. The recycling of plastic wastes has to be qualified according to the product quality standard. Accordingly, the research method is action research. It is emphasized on the actions by conducting a test of ideas into the practical or real situation within a micro scale, which is expected to be able to repair, improve the quality, and promote social recovery.

The research design is used as the foundation of this research so that the implementation could be conducted right, well, and smooth. In this section, there will be a discussion on the research object, research design up to the result, and the analysis. The research object is to design a process of PP plastic recycling management in the manufacturing system through a feasibility test of business practices. The concept of making woven bags is to make basic raw materials by mixing recycled plastic waste with pure plastic bijing or categorized as tertiary recycling in plastic waste. The alternative raw materials need to be developed due to the limit of primary raw materials which come from oil. The research is conducted in PT. Absolutech Distrindo, a manufacturing factory producing woven bags which is located in Pakis subdistrict, district of Malang, East Java. It has complete machines and tools so that it is possible to do the research in the factory.

The research design is used to determine the test parameter in order to acknowledge the woven bags' feasibility by using the alternative raw materials of PP mineral water bottle plastic wastes. The main parameter used to assess the woven bags' feasibility is the thread tenacity test, which also happens to be the woven bags' material. The test is conducted using a thread tensile strength test tool with a measurement unit of g per 1 denier. The product is confirmed to fulfill the Standard National Indonesia (SNI) if the power is around 4–6 g per 1 denier. Figure 3 shows one example of tensile strength test for experiment 1 (10% plastic wastes) with extruction temperature 175°C. According to the graph, it can be explained that the specimen will break after 14 s with maximum force at 24 N (1 N = 79.98 denier). The different experiment parameters gave different tensile strength.

The steps in the woven bag production experiment are from the raw materials of original plastic beans and plastic beans mixed with plastic bottle wastes. There are three experiments that will be conducted, which are experiment I: raw materials of 100% original plastic beans, extrusion temperature 1 = 175°C, extrusion 2 = 187°C, extrusion 3 = 200°C, extrusion 4 = 212°C, extrusion 5 = 225°C, lime percentage = 10% and cooling temperature = 20°C. Experiment II: raw materials of 90% original plastic beans, 10% plastic bottle wastes, extrusion temperature 1 = 175°C, extrusion 2 = = 187°C, extrusion 3 = 200°C, extrusion 4 = 212°C, extrusion 5 = 225°C, lime percentage = 10% and cooling temperature = 20°C. Experiment III: raw materials of 90% original plastic beans, 10% plastic bottle wastes, extrusion temperature 1 = 185°C, extrusion 2 = 197°C, extrusion 3 = 210°C, extrusion 4 = 222°C, extrusion 5 = 235°C, lime percentage = = 10% and cooling temperature = 20°C. The flowchart (Fig. 4) is presenting the general steps in the experiment process of woven bags production based on different conditions.

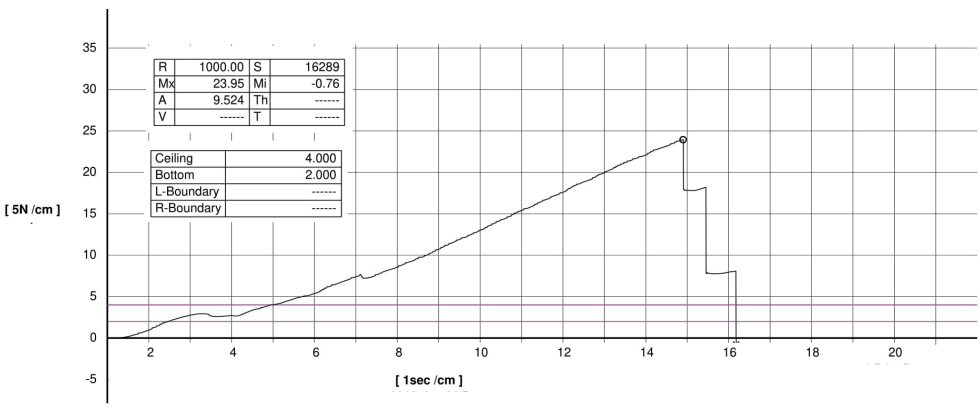

FIGURE 3. The tenacity test measurement for the woven bags' raw materials for experiment II, temperature 175°C

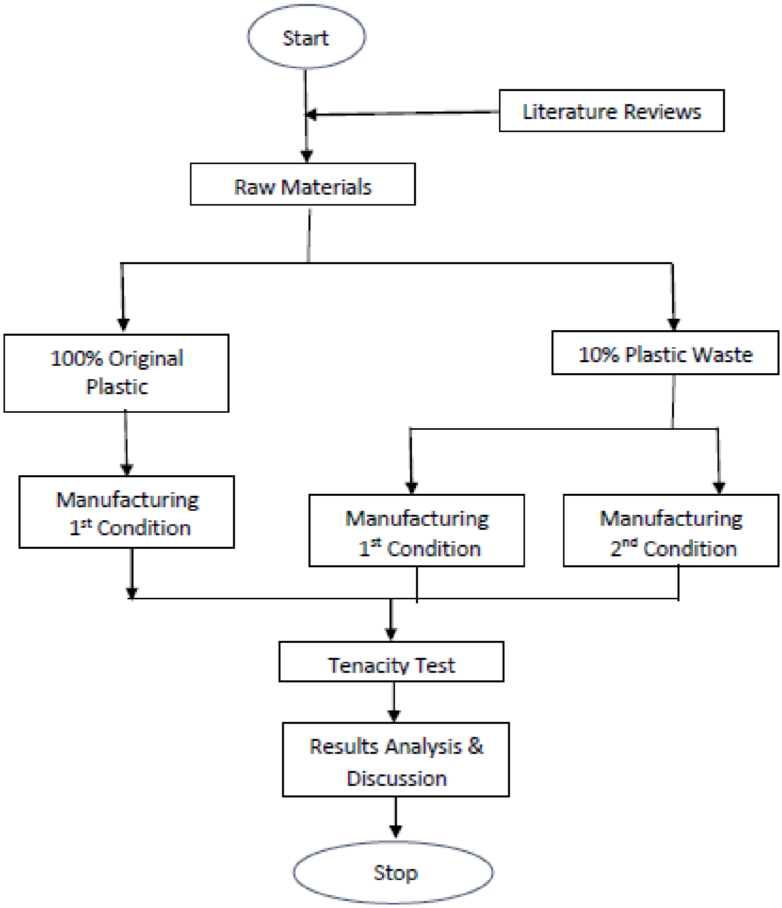

FIGURE 4. Flowchart of the woven bag manufacturing process based on differences in raw material and extrution temperature

Results and discussion

As the beginning of improvement toward the woven bag production system with the mixed raw materials between plastic beans and plastic cup wastes, created two different manufacturing process conditions. The second condition of manufacturing process works with the extrusion temperature 1 = 175°C, extrusion 2 = 187°C, extrusion 3 = 200°C, extrusion 4 = 212°C, extrusion 5 = 225°C, lime percentage = 10% and cooling temperature = 20°C. To investigate the changes in the woven bags' tenacity, the raw materials, which used 100% original plastic beans and 90% original plastic beans (with 10% plastic wastes), are compared. According to the measurement results of each material with 8 replications of each (Fig. 5), there is an average tenacity of 5.15 g per 1 denier for the raw materials of 100% original plastic beans, while the mixed one has an average tenacity = 3.38 g

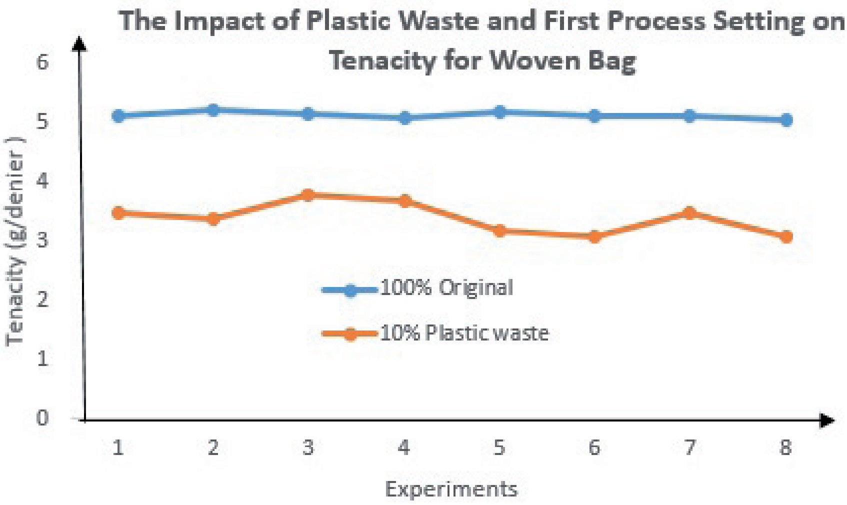

FIGURE 5. The result of tenacity measurement in setup machine condition 2 for wastes materials 0% and 10%

per 1 denier. T test has been used to decide whether the two groups of experimental data have significant differences or not. On the other hand, F test has been used to find out how much influence a parameter in the experiment determines the results. Based on the hypothesis test using the F test, concluded that $F_{\text{calcul.}} = 20$ and $F_{\text{table}} = 4.9$. With the value of $F_{\text{calcul.}} > F_{\text{table}}$, it can be considered that the original variance of tenacity is not homogenous with the recycled's tenacity. Besides, according to the result of t test, the $t_{\text{calcul.}} = 19.25$ and $t_{\text{table}} = 2.13$, which means the gap in the tenacity between the two materials is really significant.

The condition of manufacturing process 3 works on extrusion temperature 1 = 185°C, extrusion 2 = 197°C, extrusion 3 = 210°C, extrusion 4 = 222°C, extrusion 5 = 235°C, line percentage = 10% and cooling temperature = 20°C. To investigate the changes in the woven bags' tenacity, the raw materials, which used 100% original plastic beans and 90% original plastic beans (with 10% plastic wastes), are compared. According to the measurement results of each material with eight replications of each (Fig. 6), there is an average tenacity of 5.07 g per 1 denier for the raw materials of 100% original plastic beans, while the mixed one has an average tenacity = 4.76 g per 1 denier. Based on the hypothesis test using the F test, concluded that $F_{\text{calcul.}} = 97$ and $F_{\text{table}} = 4.9$. With the value of $F_{\text{calcul.}} > F_{\text{table}}$, it can be considered that the original variance of tenacity is not homogenous with the recycled's tenacity. Besides, according to the result of t test, the $t_{\text{calcul.}} = 2.17$ and $t_{\text{table}} = 2.13$, which means the gap in the tenacity between the two materials is not significant.

According to Figures 5 and 6, it can be concluded that statistically, there are changes in the woven bags' tenacity with the original raw materials and the one mixed with plastic cup wastes. There are two machine setting conditions com-

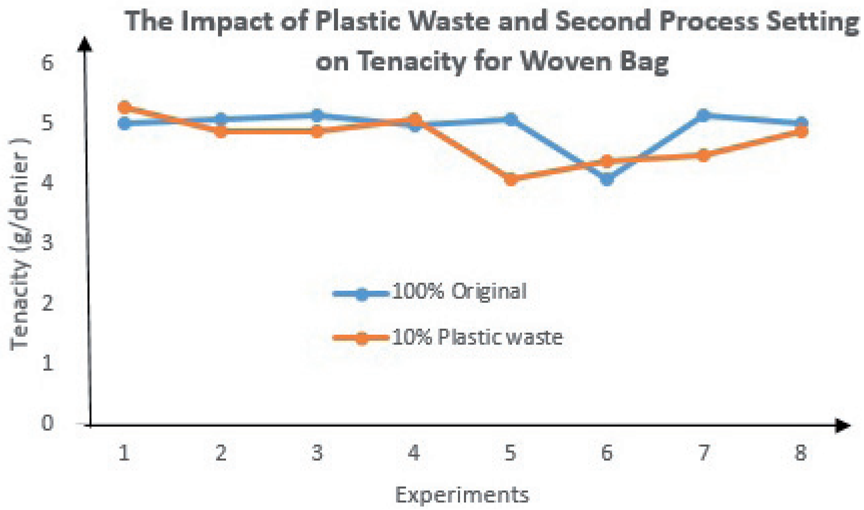

FIGURE 6. The result of tenacity measurement in the setup machine condition 2 for wastes materials 0% and 10%

pared, which are machine setting 1 and 2 that have the temperature 10°C higher than all the extrusion machines. Based on the comparison of average tenacity tests, acquired the data that tenacity value for the first machine setup has tenacity = = 3.38 g per 1 denier and for the second machine setup = 4.76 g per 1 denier. It can be concluded that the setup temperature in the second machine is able to meet the SNI standard, which is around 4–6 g per 1 denier. It indicates that the setup temperature of the extrusion machine used in the woven bags production is important to be studied. Increasing the extrusion temperature is even able to cut the gap of tenacity between the raw materials of original plastics and raw materials mixed with 10% of plastic wastes. It requires a further investigation of the relationship between the characteristics of raw materials polypropylene (C_3H_6), operational machine temperature, and the number of wastes added to the mix. An experimental design with an in-depth chemical analysis is expected to be able to find the right composition that contributes to the implementation of green manufacturing. Zhang, Wang, Lu and Yu (2005) state that; the PP melting duration around 48 s is also needed to be considered in optimizing the woven bags' tenacity.

Conclusions

Based on this research, it can be concluded that the addition of plastic cup wastes has a good chance that can be beneficial as an additive substances in the production of woven bags with the raw materials of polypropylene (C_3H_6). The tenacity in the second experiment condition with the 10% of plastic bottle wastes is able to generate a good value of 4.76 g per 1 denier, which is also allowed by the government (4–6 g per 1 denier). Statistically, the difference of tensile strength between two materials is not significance. The comparison between the first and second experiment shows that the setting of the extrusion machine's temperature is very influential to the products of woven bags. The increase in temperature as much as 10°C could improve the tenacity up to 40.38%. The understanding of the PP chemical characteristics and machine setting is helpful to generate an optimal tenacity. Therefore, in the future, the complete research design is required to increase the use of wastes in the production of woven bags.

Acknowledgements

The researcher expresses their gratitude to Ministry of National Education of the Republic of Indonesia for supporting this paper. The authors are also grateful to the Department of Mechanical Engineering of the the Brawijaya University, Malang, Indonesia for their extraordinary support.

References

Ain, Q.U & Panchal, J. (2017). Total Quality Control for Manufacturing of Plastic Woven Laminated Bags Using Six Sigma. *International Journal of Engineering Development and Research*, *5*(3), 832-842.

Al Shayeb, R. (2013). The three pillars of sustainability. Washington. Retrieved from: http://www.thwink.org/sustain/glossary/ThreePillarsOfSustainability.htm#F1 [access 21.02.2019].

Ariff, Z.M., Ariffin, A., Jikan, S.S & Rahim, N.A.A. (2012). Rheological behaviour of polypropylene through extrusion and capillary rheometry. In F. Dođan (ed.), *Polypropylene* (pp. 29-49). Rijeka: InTech.

Asmita, K., Shubhamsingh, T. & Tejashree, S. (2015). Isolation of plastic degrading microorganisms from soil samples collected at various locations in Mumbai, India. *International Research Journal of Environment Sciences*, *4*(3), 77-85.

Astuti, M., Prawoto, P., Irawan, Y.S. & Sugiono, S. (2018). The eco-innovation variables which influence the performance of creative industries center of natural stone crafts. *Journal of Ecological Engineering*, *19*(1), 14-24. https://doi.org/10.12911/22998993/79446

Comăniță, E.D., Hlihor, R.M., Ghinea, C. & Gavrilescu, M. (2016). Occurrence of plastic waste in the environment: ecological and health risks. *Environmental Engineering and Management Journal*, *15*(3). https://doi.org/10.30638/eemj.2016.073

Dornfeld, D., Yuan, C., Diaz, N., Zhang, T. & Vijayaraghavan, A. (2013). Introduction to green manufacturing. In D.A. Dornfeld (ed.), *Green manufacturing: fundamentals and applications* (pp. 1-24). New York: Springer. https://doi.org/10.1007/978-1-4419-6016-0_1

Duić, N., Urbaniec, K. & Huisingh, D. (2015). Components and structures of the pillars of sustainability. *Journal of Cleaner Production*, *88*, 1-12. https://doi.org/10.1016/j.jclepro.2014.11.030

Eriksen, M., Lebreton, L.C.M., Carson, H.S., Thiel, M., Moore, C.J., Borerro, J.C., Galgani, F., Ryan, P.G. & Reisser, J. (2014). Plastic pollution in the world's oceans: more than 5 trillion plastic pieces weighing over 250,000 tons afloat at sea. *PLoS ONE*, *9*(12), e111913. https://doi.org/10.1371/journal.pone.0111913

European Commission (2013). *Green Paper on a European Strategy on Plastic Waste in the Environment.* COM(2013)123 final of 07.03.2013. Brussels: European Commission.

Galloway, T.S. (2015). Micro- and nano-plastics and human health. In M. Bergmann, L. Gutow, M. Klages (ed.), *Marine anthropogenic litter* (pp. 343-366). New York: Springer. https://doi.org/10.1007/978-3-319-16510-3_13

Grigore, M. (2017). Methods of recycling, properties and applications of recycled thermoplastic polymers. *Recycling*, *2*(4), 24. https://doi.org/10.3390/recycling2040024

Harron, K. & Gilbert, R. (2014). Research: increasing value, reducing waste. *The Lancet*, *383*(9923), 1099-1182. https://doi.org/10.1016/S0140-6736(14)60558-4

Lithner, D., Larsson, A. & Dave, G. (2011). Environmental and health hazard ranking and assessment of plastic polymers based on chemical composition. *Science of the Total Environment*, *409*(18), 3309-3324. https://doi.org/10.1016/j.scitotenv.2011.04.038

Maddah, H.A. (2016). Polypropylene as a promising plastic: a review. *American Journal of Polymer Science*, *6*(1), 1-11. https://doi.org/10.5923/j.ajps.20160601.01

NPCS Board of Consultants & Engineers (2014). *Disposable products manufacturing*. *Handbook*. New Delhi: Niir Project Consultancy Services.

Plastics Europe (2009). *The compelling facts about plastics 2009*. Brussels: Plastics Europe.

Ryedale District Council (n.d.). *Different types of plastics and their classification*. Retrieved from: https://www.ryedale.gov.uk/attachments/article/690/Different_plastic_polymer_types.pdf [access 17.01.2019].

Seth, D., Rehman, M.A.A. & Shrivastava, R.L. (2018). Green manufacturing drivers and their relationships for small and medium (SME) and large industries. *Journal of Cleaner Production*, *198*, 1381-1405. https://doi.org/10.1016/j.jclepro.2018.07.106

Singh, N., Hui, D., Singh, R., Ahuja, I.P.S., Feo, L. & Fraternali, F. (2017). Recycling of plastic solid waste: A state of art review and future applications. *Composites Part B: Engineering*, *115*, 409-422. https://doi.org/10.1016/j.compositesb.2016.09.013

Stewart, R. (2009). Waste management. In V. Goodship (ed.), *Management, recycling and reuse of waste composites* (pp. 39-60). Boca Raton: CRC Press. https://doi.org/10.1533/9781845697662.1.39

Teodorescu, A.-M. (2012). Links between the pillars of sustainable development. *Annals of the University of Craiova. Economic Sciences*, *1*, 1-6.

Webb, H.K., Arnott, J., Crawford, R.J. & Ivanova, E.P. (2013). Plastic degradation and its environmental implications with special reference to poly(ethylene terephthalate). *Polymers*, *5*(1), 1-18. https://doi.org/10.3390/polym5010001

Verma, R., Vinoda, K.S., Papireddy, M. & Gowda, A.N.S. (2016). Toxic pollutants from plastic waste – a review. *Procedia Environmental Sciences*, *35*, 701-708. https://doi.org/10.1016/j.proenv.2016.07.069

Visvanathan, C., Adhikari, R. & Ananth, A.P. (2007). 3R practices for municipal solid waste management in Asia. In *Kalmar ECO-TECH '07 and the Second Baltic Symposium on Environmental Chemistry*. Kalmar, Sweden, 26-28.11.2007 (pp. 26-28).

Zhang, J., Wang, Y., Lu, X. & Yu, J. (2005). Study on melting behavior of polymers during burning. *Fire Safety Science*, *8*, 637-646. https://doi.org/10.3801/IAFSS.FSS.8-637

Summary

The product strength analysis of woven bag made from recycled mineral water plastic cups based on the polypropylene content. The increasing amount of plastic wastes has become a threat to the sustainability of all ecosystem in this Earth. This paper aims to provide an alternative utilization of plastic wastes as the raw material in the manufacturing process of woven bag products with a quality control in its tenacity. The initial phase of this research is a literature review on the concept of green manufacturing, woven bag quality, compositions of plastic wastes and woven bag manufacturing proses. Furthermore, it is followed by a data measurement in a form of tenacity test using a thread test gauge (tenacity). There are two types of the condition in the manufacturing process of woven bag production compared by increasing the temperature as much as 10°C in all the extraction machines. The measurement result shows that the average tensile strength in the production process of the woven bag made from the wastes of mineral water plastic cups with 10% composition and extraction temperature for the first condition is 3.38 g per 1 denier and the second condition is 4.76 g per 1 denier. The result of second condition manufacturing (increasing the extraction temperature by 10°C) after comparing it with the quality required by Standard National Indonesia (SNI) as much as 4 to 6 g per 1 denier is considered

good quality. Therefore, through the concept of green manufacturing, the utilization of plastic wastes might provide a substitution to the part of plastic core raw material in the woven bag production. This research is designed to be the beginning of innovation to acquire raw materials for the woven bag, furthermore, the optimization toward the machine setting and innovation on plastic wastes raw materials become the foundation in increasing the tenacity.

Authors' address:
Hary Sudjono
Brawijaya University
Faculty of Engineering
Department of Industrial Engineering
Indonesia
e-mail: harysudjono@ub.ac.id

Pratikto
Brawijaya University
Faculty of Engineering
Department of Mechanical Engineering
Indonesia
e-mail: pratikto@ub.ac.id

Surachman
Brawijaya University
Faculty of Economics
Department of Economics and Business
Indonesia
e-mail: surachman@ub.ac.id

Sugiono Sugiono – corresponding author
Brawijaya University
Faculty of Engineering
Department of Industrial Engineering
Indonesia
e-mail: sugiono_ub@ub.ac.id

Informacje dla autorów

Na łamach *Przeglądu Naukowego – Inżynieria i Kształtowanie Środowiska* zamieszczane są **oryginalne prace naukowe w języku polskim lub angielskim, niepublikowane** w innych czasopismach. Prawa autorskie tekstów przyjętych do druku udzielone są Wydawnictwu SGGW, a artykuły są udostępniane na warunkach Open Access na zasadach licencji Creative Commons CC BY-NC (patrz oświadczenie autorów na stronie http://iks.pn.sggw.pl).

Wymagania techniczne dotyczące przygotowania prac:

1. Tekst i tabele należy złożyć w formie elektronicznej, w plikach o formacie MS Office, a rysunki – wstawione do tekstu i w oddzielnych plikach graficznych, w programach pracujących w środowisku Windows (Excel, Photoshop itp.) w wersji czarno-białej. Rysunki i zdjęcia w wersji papierowej są drukowane w skali szarości, a na stronie internetowej czasopisma wygenerowane w wersji kolorowej.
2. Objętość artykułu wraz z ilustracjami nie może przekraczać 10 stron formatu A-4, interlinia – 1,5 wiersza, marginesy – 2,5 cm, czcionka TNR 12 pkt., tekst w układzie jednokolumnowym.

Układ pracy (zgodnie z szablonem: http://iks.pn.sggw.pl/do_autorow.html):

1. Imię i nazwisko autora(-ów) – u góry z lewej strony.
2. Pod nazwiskiem – miejsce pracy w polskim i angielskim języku.
3. Tytuł pracy – w polskim i angielskim języku.
4. Słowa kluczowe (*Key words*) – w polskim i angielskim języku.
5. Tekst pracy (w języku polskim lub angielskim) powinien obejmować: **wprowadzenie, materiał i metody, wyniki, podsumowanie i dyskusję, wnioski, literaturę, streszczenie w języku angielskim (Summary), streszczenie w języku polskim, adres autora(-ów).**
6. Tytuły tabel i rysunków, opisy główki pionowej i poziomej tabel oraz wszystkie napisy na ilustracjach muszą być w polskim i angielskim języku w wersji czarno-białej.
7. W tekstach w języku polskim do oznaczania pozycji dziesiętnej liczb należy używać przecinka, a w języku angielskim – kropki.
8. Przy powoływaniu się w artykułach angielskojęzycznych na publikacje w *Przeglądzie Naukowym* autorzy proszeni są o używanie jego angielskiej nazwy.
9. Wykaz piśmiennictwa i powołania należy sporządzić według międzynarodowego formatu APA i zestawić w porządku alfabetycznym. Bliższe informacje, przykłady formatowania i program do tworzenia opisów bibliograficznych w wymaganym formacie znajdują się na stronie *Przeglądu Naukowego* (http://iks.pn.sggw.pl/do_autorow.html), np.:
   Kowalski, J. i Nowak, P. (2009). *Analiza regresji stosowana.* Warszawa: Wydawnictwo Naukowe PWN.
   Kowalski, J., Nowak, P. i Bartnik, Z. (2009). Suspended sediment sources in two small lowland agricultural catchments in the UK. *Journal of Hydrology*, *252*(1-4), 1–24. doi:10.1016/s0022-1694(01)00388-2
   Procedura recenzowania. (2014). Pobrano z lokalizacji Przegląd Naukowy Inżynieria i Kształtowanie Środowiska: http://iks.pn.sggw.pl/recenzje.html.
10. Przy pierwszym powoływaniu się w tekście na innych autorów podaje się np.: „zdaniem Kowalskiego (2002)" lub „(Kowalski, 2002)". Przy większej liczbie autorów „(Kowalski, Malinowski i Witkowski, 2002)".
11. Streszczenia powinny zawierać ok. 500 znaków.
12. Author's address:
    Jan Kowalski
    Nazwa miejsca pracy w języku polskim (uczelnia, wydział, katedra)
    ulica, kod pocztowy miejscowość, Poland
    e-mail
13. Oświadczenie o oryginalności pracy (http://iks.pn.sggw.pl/oswiadczenie.doc).